

**KARST HYDROGEOLOGY
OF THE
CANADIAN ROCKY MOUNTAINS**

By

Stephen Richard Hurst Worthington

A thesis

submitted to the School of Graduate Studies

in partial fulfilment of the requirements

for the Degree

Doctor of Philosophy

McMaster University

© Copyright by Stephen Richard Hurst Worthington, May 1991

KARST HYDROGEOLOGY

OF THE

CANADIAN ROCKY MOUNTAINS

DOCTOR OF PHILOSOPHY (1991)
(Geography)

McMASTER UNIVERSITY
Hamilton, Ontario

TITLE: Karst hydrogeology of the Canadian Rocky Mountains

AUTHOR: Stephen Richard Hurst Worthington, B.A. (Sheffield University)
M.Sc. (McMaster University)

SUPERVISOR: Dr D.C. Ford

NUMBER OF PAGES: xx, 370

Abstract

An analysis of the discharge and hydrochemical variations of contrasting springs at Crowsnest Pass showed they were part of a vertical hierarchy in the aquifer, in which underflow and overflow components play a dominant role. It was found that karst springs at Crowsnest Pass and elsewhere show a range between two end members. Thermal springs have long, deep flow paths, with high sulphate concentrations, low discharge variance and low flow velocities. Overflow springs have local shallow flow paths, low sulphate, high discharge variance, and high flow velocities. Intermediate between these end members are underflow springs; in the Rocky Mountains these are mostly aggraded, and give the sustained winter flow and high sulphate concentrations found in major rivers.

It was found that underflow or overflow behaviour is able to explain most of the contrasts found between karst springs in discharge and sulphate concentrations. Conversely, differences in bicarbonate concentration are principally due to the ratio of allogeic to autogenic recharge to the aquifer. Hydraulic analysis showed that gradients decrease in the downstream direction, and are typically 0.0001-0.05 at maximum discharges, that friction factors vary by a factor of >1000, and that most active conduits have closed-channel flow and are in dynamic equilibrium with sediment supply.

The analysis of the hydrological data from Crowsnest Pass and elsewhere has led to the development of a new conceptual model for groundwater flow in karst, in which the Hagen-Poiseuille flow net conditions the aquifer for conduit development, and determines where the conduits will be. The model explains why most conduits are in dynamic equilibrium with sediment supply, why temperate karst springs are mostly vauclusian, what the mean time for speleogenesis is, how >98% of the solution of limestone is in the surficial zone, and why there are karstic hot springs in the Rocky Mountains and elsewhere. The model enables predictions to be made of sink to resurgence flow velocities, of conduit depth below the water table, of the ratio of beds to joints used by conduits, of the spacing between cave tiers, and of the depth of vauclusian springs.

This new understanding of how karstic aquifers develop and function gives a powerful predictive ability to karst hydrogeology.

Preface

The research upon which this thesis is based commenced as a hydrological study of some karst springs, with the aim of achieving some insight into the part played by conduits in groundwater flow in the Rocky Mountains. The hydrological and hydrochemical information collected showed that the two principal springs were strikingly different, yet no existing hypothesis of karst groundwater flow adequately explained the main differences between the springs.

A serendipitous discussion on the unpredictability of cave location, just at the time when I was wrestling with the possibilities of regional flow, led to the ideas expounded in Chapters 6, 7 and 8. These ideas help explain groundwater flow in the Rockies (and elsewhere), but most of the data used to develop the ideas are drawn from my cave exploration and research in countries around the world over the last twenty years.

Karst makes up about 7-10% of the world's rocks, and supply drinking water to more than a billion people (Ford & Williams, 1989). Groundwater flow in karst rocks is in solutionally-enlarged conduits, where turbulent flow is found, and velocities are frequently in the range of kilometres per day. However, hydrogeologists have commonly ignored these conduits in their computer simulations, instead assuming that velocities measured from well pumping tests can be applied to the whole rock.

The problem in karst hydrogeological research has largely been one of scale. Most case studies in caves or of conduit flow have been of relatively small areas ($1-100 \text{ km}^2$). At this scale, the most interesting features have been the contrasts found. There have been few studies that have considered karst hydrogeology at a regional scale ($100-10000 \text{ km}^2$). Thus there have been many descriptions of caves and of conduit flow, and some hypotheses have been proposed. However, the biggest barrier to understanding karst groundwater flow has been the difficulty in identifying what constitutes a representative sample. Thus it has been difficult to test hypotheses. In this thesis, an attempt is made to overcome this problem by collecting large and hopefully representative data sets on morphometric, hydrological and hydrochemical aspects of karst groundwater flow.

The fundamental characteristic of karst hydrogeology is that caves are the principal vectors for flow. The questions of how, when and where caves form are central to an understanding of karst hydrogeology.

It has long been thought that caves form by dissolution of the limestone by carbonic acid, but only thirty years ago it was shown that theoretically caves could not exist, as water would become saturated after travelling only a short distance through the limestone (Weyl, 1958). However, Berner and Morse (1974) showed that dissolution rates decrease by at least three orders of magnitude as saturation is approached, thus enabling undersaturated water to travel through the aquifer and produce caves. Since then research has focused on reaction processes and kinetics

(e.g. Plummer et al., 1978; Dreybrodt, 1988), and CO₂ availability (e.g. Drake, 1984), as well as the continued collection of field data to test theoretical models. However, the presence of sulphate in karst waters has been largely ignored in these studies. It will be shown in this thesis that sulphate is usually present in large quantities in the waters that initiate conduit flow, so these may play a pivotal role in the formation of conduits.

The question "when?" (of how long it takes for caves to form), has proven difficult to answer. Minimum times of ten thousand years or less have been cited by and White (1983) and Dreybrodt (1988) on theoretical grounds, and by Mylroie and Carew (1987) from field evidence. However, dating of speleothems (Ford and Williams, 1989) has often shown that even the most recent passages in caves are at least hundreds of thousands of years old (eg. Schmidt, 1982; Worthington, 1984). New evidence for the mean time it takes to form caves will be presented in Chapter 8.

The answer to where caves form has hitherto proven elusive. Despite process studies on cave hydraulics (e.g. Curl, 1974, Lauritzen et al., 1985), and morphological and structural case studies (e.g. Ford, 1963; Jameson, 1985), it is still disputed whether the water table is a meaningful concept in karst areas (see Chapter 5). In his 1988 book entitled "Processes in Karst Systems", Dreybrodt used over 300 equations to explain how and when caves form, but the long chapter on the locality of cave development was descriptive in nature, with just three equations. This "failure of cave prediction on theoretical grounds" was noted by Waltham (1981), who stated: "in practical terms the only advice which can ... be offered the concerned engineer or hydrologist is that 'the only thing predictable about caves is that they are unpredictable.'"

This thesis will show that caves are predictable.

I wish to extend my thanks to the following people who aided my research.

Derek Ford recommended what turned out to be the ideal field area, provided me with the means to collect extensive hydrological and hydrochemical data at all seasons, and encouraged me during the long gestation of this thesis.

John Drake and Henry Schwarcz, members of my thesis committee, provided helpful suggestions for the research, and critically reviewed this manuscript.

Rea Bryant worked wonders with the stage recorders over the long, cold Rocky Mountain winter, keeping them functioning at -40°.

Pam Burns, Ian Drummond, Mike Evans, Steve Grundy, Linda Hastie, Brian Hayton, Chris Larsen, Ian McKenzie, Stefan Meinke, Chris Pugsley, Olivia Whitwell and Chas Yonge helped with dye tracing and water sampling.

Martin Knyf, Steve Vermette and Chas Yonge helped with isotopic and neutron activation analysis.

Marcus Buck, Philippe Drouin, John Ganter, Ivo Karmann, David Lowe, Craig Malis, Dug Medville, Philippe Meus, Chris Pugsley, Jacques Schroeder, Ron Simmons, Ron Stenson, Chris Smart, Marc Tremblay, Sue Vajoczki, Chas Yonge, and Nadja Zupan provided me with useful information on karst areas they knew well and gave me feedback on some of my new ideas.

Finally, Jane Mulkewich provided spiritual and financial support, assisted me during eight months of field work, and critically reviewed my ideas and this thesis.

Contents

List of figures	xiii
List of tables	xxi
Symbols used	xxv
Glossary	xxvii
Chapter 1 Introduction	
1.1 Research objectives	1
1.2 Choice of study area	5
1.3 Organisation of the thesis	9
1.4 The problem of sampling bias	10
Chapter 2 The study area: Crowsnest Pass	
2.1 Geology	13
2.1.1 Stratigraphy and mineralogy	13
2.1.2 Structure	18
2.2 Topography and drainage	20
2.2.1 Surface flow and inputs to the karst aquifers	20
2.2.2 Springs	22
2.3 Modern hydrogeology	27
2.3.1 Hydraulic conductivity of the karst aquifers	27
2.3.2 Groundwater flow vectors	29
2.4 Paleohydrogeology	30
Chapter 3 Hydrological and meteorological measurements	
3.1 Introduction	31
3.2 Discharge measurement	32
3.3 Fluorometry	41
3.3.1 Aquifer hydraulics	41
3.3.2 Catchment delineation	52
3.4 Hydrochemistry	53
3.4.1 Specific conductivity and titrations	53
Sampling and analysis	53
The determination of aggressiveness	57
3.4.2 Neutron activation analysis	64
3.4.3 Stable isotope analysis	65
3.5 Meteorology	68
3.6 Characterisation of the springs at Crowsnest Pass	69

Chapter 4 The influence of boundary conditions on spring discharge

and chemistry

4.1	Introduction	73
4.2	Underflow, full flow and overflow regimes	73
4.3	Springs of the Dinaric karst, Yugoslavia	81
4.4	Valles - San Luis Potosí region, Mexico	84
4.5	The Mendip Hills, England	88
4.6	Karst springs of Nittany Valley, Pennsylvania, USA	89
4.7	Karst springs of Ariège, France	94
4.8	Conclusion	98

Chapter 5 The hydraulics of karstic groundwater flow

5.1	Introduction	99
5.2	Diffuse flow and conduit flow	100
5.3	The Darcy-Weisbach equation	103
5.3.1	Velocity	103
5.3.2	Discharge	114
5.3.3	Area	115
5.3.4	Hydraulic gradient	117
5.3.5	Friction factor	124
5.4	Conclusion	126

Chapter 6 Flow nets in karst aquifers: morphometry and initial conditions

6.1	Introduction	127
6.2	Morphometric analysis of flow paths	130
6.2.1	Introduction	130
6.2.2	Conduit density	131
6.2.3	Conduit porosity	134
6.2.4	Segment length	135
6.2.5	Sinuosity	135
6.2.6	Flow belt width	140
6.2.7	Depth of loop crests and bases	143
6.2.8	Conclusion	149
6.3	Geological controls	149
6.3.1	Fracture occurrence	149
6.3.2	Primary tube development on multiple bedding planes	151
6.3.3	To what extent are bedding planes favoured?	155
6.4	Hydraulic controls on conduit development	158
6.4.1	Flow through fractures	158
6.4.2	Aquifer inputs	159
6.4.3	Initial hydraulic gradients	161
6.5	Topological controls	164
6.6	Kinetic controls on solution	166
6.7	Models of conduit development	169

Chapter 7 Flow nets in karst aquifers: the locus of flow during one generation

7.1	Introduction	173
7.2	Flow depth as a function of catchment length, dip and strike	173
7.2.1	Mean flow depth in explored caves (as a function of dip and catchment length)	173
7.2.2	Mean flow depth in explored caves (as a function of dip, strike and catchment length)	179
7.3	Phreatic lifts and drops	181
7.3.1	Initial phreatic drops	181
7.3.2	Terminal phreatic lifts : vauclusian springs	186
7.4	Prediction of water well yields	187
7.5	Tributary junctions	188
7.6	Factors possibly modifying the initial flow net	192
7.6.1	Long vadose paths	192
7.6.2	Effects favouring shallow phreatic flow	193
7.6.3	Distortion of hydraulic conductivity ellipse by impermeable strata	194
7.6.4	The influence of topographic relief	196
7.7	Conclusion	196

Chapter 8 Flow nets in karst aquifers: response to a falling water table

8.1	Introduction	199
8.2	Longevity of flow in conduits within one tier	201
8.3	Active conduits are mostly below the water table	204
8.4	Response at initial phreatic drops and terminal phreatic lifts	206
8.5	Hydraulics of existing and developing conduits	208
8.6	There may be flooded conduits and low-gradient streams in the vadose zone	216
8.7	Cave tiers are equidistant	221
8.7.1	Previous studies	221
8.7.2	The endogenetic model	222
8.8	Hydrochemical characteristics of the flow field beneath active conduits	224
8.8.1	Expected hydrochemical characteristics	224
8.8.2	Thermal karstic springs	225
8.8.3	Sulphate / bicarbonate ratios	229
8.8.4	Implications of high sulphate values in the deep flow net	229
8.9	Conclusions	233

Chapter 9 Catchment delineation of the springs at Crowsnest Pass

9.1	Problems of catchment delineation in karst	235
9.1.1	Introduction	235
9.1.2	Groundwater boundaries do not coincide with topographic boundaries	235
9.1.3	Flows may branch to two or more springs	237
9.1.4	Flow route may vary with stage	237
9.1.5	There may be unmonitored underflow	237
9.1.6	A catchment may have non-contiguous components	238
9.1.7	Conclusion: do springs have definable catchments?	238
9.2	Catchment area model for Crowsnest Pass	239
9.2.1	Model design and validation	239
9.2.2	Model use	243
9.3	Underflow and overflow regimes	250
9.3.1	Underflow and overflow in surface creeks	250
9.3.2	Overflow springs	254
9.3.3	Ptolemy Spring: a full-flow regime	254
9.3.4	Crowsnest Spring: an underflow regime	257
	Identification as an underflow regime	257
	Quantification of the underflow component	262
9.3.5	Sublacustrine Springs: an underflow regime	264
9.4	Catchment altitude	266
9.4.1	Freeze-thaw effects	268
9.4.2	Spring temperatures	268
9.4.3	Solute concentrations	270
9.4.4	Isotopes	273
9.5	Geology of catchments	273
9.6	Definition of catchments at Crowsnest Pass	273

Chapter 10 Karst groundwater flow at Crowsnest Pass

10.1	Karst spring hydraulics	277
10.1.1	Discharge	277
10.1.2	Velocity	279
10.1.3	Area of conduits	279
10.1.4	Hydraulic gradients	281
10.1.5	Friction factors	282
10.2	Aquifer characterisation from paleohydrology	282
10.3	Aquifer characterisation from hydrochemical evidence	283
10.4	Aquifer characterisation from the karst flow model	288
10.5	Reasons for the contrasting regimes of Ptolemy Spring and Crowsnest Spring	289
10.6	Flow vectors in the Flathead and High Rock Ranges	289

Chapter 11 Karst groundwater flow in the Rocky Mountains

11.1	Introduction	293
11.2	Hydraulics	293
11.2.1	Maligne karst	293
11.2.2	Castleguard Cave	295
11.2.3	Conclusions	301
11.3	The water balance	301
11.4	Surface runoff from Rocky Mountains karst	302
11.5	Aggraded karst springs	303
11.6	Regional strike-oriented underflow in the Rocky Mountains	304
11.7	Regional dip-oriented flow in the southern Rocky Mountains	307
11.8	Regional flow to thermal springs in the northern Rocky Mountains	311
11.9	Conclusions	314

Chapter 12 Karst groundwater as a geomorphic agent

12.1	The vertical distribution of solutional erosion	317
12.2	Erosion processes and fluxes in the Rocky Mountains	322
12.3	Erosional fluxes in the Ptolemy catchment	324
12.3.1	Measurements	324
12.3.2	The altitudinal variation in erosional fluxes	329
12.4	Conclusion	330

Chapter 13 Karst hydrogeology: a new paradigm

13.1	Introduction	331
13.2	Hydrochemistry	331
13.3	Hydraulics	332
13.4	Discharge and drainage	333
13.5	Morphometric analysis of conduits and conduit flow	334
13.6	A comprehensive model of karst groundwater flow	334

Chapter 14 Conclusions 339

References 341

FIGURES

1.1	Carbonate outcrops and important karst springs of the Rocky Mountains	2
2.1	Structural and lithological relationships of the carbonate Palliser and Banff-Rundle aquifers of the Flathead and High Rock Ranges	14
2.2	Carbonate outcrops and topographic blocks of the Flathead and High Rock Ranges with groundwater flow directions, assuming a planar piezometric surface with a gradient of ≤ 0.005	16
2.3	Geological sections across the Flathead and High Rock Ranges	17
2.4	Outcrops of the Palliser and Banff-Rundle aquifers in the Flathead and southern High Rock Ranges, with areas of enclosed drainage	19
2.5	Caves of the Ptolemy and Andy Good plateaux, with dye injection points	23
2.6	Topographical subdivisions of the Flathead and High Rock Ranges, with altitude of limestone contacts and hypothetical groundwater gradients .	25
3.1	Daily temperatures at Sentinel from September 1985 to August 1986 .	34
3.2	Measurement sites in the vicinity of Crowsnest Pass, showing dye trace routes to Ptolemy Spring and Crowsnest Spring	36-37
3.3	Measurement sites in the Flathead and High Rock Ranges	38
3.4	Stage-discharge relationships for Ptolemy Spring, Crowsnest Spring, Crowsnest River and Ptolemy Creek	39
3.5	Daily discharge of Ptolemy Spring, Crowsnest Spring and Sublacustrine Springs, September 1985 to August 1986	44
3.6	Daily discharge of Crowsnest River at the outlet of Crowsnest Lake and at Frank	45
3.7	Monthly discharge of the springs and creeks at Crowsnest Pass as a percentage of the discharge in Crowsnest River at the outlet of Crowsnest Lake, from August 1985 to September 1986	45

3.8	Instantaneous discharge of Crowsnest Spring from May 1st to September 1st 1986	46
3.9	Instantaneous discharge of Ptolemy Spring from May 1st to September 1st 1986	46
3.10	Instantaneous discharge of Ptolemy Creek from May 1st to September 1st 1986	47
3.11	Dye velocities to Ptolemy Spring and Crowsnest Spring	51
3.12	Total hardness at Ptolemy Spring and Crowsnest Spring, September 1985 to August 1986	54
3.13	Mean residence time of Crowsnest Lake, 1985-1986	54
3.14	Alkaline and non-alkaline hardness concentrations at Ptolemy Spring and Crowsnest Spring, April 15 to September 22, 1986	59
3.15	Aggressiveness of spring and creek waters at Crowsnest Pass	59
3.16	Concentrations of 16 elements in precipitation and in springs at Crowsnest Pass	65
3.17	Concentrations of nine elements in Ptolemy Spring, August 21-26, 1986	65
3.18	$\delta^{18}\text{O}$ and δD measurements from Ptolemy Spring, August 10-11, 1985 .	68
4.1	Recession exponents as an indicator of aquifer boundary conditions ..	79
4.2	Ratio of maximum discharge to mean discharge at Ljubljana springs	84
4.3	Cross-section of the Sierra Madre Oriental and El Abra Ranges, Mexico, at latitude 22°N, showing deep sulphate and shallow bicarbonate flow vectors (after Fish, 1977)	86
4.4	Relationship between coefficient of variation of hardness and proportion of concentrated recharge to karst aquifers	91
4.5	Summer recessions of Fontestorbes, Le Baget, and Aliou springs, Ariège, France	95
	a) gauged flow assuming fixed catchments giving an annual water balance (Fontestorbes 86km ² , Le Baget 13km ² , Aliou 12km ² ; after Mangin, 1975)	
	b) assuming fixed catchments of 40km ² for Fontestorbes, 13km ² for Le Baget, and 5km ² for Aliou, but with an underflow loss of 15km ² for Aliou, and an underflow gain of 700ls ⁻¹ for Fontestorbes.	

5.1	Flow velocity in karstic terrains	101
5.2	Velocity-discharge relationships for six cave systems (Wookey and Cheddar data from Stanton and Smart, 1981; Maligne data from Smart, 1988a; Jordtulla data from Lauritzen, 1986)	112
5.3	Ratio of maximum to minimum annual discharge for 136 karst springs (data in Table 5.2)	116
5.4	Evolution of velocity and cross-section in a karst conduit	116
5.5	Crossing of flow paths in the vadose zone of Yorkshire System, Andy Good Plateau	119
5.6	Hydraulic gradients of 18 flow routes in the ten largest catchments of the Mammoth Cave area, Kentucky (USA), (data from Quinlan and Ray, 1981)	123
6.1	Conduit porosity and density in karst aquifers	133
a)	Porosity due to explored conduits in 15 caves (data given in Table 6.1)	
b)	Conduit density for the caves in Table 6.1, and for the longest 20 and deepest 20 known caves in the world (after Courbon & Chabert, 1986)	
6.2	Flow paths in an orthogonally-jointed aquifer, using joints or bed-joint intersections	137
a)	terminology (note that this diagram is extremely simplified, and that L_x/L_y is usually >1000)	
b)	relative length of flow paths as a function of χ	
6.3	Efficiency of flow paths in karst - plan patterns of 57 allogenic and 39 autogenic flow paths (data in Table 6.1)	141
a)	sinuosity	
b)	width/length ratios	
6.4	Plan patterns of the six longest explored flow paths in karst conduits .	142
6.5	Profiles of explored phreatic loops	146-147
a)	Doux de Coly spring, France (after Isler and Magnin, 1985)	
b)	Hölloch, Switzerland (after Bögli, 1980)	
c)	Foussoubie, France (after Le Rouk, 1989)	
d)	Wookey - Swildons, England (after Ford, 1963; Drew, 1975b; Farr, 1983)	
e)	Annette - Trou de Glaz, France (after Chevalier, 1951)	

6.6	Profiles of active and fossil caves at Crowsnest Pass, showing vertical looping	148
a)	Crowsnest Spring (after Barton, 1981)	
b)	Yorkshire System, showing two important passages developed when the water table was at or above 2230m	
6.7	Relative depth below the water table of loop crests and loop bases for 19 active and fossil phreatic paths (data listed in Table 6.3)	149
6.8	Cross-section through the low potential field surrounding a developing conduit	152
6.9	Maximum possible use of bedding planes as flow routes as a function of dip and strike	157
6.10	Relative discharge of fracture flow paths in an orthogonal flow net, using the Hagen - Poiseuille equation	157
6.11	Contrasting initial flow paths in alloigenic and autogenic karstic aquifers, modelled from the Hagen - Poiseuille equation	160
6.12	Possible hydraulic gradient configurations in karst	162
6.13	Two-dimensional model of Hagen-Poiseuille flow in karst aquifers ..	165
6.14	Relative times to breakthrough for proximal and distal inputs in a karst aquifer 50km in length, based on empirical length and hydraulic gradient functions	171
7.1	Strike-oriented flowlines on a single bedding plane ABCD:	175
a)	conduit development with the bedding plane providing structural control	
b)	conduit development at sparse primary tubes or bed-joint intersections	
c)	conduit development at closely spaced primary tubes or bed-joint intersections	
7.2	Mean phreatic flow depth as a function of stratal dip and aquifer length for 17 karst aquifers	180
7.3	Phreatic flow depth and the domain of thermal springs in karst as a function of aquifer length and stratal dip	180
7.4	Flow routes aslant the strike following fractures	182
7.5	Catchment area for Fontaine de Vaucluse, France (after Drogue et al., 1983, Michelot and Mudry, 1985, and Puig, 1987)	186

7.6	Measured well yield in Pennsylvania as a function of stratal dip (after Siddiqui and Parizek, 1971) compared to the predicted relationship from Equation 7.3	189
7.7	Tributary flow fields towards a target conduit, showing equipotential lines	191
7.8	Terminal phreatic lifts and drops of selected tributary passages	191
7.9	Mean phreatic flow depth for allogenic and autogenic karsts	195
8.1	Sequential development of conduits in a karst aquifer, shown soon after abandonment of conduit A in favour of conduit B	200
8.2	Tiers of cave passages in Nelfastla de Nieva, Mexico	203
8.3	Examples of underground deltas	208-209
8.4	Ratio of discharge in developing conduit C to discharge in existing conduit B for four growth rates, corresponding to capture at stages 8, 9, 10 and 11 in Figure 8.1	211
8.5	Altitude range of phreatic loops in Ogof Ffynnon Ddu I, Wales (after Smart and Christopher, 1989)	211
8.6	Contemporaneous distributary junctions (arrowed) in part of Yorkshire System when the water table was at or above 2230m	213
8.7	Phases in the life of karst conduits	214
8.8	Patterns of vertical shaft development in the vadose zone	218
8.9	The domain of karst in terms of horizontal fracture spacing between joint conduits	220
9.1	Problems of catchment delineation in karst	236
9.2	Catchments and precipitation gauge locations used for development of runoff model	240
9.3	Subcatchments used with runoff model	244-245
9.4	Model discharge for topographic catchments	246
9.5	Mean catchments in the karst of the Flathead and southern High Rock Range, derived from the runoff model	249

9.6	Examples of overflow (Kilmarnock Creek), full flow (Upper Fording River) and underflow (Crowsnest River) regimes in the Front Ranges	252
9.7	Identification of the underflow component of Kilmarnock Creek	253
	a) best fit to Upper Fording River discharge	
	b) computed groundwater and surface components of discharge	
9.8	Discharge of Ptolemy Spring and Parrish Spring in August 1985, showing the greater variation in Parrish Spring	255
9.9	Instantaneous discharge of Ptolemy Creek and Ptolemy Spring during the snowmelt peak in 1986	255
9.10	Discharge of Ptolemy Spring and Crowsnest Spring from September 1985 to September 1986, showing contrasts in exponential recessions	256
9.11	Recession coefficients for first 24 hours after major flow peaks at Ptolemy Spring and Crowsnest Spring	259
9.12	Response of Ptolemy Spring and Crowsnest Spring to precipitation events and temperature changes, January - March 1986	261
9.13	Specific discharge from Ptolemy Spring and Crowsnest Spring during the winter and summer recessions, assuming differences to be due to aquifer boundary conditions	263
9.14	Predicted surface overflow runoff in 1985-1986 from a 41 km ² Crowsnest Spring catchment assuming identical specific discharge to Ptolemy Spring	263
9.15	Calculated catchment area for Crowsnest Spring, assuming identical specific discharge to Ptolemy Spring	265
9.16	Mean monthly discharge for Sublacustrine Springs, Crowsnest Spring and Ptolemy Spring	265
9.17	Catchment areas of Sublacustrine Springs and Crowsnest Spring as a function of season, assuming the same specific discharge as Ptolemy Spring	267
9.18	Cumulative discharge of Ptolemy Spring, Crowsnest Spring, Ptolemy Creek and Sublacustrine Springs over the snowmelt season in 1986 from snowmelt and rainfall, excluding extrapolated baseflow recession from Fall 1985	269
9.19	Relationship between temperature and discharge at Crowsnest Spring. The equation line assumes two flow components: a fixed discharge component ($T=15^{\circ}\text{C}$), and a variable discharge component ($T=3.8^{\circ}\text{C}$)	269

9.20	Relationship between alkalinity and altitude at Crowsnest Pass	272
10.1	Mean daily discharge for Ptolemy Spring and Crowsnest Spring, and calculated discharge for Sublacustrine Springs from May to August 1986, showing karstic response of Sublacustrine Springs	278
10.2	Bimodal dye peaks at Crowsnest Spring from Phillipps Pass injections	280
10.3	Chemograph variation at Ptolemy Spring from September 1985 to September 1986	286
	a) Total hardness	
	b) Bicarbonate and sulphate	
10.4	Chemograph variation at Crowsnest Spring from September 1985 to September 1986	287
	a) Total hardness	
	b) Bicarbonate and sulphate	
10.5	Runoff vectors from the karst of the Flathead and High Rock Ranges	292
11.1	Water levels in Medicine Lake as a function of head above the flow constriction at the lake bottom (at low discharges) and above Maligne Springs (at high discharges)	296
11.2	Plan of Castleguard Cave	298
11.3	Profile of Castleguard Cave, viewed along the strike of the strata . . .	299
11.4	Discharge from Maligne Springs from September 1st 1985 to May 1st 1986, showing the nearly constant minimum discharge between February 1st and May 1st	307
11.5	Location of major thermal springs of the Rocky Mountains	312
11.6	Variation in the proportions of bicarbonate and sulphate in overflow springs (Ptolemy Spring, Parrish Spring), underflow springs (Crowsnest Spring, Sublacustrine Spring), and thermal springs (Banff, Miette, Radium and Fairmont Hot Springs) in the Southern Rocky Mountains	315
12.1	Percentage of bedrock removed by solution as a function of depth for 9 karsts	318
12.2	Model of principal solution zones in karst	323
12.3	Hypsometric curve for the Ptolemy Creek catchment	330
12.4	Geomorphological units of the Ptolemy Creek catchment	326

12.5	Specific dissolution of limestone in the Ptolemy Creek catchment as a function of altitude	327
12.6	Erosional fluxes in the Ptolemy Creek catchment as a function of altitude	327

Tables

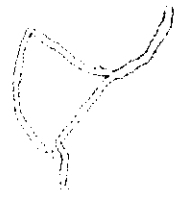
1.1	Discharge and hydrochemistry of the principal eastward-flowing catchments in the Rocky Mountains between Crowsnest Pass and Jasper	4
2.1	Mean composition of limestones at Crowsnest Pass (after Holter, 1976)	18
2.2	Limestone blocks of the Flathead and High Rock Ranges	24
2.3	Lithology and aquifers of the Front Ranges	28
3.1	Hydrological techniques used in karst aquifer studies at Crowsnest Pass	32
3.2	Rating curve coefficients for gauged streams at Crowsnest Pass	40
3.3	Monthly discharges of the springs and creeks at Crowsnest Pass, 1985-1986	42
3.4	Altitude and discharge of the karst springs at Crowsnest Pass	43
3.5	Dye traces at Crowsnest Pass	48
3.6	Hydrochemistry of Crowsnest River at the outlet of Crowsnest Lake ..	56
3.7	Alkaline and non-alkaline hardness of spring and creek waters at Crowsnest Pass	58
3.8	Coefficient of variation for hardness values at Ptolemy Spring and Crowsnest Spring	60
3.9	Aggressiveness of autogenic karst springs and cave streams	62
3.10	$\delta^{18}\text{O}$ results from Ptolemy Spring and Crowsnest Spring	67
4.1	Discharge budget for the White Peak, England (after Edmunds, 1971, and Christopher et al., 1977)	75
4.2	Discharge characteristics for distinguishing flow types	77
4.3	Major karst springs of the Valles - San Luis Potosí Platform, Mexico (data from Fish, 1977)	87
4.4	Variations in anion concentrations in overflow and underflow springs ..	93

4.5	Characteristics of Aliou, Le Baget and Fontestorbes Springs, Ariège, France (after Mangin, 1975, 1984)	94
4.6	Baseflow recession indices for Aliou, Le Baget and Fontestorbes Springs, Ariège in 1970 (data from Mangin, 1975)	96
5.1	Conduit groundwater velocities from multiple tracer tests	107
5.2	Annual variation in discharge (Q_s/Q_n) for karst springs	108
5.3	Recovery period of cave conduits	110
5.4	Hydraulic gradients in well-karstified limestones	113
5.5	Apparent friction factors for some karst conduits	125
6.1	Conduit density and porosity in karst aquifers	132
6.2	Conduit segment lengths	136
6.3	Sinuosity of flow routes in karst	138
6.4	Crest and base depths for active and fossil phreatic loops	144
6.5	Sulphate and bicarbonate concentrations in karst springs	168
7.1	Conduit and catchment characteristics for 16 caves	177
7.2	Notable initial phreatic drops and terminal phreatic lifts	184
7.3	Phreatic flow depth for caves in narrow karst aquifers in Norway . . .	196
8.1	Vertical spacing between cave tiers	202
8.2	Occupancy times of cave tiers based on radiometric and paleomagnetic dating and denudation rates	203
8.3	Loop amplitude and tier spacing	204
8.4	Vadose incision in major low-gradient river caves ($Q_m > 1\text{m}^3\text{s}^{-1}$, $L > 1\text{km}$)	207
8.5	Heat fluxes of thermal springs in the Peak District, England (data from Edmunds, 1971)	228
8.6	Contrasts of temperature and sulphate/bicarbonate ratios of karst springs	230

9.1	Runoff model catchments and results	242
9.2	Areas of karst catchments draining the Flathead and High Rock Ranges	248
9.3	Discharge characteristics of the principal springs at Crowsnest Pass	256
9.4	Karst catchment areas at Crowsnest Pass	274
11.1	Major gauged karst springs of the Rocky Mountains	294
11.2	Winter discharge to some major transverse valleys in the Rocky Mountains	305
11.3	Regional hydraulic gradients from Rocky Mountain valleys east to the Prairies and west to the Rocky Mountain Trench	310
11.4	Heat fluxes of thermal and mineral springs of the Rocky Mountains ..	313
12.1	Total hardness measurements at Waitomo, New Zealand (after Gunn, 1981b)	320
12.2	Erosion processes studied in the Ptolemy catchment	325
12.3	Sediment fluxes in high mountain basins	328

Symbols

- A** Area (cross-section) of aquifer
Area (cross-section) of conduit
Catchment area
- C** Coefficient of variation of hardness (CVH)
Concentration
- d** Passage diameter
- D** Depth of flow below water table
- f** Darcy-Weisbach friction factor
- F** Heat flux
- F** Number of flow paths
- g** Acceleration due to gravity
- h** Height above datum
- H** Total hardness
- K** Constant
Conductivity
Alkalinity
- K** Hydraulic conductivity
- L** Length
- L** Length from upstream limit of a catchment
- n** Number
- p** Wetted perimeter
- q** One component of discharge
- Q** Total discharge
- R** Ratio
- R** Hydraulic radius
- r²** Correlation coefficient from regression
- S** Slope of hydraulic gradient (=dh/dl)
- S** Sinuosity of a flow conduit
- V** Vertical spacing between tiers of conduits
- v** Velocity
- V** Apparent (straight-line) tracer velocity
- W** Width of flow belt



α	Baseflow recession exponent
δ	Difference
Δ	Change
η	Dynamic viscosity
θ	Stratal dip
λ	Angle between strike and joint directions
ρ	Density
Σ	Sum
ϕ	Angle between strike and flow directions
χ	Angle between joint and flow directions
ψ	Passage slope
ω	relative discharge with respect to flow depth

Subscripts

a-f	Coefficients
a	Apparent
b	Base
c	Crest
e	Equilibrium
g	Groundwater
h	Thermal groundwater
i	Input
j	Junction
k	Known
m	Mean
n	Minimum
o	Output
p	Principal, phreatic
r	Tributary
s	Saturation
seg	Segment
t	True
u	Underflow
up	Upstream
v	Vadose
x	Maximum

Glossary

Aggressiveness	The concentration of powdered CaCO ₃ that must be added to a water sample to bring it to equilibrium, measured in mg l ⁻¹ . Positive numbers indicate undersaturation, and negative numbers denote supersaturation.
Boundary zone	The area in a catchment which drains to more than one spring group
Breakthrough time	The time it takes to establish a conduit >5-10mm in diameter, in which turbulent flow will occur
Chemograph	A graph which shows the variation in concentration of a chemical variable with respect to time
Conduit flow	Flow through conduits. It may be laminar or turbulent.
Conduit porosity	The porosity in a karst aquifer which is due to the presence of conduits
Core zone	The area in a catchment which drains to only one spring group
CVB	Coefficient of variation of bicarbonate
CVH	Coefficient of variation of total hardness
CVS	Coefficient of variation of sulphate
Diffuse flow	Laminar flow through pores and fissures
Dynamic equilibrium phase	The mature phase in the life of a karst conduit, when the floor of the conduit is covered with sediments. There is a dynamic equilibrium between discharge and sediment movement, with accumulation at low discharges and removal at high discharges.

Dynamic phreatic	Closed-channel conduit flow that is turbulent at times
Endokarst	The non-surficial zone in karst
Enlargement phase	The period during which there is dynamic phreatic flow in a clean conduit, resulting in rapid enlargement
Epiphreatic Zone	Zone of periodic inundation, caused by an increase in the hydraulic gradient
Epikarst	The near-surface zone in a karst. It comprises the soil zone and the subcutaneous zone.
Equilibrium phase*	See dynamic equilibrium phase
Exsurgence	A karst spring fed largely or exclusively by autogenic water (q.v. resurgence)
Full-flow spring*	(Section 4.2) A spring which fully drains a catchment. Such springs are rare in karst
Initial hydraulic gradient*	The hydraulic gradient in a karst aquifer at the time of initiation of a tier of conduits
Initial phreatic drop*	The upstream limb of a conduit below the water table which descends steeply
Initiation phase	The period when a conduit is less than about 10mm in diameter, when there is only laminar flow
Low potential limit*	The boundary to the area surrounding a developing conduit, within which primary tubes (including anastomoses) may form. See Figure 6.10
Medial phreatic drop/lift*	Descending or ascending conduits below the water table, excluding the initial phreatic drop and the terminal phreatic lift
MEM	Micro-erosion meter

Nothephreatic	Conduit flow which is always laminar
Overflow spring*	A spring partially draining a catchment, which preferentially drains flood flow
Paragenetic conduit	A phreatic conduit with mud-covered walls and low flow velocities (Renault, 1968)
Paragenesis	Protection (by sediments) against downward erosion in a conduit (<Italian parare, to defend against, cf parachute)
Phreatic drop	A conduit below the water table which descends in a downstream direction
Phreatic lift	A conduit below the water table which ascends in a downstream direction
Phreatic loop base*	A low point in a phreatic conduit
Phreatic loop crest	A high point in a phreatic conduit
Resurgence	A karst spring fed largely by sinking allogenic stream(s) (q.v. exsurgence)
SPC	Specific conductivity
Spring group*	A number of springs in geographical proximity, which together drain from the same catchment
Stagnation phase	The period when a conduit is abandoned by streamflow
Siphon	Flooded cave passage
Syngenetic conduit	A phreatic conduit with clean walls and rapid flow velocities (Renault, 1968)
Terminal phreatic lift*	The section of conduit at the downstream end of a phreatic loop which ascends to the water table

Total hardness The sum of Ca and Mg ions, usually expressed as mg l⁻¹ CaCO₃

Underflow spring* A spring partially draining a catchment, which preferentially drains baseflow

Underground delta (French: delta souterrain) It appears the term was first used by E.A. Martel (Renault, 1968)

Underflow-overflow spring* An intermediate spring in a catchment, in which there is at least one underflow and one overflow spring

Victor tube The first phreatic tube to expand to a size so that turbulent flow can be established along a karstic flow route (Ford and Williams, 1989)

Indicates a term which is introduced or given a precise definition in this thesis

Chapter 1

Introduction

1.1 Research objectives

The Rocky Mountains are a major karst area in Canada, and most of the mountains in the Front and Main Ranges from Crowsnest Pass north to Banff and Jasper National Parks are composed of carbonates (Figure 1.1). The eastward flowing rivers from most of this area feed the Saskatchewan River, which is a crucial irrigation source for the prairie provinces of Alberta, Saskatchewan and Manitoba. Consequently, there has been great interest in runoff generation in the Rockies, and this is reflected by an extensive data base of precipitation and streamflow information. This makes the southern Rockies an ideal location for hydrological studies of alpine karst.

Previous karst studies in the Rockies have been of three types. There have been detailed studies on aspects of the hydrology, hydrochemistry and geomorphology of mostly small, high-altitude drainage basins during the short summer season when such areas are easily accessible (e.g. Ford, 1971a; Brown, 1970, Luckman, 1973; Smart, 1983a,b). Second, there was a regional study of the hydrochemistry of the Athabasca and North Saskatchewan Rivers, two of the principal rivers draining the eastern slopes of the Rockies (Drake, 1974). Third, there have ^{been} ~~have~~ several hydrochemical studies of thermal karstic springs (e.g. van Everdingen, 1972).

The local studies characterised the hydrochemistry of the karst aquifers as reflecting the solution of limestone and dolomite (Ford, 1971a). Discharge was dominated by conduit flow, which rapidly transmitted the summer snow- and glacier-melt through the aquifers. This resulted in steep recessions and low storage. Karst

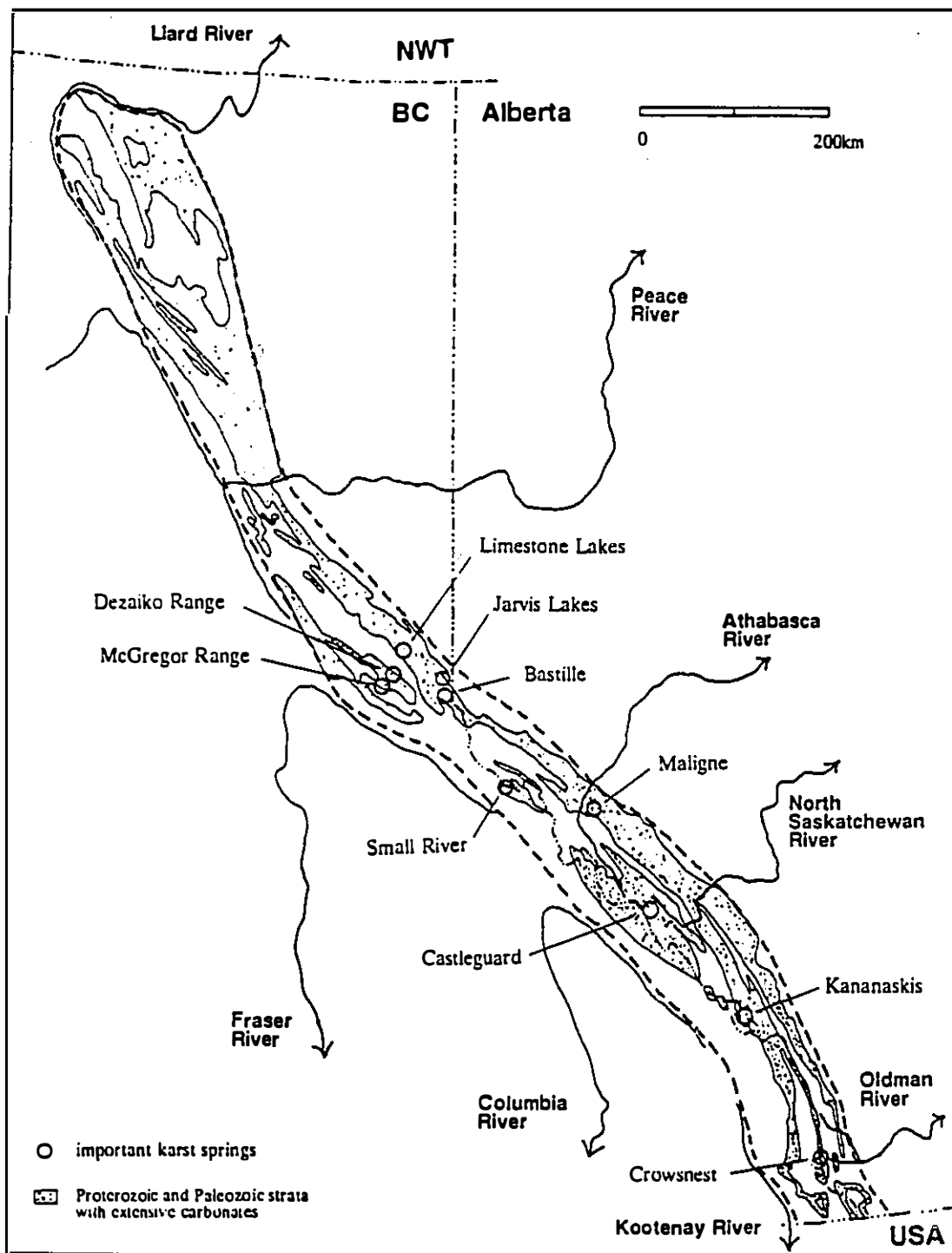


Figure 1.1 Carbonate outcrops and important karst springs of the Rocky Mountains

discharge in winter was very low, with some of the major springs having negligible or zero discharge (Smart and Ford, 1986).

By contrast, on a regional scale, Drake (1974) showed that, though limestone and dolomite are important sources for solutes, nevertheless gypsum represents 36% of the rock removed by solution. Furthermore, there is considerable storage in the whole drainage system, so that winter discharge is maintained at about 10% of the mean summer level. Drake (1974) subdivided discharge on hydrochemical grounds into a constant discharge "groundwater" component and a variable "surface water" component (Table 1.1); the constant discharge component is about $1.5 \text{ l s}^{-1} \text{ km}^{-2}$.

A further little understood aspect of karst groundwater flow in the Rocky Mountains is the role played by thermal springs such as Banff Hot Springs. Previous studies of the thermal karstic springs in the Rocky Mountains have concentrated on the hydrochemistry of the springs. It has been thought that recharge to the springs is of local origin, from within a few kilometres (van Everdingen, 1972). There has been no attempt to compare the flow fields of thermal karstic springs to those of non-thermal karstic springs.

From these studies it was not clear whether the contribution from karst to the winter baseflow was negligible, or substantial. If it were the former case, then Rocky Mountains karst aquifers could be characterised solely by conduit flow, with the water table being of little or no significance; if it were the latter case then there would be substantial diffuse flow through pores and fissures in the limestone, and the water table would be a relevant and important component of karst groundwater flow in the Rockies. Furthermore, thermal karstic springs have not been integrated into general concepts on karst groundwater flow in the Rockies.

Drake (1974) identified three unresolved problems at the conclusion of his study on hydrology and karst solution in the southern Canadian Rockies: the source of the discharge which sustains winter flow, the source of the sulphate present in the rivers, and the nature of solutional activity in the winter months.

Table 1.1 Discharge and hydrochemistry of the principal eastward-flowing catchments in the Rocky Mountains between Crowsnest Pass and Jasper

river	area km ²	HCO ₃ ⁻ mg l ⁻¹	SO ₄ ²⁻ mg l ⁻¹	Ca ²⁺ mg l ⁻¹	Mg ²⁺ mg l ⁻¹	Specific Q l s ⁻¹ km ⁻²	January -March	June -August
Crowsnest River (1)	#104	151	41	50	11	#5.8	#29	
Oldman River	1440	168	34	47	12	2.6	19	
Highwood River	774	162	33	50	11	2.2	28	
Kananaskis River	899	153	27	45	10	3.8	39	
Spray River (2)	749	155	60	52	14	5.2	41	
Bow River	2210	123	32	35	11	3.6	48	
Red Deer River	2250	154	50	46	14	2.2	24	
Clearwater River	2230	188	64	58	19	2.6	19	
N. Saskatchewan R.(3,4)	1290	104	35	31	10	2.7	73	
Athabasca River (3)	3250	84	19	26	6	3.0	58	
Miette River (3)	630	75	29	23	8	1.1	44	
Maligne River (3)	908	103	31	33	8	2.5	42	
N. Saskatchewan River at Rocky Mountain House (Drake, 1974) (4)	11000	150	60	50	15	2.3	25	
"surface water"		116	24	34	9			
"groundwater"		162	94	58	19			
Athabasca River at Hinton (Drake, 1974)	9780	133	62	46	13	3.5	42	
"surface"		91	22	28	7			
"groundwater"		156	101	63	17			

notes:

The discharge data is for 1986 (Inland Waters Directorate, 1987a); the hydrochemical data are based on up to 100 samples per river collected over several years (Inland Waters Directorate, 1975)

- (1) at the point where it leaves Crowsnest Lake
- (2) The flow is regulated at present; the discharge data is pre-regulation averages
- (3) part of North Saskatchewan or Athabasca catchments studied by Drake (1974)
- (4) Not gauged since 1970; 1967-1970 means used.

Based on the topographic catchment; the actual catchment is discussed in Chapter 3

The field research, upon which this thesis is based, was undertaken to gain a better understanding of karst groundwater hydrological and hydrochemical processes in the Rocky Mountains during all seasons to answer the problems posed by Drake (1974), and to investigate the role of conduit flow and of diffuse flow in karst aquifers in a mountain environment.

1.2 Choice of study area

The most intensive previous studies of karst groundwater flow in the Rockies have utilised stage recorders at springs during the recession from the annual snowmelt peak for periods up to two months, and have related this to hydrochemistry (Ford, 1971), or to tracer travel through the karst aquifer (Smart, 1983a,b). Also, there have been tracer studies during both high- and low-discharge periods at Maligne (Brown, 1970; Kruse, 1980; Smart, 1988). These studies have focused on three areas, Maligne, Castleguard and Crowsnest Pass, which have the biggest springs and the longest caves in Canada (Figure 1.1).

Maligne has the greatest sinking river in Canada, and one of the largest in the world. It has a catchment of 762km²; this is considerably larger than the second biggest sinking river in the Rockies, which is probably the uninvestigated 30km² Limestone Lakes catchment (Figure 1.1). More than 95% of Rockies karst drainage is autogenic, so the allogenic Maligne is not representative of Rockies karstic catchments. Studies at Maligne have characterised the calcium bicarbonate hydrochemistry (Ford, 1971), and used tracers to elucidate the nature of the principal conduit(s) connecting the sink at Medicine Lake with the risings 16km away (Brown, 1970; Kruse, 1980; Smart, 1988). It has been shown by Kruse (1980) that the Maligne karst partly drains to aggraded springs in the floodplain of the Athabasca River. While aggraded springs are characteristic of karstic catchments in the Rockies, measurement of their discharge or hydrochemistry is difficult. In this case, the high discharge of the Athabasca River precludes the possibility of accurately quantifying

the total discharge of all the aggraded springs at Maligne, though a gauge on the Maligne River close to its mouth probably records most of the discharge; the gauge has recorded a winter minimum of $1.94 \pm 0.19 \text{ m}^3\text{s}^{-1}$ ($2.1 \pm 0.21 \text{ s}^{-1}\text{km}^{-2}$) over the period 1973-1988.

Castleguard has the second largest springs in the Rockies (mean discharge (Q_m) = c. $4.6 \text{ m}^3\text{s}^{-1}$) after Maligne (Q_m = $15.2 \text{ m}^3\text{s}^{-1}$), and the longest cave in Canada (Castleguard Cave, length = 20km). It is a mixed autogenic and glacierised karst, with summer glacier melt providing daily runoff pulses (Smart, 1983a). The remote location (20km from the nearest driveable road), deep winter snow, and liability of the cave to flood in summer have ensured that surface hydrological studies have taken place only in summer (Ford, 1971a; Smart, 1983a,b), while all cave studies since 1967 have taken place only in winter (Thompson, 1976; Ford, 1983b; Yonge, 1983, 1984, 1985; Sawatsky, 1987, Thomson, 1988).

Smart (1983a) recognised more than 70 springs along a 4km stretch of the Castleguard River, with the upstream springs issuing from bedrock, while the downstream springs are aggraded. The upstream springs are dry in late winter (April), but Artesian Spring, 4km downstream of the uppermost springs, is perennial, though it has not been gauged in winter (Smart, 1983b). The uppermost perennial gauge on the North Saskatchewan River used to be located 40km further downstream at Saskatchewan River Crossing, which is 250m lower than Artesian Spring at Castleguard. The minimum discharge there over the four winters gauged was $1.70 \text{ m}^3\text{s}^{-1}$, or $1.32 \text{ l s}^{-1}\text{km}^{-2}$ over the 1290 km^2 catchment. The snow cover over Castleguard River in winter and its difficult access would make it extremely arduous to monitor discharge in the winter months.

In recent years, important springs have been found in other karst areas in the Rockies, including Kananaskis (Gadd, 1986), the Mount Robson area (Worthington 1984; Yonge and Worthington, 1985), Bastille Mountain (Miller, 1989; Buchanan, 1989), Jarvis Lakes (McKenzie, 1987a), the McGregor Mountains (Nash,

1983; McKenzie, 1984), and Dezaiko Range (Pollack, 1984a,b, 1986, 1988; McKenzie and Pollack, 1986, Koppe, 1988). All of these springs are remote from highways, and most probably have difficult-to-gauge underflow components.

Recent karst hydrological research close to Small River, in the Mount Robson area, has focused on flow from a glacier (Abobe Glacier) to two high-level karst springs (Stump Cave Spring and Middle Rising) (Smart and Huntley, 1988; Huntley and Smart, 1989; Huntley, 1990). These two springs are perched 600m above the Small River valley, and are probably perennial (Yonge, 1990); in the valley two springs presumably discharge the strike-oriented underflow from the karst aquifer (Yonge and Worthington, 1985). However, dye traces have yet to reveal the catchments for these springs, which demonstrate underflow characteristics (Huntley, 1990).

While conduit flow has been studied in summer in several of the above karst aquifers, none is suitable for studying both conduit and diffuse components of karst groundwater flow over the whole year.

The remaining area where karstic springs have been identified is Crowsnest Pass. The Pass is a 500 metre wide breach in the carbonate Front Ranges. It is the lowest point in the Front Ranges between the southern termination of the carbonate outcrop at North Kootenay Pass, 30km to the south, and Banff, which lies 160km to the north, and which is at the same altitude as Crowsnest Pass. The Pass could therefore be expected to be the discharge point for diffuse flow from a large area of karst. The meandering, low-gradient (<0.002) Crowsnest River is easily monitored at the point where it leaves the limestone. The catchment has only a minor non-karst component, so the total outflow from the karstic component can be accurately measured.

Crowsnest Pass has a number of karst springs. Crowsnest Spring is the most prominent both visually and in terms of discharge; discharge and calcium

bicarbonate hydrochemistry were monitored in July 1968 and July 1969, with total hardness increasing from 120 to 190 mg l⁻¹ as discharge dropped from 1.9 to 1.2 m³s⁻¹ (Ford, 1971a). At the same time, two samples from Ptolemy Spring had total hardnesses of 68 and 74 mg l⁻¹; the much lower hardnesses were thought to be due to a high-altitude catchment (Ford, 1971a). Some discharge and hydrochemical measurements were made of the aggraded Emerald Spring (Ford, 1971a), and Cogley (1970) suggested that there were other aggraded springs which contributed a substantial amount to runoff. Minor springs included several overflow springs above Emerald Lake and high altitude springs such as two in the east cirque of Ptolemy Creek (Ford, 1971a).

The greatest concentration of known caves in any one area in Canada is found at Crowsnest Pass, where there are 17 caves with more than 100m of passage, including Yorkshire System, the second longest cave in Canada, with 11km of mapped passages (Thompson, 1976; Barton, 1981a,b; Yonge, 1983a; Meinke, 1986; McKenzie, 1987b, 1989a,b; Rollins, 1988; Forbes, 1988). While none of these caves give access to the principal underground flow routes, nevertheless they contain several streams, which are useful as dye injection points and for understanding the hydrology of the upper 500m of the karst aquifer.

Crowsnest Pass thus contains a contrasting suite of springs, representative of most spring types in the Rockies, with the exception of glacierised karst (Smart, 1983a). The major springs (Crowsnest Spring, Ptolemy Spring, Sublacustrine Springs) are within thirty minutes walk of tracks which can be driven at all seasons, and are close to a paved highway, which eases logistics. Moreover, the area is not in a national park, so there are no bureaucratic difficulties involved in setting up instruments, and no restrictions on off-road driving or camping. Furthermore, bear hunting is popular in the area, so that the bears one inevitably meets are retiring animals. However, this did not prevent one inquisitive bear from demolishing a Stevenson Screen.

A further advantage of Crowsnest Pass is that the discharge characteristics and hydrochemistry of Crowsnest River, at the point where it leaves the karst area, are close to the average of a broad range of larger catchments in the Rockies (Table 1.1), so that interpretations made at Crowsnest Pass are applicable at a regional scale in the Rockies.

1.3 Organisation of the thesis

The physical characteristics of Crowsnest Pass will be presented in Chapter 2, and the data collected during field work there will be summarised in Chapter 3. This chapter ends with an explanation of how the data collected at Crowsnest Spring and Ptolemy Spring is inconsistent with previous models of karst hydrogeology.

A critical review of karst hydrogeology is presented in Chapters 4 through 8. The causes of variation in spring chemographs and hydrographs are investigated in Chapter 4. Chapter 5 will present a review of the hydraulics of flow in karst aquifers, and will show why hydraulic parameters at Crowsnest are comparable to other karst aquifers. Chapters 6, 7 and 8 evaluate how karst flow systems are assembled.

In order to assess the importance of different flow modes and to estimate the hydraulic gradients at Crowsnest Pass, it is desirable to estimate catchment areas, and this will be done in Chapter 9. The findings from Chapters 4 through 9 are used in Chapter 10 to rationally explain the differences between Ptolemy Spring and Crowsnest Spring. Karstic groundwater flow throughout the Rocky Mountains can then be explained in Chapter 11. Chapter 12 addresses the question of where solution is taking place at Crowsnest Pass, and compares solute with other fluxes. Finally, Chapter 13 presents an assessment of the paradigm shift represented by the preceding chapters.

1.4 The problem of sampling bias

Our present understanding of karst hydrology is largely derived from case studies. Studies of runoff from karst are biased towards visible springs, to the neglect of both surface runoff and aggraded springs, which may feed directly into the bed of surface rivers. Studies of caves are heavily biased towards areas where there are easily accessible, non-flooded caves. Known caves rarely represent more than a small fraction of the active flow routes in an aquifer. Active flow routes are largely unexplored because they are mostly flooded.

The present study tries to mitigate this bias in three ways. First, the hydrological study of Crowsnest Pass has attempted to quantify all the discharge from the karst outcrop, of which only a minority is to visible springs (Chapters 2, 3, and 10).

Second, the critical review of karst hydrology in Chapters 4 through 8 minimises sampling bias by being comprehensive. Where feasible, an attempt has been made to assemble all available published data (e.g. Tables 3.9, 4.4, 5.1, 5.2, 5.3, 5.4, 5.5, 6.3, 6.4, 7.1; Figures 4.4, 5.1, 5.2, 5.3, 6.7, ~~8.2, 8.5~~). Where such a data set would be unmanageably large, then restrictive criteria have been applied to select high-quality data from representative samples (e.g. Tables 7.2, 7.3, 8.1, 8.3, 8.4; Figures 4.2, 4.3, 4.5, 5.6, 6.1, 6.4, 6.5, 7.5, 7.6, 7.8, 8.2, 8.3, 8.5; Sections 4.3 - 4.7). This review also necessitated the introduction of several new terms to describe the configuration of karst conduits.

Third, the catchment delineation is predicated on the concept that the hydraulics of groundwater flow in adjacent karst catchments is similar. Care has been taken to ensure that the discharge budgets are balanced not only in the catchments for the Crowsnest springs, but also in the neighbouring catchments in the Flathead and High Rock Ranges.

Many hypotheses concerning karst groundwater flow have hitherto only been supported by deductive reasoning. A second thrust of the methodology in this

thesis is to use hypothesis testing to assess both published concepts and the new concepts introduced here.

PAGINATION ERROR.

ERREUR DE PAGINATION.

TEXT COMPLETE.

LE TEXTE EST COMPLET.

NATIONAL LIBRARY OF CANADA.

CANADIAN THESES SERVICE.

BIBLIOTHEQUE NATIONALE DU CANADA.

SERVICE DES THESEES CANADIENNES.

Chapter 2

The study area: Crowsnest Pass

2.1 Geology

2.1.1 Stratigraphy and mineralogy

The following stratigraphic descriptions are based upon Geological Survey of Canada publications covering the Flathead Range (deWit and McLaren, 1950, Price 1961, 1965) and the High Rock Range (Norris 1958, Douglas, 1958, Price, 1965), supplemented by field observations. The generalised stratigraphy, structural relationships and carbonate outcrop are shown in Figures 2.1, 2.2 and 2.3.

The oldest strata in the study area belong to the Devonian Alexo Formation. These are principally thin-bedded or laminated silty dolomites, with local intercalations of solution breccia. At Crowsnest Pass, the formation is 82m thick, but it thins to 30m or less in the Flathead Range. It forms a recessive zone beneath the Palliser limestones.

The Palliser Formation (Devonian) consists of limestones, which are often slightly dolomitised and slightly argillaceous. The lower part has poorly defined beds 0.3-2m in thickness, while the upper part has well defined beds less than 0.3m in thickness. The basal Palliser locally contains lenses of dolomite solution breccia (Price, 1965). The Palliser is the major cliff-forming unit in the Flathead and High Rock Ranges, being characterised by unbroken cliffs 150-200m in height.

The Exshaw Shale (Mississippian) is a black, non-calcareous shale with minor limestones and siltstones, some 12-13m in thickness. It forms a distinctive recessive zone above the Palliser cliffs.

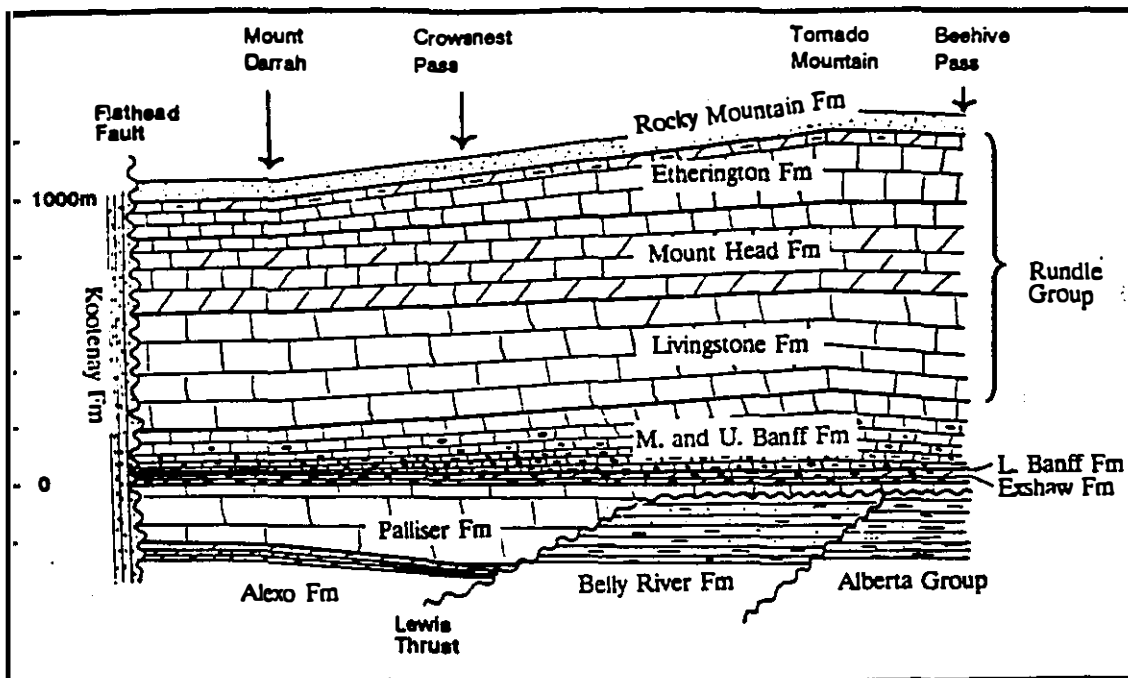


Figure 2.1 Structural and lithological relationships of the carbonate Palliser and Banff-Rundle aquifers of the Flathead and High Rock Ranges

The lower part of the Banff Formation (Mississippian) consists of black shale, which is calcareous in part, interbedded with cherty limestone, cherty siltstone and banded chert. It thickens somewhat to the north, from 33m in the southern Flathead Range to 46m at Beehive Pass, where black calcareous shales, siltstones and mudstones predominate. The limestones of the Middle and Upper Banff gradually become less argillaceous and less siliceous, with thicker beds. Consequently, while the Lower Banff forms a recessive zone with the Exshaw Shale, the Upper Banff is fairly prominent.

Above the Banff are about 800m to 1000m of limestones of the Rundle Group (Mississippian). The Rundle, together with the Palliser, forms the resistant heights of the Flathead and High Rock Ranges. This is subdivided into the Livingstone,

Mount Head and Etherington Formations. The Livingstone consists of thickly bedded or massive limestones, with occasional cherty limestones and dolomites, and forms prominent ribbed cliffs. The Mount Head consists of medium-bedded limestones, with dolomites being fairly common. The Etherington Formation has predominantly thin-bedded limestones, with occasional dolomites and thin shales and sandstones up to 0.5m thick. Below the Lewis Thrust, well logs show that anhydrite is fairly common in the Upper Livingstone and the Mount Head Formation (Douglas, 1958). The high solubility of anhydrite ensures that it has not been identified in surface outcrops, but solution breccias have been noted in these members in the Blairmore Range (15km east of the Flathead and High Rock Ranges, and below the Lewis Thrust). Above the Lewis Thrust, anhydrite has not been reported in outcrops, but there is a 14m thick breccia in the Upper Livingstone, which may be a solution breccia.

The Rundle Group is overlain by the Rocky Mountain Formation (Pennsylvanian-Permian), which consists of 200 to 300m of quartzitic and dolomitic fine-grained quartz sandstones. The Alberta Group and Belly River Formation (Cretaceous) consist of shales, sandstones and minor limestones. The Kootenay Formation (Jurassic) consists of carbonaceous sandstones and shales, interbedded with coals. The coals are no longer mined on the Alberta side of the border, but are currently being mined in open-cast operations in B.C.; the closest pit is 15km northwest of Crowsnest Pass.

Chemical analyses have been made on samples taken from limestone quarry exposures, with purities up to 99% CaCO_3 , and 99.5% $\text{CaCO}_3 + \text{MgCO}_3$ (Holter, 1976). A summary is presented in Table 2.1.

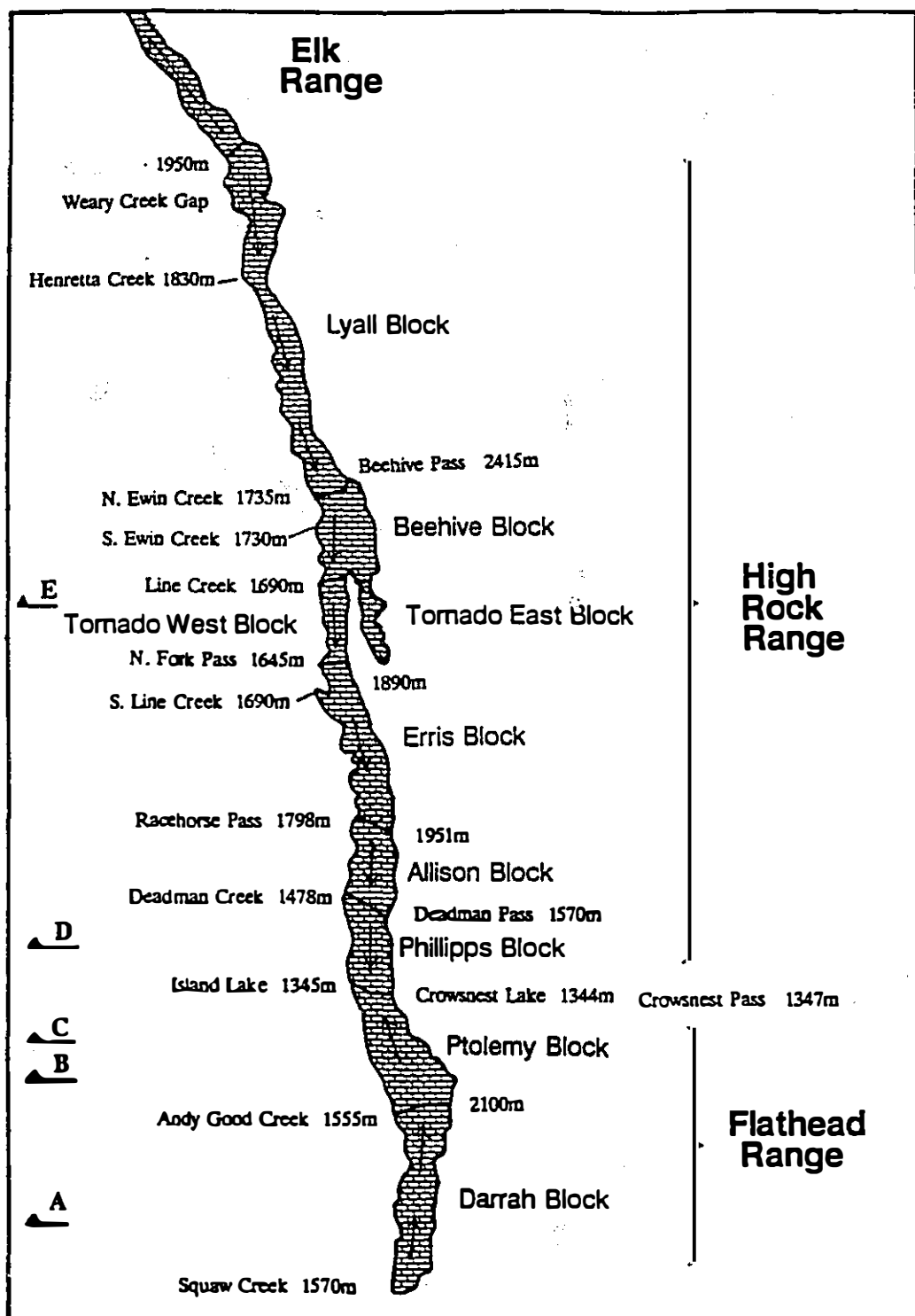


Figure 2.2 Carbonate outcrops and topographic blocks of the Flathead and High Rock Ranges.

Groundwater flow directions are shown, assuming a planar piezometric surface with a gradient of ≤ 0.005 . Geological sections A through E are shown in Figure 2.3.

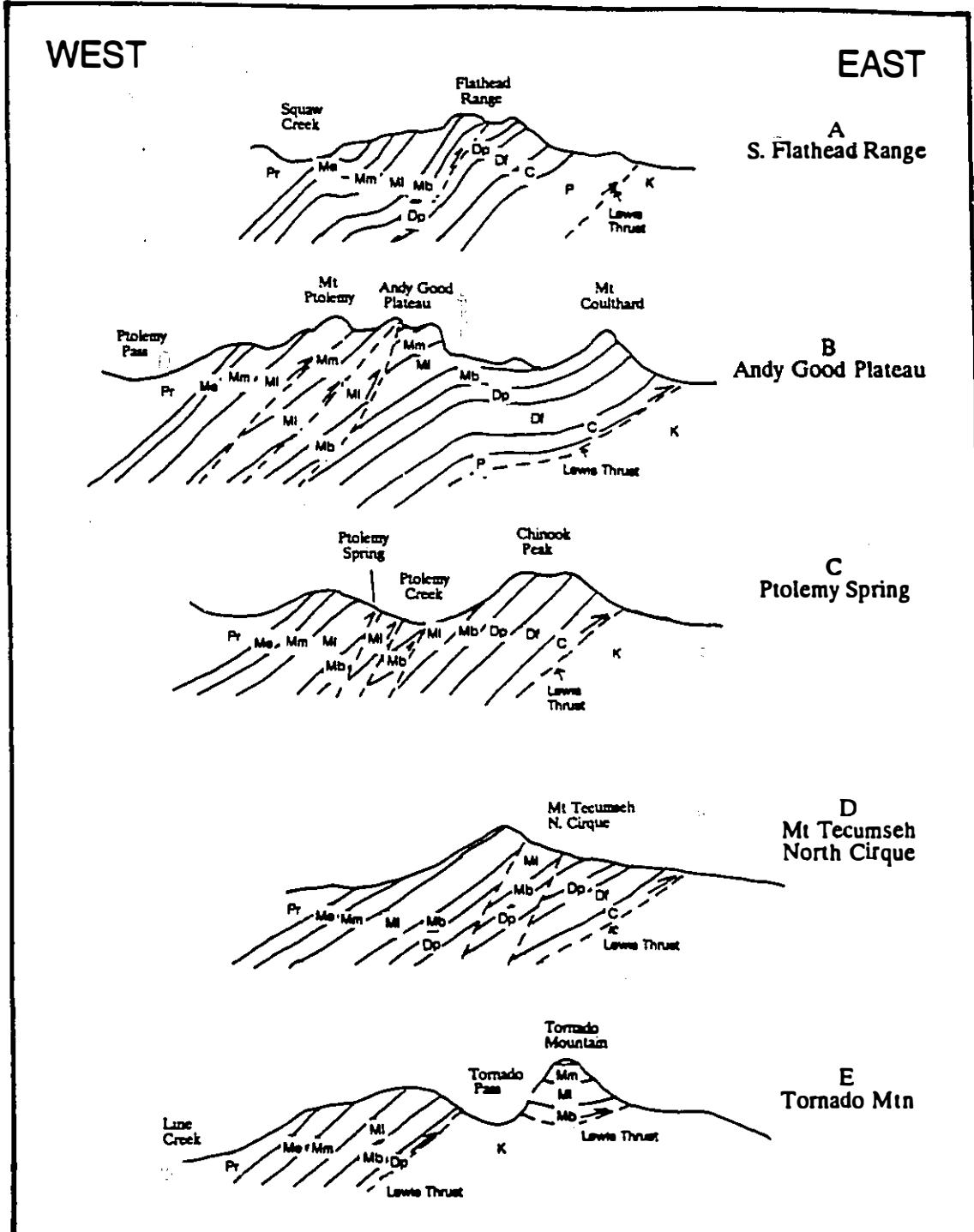


Figure 2.3 Geological sections across the Flathead and High Rock Ranges (after Price, 1961, 1965)

K= Belly River Fm; Pr= Rocky Mountain Fm; Mr= Rundle Group; Me= Etherington Fm; Mm= Mt Head Fm; Ml= Livingstone Fm; Mb= Banff and Exshaw Fms; Dp= Palliser Fm; Df= Fairholme and Alexo Fms; C= Cambrian Fms; P= Purcell Fms.

Table 2.1 Mean composition of limestones at Crowsnest Pass (after Holter, 1976)

Formation	n	CaCO ₃	MgCO ₃	SiO ₂	Fe ₂ O ₃ +Al ₂ O ₃ + insolubles
		%	%	%	%
Palliser	12	93.5	4.9	1.0	0.6
Banff	10	47.8	9.8	38.6	3.8
Livingstone	63	86.0	10.9	2.2	0.9
Mt Head	39	91.1	6.3	2.1	0.5

2.i.2 Structure

The Rocky Mountains were created during the accretion of the Intermontane Terrane to the North American Plate during the Middle Jurassic (Gadd, 1986). Compression during this Columbian Orogeny and the later Laramide Orogeny resulted in the piling up of a series of westward-dipping thrust sheets. This has resulted in the repetition several times in an east-west direction of the carbonate-dominated Paleozoic sequence.

The Front Ranges at Crowsnest Pass are part of the Lewis Thrust sheet, which currently has a maximum stratigraphic thickness of about 6000m, while the maximum stratigraphic separation across the thrust is 8000m (Price, 1962). The thrust sheet in general forms a westward-dipping homoclinal succession, though several westward-dipping thrusts repeat part of the succession in the Flathead Range and High Rock Range as far north as Deadman Pass (Figure 2.3 a,c,d). The Front Range has an average width of 3-4km of carbonates, but between Tornado Pass and Beehive Pass and at the Andy Good Plateau folding widens the outcrop of resistant limestones to more than 6km (Figures 2.3 b,e; 2.4).

The Lewis Thrust rises stratigraphically from a position in the Precambrian to the south of the Flathead Range to the upper part of the Palliser Formation in the High Rock Range west of the Allison Anticline. East of the Allison Anticline, the

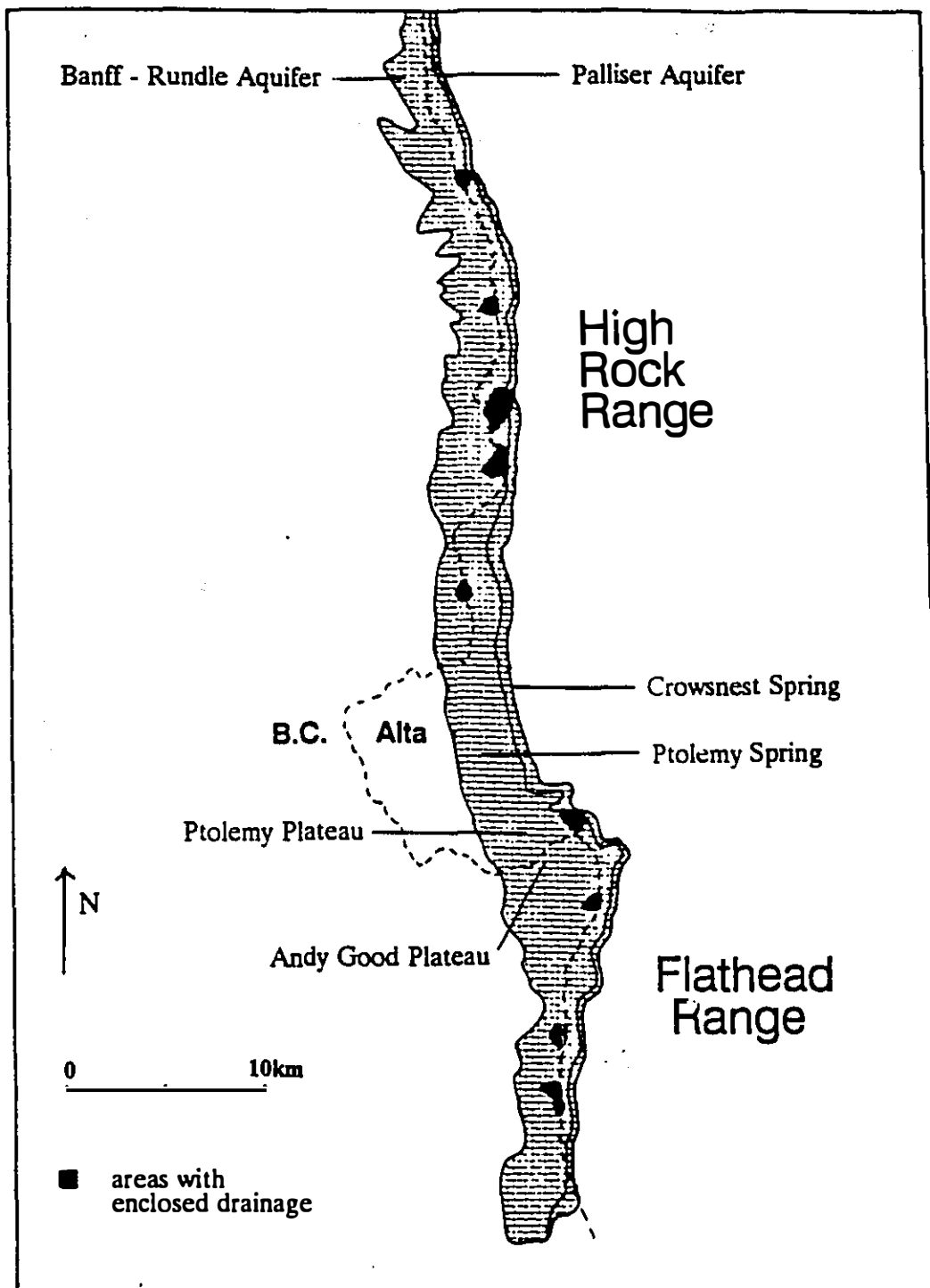


Figure 2.4 Outcrops of the Palliser and Banff-Rundle aquifers in the Flathead and southern High Rock Ranges, with areas of enclosed drainage

Lewis Thrust rises into the Banff Formation in the southern part of the Gould Dome salient (Figure 2.3e, 2.4).

In a southerly direction the Flathead Range is terminated by the Flathead Fault, a normal fault with a structural separation of 8000m. In a northerly direction the High Rock Range is structurally and topographically continuous with the Elk Range, which ends 110km north of Crowsnest Pass at Pocaterra Creek in Kananaskis Country.

2.2 Topography and drainage

2.2.1 Surface flow and inputs to the karst aquifers

Crowsnest Pass lies at an altitude of 1350m, and is occupied by three lakes, Island Lake, Emerald Lake and Crowsnest Lake. Immediately to the north and south of the Pass are the high peaks of the High Rock and Flathead Ranges, respectively, with summits ranging from 2500m up to 3100m. The crest of the Flathead and High Rock Ranges forms the topographic continental divide between the westward-flowing Elk River (draining to the Pacific via the Kootenay and Columbia rivers) and the eastward-flowing Oldman River (draining to Hudson's Bay via the South Saskatchewan, Saskatchewan and Nelson rivers).

The surface fluvial network of the Flathead and High Rock Ranges is almost intact, with the fluvial net draining 97% of the area (Figure 2.4). In this area there are just ten small areas with enclosed topographic drainage basins (discernible from 1:50,000 topographic maps). All ten areas are high-mountain cirques with floors at 2000-2200m, with enclosed basins of 0.4 km^2 to 1.5 km^2 , and eight have lakes. Some of the lakes are bedrock depressions, but others are till-dammed. In all cases there are plausible short high-gradient eastward or westward flow paths. Thus there is little evidence at the 1:50,000 map scale to suggest extensive karst aquifer development.

Despite this, however, there are powerful springs at Crowsnest Pass, and most of the drainage courses on the limestone are dry for almost all of the year. Thus

the principal drainage vectors in the Flathead and High Rock Ranges are in fact via karstic groundwater flow. Because Crowsnest Pass is the lowest pass in the Front Range between the U.S. border 70km to the south, and the Bow River 160km to the north at Banff, it has the potential to drain all of the limestone outcrop of the Flathead, High Rock and Elk Ranges, an area of 400km². That it does not drain all the discharge from this area is demonstrated by the presence of some surface flow on the limestone, by springs at other passes and by simple mass balance calculations, which suggest the 2m³s⁻¹ spring discharge at Crowsnest Pass drains about 150km² (see Chapter 9).

There is a strongly seasonal climatic regime in the Front Ranges, which results in high runoff from snowmelt in spring and early summer. All creeks flowing across the limestone lose some flow to percolation into the limestone, and when the infiltration capacity is exceeded there is surface flow. A few creeks have flow all summer long, and these are of two types. The most common are short, low-discharge streams above the tree line, fed by perennial snow patches; they usually gradually lose their flow to infiltration, and end within a few tens or hundreds of metres. The second type are spring-fed creeks, which are usually dry in the upper part of their courses, upstream of the springs.

The integrity of all stream courses on the limestone is maintained by the annual snowmelt discharge peak, which exceeds infiltration capacity for about two-thirds of the stream courses. The courses of the remaining third are sustained by lower-frequency, higher-magnitude snowmelt peaks. The time since the last flood could be identified in many creeks in the study area by the growth of vegetation in the creek bed, e.g. small bushes (a few years), trees (10-100 years), complete vegetation cover with well-developed soil profile (hundreds or thousands of years).

Present and former inputs to the karst aquifer can be examined in detail at many locations, where caves are accessible. Most of these are found 8km south of Crowsnest Pass, on the Ptolemy Plateau (2000m-2200m a.s.l.) on the Alberta side of

the border, and on the Andy Good Plateau (2300-2500m a.s.l.), which is adjacent to it, but in B.C. More than 20km of cave passages are shown in Figure 2.5. Within these caves are some twenty streams which are active in the snowmelt season, together with a large number of formerly active stream courses. Though the principal modern drainage routes feeding Ptolemy Spring have not yet been entered, several kilometres of abandoned trunk conduits have been entered; these were active when the piezometric surface was at least 600m higher than at present.

To ease identification of the different karst areas of the Flathead and High Rock Ranges, the karst was subdivided into a series of topographic blocks, which in general were named after the highest mountain in each block (Table 2.2, Figures 2.2, 2.6).

2.2.2 Springs

There are several major springs at Crowsnest Pass. On the north side of Crowsnest Lake lies Crowsnest Spring. There are two orifices to the spring; the lower one is one metre above Crowsnest Lake, is perennial, and has a maximum discharge of about 400 ls^{-1} ; the upper, overflow orifice is a few metres away, and four metres higher, and discharges the bulk of the flow in the summertime. The spring is at the base of the Palliser Limestone. The discharge and hydrochemistry of the spring was monitored during the summer of 1968 and 1969, and a dye test from the north cirque of Mt Phillipps showed that the catchment includes both Banff and Rundle strata (Ford, 1971a). A scuba diver has penetrated the spring to a depth of 40m below the water surface, at which point the cave continues vertically downward to a depth of at least -50m; it is mostly a single elliptical conduit, three to five metres in height and width (Barton, 1981).

On the opposite side of Crowsnest Lake to Crowsnest Spring lies Emerald Lake, a subsidiary lake at least 27m deep. At low stages of Crowsnest Lake, a creek flows from Emerald Lake into it, but at high stages the creek is submerged. The

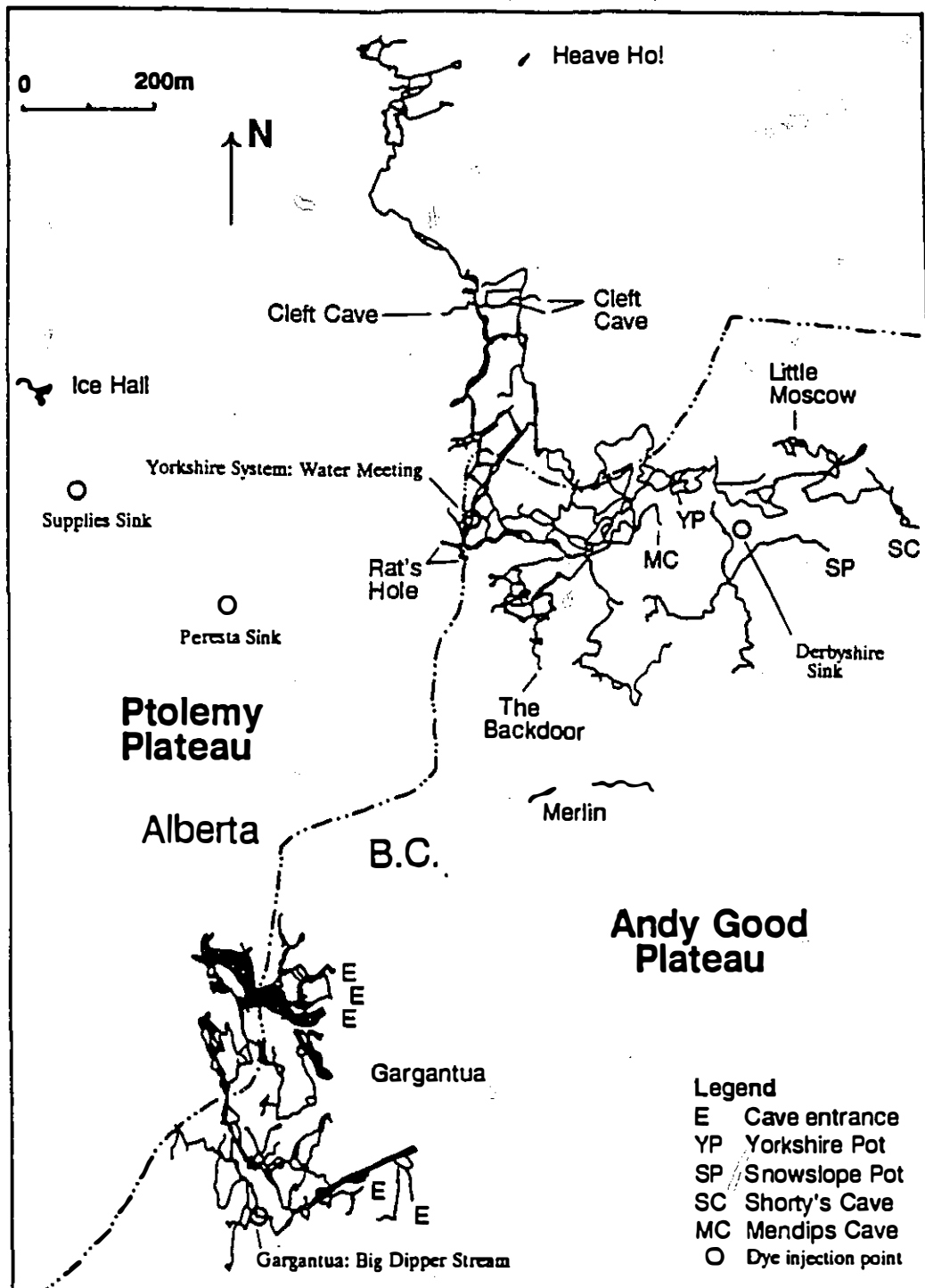


Figure 2.5 Caves of the Ptolemy and Andy Good plateaux, with dye injection points

Table 2.2 Limestone blocks of the Flathead and High Rock Ranges

block	area km ²	mean altitude	topographic division
Darrah	58.0	2104	North Kootenay Pass
Ptolemy	52.6	1962	Andy Good Creek
Phillipps	36.1	1811	Crowsnest Pass
Allison	42.6	2016	Deadman Pass
Erris	51.1	2205	Racehorse Pass
Tornado West	16.5	2215	North Fork Pass
Tornado East	13.0	2442	Tornado Pass
Beehive	36.7	2325	Tornado Pass
Lyall	100	2350	Beehive Pass
			Weary Creek Gap

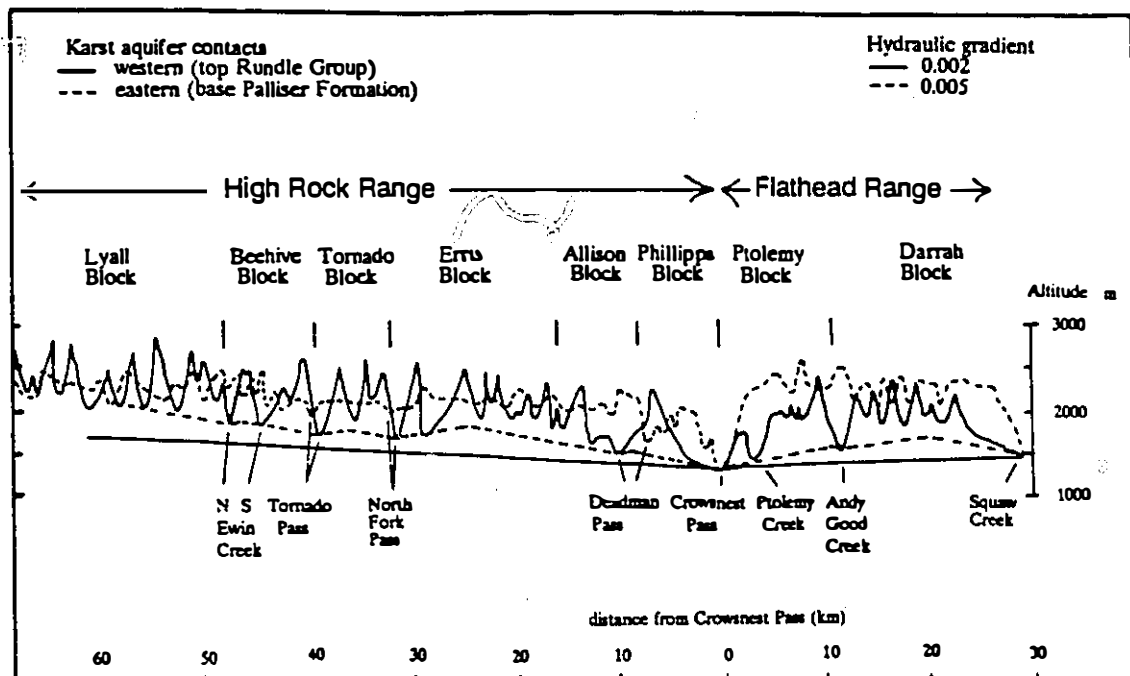


Figure 2.6 Topographical subdivisions of the Flathead and High Rock Ranges, with altitude of limestone contacts and hypothetical groundwater gradients

water from Emerald Lake presumably debouches from one or more basal Palliser springs at the bottom of the lake.

There are six springs which emerge from the Palliser Formation up to 44m above lake level on the south side of Crowsnest Pass. In 1986, the principal spring, Emerald Cliff Spring, flowed for 22 days with a maximum discharge of about 20 l s^{-1} , while the other springs flowed for 6 to 45 days, with the springs drying up in order of diminishing elevation. The maximum aggregate discharge of these springs was about 50 l s^{-1} .

Ranch Spring is the sole spring in the Banff Formation at Crowsnest Pass, and is on the north side of Crowsnest Lake, about 20m above lake level. In 1986, this flowed from March to July 10th, with a maximum flow of about 10 l s^{-1} .

There are no known springs in the Rundle Formation at Crowsnest Pass itself, but Ptolemy Spring is situated 4km south of Crowsnest Pass, at an altitude of 1550m. Its location is probably on a thrust in the Livingstone Formation (Figure 2.3c), for which a movement of 2km has been postulated at a point close to the spring (Price, 1962). The spring is obscured by a blockage of large boulders, which is readily replenished by the steep slopes above. This spring was also studied by Ford (1971a), who concluded from the low dissolved solids that the water has a high-altitude source.

The creek from Ptolemy Spring steeply descends the valley side to join Ptolemy Creek. Ptolemy Creek is fed by many springs, though only two are noticeable. These are both in the north fork of the Ptolemy valley at 2025m. The larger (northern) spring (Parrish Spring) lies at the foot of a small cliff in the uppermost part of the Banff Formation, while the smaller spring emerges at the bottom of a small lake in the Livingstone Formation.

Ptolemy Creek joins Crowsnest Creek, which mostly drains impermeable Mesozoic strata. The alluvial fan where Crowsnest Creek empties into Crowsnest Pass is highly permeable, so that Crowsnest Creek gradually sinks into its bed, losing up to 300 l s^{-1} , and failing to reach Crowsnest Lake for several months in winter. Island Creek also drains impermeable Mesozoic strata; it empties into Island Lake, and thence crosses the aforementioned alluvial fan (in summer) to enter Crowsnest Lake. During the winter, the creek sinks completely into the alluvium, and the level of Island Creek drops by about 2m, to approximately the same level as Crowsnest Lake.

The outflow of Crowsnest Lake is known as Crowsnest River, and discharges considerably more than the sum of the surface creeks that feed it. The difference in 1985-86 was 890 l s^{-1} , of which about 150 l s^{-1} is accounted for by the

spring(s) emanating from the bottom of Emerald Lake. The remainder must be from springs at the bottom of Crowsnest Lake (from the Palliser, Banff, or Livingstone Formations) and Island Lake (from the Mount Head or Etherington Formations), or into the alluvial fan separating them. The lake-bottom springs from all three lakes are collectively named Sublacustrine Springs in this thesis.

2.3 Modern hydrogeology

2.3.1 Hydraulic conductivity of the karst aquifers

The mature karstification in the High Rock and Flathead Ranges produces maximum groundwater velocities $>0.1 \text{ m s}^{-1}$ (see Section 3.3). In this context, limestones provide the major vectors of groundwater flow, while less karstified rocks such as dolomites and sandstones behave as aquitards.

There are two principal aquifers in the High Rock and Flathead Ranges, a lower aquifer in the Palliser Formation, and an upper aquifer in the Upper Banff Formation and Rundle Group. The lithologic composition and aquifers of the strata of the Front Ranges are presented in Table 2.3. and their areal distribution is shown in Figure 2.4.

The Palliser Aquifer overlies aquitards of the Alexo and Belly River Formations and Alberta Group (Figure 2.1). The bedding of these strata is concordant with the Palliser contact, and the vertical hydraulic conductivity (K_v) though these strata would be at least several orders of magnitude less than the hydraulic conductivity within the Palliser. Thus leakage through these strata is likely to be very low.

The Banff-Rundle Aquifer is overlain conformably by the sandstones, silty dolomites and cherts of the Rocky Mountain Formation, which also has a low K_v compared to the underlying Rundle Group. Consequently, leakage through this formation is also likely to be very low.

Table 2.3 Lithology and aquifers of the Front Ranges (geology after Douglas, 1958; Norris, 1958; Price, 1962, 1965)

formation	pure limestone (c.>95% CaCO ₃) m	dolomite and impure limestone m	shale chert siltstone m	potential for karstic flow
Banff-Rundle Aquifer				
Upper Etherington Formation	8	4	10	poor
Middle Etherington Formation	73	7	1	good
Lower Etherington Formation	19	4	6	moderate
Mt Head Formation				
Caernarvon member	90	0	0	good
Marston member	16	14	0	good
Loomis member	66	17	0	good
Salter member	7	51	0	poor
Upper Livingstone Formation	186	25	0	good
Lower Livingstone Formation	206	0	0	good
Upper Banff Formation	80	0	0	good
Middle Banff Formation	2	68	0	poor
Exshaw-Banff Aquitard				
Lower Banff Formation	0	5	28	very poor
Exshaw Formation	0	4	8	very poor
Palliser Aquifer				
Palliser Formation	191	11	0	good

The two aquifers are separated by 45m of shales, impure limestones, siltstones and cherts, and karstic flow would not be expected across these strata. However, tracer tests (Table 3.3, traces 3, 20, 24) have demonstrated rapid groundwater velocities from the North Cirque of Mt Phillipps (Livingstone Fm) to Crowsnest Spring (basal Palliser Fm), thus breaching the aquitard. Detailed sampling of the Rundle Group at Crowsnest Pass showed that the section is thickened from 840m to 1600m by means of high-angle thrusts, which resolve into bedding-plane thrust along incompetent horizons (Cundill, 1955). The lowest of these thrusts could provide a path to allow groundwater to breach the aquitard (Figure 2.3,d).

The subject of hydraulic conductivity in karst aquifers will be fully discussed in Chapter 5.

2.3.2 Groundwater flow vectors

Three groundwater flow vectors may be anticipated on topographic and structural grounds, with dip- or strike-oriented flow within the Front Ranges being superimposed on a regional flow field. The regional flow field appears to be quantitatively insignificant in terms of the spring analysis at Crowsnest Pass, and it will be discussed in Chapter 10.

Ford (1983a) suggested that groundwater flow in the Front Ranges at Crowsnest Pass is dominated by dip-oriented flow along the axes of the many cirque-headed valleys, with both downdip and updip flow being common; and that strike-oriented flow, though predominant in pre-glacial times, now only persists where groundwater gradients exceed 0.07. Such a groundwater gradient towards Crowsnest Pass would yield a catchment area of about 65 km².

An alternative hypothesis is that since Crowsnest Pass is the lowest point in the High Rock and Flathead Ranges where either the Palliser or Banff-Rundle aquifers outcrop, then it will be focus for groundwater flow from great distances. The carbonates of the Lewis Thrust Sheet outcrop continuously from North Kootenay

Pass, at the southern end of the Flathead Pass 28km south of Crowsnest Pass, to beyond Banff, 180km north of Crowsnest Pass. Since the Bow River at Banff is at the same altitude as Crowsnest Lake (to within a few metres), then groundwater flow from half this distance (90km) north of Crowsnest Pass might be expected. A section along the Front Ranges, showing hypothetical groundwater gradients, is shown in Figure 2.6. If the hydraulic gradient were less than 0.005, then all groundwater flow from the Flathead and High Rock Ranges would resurge at Crowsnest Pass, and the catchment would be 390 km² (Figure 2.2). Steeper gradients would result in increasing localised flow, as in the model of Ford (1983a), described above.

Hydraulic gradients in karst are discussed in Section 5.2.4, and Chapter 9 is devoted to delineation of the catchment area of Crowsnest Pass.

2.4 Paleohydrogeology

The great concentration of caves at Crowsnest Pass facilitates interpretation of the paleohydrogeology of the area. However, access to the caves is not easy, for the most significant ones are 1000m above the road, and are blocked by snow for 9-12 months of the year. Furthermore, the caves penetrated so far represent only a small fraction of the former flow routes. Existing cave maps and observations were utilised (Thompson and Coward, 1973; Thompson, 1976; Barton, 1981a,b; Meinke, 1986; McKenzie, 1987, 1989a,b; Rollins, 1988; Yonge, 1986), and these were supplemented by visits to the major caves, but little field work was carried out in them.

The instrumentation used in the study area is the subject of the next chapter.

Chapter 3

Hydrological and meteorological measurements

3.1 Introduction

Some of the hydrological techniques that may be used in studying karst aquifers are shown in Table 3.1. Most of these yield complementary information, which is valuable in testing hypotheses on the behaviour of the aquifer; conversely, one technique alone may yield information that may be interpreted in alternative ways by deductive reasoning.

All the techniques shown in Table 3.1 were utilised in the study area, though some proved more useful and hence were used more extensively. Rarely in karst studies has such a wide range of techniques been used.

3.2 Discharge measurement

Stage recorders were installed at the two principal springs (Crowsnest Spring, Ptolemy Spring) at Crowsnest Pass, and the discharge was monitored continuously for a period of fourteen months, from July 1985 to September 1986. Sublacustrine springs in Crowsnest Lake, Island Lake and Emerald Lake were found to be important, so the discharge from Crowsnest Lake into Crowsnest River was also monitored over this period by means of a recorder measuring lake level. These sites were also monitored for four weeks in August and September, 1987.

A recorder was initially set up in the river downstream of Crowsnest Lake; once a high correlation between lake level and river level and discharge was

Table 3.1 Hydrological techniques used in karst aquifer studies at Crowsnest Pass

Technique	Information gained	
	Source Area	Aquifer characteristics
discharge:		
precipitation (Q_p)	1) size	1) travel time
snowmelt (Q_s)	2) altitude	2) storage
springflow (Q_o)		
temperature	altitude	1) travel time 2) storage 3) flow depth
fluorescent dye or particulate tracers	delineation	1) storage 2) travel time 3) open/closed channel flow
isotope: O, H	altitude	travel time
major ions	1) vegetation 2) closed/open conditions	1) travel time 2) geology 3) storage
trace elements	1) geology	1) geology 2) travel time

established, the latter recorder, in a position rather exposed to vandalism, was removed and used elsewhere. The effects of seiches were of concern, especially as Crowsnest Lake is 3km long and aligned along a pass which frequently experiences strong winds. Oscillations with a period of minutes (or less) and a magnitude of several millimetres were readily apparent in the lake, so the stilling well was set back 5m from the lake edge behind a gravel beach, where these high-frequency events were greatly damped. Lake levels were checked at both ends of the lake during some strong winds, but the relative change was not significant.

Unfortunately, it was not possible to separate the proportions of springflow between Island Lake and Crowsnest Lake, due to the presence of the highly transmissive alluvial fan between them. The fan is principally composed of cobbles and gravel. There is no surface flow from Island Creek, Island Lake and Crowsnest Creek into Crowsnest Lake for about six months of the year; the threshold value in Crowsnest Creek for there to be surface flow is about 200 l s^{-1} .

Two other sites were monitored for shorter periods: a small, high altitude spring (Parrish Spring; summers of 1985 and 1986), and the spring-fed Ptolemy Creek (April to September 1986).

Four Leupold-Stevens Type F recorders and one Ott recorder were used to measure stage. The recorders were mounted on 30cm diameter plastic stilling wells, which were installed in the banks adjacent to the creeks. Sites were selected at low-energy reaches of the creeks, where stability of channel form would be high. Parrish Spring was monitored until it froze up on October 8th, but the recorders at Crowsnest Spring, Ptolemy Spring and Crowsnest River were maintained throughout the winter by Rea Bryant, a local resident. Stilling well water levels were about 1m below ground level, which gave excellent protection against the intensely cold weather (Figure 3.1); and a small quantity of oil in each stilling well also helped to prevent freezing. The only record lost over the winter due to the weather was when the recorder beside Crowsnest Lake was buried by a snowstorm for a three day period.

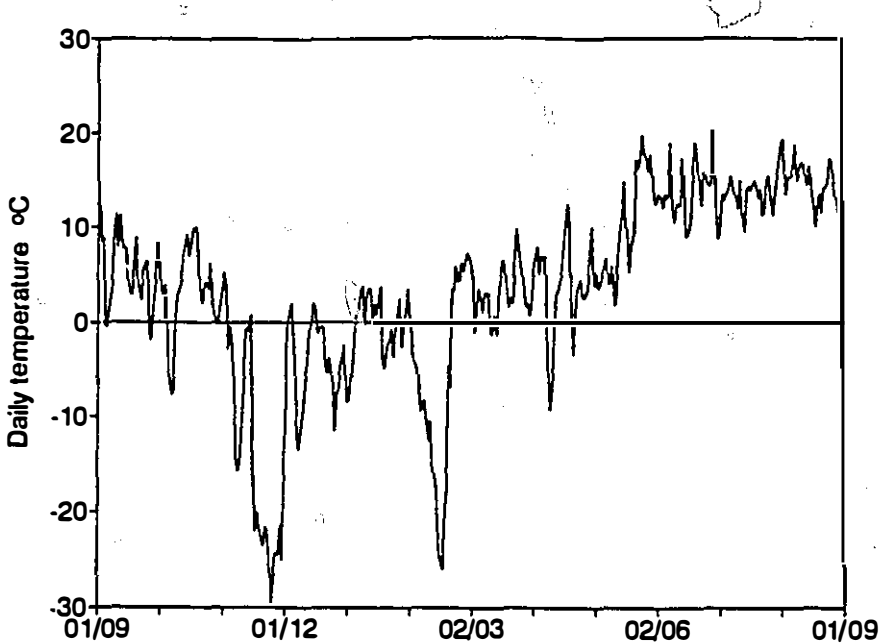


Figure 3.1 Daily temperatures at Sentinel from September 1985 to August 1986

The irregular creek cross-sections and high gradients precluded accurate gauging by the area-velocity method. Instead, Rhodamine WT was used for flow dilution gauging (Church, 1974), with a single injection of 0.2-10ml (net dye volume). This gave a satisfactorily visible dye cloud. The dye was usually pre-diluted up to a thousand fold, which facilitated easy injection and high precision of measurement. Twenty-four 30ml samples were collected after each injection to allow full definition of the dye breakthrough curve. The samples were analyzed on a Turner Designs Series 10 fluorometer. Replication of dilution gauging tests gave an accuracy better than $\pm 4\%$. Channel stability was checked by dilution gauging each field season, and after major discharge peaks; no significant change was detectable.

Crowsnest Spring was the most problematic site for discharge gauging, due to the short distance (50m) between the spring and Crowsnest Lake. However, a 4m

waterfall facilitated good mixing, and at high discharges the use of two people enabled samples to be taken at five second intervals, which resulted in good definition of the dye peak.

Stage was also measured manually at weekly intervals at Crowsnest Creek, Island Creek and Emerald Lake, and occasionally at other sites, with appropriate dilution gauging. Because the springs at Crowsnest Pass are at a lower altitude than any other discharge point in the Flathead and High Rock Ranges, there is the possibility of regional flow to Crowsnest Pass (Section 2.3.2). To test this hypothesis, all creeks on the downdip, western side of the Flathead and High Rock Ranges up to 80km north of Crowsnest Pass were gauged at low stage in late August, 1986, and in early April, 1987 (Figures 3.2 and 3.3). The basal Palliser Formation contact on the eastern, updip side of the Front Ranges is much higher than on the western side (Figure 2.5), so karstic drainage to the east is likely to be minimal; nevertheless, low points on the contact were checked. In all, more than 120 gauging measurements were made.

Stage-discharge relationships were determined for the above sites (Figure 3.4), assuming the relationship to be a power function,

$$Q = a S^b \quad (3.1)$$

which can be rearranged to

$$\log Q = \log a + b \log S \quad (3.2)$$

where S is the stage above an arbitrary datum. Coefficients a and b of the principal sites are presented in Table 3.2. The lower correlation coefficients of Ptolemy Creek, Ptolemy Spring and Ptolemy Creek are to be expected, as these are all mountain creeks with less regular cross-sections than Crowsnest River.

The discharge from the sublacustrine springs of Crowsnest Lake, Island Lake and Emerald Lake could not be accurately separated, so the springs are referred

Figure 3.2 Measurement sites in the vicinity of Crowsnest Pass, showing dye trace routes to Ptolemy Spring and Crowsnest Spring

Hydrogeology

A	Alexo aquitard	P	Palliser aquifer
E	Exshaw - Banff aquitard	B	Banff - Rundle aquifer
R	Rocky Mountain Formation aquitard		

■ Stage recorder site, weekly hydrochemical sampling

CS	Crowsnest Spring	PS	Ptolemy Spring
CR	Crowsnest River	PC	Ptolemy Creek

□ Stage recorder site, occasional hydrochemical sampling

PA Parrish Spring

● Weekly discharge and hydrochemical measurements

EL	Emerald Lake outlet	IC	Island Creek
CC	Crowsnest Creek		

○ Weekly specific conductivity, occasional discharge and titration measurements

EC	East Crowsnest Creek	WC	West Crowsnest Creek
AX	Alexander Creek	AS	Allison Creek
RS	Ranch Spring		

▲ Occasional specific conductivity and discharge measurements

PW	Ptolemy West Cirque	SS	Supplies Sink
TW	Tecumseh West Creek	TC	Tecumseh Centre Creek
PE	Peresta Sink	PL	Ptolemy Lake
ECS	Emerald Cliff Springs	LC	Leachate Creek
AGC	Andy Good Creek	DM	Deadman Creek
UAX	Upper Alexander Creek	LCC	Lower Crowsnest Creek
AG	Andy Good Plateau (Derbyshire Sink, Yorkshire Pot)		

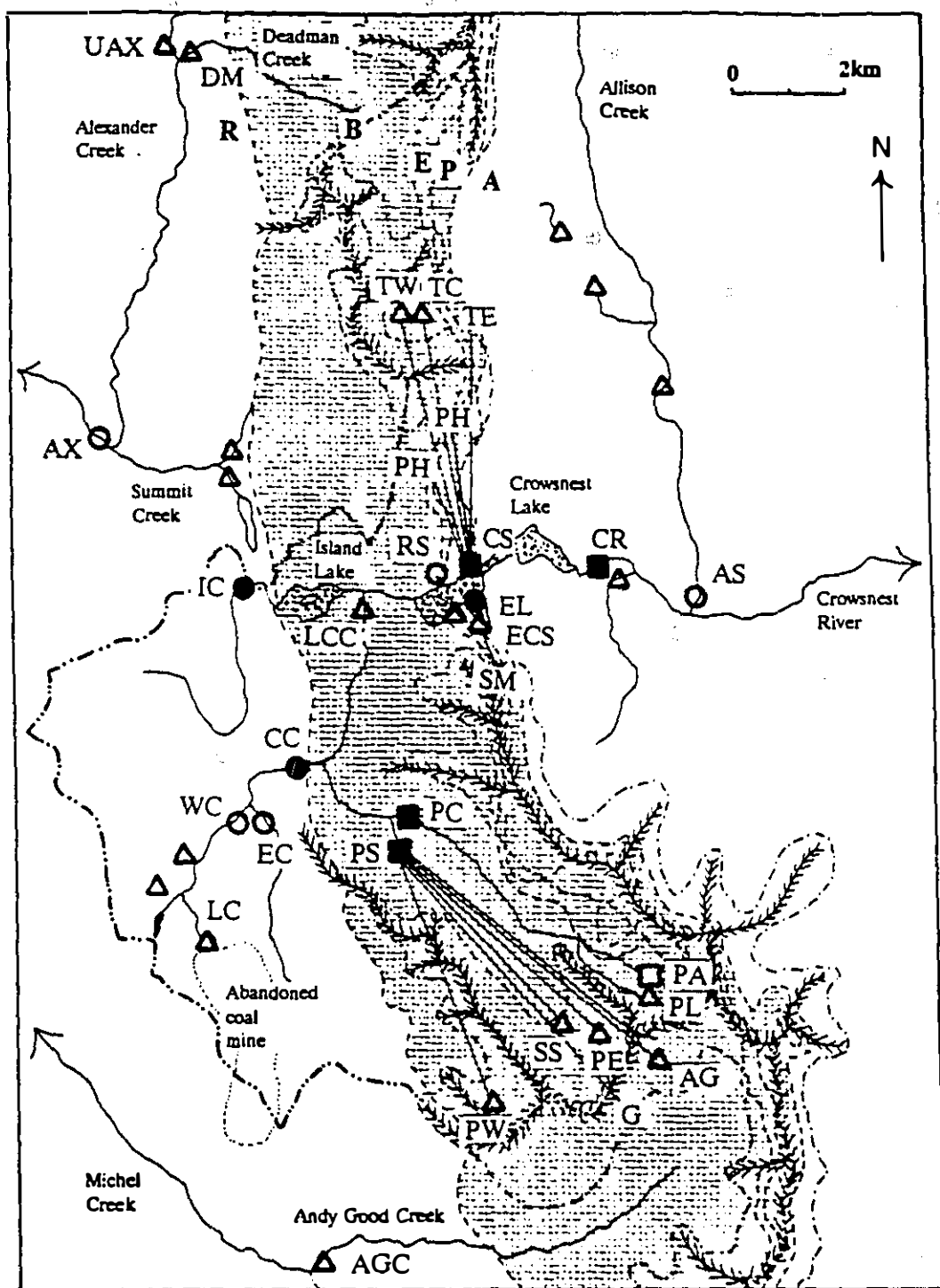
Dye injection sites

G	Gargantua	PH	Phillipps Creek
TE	Tecumseh East Creek	SM	Sentry Mountain

— dye trace

..... tree line

..... provincial boundary



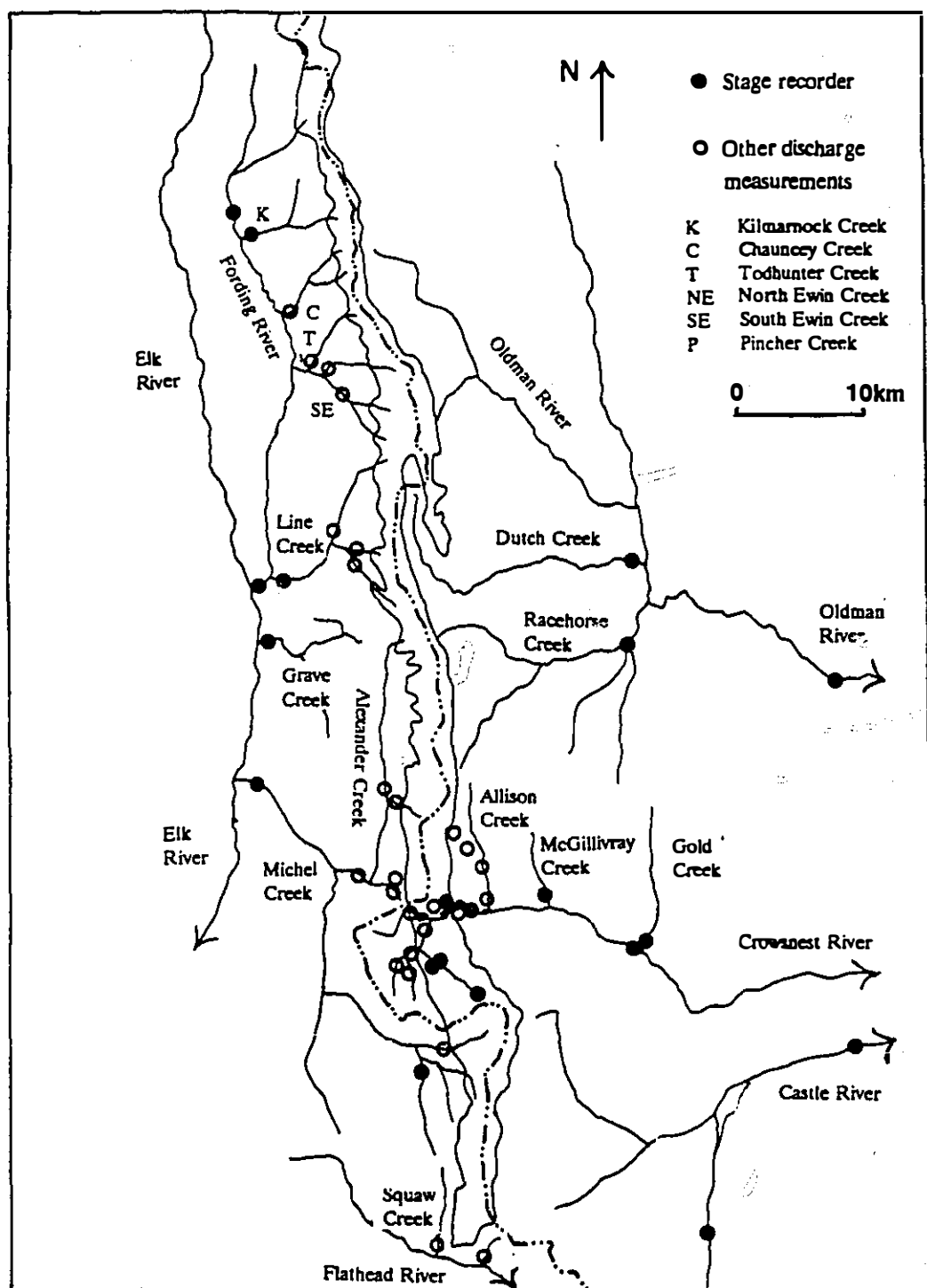


Figure 3.3 Measurement sites in the Flathead and High Rock Ranges

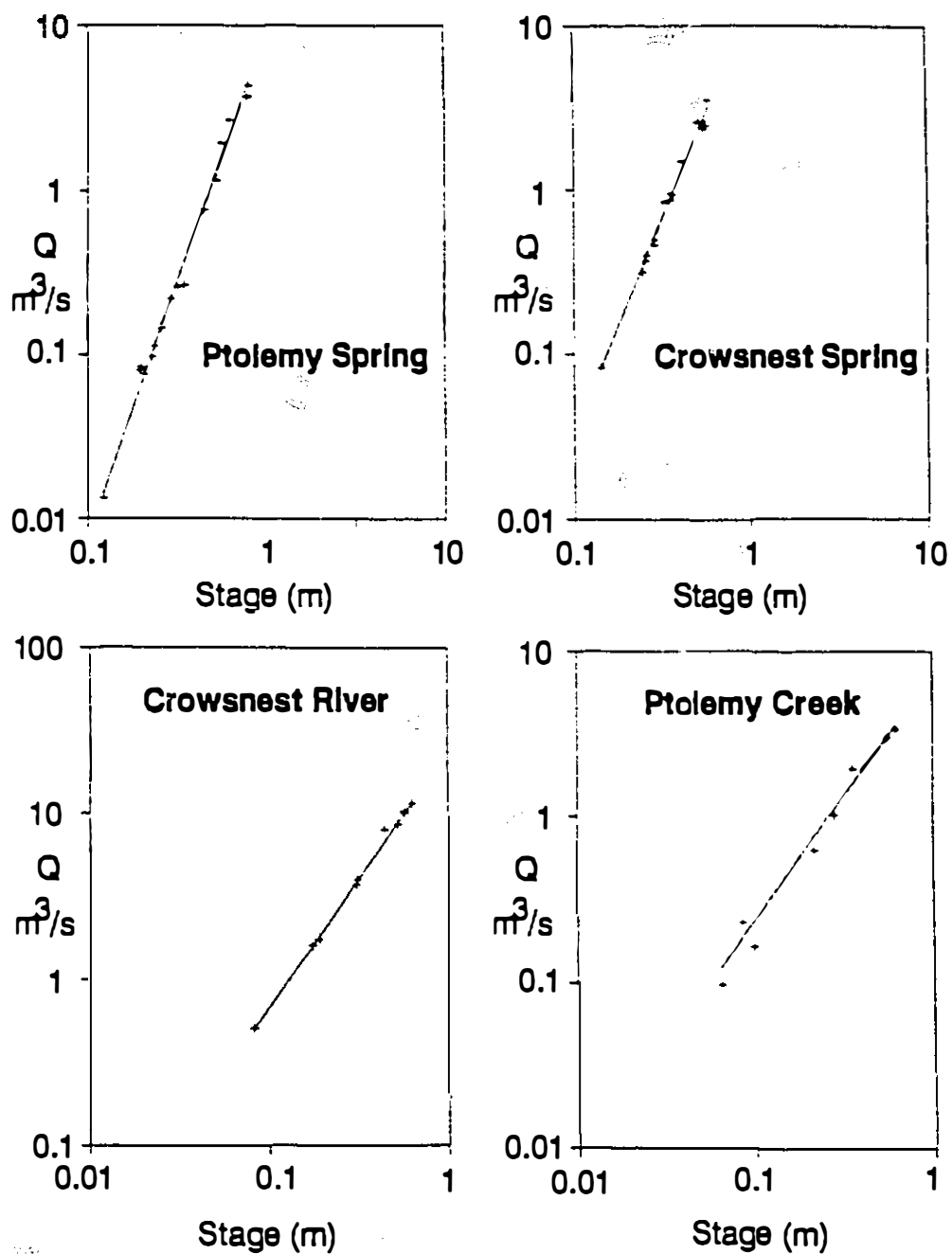


Figure 3.4 Stage-discharge relationships for Ptolemy Spring, Crowsnest Spring, Crowsnest River and Ptolemy Creek

Table 3.2 Rating curve coefficients for gauged streams at Crowsnest Pass

Gauge	a	b	r ²	n
Crowsnest River	1.377	1.543	0.997	10
Ptolemy Spring	0.930	3.009	0.990	16
Crowsnest Spring	1.134	2.624	0.988	16
Ptolemy Creek	0.869	1.552	0.980	8

to here collectively as Sublacustrine Springs. It was calculated by

$$Q_{SLS} = Q_{CR} - Q_{CS} - Q_{PS} - Q_{IC} - Q_{PC} - Q_{CC} + \Delta S \quad (3.3)$$

where Q_{SLS} , Q_{CR} , Q_{CS} , Q_{PS} , Q_{IC} , Q_{PC} and Q_{CC} are the discharges for Sublacustrine Springs, Crowsnest River at the outlet of Crowsnest Lake, Crowsnest Spring, Ptolemy Spring, Island Creek, Ptolemy Creek and Crowsnest Creek, respectively, and ΔS is the change in storage of Crowsnest Lake. However, weekly discharge measurements were made at the outlet of Emerald Lake, and this did allow a rough estimate to be made of the discharge from this lake; this is shown in Figure 3.7.

Winter discharges for the three surface creeks, Island Creek, Ptolemy Creek and Crowsnest Creek is very low; monthly means were estimated, based on observations at the end of March in 1985 and 1988 and at the end of September in 1986, and from the discharge records of local non-karstic catchments gauged by the Inland Waters Directorate (1985a,b, 1986a,b). The estimated winter discharge of the

three creeks is less than 12% of the total annual discharge of Sublacustrine Springs, so the accuracy of the latter discharge is hardly compromised.

Discharges for the springs and creeks at Crowsnest Pass for 1985-1986 are given in Tables 3.3 and 3.4, and Figures 3.5 through 3.10.

3.3 Fluorometry

3.3.1 Aquifer hydraulics

Nineteen tracer tests were carried out during 1985 and 1986, using Rhodamine WT or fluorescein (Table 3.5). Additionally, tracer results from 1969 were available (Ford, 1969). Dye was injected into small streams flowing in caves (Yorkshire Pot Alberta Avenue Stream, Gargantua Big Dipper Stream), sinking into sinkholes (Supplies Sink, Derbyshire Sink) or sinking into scree (Peresta Sink, Col Sink), or into creeks which gradually sank into their beds (Phillipps Creek, Tecumseh Creeks).

Sigmamotor water samplers collected water samples at 30 minute to 2 day intervals, depending on flow conditions. This resulted in 5-30 samples being collected during dye peaks, and many more during the tail, at Ptolemy Spring and Crowsnest Spring, allowing good definition of the breakthrough curve. After obtaining negative results at Andy Good Creek for tests 7 and 8, and negative results at Crowsnest Creek (upstream of Ptolemy Spring) for tests 12-17, no further sampling was carried out at either site. Ironically, the following test, #19, was not recovered at Ptolemy Spring. Thus it is not known whether #19 flowed to Ptolemy Creek or to Andy Good Creek.

In addition, for some of the early tests in 1986, activated charcoal detectors were placed at possible resurgences along Crowsnest Creek and Crowsnest River, but these were all negative. Since good recoveries were being recorded at Ptolemy Spring and Crowsnest Spring, later sampling was only carried out at these two springs (Table 3.5). No attempt was made to check for dye recovery at

Table 3.3 Monthly discharges of the springs and creeks at Crowsnest Pass, 1985-1986

	Discharge in L s^{-1}							
	PS	CS	PC	CC	IC	SLS	CLI	CR
1985								
August	465	494	130	40	15	788	1930	1930
September	462	679	250	150	40	824	2410	2390
October	198	596	100	130	35	811	1870	1880
November	142	472	80	110	20	890	1710	1740
December	83	315	20	40	13	509	980	1000
1986								
January	43	244	10	20	15	445	777	783
February	25	268	20	60	60	367	800	776
March	39	316	100	220	190	322	1190	1190
April	129	535	200	320	220	670	2070	2030
May	1050	1480	882	526	417	1720	6080	5860
June	1480	1830	959	370	217	2190	7040	7230
July	609	831	325	230	78	1080	3150	3200
August	353	431	118	40	15	969	1930	1950
September	307	346	175	80	20	504	1430	1430
Mean	380	660	250	180	110	880	2460	2460

Legend: PS Ptolemy Creek; CS Crowsnest Spring; PC Ptolemy Creek; CC Crowsnest Creek; IC Island Creek; SLS Sublacustrine Springs; CLI Crowsnest Lake inflows; CR Crowsnest River at outflow of Crowsnest Lake

Table 3.4 Altitude and discharge of the springs at Crowsnest Pass

	Altitude m	Days flowing	Q_s	Q_m	Q_n	Q_s/Q_n
Sublacustrine Springs <1347*	365	(5000)	(890)	(300)	(17)	
Crowsnest Spring (combined)		365	3830	670	184	21
upper spring	1351	150	(3400)	(300)	0	•
lower spring	1348	365	(400)	(350)	184	(2.2)
Ptolemy Spring	1560	365	5550	390	20	280
Parrish Spring	2040	(120)	122	(10)	0	•
Ranch Spring	1370	(120)	(10)	2	0	•
Ptolemy Lake Springs	2050	(120)	(100)	(10)	0	•
Emerald Cliff Spring #1	1391	(2)	(15)	<1	0	•
#2	1389	(4)	(30)	<1	0	•
#3	1387	(18)	(10)	<1	0	•
#4	1387	(18)	(10)	<1	0	•
#5	1352	(50)	(3)	<1	0	•
Peresta Spring	2310	(100)	(10)	<1	0	•
Ptolemy Creek Springs*	1500-1650	365	(2000)	(150)	2	(1000)

Note:

* Lake level is 1347m. Sublacustrine Springs may be at depths up to 40m below this

* Sum of all the springs feeding Ptolemy Creek, excluding Ptolemy Spring, Parrish Spring, and Ptolemy Lake Springs

Data in parentheses are approximations

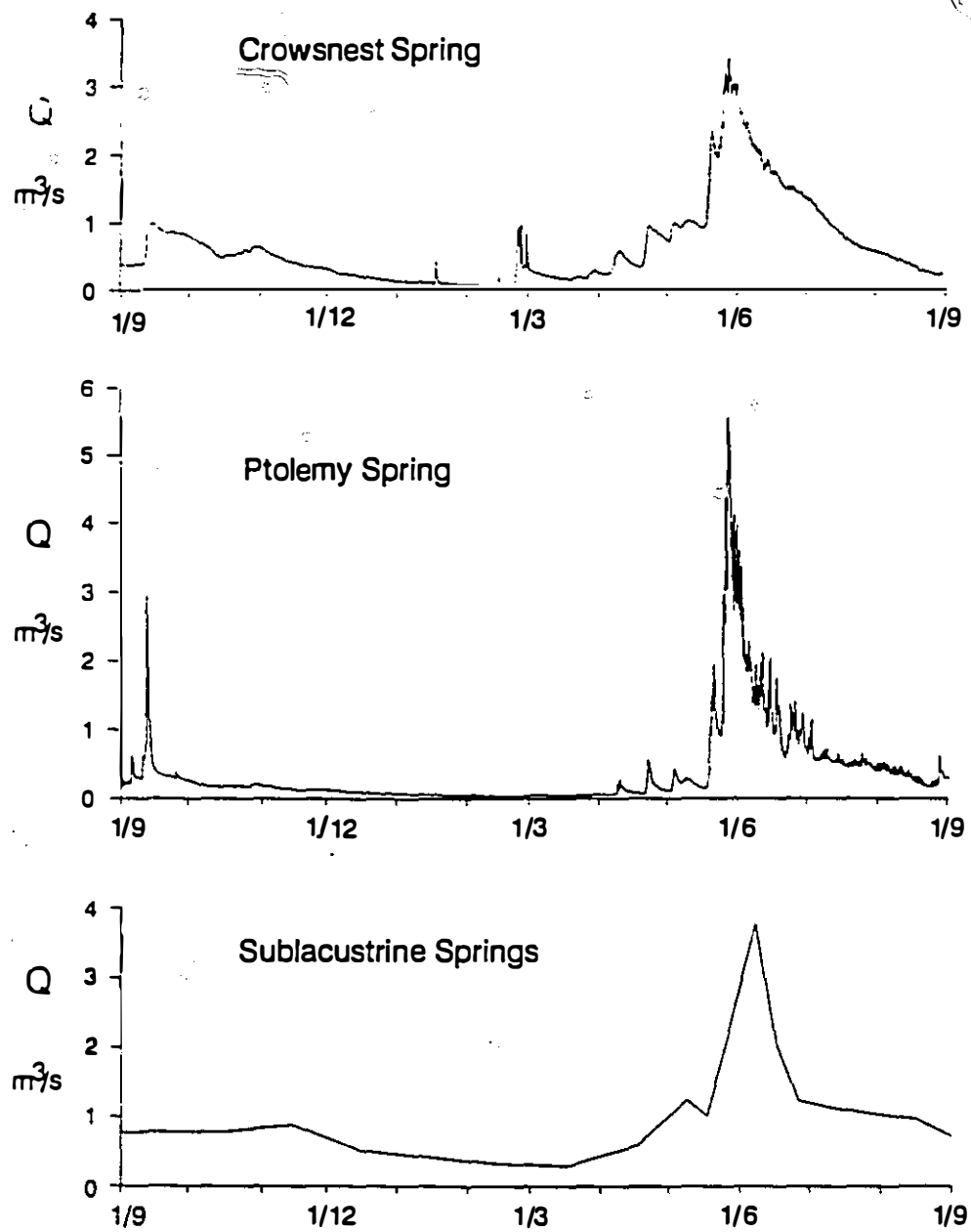


Figure 3.5 Daily discharge of Ptolemy Spring, Crowsnest Spring and Sublacustrine Springs, September 1985 to August 1986

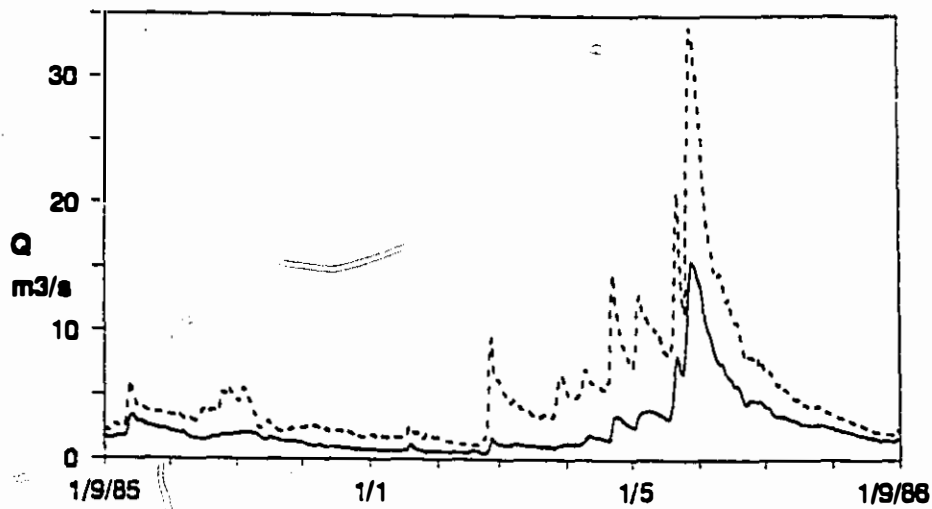


Figure 3.6 Daily discharge of Crowsnest River at the outlet of Crowsnest Lake (—) and at Frank (----)

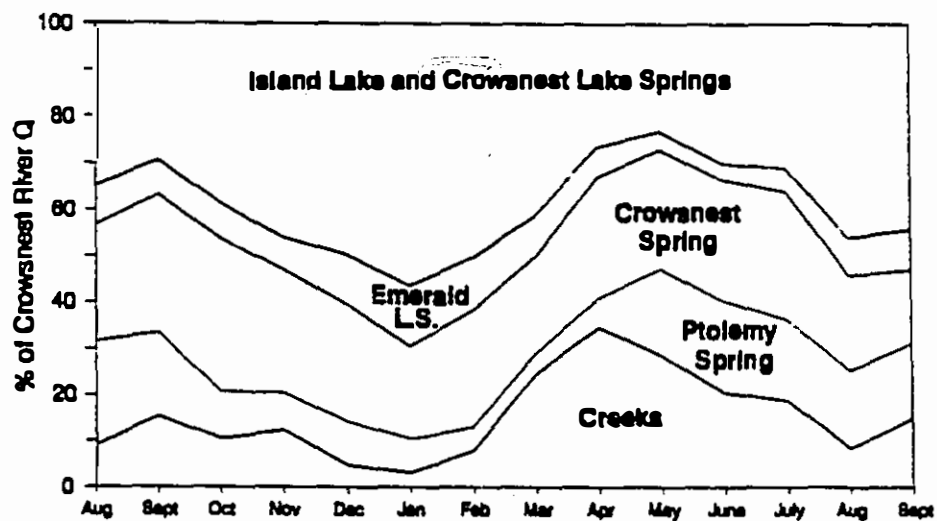


Figure 3.7 Monthly discharge of the springs and creeks at Crowsnest Pass as a percentage of the discharge in Crowsnest River at the outlet of Crowsnest Lake, from August 1985 to September 1986

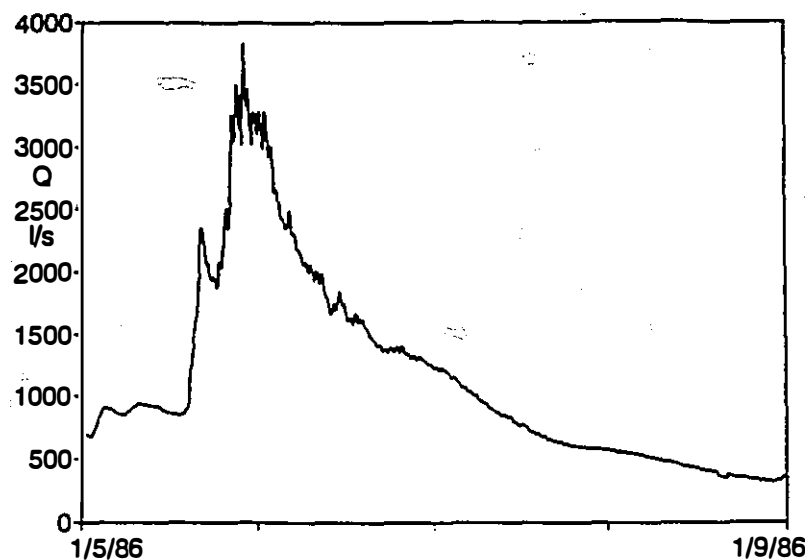


Figure 3.8 Instantaneous discharge of Crowsnest Spring from May 1st to September 1st 1986

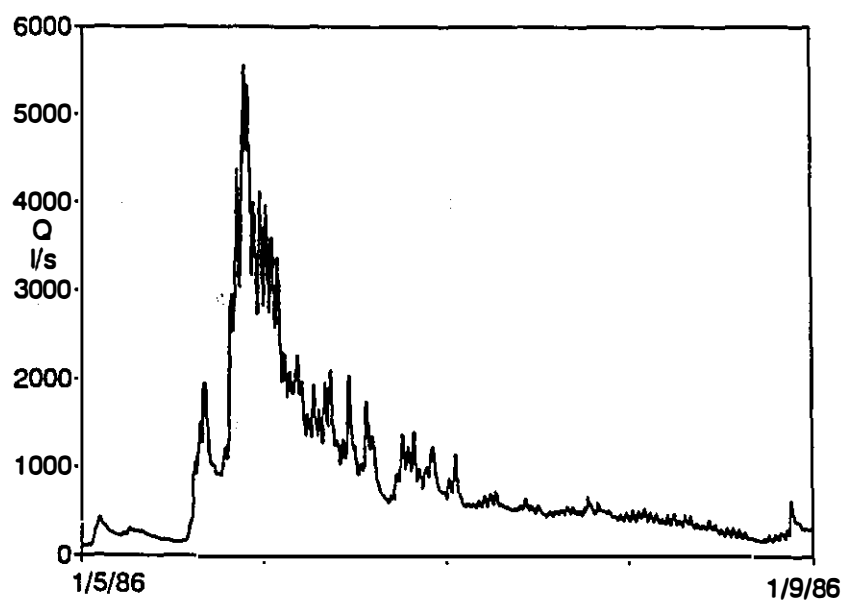


Figure 3.9 Instantaneous discharge of Ptolemy Spring from May 1st to September 1st 1986

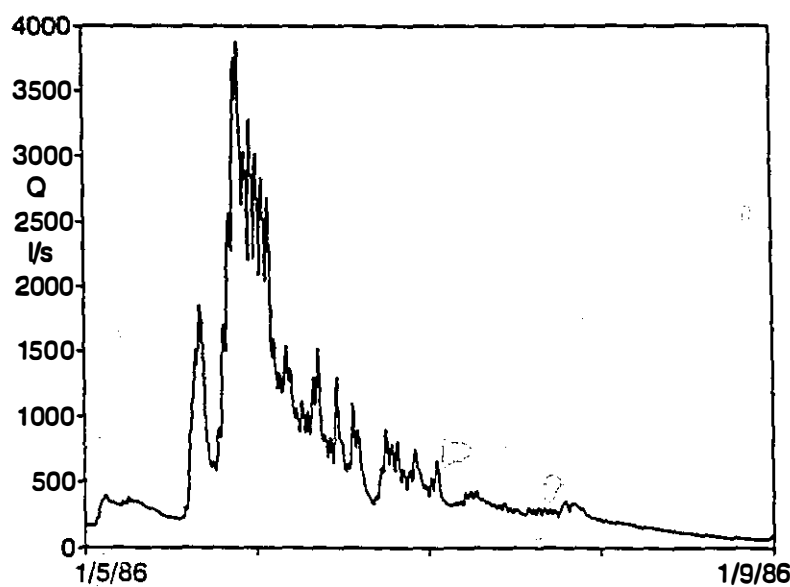


Figure 3.10 Instantaneous discharge of Ptolemy Creek from May 1st to September 1st 1986

Sublacustrine Springs; dilution and storage in the lakes would have required prohibitively large dye injections and long monitoring periods.

The principal aim of the tracing was to investigate conduit velocities in the aquifer, and the change in velocity due to changes in discharge. Thus, repeated tracings were carried out to both Ptolemy Spring and Crowsnest Spring at different spring discharges. Discharges at injection points could only be roughly estimated, as the streams were gradually sinking into their beds, and the sinks listed in Table 3.5 were often trickles down cliffs or into scree.

The relationship between tracer velocity and discharge can be expressed as a power function

$$v_a = a Q^b \quad (3.4)$$

Table 3.5 Dye traces at Crowsnest Pass

#	Injection Point	Date	Dye/Mass g	Recovery Point/%	Discharge Q_i 1 s^{-1}	Discharge Q_o 1 s^{-1}	Velocity mm s^{-1}	Note
---	-----------------	------	---------------	------------------	---	---	--------------------------------	------

1969 D.C. Ford, M.C. Brown, J.J. Drake, T. Wigley

1	Middle Sentry Mtn	4/7/69	Fl	EL3	-	-	250	
2	Phillipps Ck	6/7/69	Fl 680	-	-	-	-	
3	Tecumseh W Ck	13/7/69	RWT 3620	CS	<30	1500	>27	
4	Mt Ward NE cirque	19/7/69	Fl 900	-	-	-	-	1
5	Ice Hall	20/7/69	Fl 1140	-	-	-	-	2
6	Racehorse Pass	1/8/69	RWT 1800	-	-	-	-	

1985-1986 S.R.H. Worthington, J.L. Mulckovich

7	Gargantua BDS	5/8/85	RWT 220	PS	(1)	320	>7.2	3
8	Yorkshire Pot WM	6/8/85	RWT 220	PS	(1)	320	>7.2	3
9	Gargantua BDS	27/8/85	RWT 220	-	(1)	-	-	4
10	Lower Phillipps Ck	26/5/86	RWT 228	CS 24	50	2710	90	
11	Lower Phillipps Ck	4/6/86	RWT 229	CS 43	20	2450	52	
12	Supplies Sink	15/6/86	Fl 1893	PS 79	1	1310	23	
13	Gargantua BDS	15/6/86	RWT 425	PS 47	2	1350	37	
14	Derbyshire Sink	27/6/86	RWT 205	PS 46	0.7	1020	28	
15	Peresta Sink	27/6/86	Fl 745	PS 50	10	1050	32	
16	Ptolemy West	30/6/86	Fl 745	PS 29	3	686	8.6	
17	Peresta Sink	8/7/86	Fl 780	PS 63	8	600	15	
18	Col Sink	8/7/86	RWT 220	-	1	-	-	5
19	Peresta Sink	12/7/86	Fl 1075	PS 51	5	539	13	
20	Tecumseh W Ck	14/7/86	Fl 1075	CS 34	1	868	22	
21	Tecumseh E Ck	14/7/86	RWT 476	CS 15	0.1	831	12	
22	Upper Phillipps Ck	21/7/86	Fl 645	CS 5*	0.3	683	12	
23	Peresta Sink	10/9/86	RWT 228	PS 9*	0.2	291	3.6	
24	Tecumseh C Ck	11/9/86	RWT 461	CS 5*	0.8	275	4.6	
25	Upper Phillipps Ck	12/9/86	Fl 860	CS 25*	0.13	264	11	

Notes:

EL3 = Emerald Lake Spring #3; CS = Crowsnest Spring, PS = Ptolemy Spring

BDS = Big Dipper Streamway; WM = Water Meeting

FL = Fluorescein; RWT = Rhodamine WT

1 Detector at Racehorse negative after 2 days

2 Detectors at Ptolemy Spring and Ptolemy Creek negative

3 Inadequate sampling - only single peak detected

4 Not detected: sampling ended 2/9/85

5 Sampled only at Ptolemy Spring

• Sampling ended before end of dye recovery

where v_a is the apparent (straight-line) tracer velocity, Q is the resurgence discharge, and a and b are coefficients. This relationship will be true where

$$Q_i = Q_o \quad (3.5)$$

or

$$Q_i / Q_o = K \quad (3.6)$$

where Q_i is the discharge at the injection point, Q_o is the discharge at the recovery point, and K is a constant. Equation 3.5 can often be applied where large alloegenic rivers cross karstic terrains for short distances. Equation 3.6 is applicable where infiltration is even over a whole catchment, as with cyclonic rainfall onto a holokarst. It is less likely to be useful where infiltration is uneven, as with orographic or convectional precipitation, with snowmelt where there is an uneven snow cover, or where the path of the inlet stream is long before the main stream is reached.

There is both orographic precipitation and localised snowmelt at Crowsnest Pass. Moreover, the 300-800m altitude difference between dye injection and recovery points means that input streams have a substantial length before the main drainage conduits are reached; thus Q_i has an important bearing on overall tracer velocity. Because of these factors, a better approximation of flow velocity in the karst at Crowsnest will result from

$$v_a = 1 / (c Q_i^d l_i + e Q_o^f l_o) \quad (3.7)$$

where l is the sum of l_i , the straight-line length of the input stream, and l_o , the straight-line length of the output stream, Q_i and Q_o are the discharge of the input and output streams, respectively, and $c-f$ are coefficients.

Perhaps the first studies to demonstrate that there is a wide range of velocities in karst conduits at different ^{discharges} was Brown (1970), who studied the Maligne karst, Alberta. The relationship was quantified by Stanton and Smart (1981),

who investigated three caves in England. They found coefficient b to be close to 1 in each case, indicating flooded conduits. There is considerable evidence that almost all principal conduits in karst aquifers are flooded (see Section 8.3). Smart (1981) measured stream velocities in streams in bedrock in the vadose zone in the Mendip Hill caves, England, and found coefficient d to be about 2/3. However, recent tests in West Virginia (Worthington, 1990) have revealed a wide variation in coefficient d in low-gradient vadose passages with alluvial sediments. In these passages pool and riffle sequences have developed, and there is considerable on-line storage within the pools as discharge approaches zero ($d=0.9-1$). Conversely, at high stages the cave stream behaves more like a surface stream, as the channel width increases, so that $d=<0.5$.

An approximation for \mathbf{l}_i and \mathbf{l}_o are, respectively, a vertical vector \mathbf{V} from the input altitude to the resurgence altitude, and a horizontal vector \mathbf{h} from below the input point to the output point. Modelling vadose flow along \mathbf{V} , and phreatic flow along \mathbf{h} , Equation 3.7 can be simplified to

$$v_a = l / (c Q_i^d V + e Q_o h) \quad (3.8)$$

A full solution for a karstic drainage system would require the consideration of flow in each constant-discharge stream segment of the flow route. This is beyond the means of surface measurement, and hence has little practical use.

Apparent (straight-line) tracer velocities of the 17 successful traces to Ptolemy Spring and Crowsnest Spring are shown in Figure 3.11. Conduit velocities to both springs show a similar range. Regression of the Ptolemy Spring data set gives

$$v_a = 0.0232 Q^{1.258} \text{ m s}^{-1} \quad (n=9, r^2=0.85) \quad (3.9)$$

However, six of the nine traces form a linear array in Figure 3.6

$$v_a = 0.0275 Q^{1.180} \text{ m s}^{-1} \quad (r^2=0.994) \quad (3.10)$$

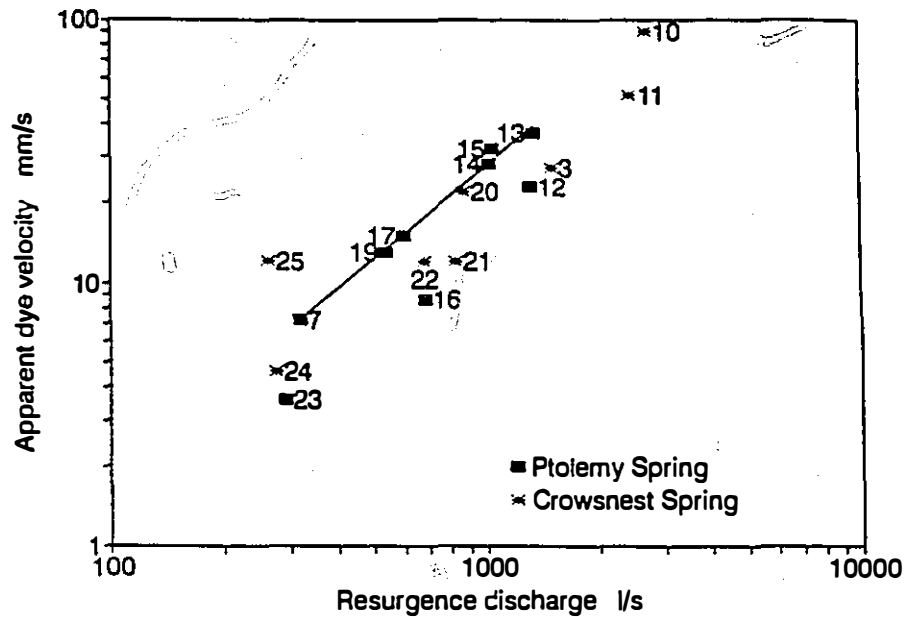


Figure 3.11 Velocities of dye traces to Ptolemy Spring and Crowsnest Spring

Equations 3.9 and 3.10 yield an estimated maximum apparent velocity of 0.20 m s^{-1} and 0.21 m s^{-1} , respectively, for Ptolemy Spring in 1986. Traces 12 and 16 were the only traces from Supplies Sink and Ptolemy West Sink, respectively, and both probably have long courses in the vadose zone before reaching the main phreatic axis of drainage; the remaining trace, number 23, was injected into a very low discharge stream.

Regression of the Crowsnest Spring data set gives

$$v_a = 0.0222 Q^{0.971} \text{ m s}^{-1} \quad (n=8, r^2=0.83) \quad (3.11)$$

which yields an estimated maximum apparent velocity of 0.082 m s^{-1} in 1986.

The eight traces were all injected into losing creeks, so that none of the traces were from the same sinkpoints. For instance, trace 25 was injected where Phillipps Creek

sank on September 12; this was more than 800m upstream of the final sinkpoint during traces 10 and 11. Both the slope (V/h) and the traced distance (l) are much more varied for Crowsnest Spring ($V/h=0.083-0.30$; $l=2.1-4.5\text{km}$) than for Ptolemy Spring ($V/h=0.11-0.13$; $l=4.7-5.8\text{km}$), so it is not surprising that the correlation is lower in Figure 3.11.

In all these cases, coefficient b is close to or greater than 1. The data of Smart (1981) reveals a similar pattern, with coefficient b always >1 . In both cases it is due to the greater variance of Q_i than Q_o . For instance, with the Longwood - Cheddar Springs data (Smart, 1981) the ratio of maximum annual discharge (Q_x) to minimum annual discharge (Q_n) for the input is 144, while over the same period at the output Q_x/Q_n is only 23.

The velocity of cave streams will be discussed further in Section 5.2.1.

3.3.2 Catchment delineation

A second aim of the tracing programme was catchment delineation. Positive traces are shown in Figure 3.2. The traces from Andy Good Plateau (#7,8,9,13,14) to Ptolemy Spring proved flow across the topographic Continental Divide, and #16 proved flow from the Crowsnest Creek topographic catchment to Ptolemy Spring. No tracing was attempted from Allison Block to Crowsnest Pass: two traces were attempted from here in 1969, with negative results (Table 3.5). Since Sublacustrine Springs have a higher discharge than Crowsnest Spring, there is a good possibility that dye would flow to the former. Sampling of Sublacustrine Springs would be awkward, for the location of the springs is not yet known, but they are probably at a depth of 20m or more below the surface of Crowsnest Lake and Emerald Lake, and at a shallower depth below Island Lake. A realistic alternative would be to sample at the outlet of Crowsnest Lake. Dilution of dye in the lakes would require large injections ($>100\text{kg}$) and long sampling periods (several months),

so that only one trace per dye could be performed per year. This is clearly beyond the scope of this research project.

The size of the catchments mean that dye tracing was only partially effective in delineating catchments at Crowsnest Pass. Alternative approaches are considered in Chapter 9.

3.4 Hydrochemistry

3.4.1. Specific conductivity and titrations

Sampling and analysis

A weekly water sampling programme was carried out between April and September in 1986 from eleven major springs and creeks at Crowsnest Pass (Figure 3.2, 3.3). This period covers 75% of the annual discharge from the karst area at Crowsnest Pass (Table 3.3). During the winter monthly samples were collected at Crowsnest Spring and Ptolemy Spring (Figure 3.12); these showed that there is little variation in Ca and Mg concentrations from October to March.

In addition, there was weekly sampling at Ranch Spring and the five Emerald Cliff Springs while they were flowing, and occasional sampling at other karst waters in the High Rock and Flathead Ranges (Figure 3.2, 3.3). Specific conductance, temperature and stage were recorded at the sampling sites, and samples were collected for titration, neutron activation and isotope analysis.

All samples from seven of the eleven sites were titrated for total hardness and alkaline hardness. The seven sites included four karst sources: Ptolemy Spring, Crowsnest Spring, Emerald Lake, Ptolemy Creek. The two non-karstic creeks feeding Crowsnest Lake plus the outlet of Crowsnest Lake into Crowsnest River were also sampled so that the chemistry of Sublacustrine Springs could be calculated. This was hindered by the long residence times in Crowsnest Lake, which had mean residence times in 1986 varying from 16 days on June 9th to 167 days on April 21st (Figure 3.13).

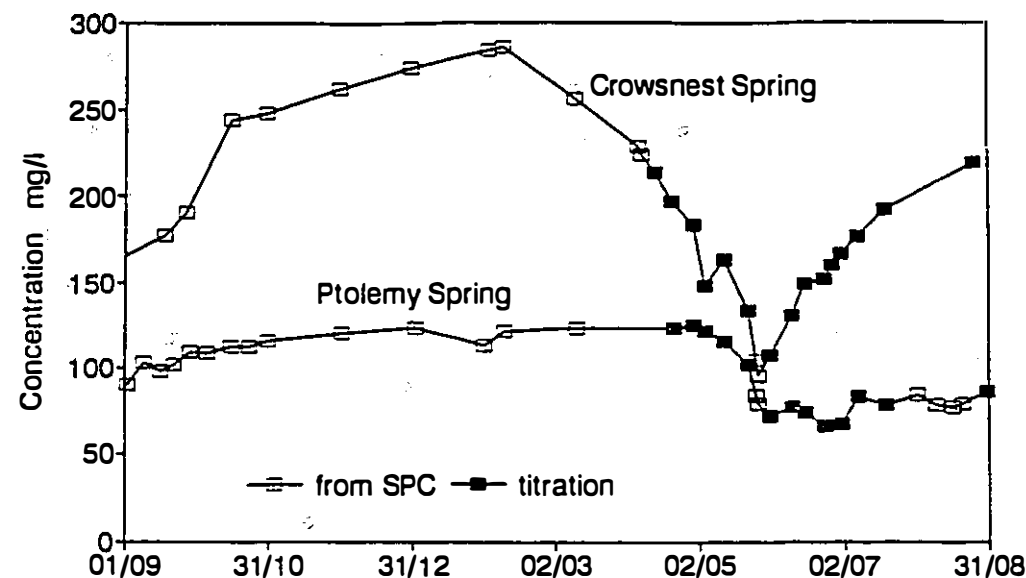


Figure 3.12 Total hardness at Ptolemy Spring and Crowsnest Spring, September 1985 to August 1986

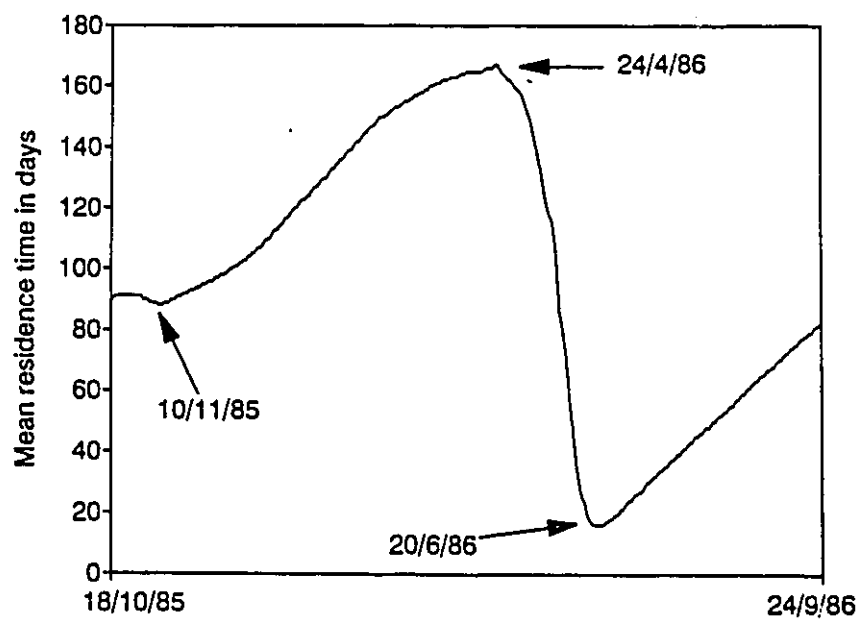


Figure 3.13 Mean residence time of Crowsnest Lake, 1985-1986

The remaining four sites were East Crowsnest Creek (partially fed by karstic water), West Crowsnest Creek (partially fed by tailings water from an abandoned coal mine), and Allison Creek and Alexander Creek, two creeks partially draining the karst of the High Rock Range.

Continuous recordings of spring temperature and conductance were made at Ptolemy Spring and Crowsnest Spring for several periods of 4 to 24 days. The Peabody Ryan model J submersible temperature recorder had a stated accuracy of 0.6°C; the mean diurnal temperature variation at the two springs was less than the instrument precision of 0.2°C. The precision of the pHOX Systems Series 57 Conductivity /T.D.S indicator recorder depended on the scale utilised. For all measurements at Crowsnest Spring and most at Ptolemy Spring the precision was $5\mu\text{S cm}^{-1}$. However, when the conductance dropped below $100\mu\text{S/cm}$, a more sensitive scale could be used, giving a precision of $0.5\mu\text{S cm}^{-1}$. Diurnal conductance variation at the two springs was $4\text{-}10\mu\text{S/cm}$, and thus were barely greater than the instrument precision. Spot readings of conductance were made with a Y.S.I. Model 33 S.C.T meter, with a precision of $1\mu\text{S cm}^{-1}$.

Titrations for alkalinity followed the methodology of Stenner (1969), but with addition of a blank measurement to improve accuracy (Rose, 1983). Non-alkaline hardness was determined by subtraction of alkaline hardness from total hardness. Hydrochemical determinations by the Inland Waters Directorate (1975, 1980, 1982, 1984) showed that the non-alkaline hardness is almost exclusively sulphate (Table 3.6).

Titrations for total hardness followed the methodology of Stenner (1969), with determinations for both saturated and unsaturated samples. This gave a direct indication of aggressiveness. At the beginning, pH measurements were attempted, but it was impossible to achieve a precision much better than 0.1 pH units, which was considered to be inadequate for near-equilibrium waters.

Table 3.6 Hydrochemistry of Crowsnest River at the outlet of Crowsnest Lake

	this thesis 1985-1986	I.W.D.# 1964-1977
	discharge-weighted mean	mean
total hardness	mg l ⁻¹ as CaCO ₃	173°
saturation index		164 (100)
Ca ⁺⁺	mg l ⁻¹	0.5 (92)
Mg ⁺⁺	mg l ⁻¹	50 (113)
Na ⁺	mg l ⁻¹	11 (35)
K ⁺	mg l ⁻¹	1.5 (113)
alkalinity	mg l ⁻¹ as CaCO ₃	0.4 (113)
SO ₄ ⁻	mg l ⁻¹	125 (116)
Cl ⁻	mg l ⁻¹	40 (113)
F	mg l ⁻¹	0.7 (113)
NO ₃ ⁻	mg l ⁻¹	0.3 (90)
non-alkaline hardness	mg l ⁻¹ as CaCO ₃	0.07 (104)
		47°

Inland Waters Directorate, 1975, 1980, 1982, 1984

° from 15 analyses

Numbers in parentheses represent the number of analyses

The precision of the titrations can be estimated by calculating the difference of each titration from the mean of the individual titrations on each sample. This gives a standard error of 0.58 mg l^{-1} ($n=571$) for total hardness, and 0.48 mg l^{-1} ($n=293$) for alkalinity. Rose (1983) disproved the myth that alkalinity is dependent on CO_2 concentration, and showed that with the use of blank measurements alkalinity can be accurately measured.

Conductance measurements were converted to specific conductivity at 0°C (K_0) by using the empirical relationship of Albutt (1977)

$$K_T = K_0 (1 + 0.0361T + 0.000127T^2) \quad (3.12)$$

where K_T is the conductance at $T^\circ\text{C}$. Linear regression of total hardness H (from titrations) against K_0 gave

$$H = 1.137K_0 - 3.9 \pm 8.4 \text{ mg l}^{-1} \quad (n=110, r^2=0.98) \quad (3.13)$$

No significant difference in the coefficients was found between calcium bicarbonate waters and calcium bicarbonate plus sulphate waters.

A summary of the hydrochemical results is given in Table 3.7. The principal findings were that the total hardness of Ptolemy Spring and Crowsnest Spring were found to vary substantially seasonally, with May - June minima coinciding with the snowmelt discharge maxima (Figure 3.12); that sulphate is a much more important ion at Crowsnest Spring than at Ptolemy Spring (Figure 3.14); that sulphate/bicarbonate ratios do not remain constant (Table 3.8); and that almost all springs and creeks at Crowsnest Pass are supersaturated with respect to CaCO_3 , (Figure 3.15). The significance of these findings will be discussed in Chapter 9.

The determination of aggressiveness

There are two methods by which the equilibrium status of karst waters may be determined. The direct method involves adding powdered CaCO_3 to a water

Table 3.7 Alkaline and non-alkaline hardness of springs and creeks at Crowsnest Pass

Locations	Aquifer	Total hardness	Alkalinity	Non-alkaline hardness
----- mg l ⁻¹ as CaCO ₃ -----				
Karstic waters				
Crowsnest Spring	both	168	110	59
Ptolemy Spring	upper	86	75	11
Sublacustrine Springs	both	208	148	60
Ptolemy Creek (above Ptolemy Spring)	upper	119	105	14
Emerald Lake	lower	143	117	26
Non-karstic and mixed waters				
Island Creek		186	167	19
Crowsnest Creek (above Ptolemy Creek)	-	232	158	74
Crowsnest River	-	173	128	45

Notes:

- 1) The above data represent mean annual discharge-weighted values, calculated from 15 samples at each location.
- 2) Upper aquifer = Banff-Rundle; Lower aquifer = Palliser (see Table 2.3)

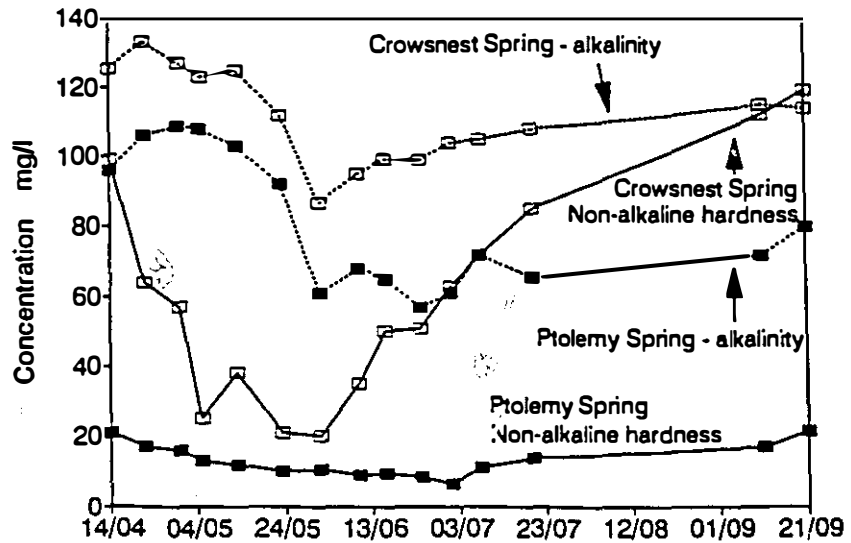


Figure 3.14 Alkaline and non-alkaline hardness concentrations at Ptolemy Spring and Crowsnest Spring, April 15 to September 22, 1986

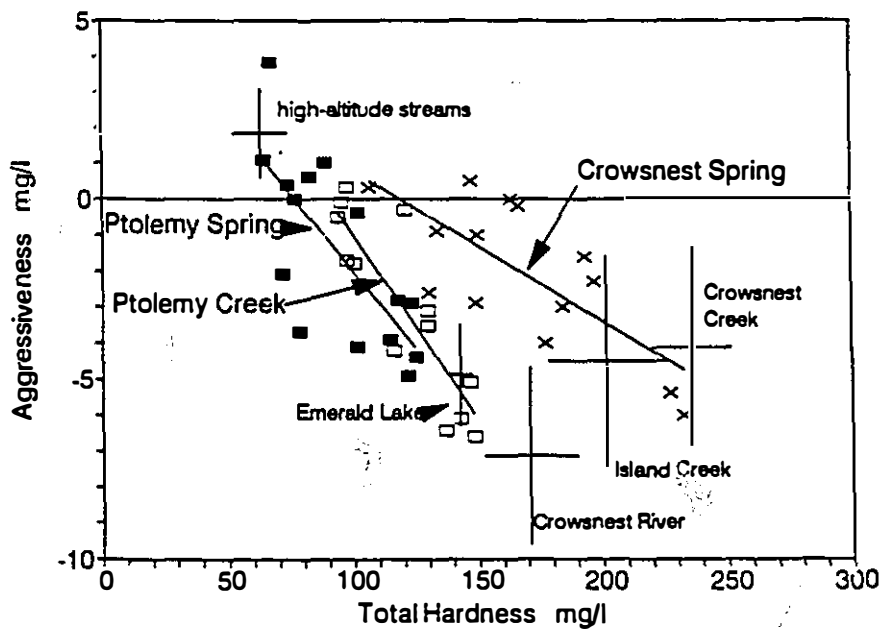


Figure 3.15 Aggressiveness of spring and creek waters at Crowsnest Pass
The data from Crowsnest Creek, Island Creek, Crowsnest River, and Emerald Lake represent the means and standard deviations of 15 samples. The high-altitude data represent 7 samples.

Table 3.8 Coefficient of variation for hardness values at Crowsnest Spring and Ptolemy Spring

	Crowsnest Spring			Ptolemy Spring			
	n	Mean	C.V.	n	Mean	C.V.	
		mg l ⁻¹	%		mg l ⁻¹	%	
Annual means							
Total hardness	28	168	32.5		33	86	24.3
April-September							
Total hardness	15	172	21.1		15	95	21.9
Alkaline hardness	15	111	11.6		15	81	22.2
Non-alkaline hardness	15	60.7	50.5		15	13.6	35.8

sample to bring it to equilibrium. The large surface area of the powder ensures rapid equilibration. The total hardness (or alkalinity) of both original and equilibrium samples are then measured, and the difference between these is known as the aggressiveness (in mg l⁻¹). The positive sign is assigned to undersaturated samples, and the negative sign to supersaturated samples. For instance, an aggressiveness of -5 mg l⁻¹ in a sample with a total hardness of 200 mg l⁻¹ indicates that the water sample is supersaturated by 5/200 mg l⁻¹, or 2.5%. In theory, the SI of such a water would be +0.0107. Aggressiveness is the preferred method chosen by several karst hydrochemists (e.g. Picknett et al., 1976; Bray, 1976, 1977; Gascoyne, 1977; Lauritzen, 1981).

The indirect method is to measure pH along with ion concentrations. Equilibrium can be determined graphically with reference to the equilibrium curves prepared by Trombe (1952), and corrected by Picknett (1976). Alternatively, a saturation index (SI) can be calculated, which expresses saturation with respect to

theoretical thermodynamic equilibrium conditions. This method has been widely used in the last twenty years. In theory it is a better method as it allows calculation of PCO_2 and of saturation indices for different ionic species. However, in practice the use of SI suffers from several drawbacks in karst studies:

1) Magnesium (from dolomite) and sulphate (from gypsum) are common in karst waters, and an accurate SI_c cannot be calculated without their measurement. This is frequently not done (see, for instance, the criticism by Fish (1977, p355) of the work of Harmon).

2) Trace elements are currently not allowed for in carbonate equilibria programs (Ford and Williams, 1989), though they can have a substantial effect on calcite solubility. Terjesen et al. (1961) found significant inhibitory effects, in decreasing order of effectiveness, with Pb^{2+} , La^{3+} , Y^{3+} , Sc^{3+} , Cd^{2+} , Cu^{2+} , Au^{3+} , Zn^{2+} , Ge^{4+} , Mn^{2+} , followed by Ni^{2+} , Ba^{2+} , Mg^{2+} , and Co^{2+} which had an equal but smaller effect. They found that a concentration of as little as 10^{-7} mol Sc l^{-1} ($4.5\mu\text{g l}^{-1}$) depressed the apparent equilibrium concentration of Ca^{2+} by 5%. Berner and Morse (1974) found that trace concentrations of phosphate depressed calcite solubility rates by up to three orders of magnitude. Nine of fourteen trace elements measured in the springs at Crowsnest Pass have mean concentrations $>10\mu\text{g l}^{-1}$ (Figure 3.16), so that it must be assumed that trace elements affect SI_c .

3) It is difficult to measure pH to sufficient accuracy in karst waters. The difficulties of making accurate pH readings in karst areas have been described by Shuster and White (1971), Picknett et al. (1976) and Lauritzen (1981). Ford and Williams (1989) state that the reproducibility of pH is about ± 0.05 , using modern portable pH meters, and they suggest that SI values will normally have an error of 0.1-0.2.

Autogenic springs and streams in caves (such as in the Canadian Rockies) are commonly very close to saturation, and there is little range in the data (Table 3.9). It will be shown in Chapter 12 that autogenic waters on average accomplish 99% of

Table 3.9 Aggressiveness of autogenic karst springs and cave streams

	Undersaturated or supersaturated	Parameter measured	Mean	\pm	n	note
Studies where aggressiveness was measured						
St Dunstan's East, Mendips, England	U	pH	0.04	0.05	30	1
St Dunstan's West, Mendips, England	S	pH	0.08	0.14	30	1
Lower Ashmead, Mendips, England	S	pH	0.01	0.07	16	1
Upper Ashmead, Mendips, England	U	pH	0.04	0.08	16	1
Wishing Well, Mendips, England	S	pH	0.03	0.05	16	1
Cheddar, Mendips, England	U	aggressiveness	2.4	6.2	39	2
Wookey Hole, Mendips, England	U	aggressiveness	6.9	8.1	39	2
Rodney Stoke, Mendips, England	S	aggressiveness	6.0	8.6	38	2
Norway (A)	U	aggressiveness	3.4	1.9	17	3
Norway (B)	U	aggressiveness	5.3	6.6	20	3
Crowsnest Spring	S	aggressiveness	1.9	2.1	14	4
Ptolemy Spring	S	aggressiveness	1.5	2.6	15	4
Ptolemy Creek Springs	S	aggressiveness	3.2	2.5	15	4
Emerald Lake Springs	S	aggressiveness	4.9	1.5	15	4
Studies where aggressiveness was calculated						
Cuves de Sassenage, Isère, France	S	pH	0.21	0.20	33	5
Baget, Ariège, France	U	pH	0.02	0.10	45	6
Ljubljanica, Slovenia, Yugoslavia	S	pH*	0.26	0.22	39	7
Kani Kedri, Iraq	S	pH	0.11	0.24	144	8
Crowsnest Spring	U	SI	0.005	0.01	6	9
El Abra, Mexico	S	SI	0.03	0.07	6	10
El Abra, Mexico	U	SI	0.45	0.15	4	11
Caves Branch, Belize	S	SI	0.07	0.28	64	12
Thompson Sp., Pa, USA	U	SI	0.03	0.14	16	14
Thompson Sp., Pa, USA	U	SI	0.23	0.04	30	15

Notes:

- Uses Trombe curves for equilibrium. These may underestimate saturation by up to 0.25 pH (Picknett, 1972)
- 1 Sampling over 12 months (Drew, 1970b)
- 2 Sampling over 12 months (Atkinson, 1977a)
- 3 Seventeen single samples in July or August from exsurges with catchments above the tree line (A) and below the tree line (B) (Lauritzen, 1981)
- 4 From this study
- 5 Sampled in 4 seasons over 4 years (Delannoy, 1983)
- 6 Regular sampling over 19 months (Bakalowicz, 1979)
- 7 Sampled August-February (Miserez, 1976)
- 8 From 6 springs, regularly sampled over 4 years (Jawad & Hussien, 1986)
- 9 Sampled in July (Ford, 1971)
- 10 Representative baseflow values from six major springs (Fish, 1977, p357)
- 11 Representative flood flow values from two major springs (Fish, 1977, p357)
- 12 From >20 autogenic cave streams, mostly in wet season (Miller, 1982)
- 13 Single samples or means from 30 exsurges (Christopher & Wilcock, 1981)
- 14 Sampled April, 1967 to January, 1968 (Shuster & White, 1971)
- 15 Sampled January to August, 1972 (Jobson & Langmuir, 1974)
- 16 From 15 springs, principally autogenic, sampled June-November (Cowell, 1976)

their dissolutional work in the epikarstic zone. The 1% accomplished in the endokarst is equivalent to $\Delta SI = 0.004$, or a mere 2-4% of the average measurement error of 0.1-0.2SI. This means that many endokarstic autogenic waters are statistically identical in SI units, with $SI_c = 0.0$.

4) The final advantage of measuring aggressiveness rather than calculating pH or SI equilibrium is that aggressiveness plots yield linear relationships which can be readily recognised and calculated (Figure 3.15). Such relationships would not be apparent on pH or SI plots, where these trends would be curvilinear (compare, for instance, Figures 8 and 9 in Lauritzen, 1981).

The above four reasons make it clear that aggressiveness determinations are more useful than SI in understanding autogenic endokarstic waters.

3.4.2. Neutron activation analysis

Several hundred water samples were collected in 8mm glass vials or 30ml polyethylene bottles for possible neutron activation analysis. It was found that the cardboard liners of the lids of the glass vial produced excessive contamination of dilute waters such as precipitation samples, and henceforth pre-rinsed polyethylene bottles only were used. Additionally, rock samples were collected, and analyses were also made of speleothem samples previously collected for radiometric dating.

Samples were analyzed on the nuclear reactor at McMaster, measuring concentrations of the elements Al, Ba, Br, Ca, Cl, Co, Cu, I, K, Mg, Mn, Na, Sr, Ti, U and V. The analytical technique is described by Vermette (1990), who found an accuracy of $\pm 5\text{-}20\%$ for different elements, using rainwater samples.

The Ca + Mg hardness of 11 samples was measured both by titration and by neutron activation analysis (NAA). The ratio NAA concentration / titration concentration was 0.993 ± 0.077 . The low standard error for titrations (0.58mg l^{-1})

compared to NAA (about $\pm 10\%$ for Ca + Mg: Vermette, 1989) suggests that most of the error lies with the NAA determinations.

A systematic variation in Sr/V ratios seemed to be evident between stalagmites recovered from Palliser Formation caves and Rundle Group caves, though many values were close to background levels. It was hoped that differences in trace element concentrations in groundwater samples might also reflect the strata traversed. However, element concentration in precipitation was very variable between precipitation events, and the only trace element systematically enriched in groundwater was Sr (Figure 3.16).

The greatest variation in spring trace element concentration was found in Cl, Na and Br, with concentrations sometimes varying by a factor of two over a period of hours (Figure 3.17). This variation is much greater proportionally than that of Ca and Mg, which are enriched to about the same degree whatever the flow path through the aquifer. The high variance is because Cl, Na, and Br concentrations are a function of sea-water enrichment of the precipitation, which has variable aquifer residence times. This ranges from days in the case of sinking streams to at least months in the case of infiltration through soils.

3.4.3. Stable isotope analysis

Samples were collected in 8ml glass vials for O and H isotopic analysis. Oxygen analyses were carried out by Martin Knyf at McMaster, and hydrogen analyses were made at the University of Calgary under the supervision of Chas Yonge. A large number of samples were collected, though some were rejected before analysis as the caps worked loose and there was visible evaporation.

It has been shown by Yonge et al. (1985) that the soil zone and upper few metres of bedrock are effective in homogenising the O and H isotopic signature of infiltration. Measurements from three caves gave a range $\delta^{18}\text{O}$ in cave seepage

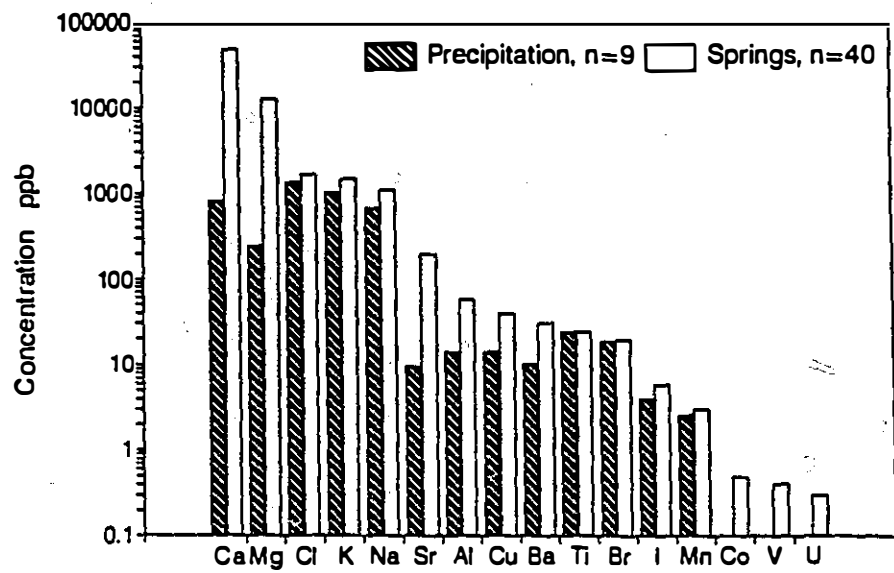


Figure 3.16 Concentrations of 16 elements in precipitation and in springs at Crowsnest Pass

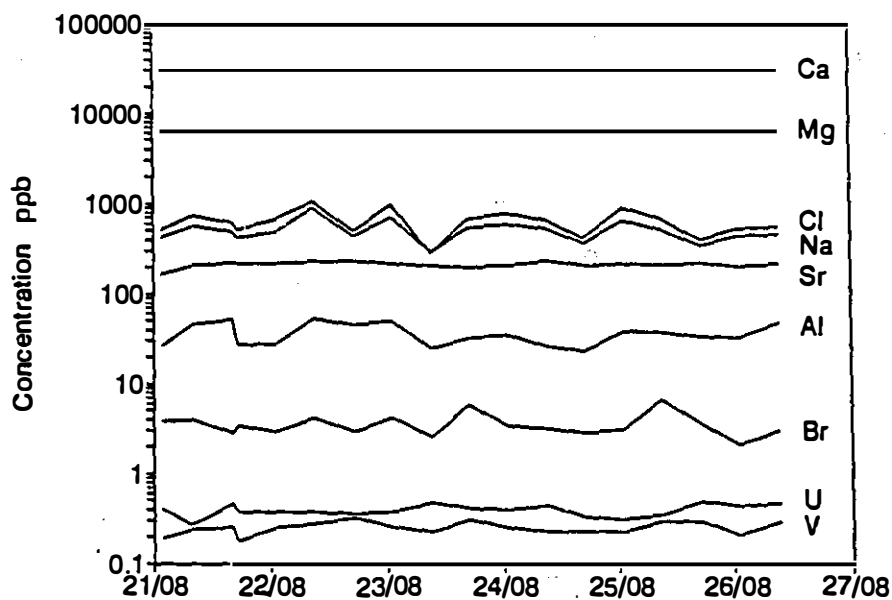


Figure 3.17 Concentrations of nine elements in Ptolemy Spring, August 21-26, 1986

waters of about 1‰, which is an order of magnitude less than the variation in precipitation.

On the other hand, sinking streams may rapidly conduct precipitation through a karst aquifer. The admixture of this allochthonous water to homogenised percolation water can produce a rapidly changing spring $\delta^{18}\text{O}$ chemograph. This is shown by the Baget Spring, France, which is fed in flood by a significant sinking stream. Hourly sampling over 18 hours during the rising limb of a flood event by Eberenz (1976) revealed four $\delta^{18}\text{O}$ peaks, with changes >2‰ occurring between successive samples on five occasions. This short-term variation is greater than the annual variation of 1.9‰ ($n=48$) recorded earlier by Bakalowicz et al. (1974). Moreover, the water in this single storm is markedly heavier ($-7.56 \pm 0.95\text{‰}$, $n=19$) than the mean recorded over two years ($-9.10 \pm 0.37\text{‰}$, $n=48$). These contrasts show that representative sampling of karst springs for isotopic analysis is difficult to achieve where there are significant sinking streams.

It was thought that $\delta^{18}\text{O}$ at Ptolemy Spring and Crowsnest Spring would vary little as both catchments are holokarstic. It was hoped to sample in September 1986 or 1987 the results of a late summer rainstorm, such as occurred in September 1985 (Figure 3.5). Such an event would be uncomplicated by the presence of snowmelt, and the high discharge would result in rapid flow through times. However, there were no suitable events in either year.

Results obtained from the two springs are shown in Table 3.10. They demonstrate rapid changes in $\delta^{18}\text{O}$ in both springs. As was found at the Baget Spring by Eberenz (1986), $\delta^{18}\text{O}$ changes >2‰ can occur in one hour. In the two comparable data sets, the $\delta^{18}\text{O}$ variation at Ptolemy Spring is greater than at Crowsnest Spring; this suggests a more dynamic flow system, and is in line with the hydrograph differences (Figure 3.5). The data also suggest that the mean catchment altitude of Crowsnest Spring may be marginally higher.

Table 3.10 $\delta^{18}\text{O}$ results from Ptolemy Spring and Crowsnest Spring

period	Ptolemy Spring		Crowsnest Spring	
	mean	n	mean	n
15/8/85-15/4/86	-18.20±0.57	18	-18.39±0.29	15
24/9/86-5/10/86	-14.52±1.56	24	-15.79±0.68	24
10/8/85-11/8/85	-16.78±1.01	24		

One set of samples from Ptolemy Spring, collected 10-11/8/85, was analyzed for both $\delta^{18}\text{O}$ and $\delta^2\text{H}$ (δD). The $\delta^{18}\text{O}/\delta\text{D}$ ratio plots along a line with a slope of 3.2 (Figure 3.18). Several interpretations of this data are possible:

- 1) The data represents extreme evaporation effects from a precipitation event of composition A in Figure 3.18. This can be dismissed as the soil cover over the lower part of the Ptolemy catchment must result in infiltration times of at least weeks.
- 2) The data represent mixing of two water sources, A and B. B could be derived from partial evaporation of high altitude precipitation of composition C in Figure 3.18, and/or melting of enriched firn (Arnoso, 1981). An orographic effect of $-5\text{\textperthousand km}^{-1}$ (Yurtsever and Gat, 1981) would result in mean difference of about 3\textperthousand between below and above the tree line mean values in the Ptolemy catchment. An annual $\delta^{18}\text{O}$ variation of $24\text{\textperthousand}$ has been recorded in precipitation at Calgary (Yonge, 1987), and firn from winter snowfall could be considerably depleted. Depletion of high-altitude precipitation is confirmed by two $\delta^{18}\text{O}$ analyses from Parrish Spring, which is 380m higher than Ptolemy Spring. On August 20th, spring flow was $-21.4\text{\textperthousand}$, and six days later it was $-17.6\text{\textperthousand}$.

The two above analyses from Parrish Spring, varying by $3.8\text{\textperthousand}$, well illustrate the problems of using $\delta^{18}\text{O}$ and δD for karst spring analysis. The input variation in these isotopes in mountainous catchments from snowmelt, from rapid infiltration over

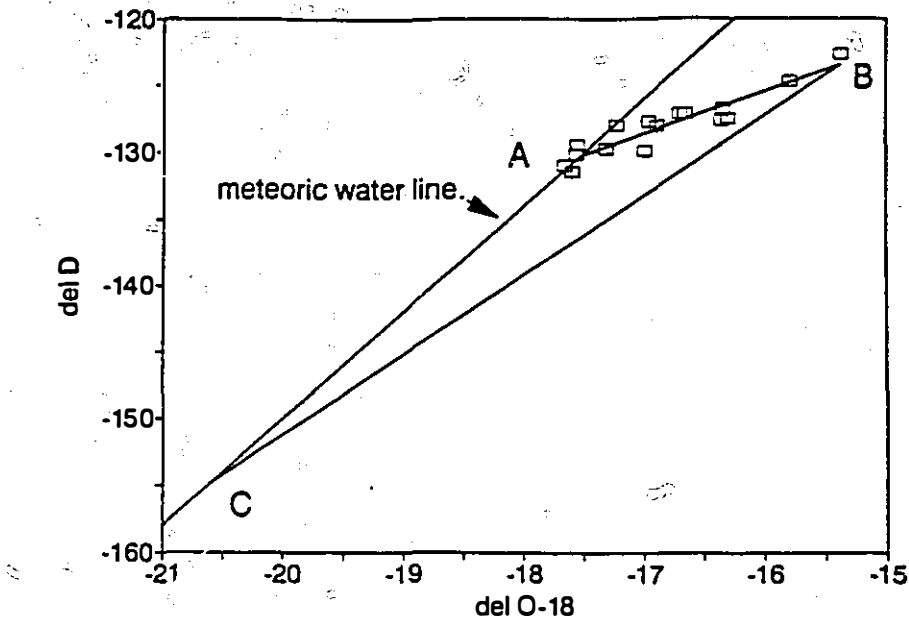


Figure 3.18 O and H isotope ratios at Ptolemy Spring, 10-11/8/85

bare rock, and from slow infiltration from soil percolation produces a spring output signal that is highly variable. This signal is only likely to be accurately measured once instantaneous recording field mass spectrometers become available.

3.5 Meteorology

Due to the large study area, the limited field seasons, difficult access to the higher parts of the field area for most of the year, and expected large spatial variation in precipitation due to aspect and altitude, it was considered to be unrealistic to gain comprehensive precipitation and temperature records from field measurement alone. Thus only a limited field programme was implemented, and this was supplemented by daily records collected by the Atmospheric Environment Service (1985, 1986).

Continuous temperature measurements were made at Crowsnest Pass (6 months), Andy Good Plateau (2 months) and the West Cirque of Andy Good Peak (3 months). These were complemented by daily maxima and minima recorded at Sentinel, 5km east of Crowsnest Pass (Figure 3.1).

Instantaneous precipitation was measured in the valley at Crowsnest Pass (altitude 1350m) over a six month period, and for two months in mid-summer on Andy Good Plateau (2320m), using tipping-bucket rain gauges. Regular rain gauges were set up in these locations and on Ptolemy Plateau. These measurements were complemented by using precipitation data from the Sacramento storage gauges network. This network was set up in the Fifties, in order to understand the distribution of precipitation on the eastern slopes of the Rockies, together with the effects of deforestation and reforestation, because of the vital role of this area in providing recharge to the Prairie provinces (Curry and Mann, 1965).

3.6 Characterisation of the springs at Crowsnest Pass

The principal challenge that emerged at an early stage of the field work for this thesis was to explain the considerable contrasts in regime and hydrochemistry between Ptolemy Spring and Crowsnest Spring. Discharge is much more variable at Ptolemy Spring than at Crowsnest Spring, with a lower maximum but much greater baseflow at the latter (Figure 3.5). Conversely, chronographs show a greater variability at Crowsnest Spring than at Ptolemy Spring (Figures 3.12, 3.14).

Though the response of the two springs is so different, most physical attributes suggest that they should be very similar. Both are holokarstic exsurgences. Flow velocities to the two springs (derived from dye traces) are essentially identical (Figure 3.6). The stratigraphy in both catchments is essentially the same (both mostly well-bedded pure Paleozoic limestones, with minor amounts of dolomite and impure limestone: Table 2.3), and the structure is the same (steeply dipping strata). Flow paths should be comparable, with flow along the strike towards Crowsnest Pass from

high-altitude inputs. The age of karstification is the same: the karst at Crowsnest Pass has been developing for about 85 million years since the formation of the Front Ranges (Gadd, 1986), and radiometric dating has shown that base level has dropped little during the Pleistocene (Ford et al., 1981).

Mean catchment altitudes are very similar. The isotope data (Table 3.10) suggests that the Crowsnest Spring catchment may be slightly higher in altitude, but the alkalinity data (Figure 3.8) suggests that this catchment is somewhat lower in altitude. Further details of catchment altitude are given in Section 5.6.

Despite all these similarities, existing karst aquifer classification systems based on hydrograph or chemograph analysis would classify the aquifers of the two springs as being very different, without being able to offer a convincing explanation for this. How to explain the contrasts is the central question of this thesis.

The spring contrasts may be due to differences in conditions within the aquifer (flow or storage) or at the boundaries of the aquifer (discharge or recharge).

Flow conditions within the aquifers must provide the explanation for the chemograph contrasts, since recharge to both aquifers (i.e. precipitation) has low solute loads. This groundwater flow must explain the dissolution not only of limestone, but also of the source rock for the sulphate (Figure 3.14).

Differences in flow velocity have often been cited as the cause of contrasts in both spring regimes and hydrochemistry. This usually follows the interpretation of Shuster and White (1971), who explained high-variance springs as being fed by conduit flow, while low-variance springs were fed by diffuse flow. However, it will be shown in Section 4.2.3 that the data of Shuster and White (1971) can be simply explained as differences between resurgences and exsurgences, and that there is not necessarily any difference in aquifer flow conditions indicated by their data. The hydraulics of flow in karst will be discussed in Chapter 5, and flow paths in karst aquifers will be investigated in Chapters 6 through 8.

A second possibility is that stratigraphic differences are the principal cause of aquifer differences. For instance, the sulphate might be derived from the Exshaw Shale, for it has been shown that flow paths to Crowsnest Spring do breach the Exshaw Shale (Figure 3.2). The subdued hydrograph might then be due to restricted flow through the Exshaw Shale, causing the ponding of water above it. However, the high sulphate values of Crowsnest Spring cannot be principally due to the fact that it emanates from the Palliser aquifer, for the Palliser springs of Emerald Lake have low sulphate values (Table 3.7). Furthermore, there is no hydrogeological reason why water should be ponded by the Exshaw Shale, for the principal flow vectors are on bedding planes and thrust faults. These flow vectors from the Banff Formation and Rundle Group would be directed along the strike towards Crowsnest Pass, with no need to traverse the Exshaw Shale.

A third possibility is that the contrasts are due to storage differences, associated with greater karstification of the Crowsnest Spring catchment. This would be the interpretation of the model of Mangin (1975, 1984). The similar geology and time for karst development, noted above, shed doubt upon this hypothesis. Moreover, it will be shown in Section 4.2.4 that the differences between the springs used by Mangin (1975) can be simply explained in terms of a vertical hierarchy of underflow and overflow springs.

The fourth possibility is that contrasts are due to part of the discharge emerging at other springs, as overflows or underflows. Occasionally, it has been shown that two or more springs belong to a vertical hierarchy, with the higher, overflow spring drying up during low-flow conditions, while the lower, underflow spring is perennial (e.g. Smart, 1983a,b). There are no overflows to either Ptolemy Spring or Crowsnest Spring. Both springs are perennial, so it would be thought that underflow springs would not be associated with either catchment. The little investigated properties of underflows and overflows will be discussed in Section 4.2.1, and the discussion will be extended to Crowsnest Pass in Chapter 9.

The remaining possibility is that spring contrasts are due to recharge differences. Both catchments are holokarstic, so there are no allogenic sinking streams, which would provide great contrasts in spring response. However, surface overflow during snowmelt was noted in Section 2.2.1, and this must affect the hydrographs at Ptolemy Spring and Crowsnest Spring. Such effects will be discussed in Section 4.2 and Chapter 9.

The causes for the contrasts between Crowsnest Spring and Ptolemy Spring will be explained in Chapter 10, once the characteristics of flow in karst have been thoroughly investigated in the intervening chapters.

Chapter 4

The influence of boundary conditions on spring discharge and chemistry

4.1 Introduction

The variability of discharge of karst springs is due to the attenuation of precipitation, snowmelt or streamflow input to the aquifer. The attenuation may be attributed to input, output or aquifer factors, or to a combination of the three. On the other hand, variability in spring chemographs is a function of concentration of dissolved ions in precipitation, snowmelt or streamflow recharge, aquifer processes which modify the concentration, and of flow velocities in the aquifer. Chemographs are thus more difficult to interpret.

There have been a large number of case studies of spring discharge and hydrochemistry in the last thirty years. Many of these have made inferences on the structure and behaviour of the karst aquifer, without fully considering the influence of boundary factors of the aquifer on the parameters measured. The important role played by boundary factors will be assessed in this chapter.

4.2 Underflow, full flow and overflow regimes

It was shown by Jakucs (1959) that the nature of recharge to a karst aquifer is an important factor in spring response, with low-variance springs being associated with autogenic percolation recharge, and high-variance springs being associated with concentrated allogeic recharge. There appear to have been no

studies specifically of spring response to surface streams which lose a part of their discharge to underlying karst aquifers, though this occurs frequently, and has been noted with many rivers in France, Yugoslavia, and elsewhere (e.g. Sweeting, 1973; Gospodarić and Habić, 1987; Bonacci, 1987). Spring altitude with respect to neighbouring springs can also be an important cause of discharge variation, though this too has been little discussed in the literature.

Springs which fully drain an area are here termed *full-flow springs*. Where streams exhibit distributary flow, then the lower element may be termed *underflow* and the upper element may be termed *overflow*. Where there are three or more springs, then the intermediate springs are *underflow-overflow springs*. Underflow and overflow occur both underground and on the surface. In the former case, it must usually be inferred from spring hydrographs. In the latter case, it may be obvious where surface streams leak part of their discharge to a karst aquifer.

Water budget calculations are helpful in determining if there may be ungauged underflow springs. For instance, calculations revealed that 33% of the discharge from the Mendip Hills, England is ungauged (Drew, 1975a; see Section 4.5). In the White Peak, England, the ungauged underflow proportion is 57% (Table 4.1). At the White Ridges, Vancouver Island, it is 86% (Ecock, 1984), and at Dorvan, France, it is 56% (Gibert et al., 1983). At Crowsnest Pass, only 34% of the discharge from the karst is to visible springs, with 31% discharging from aggraded springs, and 35% remaining as surface runoff (Section 10.6). Thus in five well-documented aquifers ungauged discharge accounts for 33-86% of the runoff.

Tracer tests have also shown that the streams in well-developed cave systems may resurge at aggraded springs. Examples include the deepest known cave in the world (Jean Bernard, France: Maire, 1990), and the deepest known cave in Canada (Arctomys Cave: Thompson, 1976).

It is difficult to characterise karst aquifers which have unobserved springs, since such springs may well be underflows, with different discharge and

Table 4.1 Discharge budget for the White Peak, England (after Edmunds, 1971 and Christopher et al., 1977)

Discharge	m^3s^{-1}	m^3s^{-1}	%
Recharge to limestone aquifer		13.5	100
Discharge from limestone aquifer			
Lower Dove resurgences	1.05		
Ilam resurgences	0.80		
Meerbrook Sough	0.74		
Wormhill Springs	0.53		
Magpie Sough	0.47		
Bradwell Brook	0.38		
Hillcar Sough	0.37		
Peaks Hole Water	0.26		
other smaller springs	0.52		
Water Authority abstractions	0.66*		

Total gauged discharge	5.8	5.8	43

Ungauged discharge		7.7	57

* This is the guaranteed (i.e. minimum) yield only, and peak abstraction rates would be more. The Meerbrook Sough discharge is also utilised.

hydrochemical characteristics than the observed springs.

Such behaviour has been documented. For instance, Smart (1988b) studied a series of about 80 karst springs over a 150m vertical range along the Castleguard valley, Alberta and concluded that "the springs appear to be organised into a vertical hierarchy with steady sustained flow from the lowest "underflow" members, short-lived, highly variable flow from higher level outputs, and complete abandonment of the highest outlets" (see Section 11.2.1). A similar hierarchy is apparent at Maligne, Alberta where there are >60 springs (Smart, 1988a; Ford, 1991) (see Section 11.2.2).

At Crowsnest Pass, the five overflow springs along Emerald Cliff demonstrate similar behaviour, with the highest spring flowing for the shortest period, and permanent flow being sustained by sublacustrine springflow from Emerald Lake. There are many other seasonal overflow springs at Crowsnest Pass. The extent to which these are complemented by underflow from the low altitude springs is discussed in Chapter 7.

Underflow and overflow springs seem to be equally important in other karst areas, so it is worthwhile to be able to recognise underflow, overflow and full-flow behaviour. Overflow springs (*trop pleins* in French) have been widely recognised in karst areas, for the cessation of flow is easily recognised. However, underflow springs have not been widely described, and there is no term in French for underflow (Meus, 1990).

The simplest method of differentiating spring types is on the basis of the ratio between maximum annual discharge (Q_x) and minimum annual discharge (Q_n) and the proportion of time when $Q>0$ (Table 4.2).

Table 4.2 Discharge characteristics for distinguishing flow types

	Q/Q_n	days with $Q > 0$
full flow	high	all
underflow	low	all
overflow	∞	few - all
underflow-overflow	∞	few - all

In practice, this approach is often hindered by two factors. The discharge record for a complete year is often unobtainable; this is especially true in the Rocky Mountains, where many springs are buried under several metres of snow in winter. Second, many (or perhaps most) springs are compound types, and may have minor underflow and overflow components which are difficult to identify. A more sophisticated approach is thus needed.

One of the principal tools in the analysis of spring hydrographs is recession analysis. Recessions are divided into two stages, an initial quickflow stage when discharge falls rapidly, followed by a baseflow stage when discharge declines exponentially so that

$$Q_t = Q_0 e^{-\alpha t} \quad (4.1)$$

where Q_0 is the baseflow at the beginning of the recession ($t=0$), and α is the recession exponent. By convention, Q is normally expressed in $m^3 s^{-1}$, while t is expressed in days. Equation 4.1 has been used in many studies of karst springs (e.g. Mangin, 1975; Atkinson, 1977a; Milanovic, 1976, 1981). Baseflow usually can be fitted to a single value of α , though this may vary seasonally. For instance, Worthington (1984c) found that five summer and fall baseflow recessions at Locust Spring measured by Coward (1975) fitted the equation

$$Q_t = 0.26 e^{-0.019t} \quad (4.2)$$

However, three winter recessions exhibit both higher baseflow discharges and faster recessions, with

$$Q_t = 0.51 e^{-0.022t} \quad (4.3)$$

Figure 4.1 shows how six types of spring may be recognised on the basis of recession exponents. This interpretation is based on the assumption that recession form is a function of aquifer boundary factors. It should be noted that the conventional hypothesis for variation in recession exponents is that it is a function of aquifer differences, unless there are obvious discrepancies such as the spring drying up. The question of aquifer differences is returned to in the conclusion of this chapter.

The simplest case is a linear log-normal recession (α constant with time), which reflects *full flow* (Figure 4.1 - type 1). Most karst spring recession analysis has made the assumption of full flow, though this needs to be tested before interpretations are made (Ford and Williams, 1989, p195). In fact, it appears that full-flow karst springs are rare. For instance, Quinlan and Ewers (1989) found that all but one of the 21 larger catchments in the Mammoth Cave area were drained by multiple springs.

Convexlog-normal baseflow recessions (α increasing with time) distinguish overflow springs. Almost all overflow springs that have been recognised are of type 2 in Figure 4.1, with a minimum annual discharge of zero. Such springs are rarely monitored, though Smart (1983a,b) studied several examples. Perennial overflow springs are also possible (Figure 4.1 - type 3), though it seems that most authors equate overflow springs solely with lack of permanency.

Underflow springs are of two types. The first is characterised by the absence, or loss, of quickflow (Figure 4.1 - type 4A). This may be called a *losing* or

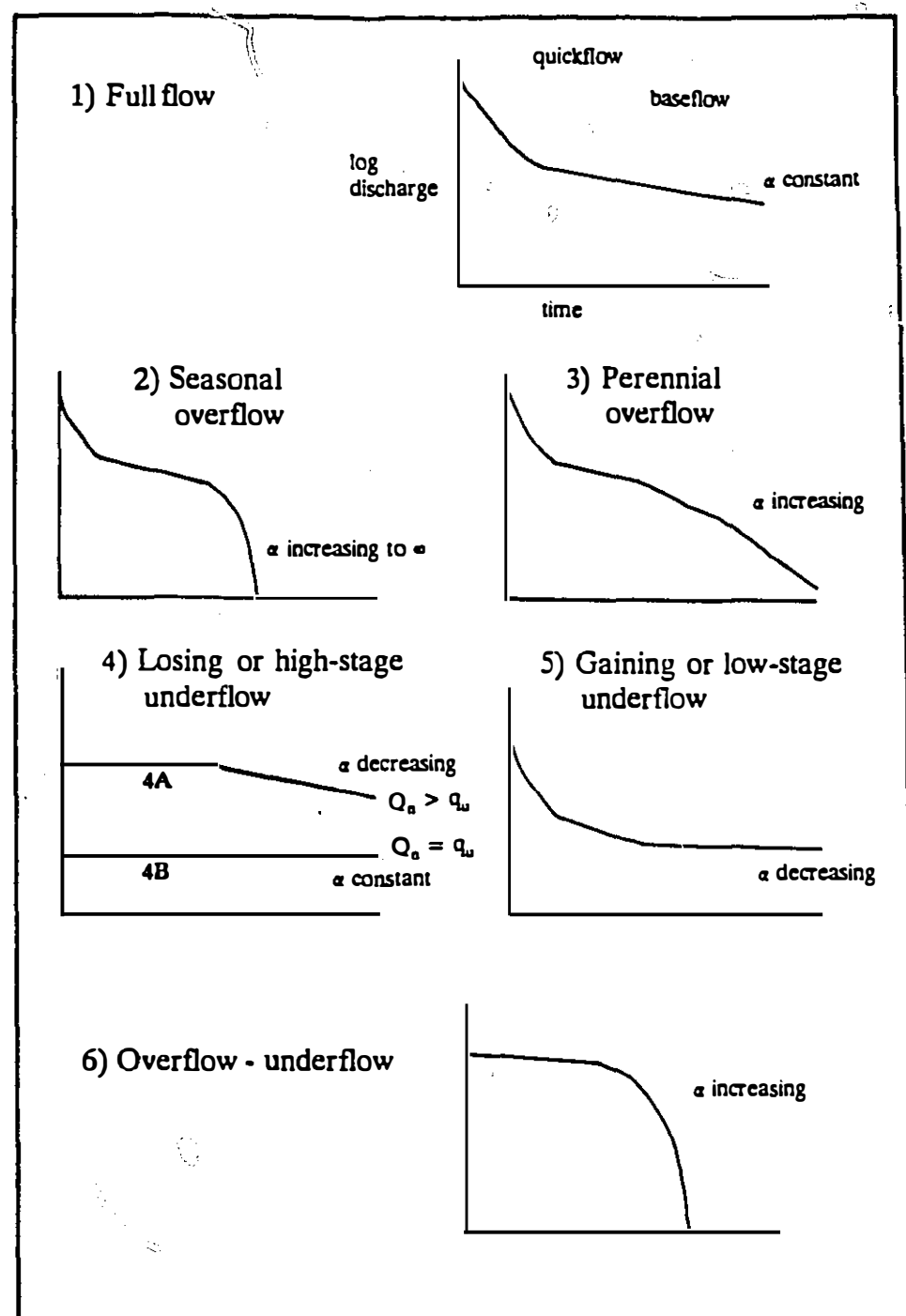


Figure 4.1 Recession exponents as an indicator of aquifer boundary conditions

high-stage underflow. Maximum discharge is controlled by a constriction close to the output. At high stages, the water level in the conduit upstream of the constriction backs up until an overflow is found. This thereafter provides a constant head to the constriction, and hence a constant discharge, resulting in the "plateau". Where plateau discharge is less than minimum catchment discharge, then a constant discharge hydrograph will result (Figure 4.1 - type 4B).

The second type of underflow is characterised by a concave log-normal baseflow recession (α decreasing with time) (Figure 4.1 - type 5). This may be called a *gaining* or *low-stage underflow*, as a normal full-flow recession is supplemented by underflow. The underflow could be from an external source (a surface stream leaking into its bed) or from an internal source (leakage from other cave streams).

The remaining type of karst spring is the underflow-overflow spring. The simplest form is shown in Figure 4.1 - type 6).

The variety in recession form shown in Figure 4.1 encompasses all the differences found in karst springs, so that it could be argued that all spring variance is due to boundary factors, and none to aquifer variance. To test this hypothesis, the boundary factors will be examined of examples from five of the most influential and best-studied karsts.

The karst in Slovenia, Yugoslavia has been called the Classical Karst (Sweeting, 1973), and is the type area for karst. Yugoslavia probably has the most extensively studied karst hydrogeology (e.g. Herak, 1972; Milanovic, 1976, 1981; Torbarov, 1976; Gospodaric and Habic, 1976; Bonacci, 1987), though much of the information has not been published in English.

The Valles - San Luis Potosi area, Mexico has three of the largest karst springs in the world (Frio, Coy, Mante), the deepest spring explored by diving (Mante, -280m), long groundwater flow distances (≈ 200 km), as well as spectacular

surface karst which includes the deepest shaft in the world (El Sótano del Barro). The hydrology and hydrochemistry of this area was studied by Fish (1977).

The remaining three areas have given rise to some of the most influential ideas on karst aquifers (see White, 1988, p171-192; Ford and Williams, 1989, p193-218). They are the Mendip Hills, England (Ford, 1965; Drew, 1975a; Newson, 1971; Smith and Newson, 1974; Smith et al., 1976; Atkinson, 1977; Friederich and Smart, 1981; Stanton and Smart, 1981), three springs in Ariège, France (Mangin, 1975, 1984), and several springs in central Pennsylvania, USA (Shuster and White, 1971; Jacobson and Langmuir, 1974).

In the following discussion, three axioms of karst groundwater flow will be used. First, each overflow stream or spring has a complementary underflow stream or spring, and vice versa. Second, any surface stream on karst either loses water to, or gains water from groundwater, or frequently both. Third, hydraulic gradients ensure that at least some groundwater flow emerges at the lowest outcrop point of the catchment (except in coastal aquifers, where the denser seawater will limit freshwater flow depth).

4.3 Springs of the Dinaric karst, Yugoslavia

Studies of the Dinaric mountains of Yugoslavia have had a profound influence on karst studies, giving such terms as doline, polje, and karst to the discipline. Groundwater flow is generally south towards the Adriatic, or north, towards the Sava, a tributary of the Danube. Karstic springs such as Trebišnjica, Buna, Ljubljanica, Ombla and Ruda are amongst the largest in the world (Ford and Williams, 1989, p155).

The Dinaric mountains are characterised by rugged topography with no surface flow, interspersed with poljes which often have large surface rivers. Dye

tracing and discharge measurements has shown that most of these rivers gradually sink into their beds, and that groundwater flow is often divergent, to different springs from the same stretch of river. Well-documented examples include Glamočko, Popovo and Nikšićko poljes (Herak, 1972), and Cerkniško, Loško and Planina poljes (Gospodarić and Habič, 1976). Discharge losses can equal the flow of the largest springs. For instance, the Trebišnjica River in Popovo Polje loses up to $130\text{m}^3\text{s}^{-1}$ in sinks along its river bed along a 70km stretch of the river (Milanović, 1981). The largest spring receiving leakage from the Trebišnjica River is Ombla Spring. This spring exhibits sustained discharge with a low α (0.0058) at low stages, which corresponds to type 5 in Figure 4.1. This could simply be a function of sustained recharge from the Trebišnjica River, rather than be a function of a sustained aquifer recession, as Milanovic (1981) inferred.

It is difficult to fully characterise groundwater flow towards the Adriatic, for unmonitored submarine springs play an important role. On the other hand, this problem is absent in the Sava catchment, which drains eastward to the Danube. The most important springs in the Sava catchment are the Ljubljanica springs, with a mean discharge (Q_m) of $39\text{m}^3\text{s}^{-1}$. The following is based upon a major cooperative study culminating in the simultaneous injection of 14 tracers, with subsequent recovery at 20 springs (Gospodarić and Habič, 1976).

The Ljubljanica springs are spread over a distance of 5km. They can be split geographically into four groups. The most important, with 57% of the discharge is a 1100m long linear array of springs which feed the Velika Ljubljanica and Lubija Rivers. Precise altitude measurements ($\pm 0.01\text{m}$ or better) and Q_s , Q_m and Q_n for eight springs during a 43 day period are given in Hribar (1976). A ninth spring was almost always dry; this was the highest spring, at an altitude of 292.8m. The ratios Q_s/Q_m , Q_m/Q_n and Q_s/Q_n all show a positive correlation with altitude. However since

Q_n for the two highest of the eight monitored springs is zero, it is more useful in this case to use Q_x/Q_m .

Figure 4.2 shows spring altitude and Q_x/Q_m for these eight springs. The vertical separation between the highest and lowest spring is only 1.53m, yet Q_x/Q_m varies by a factor of four. This is an impressive demonstration of the effect that minute spring altitude differences can have on spring hydrographs, with the lowest underflow (#41) varying little (Figure 4.1, type 4), while the highest overflows (#24, 45, 44) vary most, with all these drying up in low flow conditions (Figure 4.1, type 2).

Six of the springs in Figure 4.2 show a near-perfect exponential correlation:

$$Q_x/Q_m = 1.39 \cdot 2.66^H \quad (n = 6, r^2 = 0.995) \quad (4.4)$$

where H is the altitude above the lowest spring (#41). This suggests that all six springs are connected by well-developed flooded conduits. The slightly anomalous ratios of springs 21 and 42 could be due to vadose passage between the main conduits and the springs, amounting to an altitude drop of 0.28m for spring 21, and 0.12m for spring 42. These altitude differences are shown as 21-21A and 42-42A in Figure 4.2.

The dye tracing demonstrates rapid flow to all springs (mean velocity $v_m = 0.05 \text{ m s}^{-1}$). However, contrasts in dye velocity and concentration show that they are not fed by a single conduit with distributaries to all springs. Instead there must be a complex tributary-distributary network of conduits (Gospodarić and Habić, 1976).

The Ljubljanica study shows that catchment output boundary factors (spring altitude in this case) can be the main determinant of spring hydrograph form. Conversely, the response of Ombla Spring may be dominated by input boundary factors (leakage rate from the Trebišnjica River). In both cases, the large catchments and complex hydrogeology make spring hydrograph interpretation difficult.

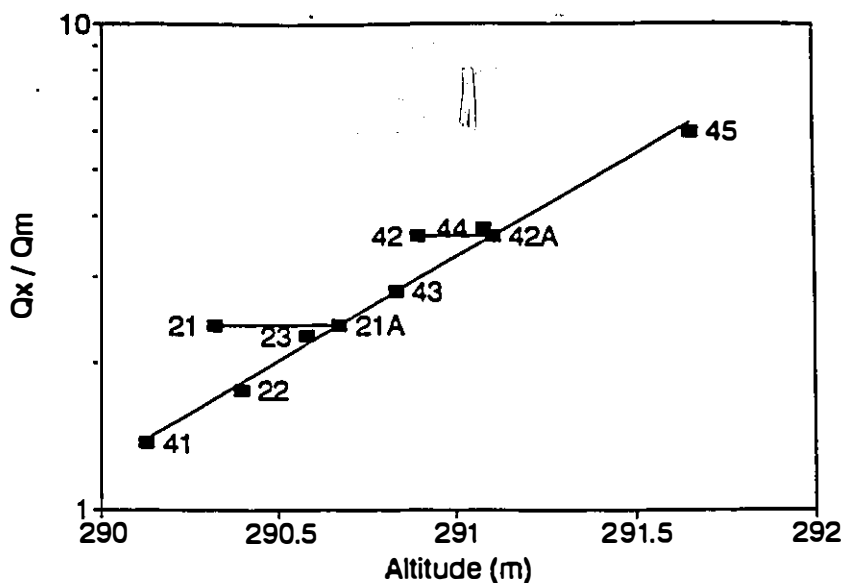


Figure 4.2 Ratio of maximum discharge to mean discharge at Ljubljanica springs (data from Gospodarić & Habić, 1976)

4.4 Valles - San Luis Potosí region, Mexico

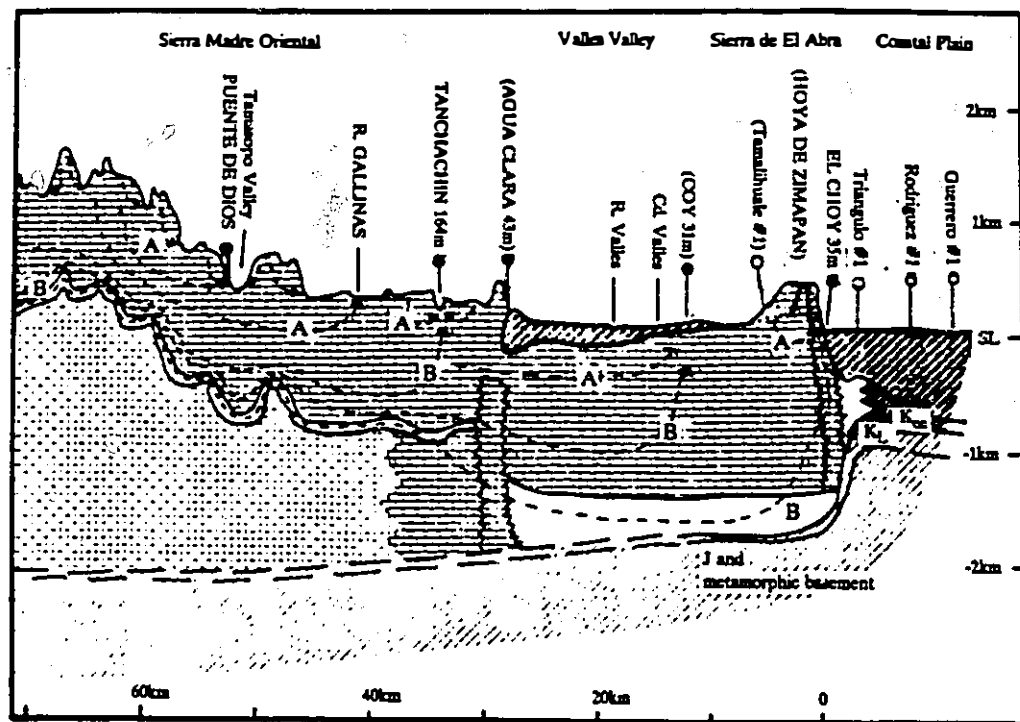
Fish (1977) investigated the large karst springs of part of the Sierra Madre Oriental in northern Mexico. These included Frio ($Q_m = 28 \text{ m}^3 \text{s}^{-1}$), Coy ($Q_m = 24 \text{ m}^3 \text{s}^{-1}$), Huichihuayán ($Q_m \approx 10\text{-}20 \text{ m}^3 \text{s}^{-1}$), San Juanito ($Q_m \approx 10\text{-}20 \text{ m}^3 \text{s}^{-1}$), Mante ($Q_m = 12 \text{ m}^3 \text{s}^{-1}$), Choy ($Q_m = 5 \text{ m}^3 \text{s}^{-1}$), Media Luna ($Q_m = 4.5 \text{ m}^3 \text{s}^{-1}$) and Santa Clara ($Q_m \approx 4 \text{ m}^3 \text{s}^{-1}$). All of these except Media Luna are situated at or close to the eastern boundary of the mountains. Water balance estimates indicated drainage distances of up to 200km. Some surface rivers cross the catchment area, losing underflow to the karst. For instance, the Rio Verde at Tanlacut has a surface catchment area of 6039km², a mean discharge of 7.6m³s⁻¹, but a minimum discharge of nil. However,

60km further upstream, annual discharges sometimes exceed the discharge at Tanlacut (Fish, 1977, p128).

Fish (1977) found elevated temperatures and high sulphate concentrations in many of the springs. He reasoned that the flow of these springs had been in contact with anhydrite deposits buried >1km below the surface under folded platform and reef limestones (Figure 4.3). Furthermore, Mante is a vauclusian spring, which has been dived to a depth of 270m and which continues to descend steeply beyond this point. Several large fossil springs have also been found, with similar deep vauclusian characteristics. The principal examples are Hoya de Zimapán (295m deep), Cueva de la Ceiba (195m deep), and Cueva del Nacimiento del Río Choy, a fossil resurgence which rises vertically for 100m above the present Choy spring.

The springs at the eastern boundary of the area may be divided into two groups, with Coy and Mante being the lowest springs in the southern and northern groups, respectively. High-sulphate springs have high temperatures, low Q_w/Q_n , and an altitude close to the lowest springs. Low-sulphate springs generally have low temperature, high Q_w/Q_n , and are located some tens of metres higher than the base-level springs (Table 4.3). Fish (1977) concluded that the low-altitude, high-sulphate springs receive water from two sources, a deep long-distance circulation, and a shallow more local flow. On the other hand, the low-sulphate springs receive only shallow local flow (Figure 4.3).

The range in discharges suggests that the springs are part of two underflow-overflow hierarchies, with Coy and Mante being the lowest members of each spring group. Furthermore, even as a set they are not full-flow springs, for there is considerable surface overflow from the catchment.



- K_u, T, K_o (Cuesta del Cura): impermeable
- Tamasopo, El Abra & K_L reef and platform facies; karstic
- El Abra basal or forereef dolomites
- K_L Guaxcamá gypsum, anhydrite, limestone and dolomite
- Tamaulipas, other basal K_o and below
- A Ca, HCO₃
- B Ca, Mg, SO₄, HCO₃
- > flow path
- spring
- well

Figure 4.3 Cross-section of the Sierra Madre Oriental and El Abra Ranges, Mexico, (after Fish, 1977). The topography is shown at latitude 22°N. In the El Abra Range, the topography at 22°N is shown by a dotted line, while the solid line represents the topography 25km further north at Hoya de Zimapán (a fossil phreatic conduit). Names in brackets represent locations not exactly on the line of the section. Coy spring is one of the largest springs in the world, with a mean discharge of 24 m³s⁻¹; it is located in platform facies El Abra Limestone, which forms a 3 km² inlier in shale. At this spring and at El Choy spring there is a large positive water balance, which shows that the major groundwater vectors must be below the 20km wide impermeable outcrop in the Valles valley. This flow is driven by a hydraulic gradient <0.001. The deep flow paths are indicated by high spring temperatures, and are characterised by high sulphate values.

Table 4.3 Major karst springs of the Valles - San Luis Potosí platform, Mexico (data from Fish, 1977)

	SO ₄ ²⁻ max. mg l ⁻¹	Temp. max. °C	Q _w /Q _n m ³ s ⁻¹	Q _n m ³ s ⁻¹	Alt. m	Alt.* m
high sulphate						
Coy	836	24.6	1.87	15	31	0
Mante	535	26.5	1.87	8	80	0
Choy	445	26.4	2.8	2.5	35	4
Agua Clara	500	24.0	2.2	1	43	12
medium sulphate						
Frió	180	23	4.4	6	90	10
Pimienta	300	22.5	~	0	105	74
low sulphate						
Sabinas	12	21	54	0.3	160	80
San Juanito	5	19.6	(20)	1	100	69
Huichihuayán	4	20	24	1	100	69
Santa Clara (7)	24	15	0.3	75-100	44-69	

* altitude in metres above lowest regional karst spring (Coy for the southern El Abra, and Mante for the northern El Abra)

4.5 The Mendip Hills, England

The Mendips are an isolated range of hills rising above the Somerset Levels, a former marsh just above sea level. They are principally composed of limestone, and percolation water makes up 74-100% of the discharge of the various karst springs (Drew, 1975a).

Newson (1971) studied total hardness in streams sinking into caves, in percolation water and in spring waters, and found that spring total hardness could be expressed in terms of a simple two-component mixing model. For instance, Rickford Spring received 1-15% sinking stream water of calculated mean hardness 124 mg l^{-1} mixed with 85-99% percolation water of calculated mean hardness 288 mg l^{-1} . Furthermore, the coefficient of variation of hardness (CVH) of different springs was found to be a function of the average sinking stream component of resurgence discharge.

The factors causing spring variability have not been definitively studied in the Mendips. Drew (1975) suggested that spring variability was greater for springs with a larger percentage of their catchments fed by sinking streams. Underflow /overflow differences also seem to be important. The evidence for this is threefold. First, ten sinking streams have been tested by tracers to more than one spring (Drew, 1975; Atkinson, 1977a). Second, several springs have known overflows (e.g. Ashwick Higher, Ashwick Lower, Cheddar: Drew 1970b, 1975b). Third, at least one spring (Langford: Smith and Newson, 1974) dries up during droughts, indicating there must be an underflow component. Fourth, and most important is the indication of underflow that comes from water balance calculations (Drew, 1975a).

Drew computed a water budget for the whole of the Mendip Hills for 1969, and found that measured spring discharge accounted for only 67% of the aquifer recharge. He offered two explanations. There could be local underflow to

fluvioglacial deposits adjacent to the Mendips. Alternatively, or additionally, there could be deep groundwater flow. He cited borehole evidence from areas close to the Mendips and freshwater springs in the Bristol Channel around the islands of Steepholme and Flatholme to support this. Furthermore, deep karstic flow has been shown to exist from the northern shore of the Bristol Channel, where the Great Spring in a submarine railway tunnel has a mean discharge of 860 l s^{-1} (Drew, Newson and Smith, 1970).

The putative underflow loss from the Mendips karst casts doubt on existing hydrogeological interpretations of flow. For instance, the water budget calculations of Drew (1975a) indicate the Cheddar catchment may be 55 km^2 , rather than the 39 km^2 calculated by Atkinson (1977), with the difference being represented by ungauged underflow. If this is true, then quickflow to known springs in the Cheddar catchment would represent about 36% of runoff, rather than the 50-54% calculated by Atkinson (1977).

The evidence from the Mendip Hills thus suggests that variation in spring chemographs is principally a function of input boundary factors (sinking stream or percolation). On the other hand, contrasts between spring hydrographs may be due to input boundary factors (sinking streams or percolation), and overflow/underflow both within the aquifer and at the outputs.

4.6 Karst springs of Nittany Valley, Pennsylvania, USA

The Nittany Valley area is composed of dolomites and limestones, interbedded with siliciclastic strata. Structural dips are steep ($>15^\circ$), so that groundwater flow is principally strike-oriented towards the surface streams which cut across the strata.

Shuster and White found the karst springs to be of two contrasting types (Shuster and White, 1971). Six springs with low variability in chemistry, temperature and discharge had a median Q_s/Q_n of 6.7. Seven other springs had high variability in chemistry, temperature and discharge, with a median Q_s/Q_n of 20 (Shuster and White, 1971). The low-variability springs were "located in mid-valley areas. They receive water primarily from these areas, and via deeper and distant groundwater flow patterns" (Jacobson and Langmuir, 1974, p263). The high-variability springs are "normally near the foot of major sandstone-shale ridges along strike from a sinking stream" (Jacobson and Langmuir, 1974, p262).

The coefficient of variation of hardness (CVH) was used by Shuster and White (1971) as the principal statistical parameter for distinguishing the two sets, with the values for the low- and high-variability springs being 2% and 23% respectively. Shuster and White (1971) attributed the differences between the two types as being due to aquifer contrasts (diffuse flow or conduit flow). However, in the Mendip Hills (see Section 4.5), and in Scotland, Ireland and Wales, Newson (1971) found a strong correlation between CVH and aquifer boundary factors (i.e. percolation or sinking stream input). This relationship might be anticipated. Sinking stream water is highly variable in discharge and temperature, and sometimes in chemistry as well, and will pass through a short underground flow route with little change in any of these parameters. On the other hand, percolation water may have a residence time of several months in the soil zone, and so will become homogenized with respect to isotopic composition, temperature, and chemical composition (Drew, 1970a; Pitty et al., 1979; Friederich and Smart, 1981; Gunn, 1983; Yonge et al., 1985).

The relationship between CVH and aquifer boundary factors is shown in Figure 4.4 for the combined data sets from the aforementioned papers, together with other results from England (Ternan, 1972; Pitty, 1974), Mexico (Fish, 1977), Wales (Ede, 1972), France (Bakalowicz, 1979; Delannoy, 1983), the USA (Hess and White,

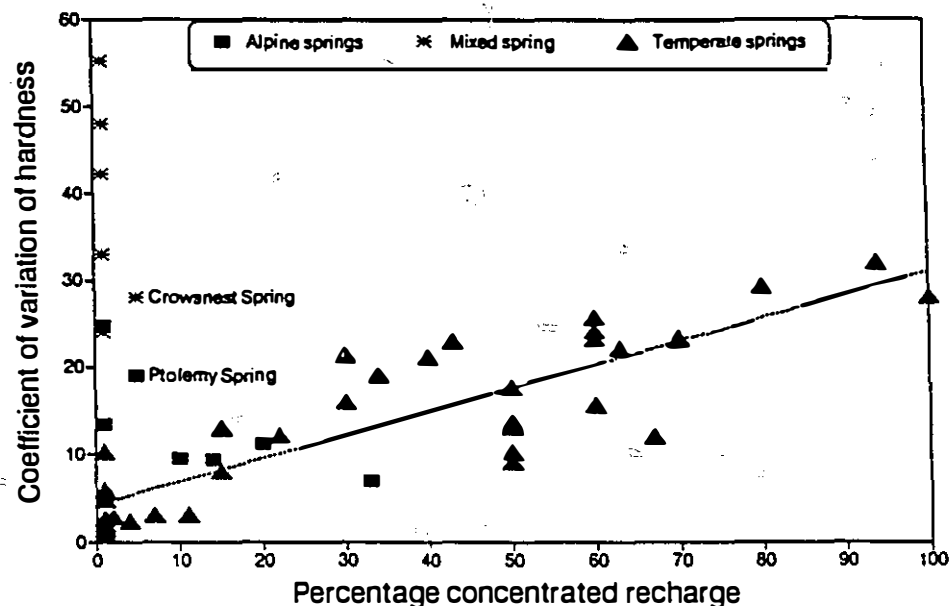


Figure 4.4 Relationship between coefficient of variation of hardness and proportion of concentrated recharge to karst aquifers
The data sets are explained in the text

1989), and Alberta (this thesis). The alpine and Mexican data are clearly anomalous, while linear regression of the temperate data gives

$$C = 0.27 R + 4.1 \quad (n = 36; r^2 = 0.76) \quad (4.5)$$

where C is the CVH, and R is the % of recharge to the karst aquifer that is concentrated in streams.

Drew (1970b) and Drake and Harmon (1973) studied both sinking streams and springs, and found input hydrochemistry to be an important factor in spring response. This concept is reinforced by Figure 4.4. The sinking streams in Gower (Wales), Clare (Ireland) and Sutherland (Scotland) flow off carbonate-poor

catchments, so that chemical contrasts between allogenic and autogenic components of the catchments are high, and so the CVH values for these springs are somewhat greater than recession line values.

The high CVH values of the anomalous alpine and Mexican data in Figure 4.4 also reflect mixing of different water types. In these cases, the coefficient of variation of bicarbonate (CVB) and of sulphate (CVS) help to show the character of the different water types (Table 4.4). It will be shown in Chapters 9 and 10 that the high CVB at Ptolemy Spring and Crowsnest Spring represents the mixing of low-altitude and high-altitude water, and the high CVS represents the mixing of dynamic phreatic and non-phreatic water. Fish (1977) similarly explained the variance of Choy and other Mexican exsurges in terms of the mixing of local low-temperature calcium bicarbonate waters with distant thermal calcium bicarbonate plus sulphate waters.

Though Figure 4.4 suggests that most of the CVH variance may be due to input differences (sinking stream or percolation), these are probably complemented by underflow and overflow at the output of the aquifer. The mean altitude of the high-variability springs of Shuster and White (1971) is 40m higher than the low-variability springs. Moreover, all seven high-variability springs are situated above local base level; there must be some groundwater flow along the strike to the transverse base-level creeks (Spring Creek and Juniata River; axiom 3, p81). Groundwater gradients downstream of the springs of 0.0011-0.0066 should be enough to cause significant underflow over the 5-30km distances to Spring Creek and Juniata River, where they should emerge as low-variability springs. Jacobson and Langmuir (1974) studied 19 springs in the Spring Creek area, and found a number of low-variability springs at low altitude along Spring Creek.

The evidence from Nittany Valley thus supports the hypothesis that spring hydrology and hydrochemistry are principally a function of boundary factors.

Table 4.4 Variation in anion concentrations in underflow and overflow springs

	n	Coefficient of variation of total hardness (CVH) %	bicarbonate (CVB) %	sulphate (CVS) %
Crowsnest Pass				
Crowsnest Spring	15	21.1	11.6	50.5
Ptolemy Spring	15	21.9	22.2	35.8
Pennsylvania, USA (Jacobson & Langmuir, 1974)				
Rock Spring	36	26.0	28.6	12.7
Thompson Spring	30	4.8	2.7	17.8
Indiana, USA (Bassett, 1976; Krothe & Libra, 1983)				
Orangeville	36	29	24	75
White R. freshwater spr.	4	62	37	69
White R. mineral spr.	4	25	13	29
El Abra, Mexico (Fish, 1977)				
Choy	22	42.2	7.3	83
Coy	11	55.2	15.3	78.5
Frio	4	23.9	8.2	48.6
Tananchin	4	48.0	15.6	77.0
Taninul sulphur pool	8	8.6	8.0	19.9
Dorvan, France (Gibert et al., 1983)				
Cormoran	34	33	3.1	56
Pissoir	29	9.5	12.4	24

Note:

The Crowsnest data are discharge-weighted values from April-September 1986. The annual CVH from 1985-1986 is 33% for Crowsnest Spring and 24% for Ptolemy Spring (Table 3.8).

Hydrochemistry is largely controlled by input differences (Drake and Harmon, 1973), while discharge may be a function of the overall groundwater flow, of which underflow and overflow springs are complementary parts.

4.7 Karst springs of Ariège, France

Three karstic springs in Ariège, France have been studied over a period of years by Mangin (1975, 1984), Bakalowicz (1979), and others. The principal characteristics of the springs are given in Table 4.5.

Table 4.5 Characteristics of Aliou, Le Baget and Fontestorbes Springs, Ariège (after Mangin, 1975, 1984)

	Aliou	Le Baget	Fontestorbes
catchment area (km^2)	11.93	13.25	85
karstic % of catchment	80	67	83
mean catchment altitude (m)	931	923	1295
spring altitude (m)	441	498	510
mean discharge 1970-1979 ($\text{m}^3 \text{s}^{-1}$)	0.484	0.552	2.418

The discharge response of the three springs is very different. Figure 4.5a shows the three most sustained recessions studied by Mangin (1975). Both specific discharge maxima and baseflow recession indices (α) are highest for Aliou, intermediate for Le Baget, and lowest for Fontestorbes.

These contrasts were explained by Mangin (1975, 1984) as being due to storage differences between the three catchments. However, they could equally be due to overflow and underflow. Recession indices for the last 60 days of the 1970

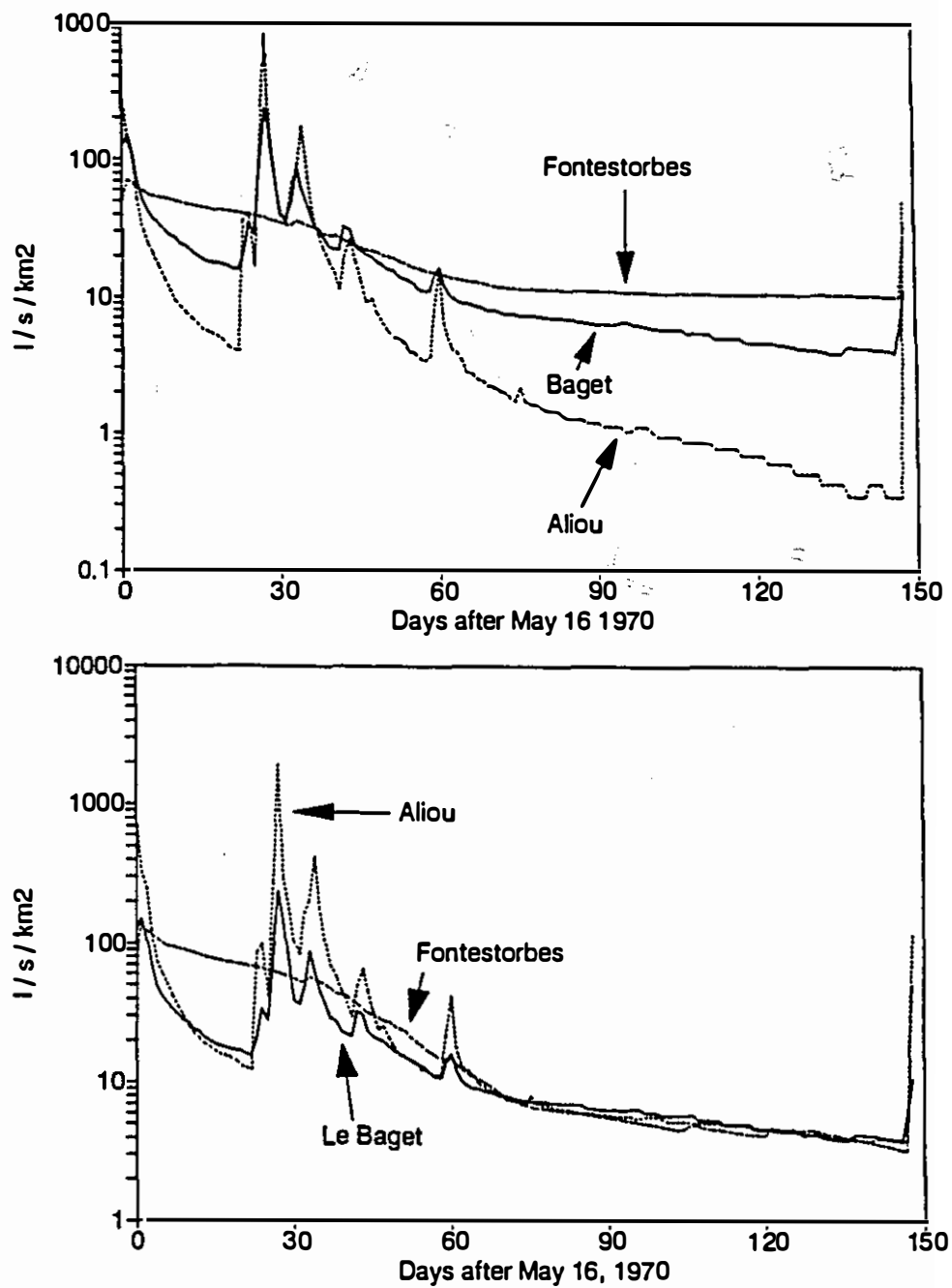


Figure 4.5 Summer recessions of Fontestorbes, Le Baget, and Aliou springs, Ariège, France

a) gauged flow assuming fixed catchments giving an annual water balance (Fontestorbes 86km², Le Baget 13km², Aliou 12km²: after Mangin, 1975)

b) assuming fixed catchments of 40km² for Fontestorbes, 13km² for Le Baget, and 5km² for Aliou, but with an underflow loss of 15km² for Aliou, and an underflow gain of 700l s⁻¹ for Fontestorbes.

recession (days 86-146) are given in Table 4.6.

Table 4.6 Baseflow recession indices for Aliou, Le Baget and Fontestorbes Springs, Ariège in 1970 (data from Mangin, 1975)

period	baseflow recession index (α)		
	Aliou	Le Baget	Fontestorbes
August 11 - October 10	0.022	0.0088	0.0019
August 11 - September 10	0.017	0.0089	0.0024
September 10 - October 10	0.027	0.0087	0.0015

The increasing α of Aliou over time suggests that it is a perennial overflow spring (Figure 4.1, type 3). The constant α of Le Baget suggests that it is a full-flow spring (Figure 4.1, type 1). The increasing α of Fontestorbes suggests that it is a low-stage underflow spring (Figure 4.1, type 5).

Le Baget and Aliou are adjacent catchments, and both share flow from the Balagué polje with a third catchment (Plamicou). A dye test carried out when the polje was flooded for a month resulted in dye recoveries at both Plamicou and Le Baget. There is no reason to suppose that discharge vectors would be identical at high and at low flow; thus there are presumably overflow/ underflow effects from this polje.

Upstream from the main gauging point at Le Baget, there are three overflow springs, which flow for about 25, 60 and 110 days a year (Mangin, 1975, p548). Downstream from the gauging point some of the water sinks into the streambed and resurges at Alas Spring. The hydraulic gradient along the strike in the karstic limestone from the main stage recorder at Le Baget Spring to Alas Spring is

0.016 (Mangin, 1975). From axiom 3 (p81), there must be some karst groundwater underflow along the strike which bypasses the Baget gauging point.

There are no visible overflow or underflow springs in the Aliou catchment. However, there could be unnoticed underflow downstream of the spring into the alluvium of the valley. Alternatively, there could be underflow to neighbouring karst catchments such as Le Baget, Plamicou or Arbas.

The Fontestorbes catchment is much larger than the other two. Fontestorbes Spring is situated at the faulted contact between the karstic limestones and marls, close to a low-gradient river, so underflow below Fontestorbes is unlikely to be significant.

Mangin (1975) noted the complex nature of recharge to the catchment. There are ungauged overflow springs in the Frau Gorge which flow when discharge at Fontestorbes exceeds $4 \text{ m}^3 \text{ s}^{-1}$ (making Fontestorbes a Type 4 spring). However, when Fontestorbes discharge exceeds $5.2 \text{ m}^3 \text{ s}^{-1}$, then it receives surface overflow from the Montaillou catchment (adding a Type 2 component to Fontestorbes).

But Fontestorbes is the westernmost of three major springs of the 230km^2 Sault karst, the other two being Aiguo Niret in the centre and Font Maure in the east. Aiguo Niret is the highest of the three (630m), and is an overflow, ceasing to flow between July and the first floods of winter (Mangin, 1986). The complementary underflow to Aiguo Niret (axiom 1, p81) must emerge at Font Maure (which is lower than Fontestorbes) and/or at Fontestorbes (which is closer than Font Maure). This then adds a Type 5 component to Fontestorbes.

These complex hydrogeological possibilities suggest that these three karst springs may be much more complicated than the simple assessment at Aliou as a perennial overflow spring, Le Baget as a full-flow spring, and Fontestorbes as a low-stage plus high-stage underflow. However, this assessment may be true as a first approximation.

The summer recessions for the three springs in 1970 are shown in Figure 4.5a. If it is assumed that the three catchments produce similar baseflow recessions, then pattern-matching can be used to calculate underflow and overflow components (Figure 4.5b). This pattern matching shows that underflow and overflow differences may be responsible for the majority of the hydrograph differences in Ariège.

4.8 Conclusion

It follows from the three axioms of karst groundwater flow on page 81 that full-flow springs only occur in catchments where there are no overflow springs, where the spring is at the lowest topographic position in the catchment, and where there are no surface streams in the catchment which bypass the spring. The above analysis of four examples has shown that full-flow karst springs may be rare, and that spring discharges (and hydrochemistry) can be largely explained in terms of aquifer boundary conditions.

On the other hand, Shuster and White (1971) attributed the contrasts between the two spring types in Pennsylvania principally to flow velocity (diffuse flow versus conduit flow). Conversely, in Ariège, Mangin (1975, 1984) attributed spring contrasts to storage differences. Neither of these hypotheses is easy to falsify as the proposed differences lie hidden within karst massifs. However, in the absence of supporting evidence for either of these hypotheses of aquifer differences, it is perhaps simpler to apply Ockham's Razor and assume that contrasts in the hydrology and hydrochemistry of karst springs are due to the observable contrasting boundary factors.

The next chapter will look inside karst aquifers rather than at their boundaries, and identify their essential hydraulic characteristics.

Chapter 5

The hydraulics of karstic groundwater flow

5.1 Introduction

There are three approaches to the study of the hydraulics of karst groundwater flow. The first is to assume that the karst behaves as a diffuse flow aquifer. It can then be modelled using traditional methods such as drawdown tests in wells (Freeze and Cherry, 1979). This technique has been the standard method used in applied studies in North America, though recently there have been some changes following scathing criticism from some karst hydrogeologists (e.g. Quinlan and Ewers, 1986).

The second approach considers that cave conduits are the principal vectors for groundwater flow, and uses vadose or drained phreatic conduits as analogues for present flow. This method uses passage morphology (e.g. scallops, cross-sectional shape) and topography (slope, direction, bifurcation) to infer past hydraulics (e.g. Lauritzen, 1982; Gale, 1984). Such information has then been extrapolated to explain how caves have formed (see Chapter 6). The principal problems are the interpretation of the features studied, ^{and} in the small sample size used, which may be unrepresentative of the whole aquifer.

The third approach studies modern water flow in phreatic conduits. Recent cave exploration by scuba divers has begun to show the extent of flooded conduits, which appear to be of overwhelming importance in karst drainage (see Section 8.3). Spring monitoring and water level studies provide an indirect approach to modelling hydraulics (e.g. Atkinson, 1977a; Smart, 1988a). The direct approach of

scuba diving into the conduits is both dangerous and arduous; data collected may be of low precision, but it will of high accuracy because modern hydraulic relationships will be observed (e.g. Lauritzen et al., 1985). This latter study found that the scallops in one Norwegian conduit represented the highest 2% of flows or less; hitherto, it had been assumed that scallops represent mean discharge, which may be an order of magnitude less.

The theme that has emerged from most of the studies using the second and third approaches is that there is a wide variation in such basic hydraulic parameters as flow velocity and hydraulic gradient, but that such variation is essentially unpredictable. The following review will compare the tracing results at Crowsnest with other studies, and derive some fundamental relationships, showing that conduit velocity is predictable.

5.2 Diffuse flow and conduit flow

Perhaps the most useful and widely used parameter that may be measured from the surface for characterising karstic groundwater flow is velocity. Measurements fall into two categories in karst areas. The commonly used method where boreholes are available is to undertake recharge or drawdown tests (Freeze and Cherry, 1979). The second method is to undertake tracer or flood pulse tests between an input sinkpoint and one or more resurgences (Ashton, 1966). Occasionally, these may be supplemented by in-cave studies using stable isotopes (e.g. Atkinson, 1984; Yonge et al., 1985), tracers (e.g. Friederich and Smart, 1981, 1982), or discharge and hydrochemical differences (e.g. Pitty, 1968; Gunn, 1983).

The spectrum of flow velocities in karst covers about ten orders of magnitude (Figure 5.1). This large range can be subdivided into two modes of flow. Soil, seepage and subcutaneous flow velocities are $<10^3 \text{ ms}^{-1}$. This flow is laminar,

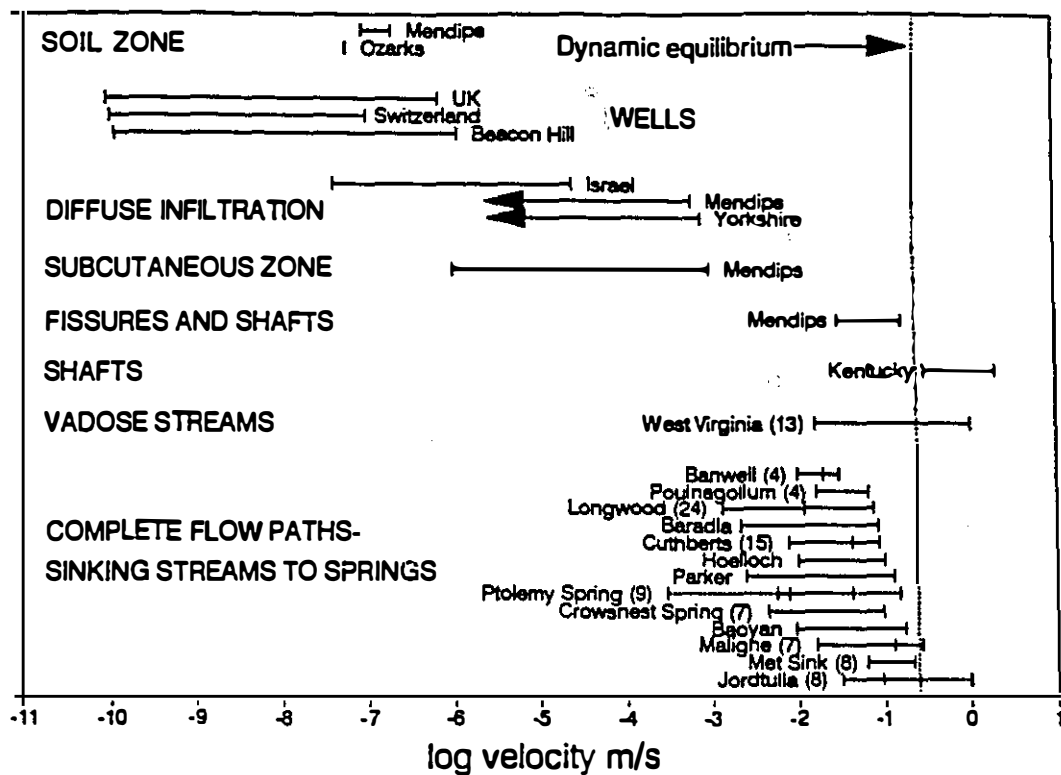


Figure 5.1 Flow velocity in karstic terrains

Data from Friederich and Smart, 1981 (Mendips, England); Yonge et al., 1985 (Ozarks, USA); Hart, 1977 (Oregon, USA); Smith et al., 1976 (UK); Kiraly, 1975 (Switzerland); Atkinson, 1984 (Yorkshire, England); Hobbs and Smart, 1988 (Beacon Hill, England); Even et al., 1986 (Israel); Brucker et al., 1972 (Kentucky, USA); Worthington, 1990 (West Virginia, USA); Denes & Szilagyl, 1989 (Baradla Barlang, Hungary); Stanton and Smart, 1981 (Banwell, Longwood, Cuthberts: England); UBSS, 1969 (Poulnagollum, Eire); Bögli, 1980 (Hölloch, Switzerland); Quinlan and Ewers, 1989 (Parker Cave, USA); this thesis (Ptolemy, Crowsnest); Song, 1986 (Baoyan, China); Smart, 1988a (Maligne, Alberta); Komatina, 1984 (Caprazlije, Yugoslavia); Smart, 1988b (Met Sink - Castleguard Big Springs, Alberta); Lauritzen, 1985 (Jordtulla, Norway).

- Note:
- 1) K from well data has been converted to velocity, assuming a hydraulic gradient of 0.001.
 - 2) Figures in parentheses represent the number of tracer tests. The indicated velocity range only represents velocities measured by these tests, except at Ptolemy Spring and Jordtulla, where dotted lines represent calculated extrapolations to measured Q_n and Q_r . Q_n at Jordtulla is zero, so minimum velocity is zero.
 - 3) The velocity at mean discharge is shown where available (at Banwell, Longwood, Cuthberts, Ptolemy Spring, Crowsnest Spring, Maligne and Jordtulla).

through pores and narrow fissures, and can be characterised by Darcy's Law

$$Q = -K A dh/dl \quad (5.1)$$

where Q is the discharge, K is the hydraulic conductivity, dh/dl is the hydraulic gradient, and A is the cross-sectional area. There is voluminous literature on Darcy flow, and computer modelling of Darcy flow in homogeneous rocks has met with considerable success (e.g. Freeze and Cherry, 1979; Domenico and Schwartz, 1990).

Laminar flow through fissures is described by the Hagen-Poiseuille equation

$$Q = \pi \rho g r^4 S / 8 \eta \quad (5.2)$$

where ρ is the fluid density, and η is the dynamic viscosity of the fluid. The Hagen-Poiseuille equation has been used in modelling the early stages of flow in karst terrains (e.g. Thraikill, 1968; Smith et al., 1976).

Burdon and Papakis (1963) introduced the term diffuse circulation for Darcy flow through pores and fissures in karst, differentiating it from the second mode of flow, concentrated circulation. White and Schmidt (1966) adopted the now more commonly used terms diffuse flow and conduit flow. Conduit flow takes place in conduits $>5-10\text{mm}$ in diameter (White and Longyear, 1962), where velocities generally exceed 10^3ms^{-1} , and so flow is usually turbulent. In both open channels and flooded conduits, flow can be described by the Darcy-Weisbach equation

$$Q = (8gRSA^2/f)^{0.5} \quad (5.3)$$

where R is the hydraulic radius of the passage (= area / wetted perimeter), g is the acceleration due to gravity, S is the slope of the hydraulic gradient ($=dh/dl$), A is the passage cross-sectional area, and f is the Darcy-Weisbach friction factor. The lack of data and the perceived variability of these parameters has hindered the modelling of

karst aquifers using the Darcy-Weisbach equation, except for short sections of conduit (e.g. Gale, 1984), or for the one cave intensively studied by scuba divers (Lauritzen et al., 1985). However, sufficient data has now been published so that the domains of these variables can be identified more precisely than has been possible in the past. Each of the five variables in the Darcy-Weisbach equation (velocity, discharge, area, hydraulic gradient, friction factor) will now be examined.

5.3 The Darcy-Weisbach equation

5.3.1 Velocity

Most general reviews of flow velocities in karst have stressed its variability. For instance, Gaspar (1987, p68) stated "the velocity measured along a flow profile is a local characteristic, specific to the karst network under study, which can by no means be applied to the karst volume as a whole". This viewpoint has been supported by almost all tracer studies.

Most velocity data in karst aquifers has come from tracer studies. Yet the fundamental aim of tracer studies over the last century has been to establish flow routes rather than flow velocities. The velocity data derived from these studies has usually been restricted to one value per route. Such single values are then used to characterise the velocity of that route. Where repeat tracing has shown variability in velocity, this has sometimes been taken as indicating measurement error (see book review by Quinlan, 1986).

However, the great variation in discharge of karst springs (e.g. Figure 3.5) described in the following section causes an equally great variation in velocity, since most conduits are flooded (Figure 3.6; Section 7.7). Thus, characterising karst groundwater velocities by single dye traces is as invalid as characterising karst spring discharges by single measurements (see Figure 3.6).

In order to allow comparisons to be made between karst systems, Stanton (1981) suggested that velocities in cave conduits could be expressed as a *standard travel time*, the travel time for a tracer during mean resurgence discharge. Perhaps a more useful parameter is *standard velocity*, the velocity at mean resurgence discharge. This has a direct rather than inverse relationship with discharge, and allows easy comparison between data sets and with parameters such as sediment entrainment velocities.

The velocity in cave conduits may be derived by rearranging the Darcy-Weisbach equation to give

$$v = (8gRS/f)^{0.5} \quad (5.4)$$

This is not very useful in practice, as R , S and f are poorly known. With time, solution will increase the value of R , so that in theory v should drop, as long as Q is constant. This corresponds with the proposition by White (1988) that there are three stages in the life of a cave passage, each associated with different growth rates: initiation ($d < 10\text{mm}$; growth (wall retreat) $\approx 0.001 \text{ mm a}^{-1}$), enlargement ($d > 10\text{mm}$; growth $\approx 0.02-1 \text{ mm a}^{-1}$), stagnation (d variable; growth=0). Geomorphological studies of abandoned cave passages, and exploration by scuba divers of active cave passages, both suggest that the passages behind springs are often single passages, draining all the flow from a catchment for as long $> 10^5$ years. These observations support the hypothesis of a constant Q and falling v over time in active cave passages.

The ergodic principle may be used to test this hypothesis, substituting space (data from different areas) for time. In recent years there have been a number of studies where repeated dye injections have been made at different discharges, and these are shown in Figure 5.1. The surprising result from the repeated dye tracings is that velocities, and particularly maximum velocities, are similar. With the exceptions of Banwell (a small data set, possibly with no high-discharge measurement), and

Jordtulla, maximum flow velocities for the remaining eleven data sets are very similar (Figure 5.1). These are apparent, straightline flow velocities (v_s), and actual flow velocities (v) through sinuous cave passages are likely to be 50% higher (see Section 6.2.1).

These similar velocities contradict the hypothesis of falling v over time, but may be simply explained by considering Hjulstrom's diagram. Flow velocities $>0.2\text{ms}^{-1}$ are sufficient to entrain and transport any unconsolidated clay, silt or sand that has been deposited at periods of low flow. During the period of passage enlargement, maximum annual velocities would be sufficient to prevent sediment deposition. Enlargement rates of $0.02\text{-}1\text{mma}^{-1}$ would restrict this enlargement period to $10^4\text{-}10^5$ years, on average possibly 10% of the total active life of a cave conduit.

Eventually, a threshold is reached when maximum velocity (v_s) drops below 0.2ms^{-1} , and the sediments deposited during low flow cannot be removed by the annual flood. Renault (1968) classified flooded conduits as being of two types, which he called *syngenetic* and *paragenetic*. He described *syngenetic conduits* as having clean walls and velocities $>0.1\text{ m s}^{-1}$, while *paragenetic conduits* had sediment-covered walls and velocities $<0.1\text{ m s}^{-1}$. He went on to describe how the accumulating sediment load on the floor of paragenetic conduits would cause upward migration of the conduit over time.

In a paragenetic passage clays and silts will be deposited in periods of low flow, and partially or completely eroded at periods of high flow. The velocity in the passage (and hence the cross-section of the passage) will thereafter maintain a *dynamic equilibrium* maximum velocity of about 0.2ms^{-1} . The deposition of sediments on all surfaces of a paragenetic passage must lead to a dramatic reduction in solutional passage enlargement. This new phase of dynamic equilibrium may last for $10^5\text{-}10^6$ years, until the stagnation phase is reached when the cave stream finds a new, lower course. Phases of cave passages are further discussed in Section 8.5.

Evidence to support this new concept of an equilibrium phase between the enlargement and stagnation phases comes from several sources. First, observations by divers in several of the 13 conduits in Figure 5.1. support the concept. Jordtulla ($Q_x=2\text{ms}^{-1}$) is the only dived site (of the 13) with clean bedrock walls (Lauritzen, 1985), and abundant sediments have been noted at other sites such as Wookey Hole, Cheddar, and Mill Hole (Farr, 1980, 1983; Anon. 1988).

Second, dye velocity data assembled from many sources almost all give mean velocities (v_s) of $0.02\text{-}0.05\text{ms}^{-1}$ (Table 5.1). Given a ratio of maximum discharge (Q_x) to mean discharge (Q_m) of 3-12 for most perennial springs (Table 5.2), and mean sinuosities of 1.5 (Table 6.1), this suggests that most of these springs have v_s close to the dynamic equilibrium value of 0.2ms^{-1} .

Third, cave divers report that almost all siphons (flooded passages in caves) have sediments, with unconsolidated silt and clay being mobilised by the passing diver, thereby frequently reducing the visibility to near zero (Farr, 1980; Simmons, 1990; Buck, 1990). Renault (1968) cited several cases of mud-coated walls in siphons that had been pumped dry. Furthermore, many passages in the epiphreatic zone of caves have walls that are entirely coated by mud several millimetres in thickness. The major exceptions are siphons close to sea level in areas such as Florida (USA), the Yucatan (Mexico) and the Bahamas; however, speleothems in these caves attest that they are relict, and are flooded due to a rise in sea level since the Pleistocene.

Fourth, measurements of suspended sediment concentrations at karst springs show a large increase at higher discharges. The only study known to the author is by Newson (1971). He studied three karst springs in the Mendip Hills, England. Particulate loads in the springs were usually $<10\text{mg l}^{-1}$, and often $<1\text{mg l}^{-1}$, confirming the observed limpid clarity of karst springs at low discharges. However, at higher discharges ($Q>0.5Q_m$), there was a rapid increase in suspended sediment concentrations. At Cheddar Spring, this can be described by

Table 5.1 Conduit groundwater flow velocities from multiple tracer tests

Area	Range mm s ⁻¹	Straightline velocity Mean mm s ⁻¹	Surface gradient	Reference
Multiple traces on one flow route				
Jordtulla, Glomdal, Norway	32-250	***110	l	Lauritzen, 1986
Parker Cave-Mill Hole, Ky, USA	3-130	*67	l	Quinlan & Ewers, 1989
St Cuthbert's-Wooley, England	8.2-89	**43	m	Stanton & Smart, 1981
Longwood-Cheddar, England	1.3-74	**12	m	Stanton & Smart, 1981
Swan Inn-Banwell, England	10-31	**21	m	Stanton & Smart, 1981
Poulnagollum-Killeany, Eire	16-65	*41	m	Tratman, 1969
Caprazlige-Mali Rumin, Yugoslavia	51-290	*170	m	Komatina, 1984
Main Sinks-Maligne Springs	17-280	**#120	m	Smart, 1988a
Baradla, Hungary	22-65	**12	m	Denes & Szilagyi, 1989
Baoyan, China	8-170	*89	?	Song, 1986
Met Sink-Big Spring, Castleguard	63-220	**#130	h	Smart, 1988b
Phillips Pass - Crowsnest Spring	11-90	**14	h	Table 3.5
Peresta Sink-Ptolemy Spring	3.6-32	**9.0	h	Table 3.5
Multiple traces in one area				
Midwestern USA	0.8-64	**29	l	Aicy and Fletcher 1976
Manavgat, Turkey	4-58	*31	l-m	Bakalowicz, 1973; Chabert, 1977; Karanjac & Altug, 1980; Courbon & Chabert, 1986
Peak District, England	2-82	**22	m	Christopher et al., 1977, 1981
Eastern Mendips, England	43-146	**66	m	Drew, 1975a; Smith et al., 1976
Mendip Hills, England	6-240	**73	m	Atkinson, 1977
Yorkshire, England		**8	m	Smith & Atkinson, 1977
Dinaric mountains, Yugoslavia	0.6-120	**36	m	Herak, 1972
Causse Comtal, France	16-50	*33	m	Dodge, 1985
Guizhou - Guangxi, China	<0.04->87	**44	m	Lu, 1988
White Limestone, Jamaica		**40	m	Smith et al., 1976
Mulu, Malaysia	>33-128	**94	m	Smart & Friederich, 1982
Waitomo, New Zealand		**56	m	Gunn & Turnpenny, 1985
Middle Alb, Germany	6-49	**24	m	Strayle, 1970
Franconian Alb, Germany	10-54	**+26	m	Seiler et al., 1989
Ariège, France	2-120	**43	m-h	Mangin, 1975
Vercors, France	0.8-116	**30	m-h	Delannoy, 1984
N Limestone Alps, Austria	3-70	*37	h	Bauer and Zötl, 1972
Glattalp, Switzerland	11-100	*56	h	Bögli, 1970
Caucasus, USSR	20-60	*40	h	Kiknadze, 1982
Small River, B.C.	190-1020	**#590	h	Huntley, 1990
Castleguard, Alberta	63-217	**#139	h	Smart, 1988b
Platé, France	5-400	**68	h	Maire, 1990

notes:

+ most tests undertaken in low water conditions

most tests undertaken in high water conditions

Surface gradients: l=<0.01, m=0.01-0.1, h=>0.1

*** Mean velocity is based on long-term (≥ 1 year) discharge records

** Mean velocity is based dye-trace velocities, which may not represent the range of velocities found in the aquifer

• Mean velocity is the mean of the fastest and slowest dye traces

Table 5.2 Annual variation in discharge (Q_s/Q_n) for karst springs**Rocky Mountains karst springs**

	Q_s/Q_n mean	n	reference
Sublacustrine Springs	17	>3	this thesis
Crowsnest Spring (total)	21	1	
Crowsnest Spring (upper)	∞	1	
Crowsnest Spring (lower)	2.2	1	
Ptolemy Spring	193	1	
Parrish Spring	∞	1	
Emerald Cliff Springs	∞	5	
Ranch Spring	∞		
Maligne Springs	23.4	>60	Smart (1988a), Ford (1991)
-uppermost springs	∞		
-lowermost springs	<<23.4		
Castleguard - Big Spring	∞		Smart (1983a)
- Cave	∞		
- Red Spring	52		
- Artesian Spring	<20?		

Karst springs from other areas

	range	median	n	reference
Spain	4-100	7.8	14	Oberti et al., 1988
Rellinars, Spain	20- ∞	∞	7	Freixes, A., 1986
Switzerland	34- ∞	750	7	Maire & Nicod, 1984; Lavanchy et al., 1988
Germany	3.6-120	47	4	Bögli, 1980
N. China	1.2-6.8	1.7	5	Song, 1986
S. China	13-120	110	7	Song, 1986
Vercors, France	33- ∞	141	23	Delannoy, 1984
N. Pre-Alps, France	>20-800	135	12	Maire & Nicod, 1984
Ariège, France	25-5300†	190	3	Mangin, 1975
Dinaric Mtns, Yugoslavia	6- ∞	16	10	Bonacci, 1987
W. Virginia, USA	75-116	106	3	Coward, 1975
Cheddar, England		46	1	Atkinson, 1977
Yorkshire, England	21- ∞	49	10	Halliwell et al., 1974
Waitomo, New Zealand	25-747	72	3	Gunn & Turnpenny, 1985
Styria, Austria	7-64	36	2	Bauer & Zötl, 1972
El Abra, Mexico,	12- ∞	79	6	Fish, 1977
Manavgat, Turkey		32	#	Chabert, 1977

* mean discharge

from combined discharges ($Q_n = 157 \text{ m}^3 \text{s}^{-1}$) of >35 springs, several of which dry up

† from 3 main springs; there are also overflows e.g. in Gorges de la Frau

$$C = 13.0 Q^{1.84} \text{ mg l}^{-1} \quad (n=5, r^2=0.992) \quad (5.5)$$

where C is the suspended sediment concentration. Suspended sediment concentrations at Rickford Spring showed an even more rapid rise with discharge. A major part of the sediment load was calcareous (98% at Cheddar, 38% at the other two springs), and 86-95% of the sediment was silt- or clay-sized. The high calcareous content and high flux ($180 \text{ m}^3 \text{ a}^{-1}$; Table 5.3) indicate that the sediment source is from short-term (<1000 years) storage within the karst aquifer. Dye tracing has shown that almost the whole flow route is phreatic (Section 3.3.1 and Equation 5.7), so the principal temporary storage location is most likely to be in flooded conduits.

Most limestones (including the Mendip ones) are largely made up of silt to sand-sized clasts, and it has been shown that there is differential dissolution of limestones of different texture (Rauch and White, 1970). So perhaps it is not surprising that the dissolution of limestone releases limestone clasts which are then removed by streamflow to a low-energy environment in the cave where they will accumulate. This is similar to the mechanism proposed by Bull (1981) for the accumulation of fine sediments in Ogof Agen Allwedd (Wales), by being washed down fissures by flood events.

Carbonate content of silts and muds in caves has rarely been measured, for it has been presumed to be very low. Yet four studies in England, Yugoslavia, Canada and France, which made carbonate analyses all found some high carbonate percentages. The high carbonate loads in Mendips (England) springs has been described above. In Slovenia (Yugoslavia), Zupan (1990) analyzed 50 stream samples from nine caves. She found that carbonate loads increased progressively from 5-10% at the points where alloigenic streams entered the caves up to 30-70% within the caves, and that authigenic stream sediments were usually >90% calcite. Microscopic analysis showed that most of the calcite was sparite. In one high-altitude cave, Velika

Table 5.3 Recovery period of cave conduits

		Friars H.S.	Ptolemy	Cheddar
catchment area	km ²	85.7	18.6	55.2
allogenic catchment	%	96	0	2
insolubles in runoff	%	80	4	3
mean discharge	m ³ s ⁻¹	1.5	0.39	0.95
mean solute concentration	mg L ⁻¹	-	86	240
flux of solutes	m ³ a ⁻¹	-	410	2700
flux of insolubles	m ³ a ⁻¹	700#	16§	80§
flux of particulate solubles	m ³ a ⁻¹	?	?	100
siphon volume	x10 ⁵ m ³	8	1.2¶	1.1¶
recovery period*	years	<1100	<.500	600

calculated from estimated age of cave and total sediments removed over that period

§ calculated from solute flux and % insolubles in catchment

¶ calculated from tracer tests

* period of sediment deposition needed to return conduit to dynamic equilibrium following a flood of 2x annual flood; assumes that flood maintains peak long enough to remove enough sediment from cave to reduce velocity to equilibrium

data sources: Friars Hole System - Coward (1975), Worthington (1984).

Cheddar - Newson (1971), Smith and Newson (1974), Drew (1975a), Atkinson (1977a)

ledenica v Paradani, developed in dolomite and dolomitic limestone, Zupan (1990) found two facies. Near the surface, there is a lithified (paleokarstic) quartz sandstone, with minor plagioclase, hornblende and calcite. Deeper within the cave, below each waterfall, there are sand beaches composed of dolomite and ankerite. In Castleguard Cave (Alberta), Schroeder and Ford (1983) found >60% carbonate in laminated silts. In the Niaux - Lombrives - Sabart System (Ariège, France), Sorriaux identified an authigenic calcite sand facies, composed of "subangular to rounded grains up to

several millimetres in diameter" (Sorriau, 1982, p183). Research is clearly needed to document the carbonate content of silts in active phreatic passages in holokarsts.

Fifth, calculations show the recovery period following low-probability flood events is sufficiently short to maintain quasi-equilibrium conditions in most siphons. Calculations for three karst catchments are given in Table 5.3. The recovery periods of some hundreds of years (or possibly thousands if calcareous silts are not present) suggest that equilibrium conditions may represent on average the hydraulic conditions of a 50-100 year flood, rather than an annual flood. Evidence below (Equation 5.7) suggests that annual maximum velocities in karst conduits are about 0.1m s^{-1} , which would correspond with occasional floods (1 per 50-100 years) producing velocities of about 0.2m s^{-1} .

The five strands of evidence described above offer powerful support to the concept of a dynamic equilibrium phase as being the dominant phase in the life of a flooded cave conduit. Velocities for dynamic equilibrium conduits may be predicted by

$$v_t = a Q_t/Q_x \text{ ms}^{-1} \quad (5.6)$$

where Q_t is the discharge at time t of a system with maximum annual discharge Q_x , v_t is the velocity at time t , and a is a coefficient which depends on the recovery period of the conduit.

Figure 5.2 shows data from Ptolemy Spring, Crowsnest Spring, and the four other cave systems with published data, where Q_x and velocity over a wide range of discharges is known (with $r^2 > 0.8$ for each cave in Equation 3.4). The Ptolemy, Crowsnest, Wookey and Cheddar data show a similar relationship, and give

$$V_t = 0.096 (Q_t/Q_x)^{1.08} \text{ ms}^{-1} \quad (r^2 = 0.89) \quad (5.7)$$

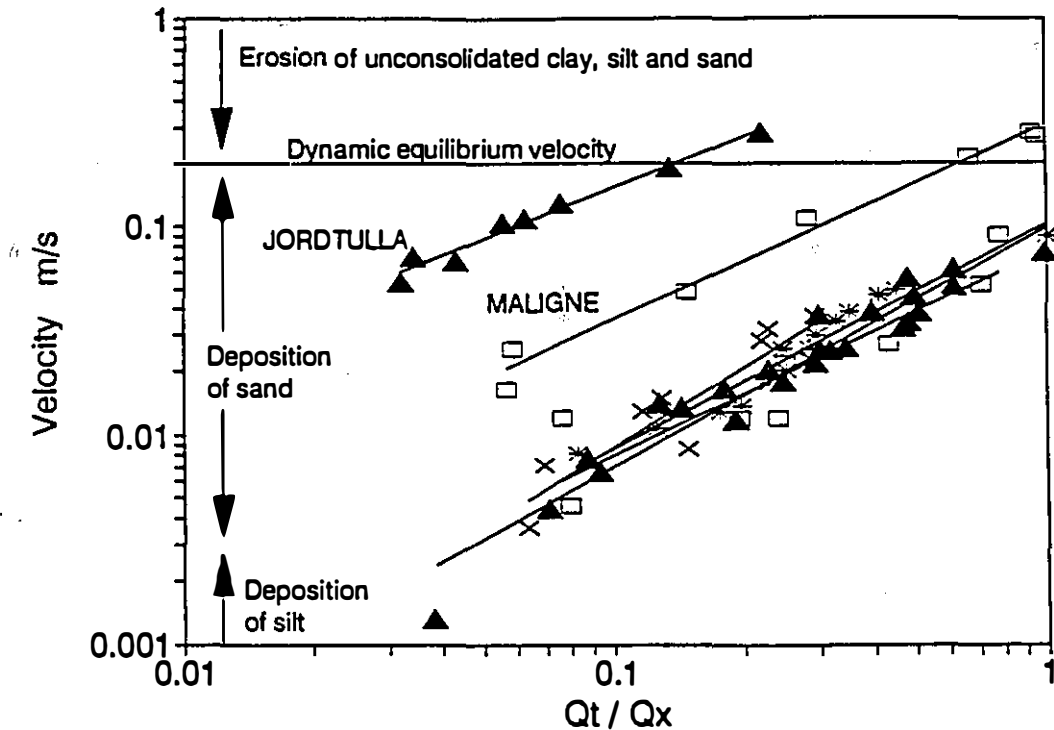


Figure 5.2 Velocity-discharge relationships for six cave systems

Crowsnest Spring (\square) and Ptolemy Spring (\times) data from Table 3.5; Wookey (*) and Cheddar (\blacktriangle) data from Stanton and Smart, 1981; Maligne data from Smart, 1988a; Jordtulla data from Lauritzen, 1986.

The exponent greater than unity reflects the influence of the greater variance in input discharge than in output discharge (see Section 3.3.1). These four caves would thus appear to all have phreatic conduits in dynamic equilibrium. The remaining two caves have not yet reached equilibrium, and this is supported in both cases by surface overflow during snowmelt maxima.

The approximate sink to rising gradient has been noted in Table 5.4. It should be noted that the velocity data lends no support to the hypothesis that V is a

Table 5.4 Hydraulic gradients in well-karstified limestones

	m/km	average	low	high	
Maligne, Alberta	-	0.06	25		Section 11.2.1
Gavel-Leck Beck Head, UK	<1	-	-		Waltham et al. 1983
Stoke Lane, UK	<2	-	-		Atkinson 1977
Reservoir Hole, UK	-	7°/(0.005)	10		Atkinson 1977
Luire-Arbois, France	-	1.3*	26		Delannoy and Maire, 1984
Vaucluse, France	-	-	<2.8		Courbon and Chabert, 1986
Apulia, Italy	0.3-10	-	-		Grassi and Tadolini 1985
Höllloch, Switzerland	-	<0.8	46		Bögli 1980
Jordtulla, Norway	-	0	1.5		Lauritzen 1985
W.Balcony Mtns, Hungary	0.8-6.5	-	-		Erdélyi and Gálfy, 1988
Tlemcen, Algeria	0.3	-	-		Collignon, 1987
Trebiciano-Timavo, Yug.	-	<0.46	3.8		Belloni et al., 1972
Gunung Sewu, Indonesia	2.8-5	-	-		Waltham et al 1980b
Niangziguan, China	0.9-13	-	-		Chen and Bian, 1988
Friars Hole System, USA	-	2*	<3		Coward, 1975; Worthington 1984
Elk River Cave, WV, USA	-	0.6	5		Medville and Storage, 1986
The Portal, WV, USA	-	0.3	-		Medville, 1990
Florida, USA	0.2-1	-	-		Stringfield, 1966
Mammoth Cave area, USA					
Mill Hole- Green R.	-	0.095	2.8		Quinlan et al. 1983
most major conduits	0.5-2	-	-		Quinlan and Ray 1981
away from conduits	2-10	-	-		Quinlan and Ray 1989
Yucatan, Mexico	0.02	-	-		Back & Hanshaw (1970)

* gradients probably reflect perched siphons

Data in parentheses represent calculations based on $Q \propto \sqrt{h}$ and Q_x/Q_n

function of sink to rising gradient. This is a myth which has been falsified before (Zötl, 1974):

A minimum of a pair of tracer tests, at low and high flows, will show whether a karst flow route is phreatic or vadose (assuming proportionality of input/output discharge: Equation 3.6). If it is predominantly phreatic, as expected (see Section 8.3), then velocity in an equilibrium conduit will approximate Equation 5.7. It is believed that as many as 90% of karst aquifers obey these conditions. If this is so, then most conduit velocities may be predicted with *no* tracer tests.

5.3.2 Discharge

Karst springs include most of the largest springs in the world, with several having mean and maximum discharges of $>20\text{ m}^3 \text{ s}^{-1}$, and $>100\text{ m}^3 \text{ s}^{-1}$, respectively, emanating from a single cave conduit (Ford and Williams, 1989). The springs at Crowsnest Pass have more modest discharges (Figure 3.5), but these are more representative of spring discharges commonly found in karst areas.

The threshold passage diameter for conduit flow in a karst aquifer is about 10mm (White and Longyear, 1962), and maximum diffuse flow velocities are $<10^{-2}\text{ m s}^{-1}$ (Figure 5.1). This gives a discharge of $<10^{-6}\text{ m}^3 \text{ s}^{-1}$ for diffuse flow in a fissure, and discharges of such a magnitude have been referred to as seeps (Gunn, 1983). Karstic springs referred to in the literature invariably have mean discharges $>10^{-4}\text{ m}^3 \text{ s}^{-1}$, so that these *must* be issuing from conduits. Thus it is concluded that the term diffuse karstic spring is a contradiction in terms, and *all* karst springs are conduit springs.

The hydrochemical analysis of Drake and Harmon (1973), the hydraulic and hydrochemical analysis of Atkinson (1977a,b), and the high correlation between proportion of concentrated recharge and spring hydrochemical variance (Newson, 1971; Figure 3.4) all support the hypothesis that low variance in spring discharge,

hardness and temperature indicate autogenic recharge rather than diffuse flow. The fact that at least 90% of the world's deepest caves and more than half of the world's longest caves have only autogenic recharge (Courbon and Chabert, 1986) graphically illustrates the high incidence of conduits in autogenic karsts.

The high variability of discharge from karst springs distinguishes them from springs discharging from homogeneous aquifers. Discharge variations for the springs from Crowsnest Pass, together with many examples from the literature, are presented in Table 5.2 and Figure 5.3. It is often the case that all the karst springs in one area emerge from the same rock type. Intra-area variability is greater than inter-area variability in Table 5.2 and Figure 5.3. This suggests that it is neither lithology nor regional factors such as seasonality of recharge that is the dominant factor in determining discharge variability. This is because the springs are often part of a vertical hierarchy of low-variability underflow springs and high-variability overflow springs (see Section 4.2).

Maximum conduit discharge of equilibrium conduits may be predicted by rearranging Equation 5.7 to give

$$Q_x = 0.1 Q_t / v_t \text{ m}^3 \text{s}^{-1} \quad (5.8)$$

Unfortunately, this approach cannot be used to determine Q_n or Q_m .

5.3.3 Area

It has been noted in Section 5.2.1 how the enlargement phase of conduits is fairly short (10^4 - 10^5 years), and how passage expansion in the subsequent equilibrium phase is greatly retarded. This concept is illustrated in Figure 5.4. The cross-sectional area of an equilibrium conduit (A_e) may be derived from Equation 5.7

$$A_e = Q_x / 0.1 \text{ m}^2 \quad (5.9)$$

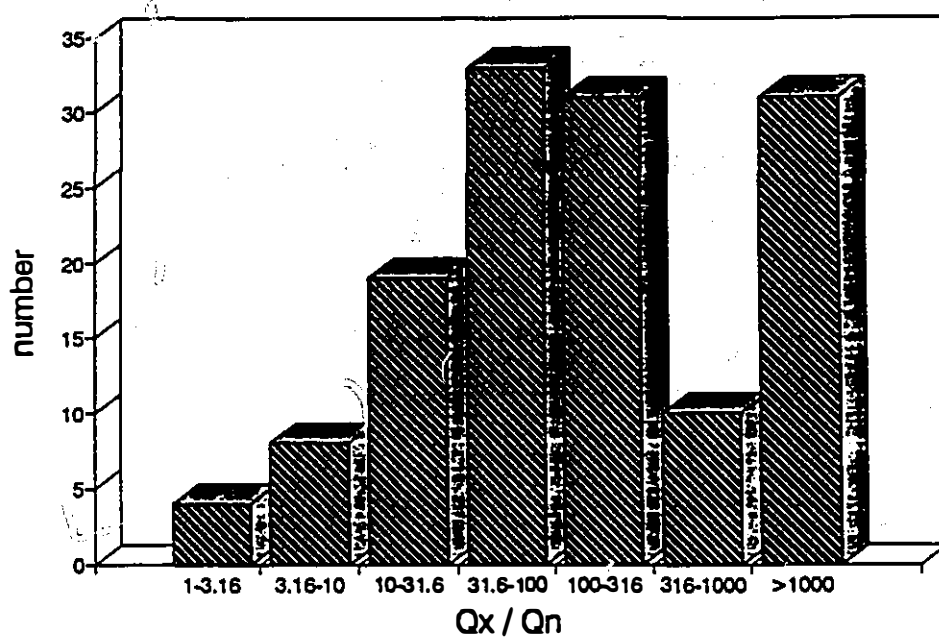


Figure 5.3 Ratio of maximum to minimum annual discharge for 136 karst springs (data in Table 5.2)

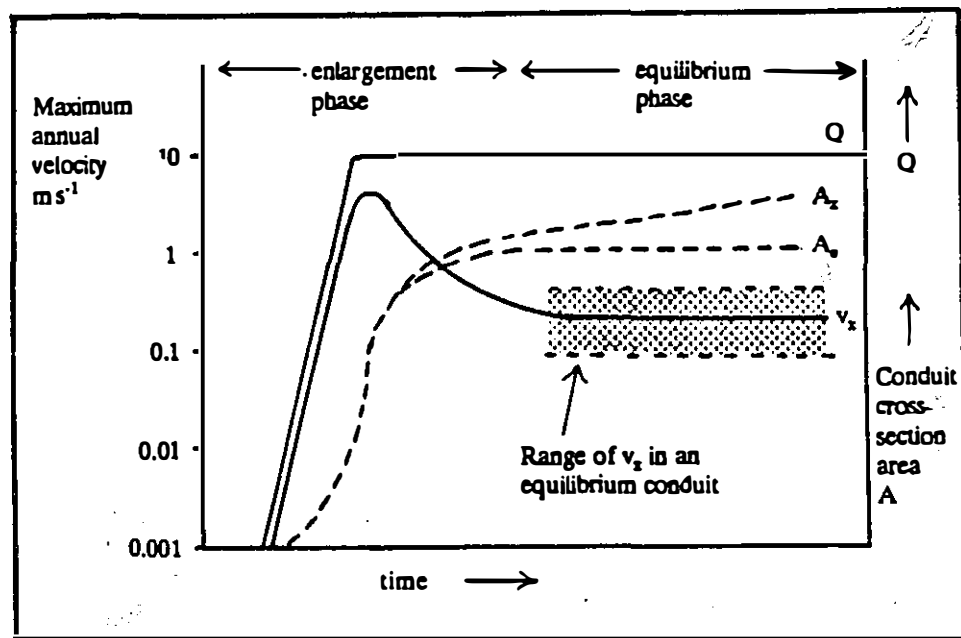


Figure 5.4 Evolution of velocity and cross-section in a karst conduit

Equation 5.9 may be tested against the range of known values for A. The largest karst springs in the world have maximum discharges occasionally exceeding $100\text{m}^3\text{s}^{-1}$, which gives equilibrium passage cross-sections $>1000\text{m}^2$, or a circular tube with a diameter $>36\text{m}$. This is approximately the size of the largest known phreatic passages that have been found.

It should be noted that much larger passages have been found in caves, with maximum sizes exceeding 10^4m^2 . These have been formed by vadose solution, usually accompanied by ceiling collapse due to loss of buoyant support following dewatering. For instance, Worthington (1984) found that stream solution of breakdown in just five localities out of 69km of passage accounted for 28% of the total cave volume of Friars Hole System. This created voids up to $3.5 \times 10^5\text{m}^3$. The largest chamber currently known (in Lubang Nasib Bagus, Malaysia) has a volume of $1.2 \times 10^7\text{m}^3$, with $A=4.5 \times 10^4\text{m}^2$. This too has a floor of collapsed debris from the ceiling, with a large stream flowing through the breakdown progressively removing it by solution. The main passage, where unmodified by breakdown, has $A=220\text{m}^2$.

5.3.4 Hydraulic gradients

The hydraulic gradient in karst aquifers refers to the slope of the water table, the upper limit of the saturated or phreatic zone, and the lower limit of the unsaturated or vadose zone. In granular aquifers, the water table is often considered to be a subdued reflection of the land surface. This is not the case in karst, where the slope of the water table usually relates poorly to the land surface above.

In the vadose zone, there is an important vertical component of flow downwards to the water table, while in the phreatic zone, this vertical component is much reduced. For instance, the slope of passages in the vadose zone (ψ_v) of the twenty deepest caves in the world (Courbon and Chabert, 1986) varies from 26° to

81°, with a median of 48°. All these caves now have vadose zones >1km in thickness. Within the vadose zone both joints and bedding planes are important, and where bedding planes are followed the flow is usually downdip.

Conversely, in the phreatic zone, overall conduit slopes are controlled by the hydraulic gradient, which is usually <<1°. However, the slopes of individual conduit segments are also a function of structure. For example, the mean passage slope of phreatic passages in the twenty longest caves in the world (Courbon and Chabert, 1986) varies from 0.6° to 9°, with a median of less than 2°. At Crowsnest Pass, slopes average about 10°, due to the steep dip, where the undulations of the steeper phreatic passages have given rise to passage names such as Roller Coaster and Big Dipper, the latter being the British name for a roller coaster.

Despite the non-overlapping data sets of vadose flow and phreatic flow mentioned above, confusion has been created by two further characteristics of the vadose zone. These are the crossing of flow paths and perched siphons. It is worth discussing these in detail, for these, together with the wide range of well yields from karstic aquifers (Parizek, 1976), and the perceived unpredictable nature of conduit development in flooded passages, have been used as evidence to argue against the existence of a continuous water table of relevance either to aquifer discharge (Smith, 1971; Smart and Ford, 1986), or to cave formation (Waltham, 1974).

Flow routes of streams in the upper part of the vadose zone in Yorkshire System are shown in Figure 5.5, though the circuitous flow paths shown are only a small proportion of the total number that exist in this area. The crossing of flow paths in the vadose zone has been proved in several karst areas by tracer tests (e.g. Atkinson, 1977a), but has been recorded more precisely on many cave maps.

Siphons are often considered to be an indication of the water table, but they may be perched well above it. For instance, several siphons occur in Yorkshire System at altitudes of 2067m to 2147m, giving apparent hydraulic gradients of 0.082-

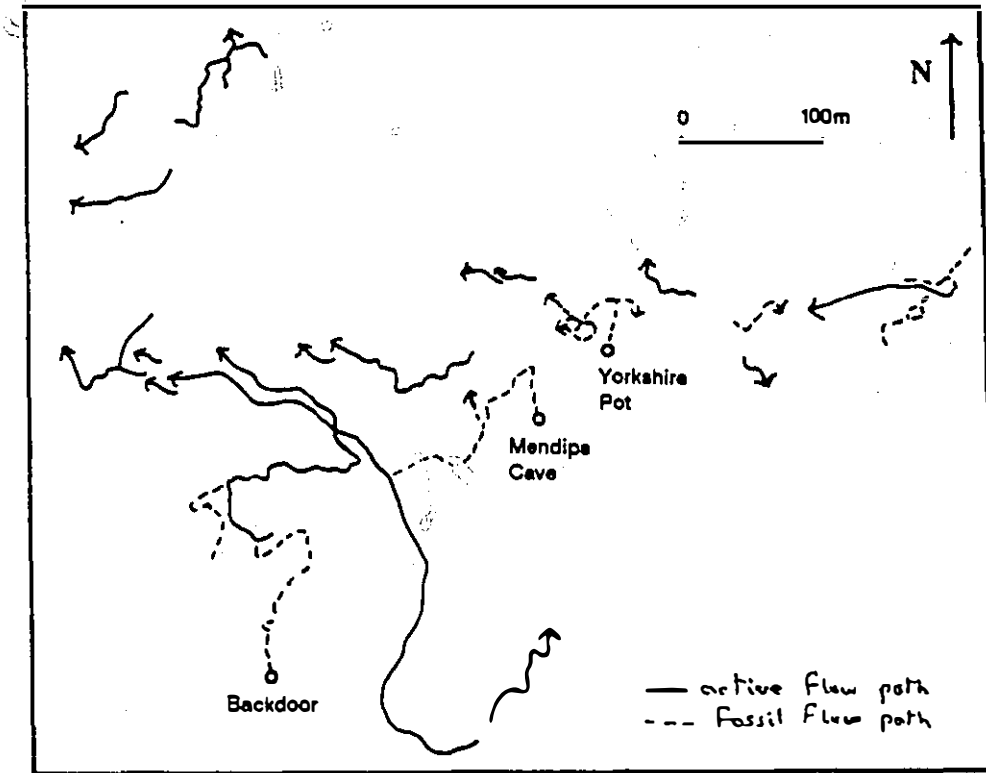


Figure 5.5 Crossing of flow paths in the vadose zone of Yorkshire System, Andy Good Plateau

0.096 to Ptolemy Spring, and gradients up to 0°2 between siphons. From the Darcy-Weisbach equation (5.3)

$$Q \propto (\Delta h)^{0.5} \quad (5.10)$$

where Δh is the change in head. Palmer (1987) showed that if an xy plot of these two variables did not extrapolate to the origin, then the siphon must be perched. Constancy of level of the Yorkshire System siphons shows they are all perched siphons. Catchment evidence (Chapter 8; also see Figure 2.5) indicates these siphons

are perched perhaps 500m above the water table. Perched siphons in such situations high in the vadose zone have sometimes been passed by scuba divers (e.g. in Green Link (NZ); Anou Ifflis (Algeria); V. Yukhin (USSR); Courbon and Chabert, 1986).

Both the crossing of flow paths and perched siphons are a result of an essential attribute of karstic limestones: that they have very low initial permeability. Limestones with high initial permeability (e.g. the Chalk in England and France, and many dolomites and recent limestones) develop as diffuse flow aquifers. On the other hand, the selective solutional opening of fractures in karstic limestones creates an extremely anisotropic aquifer, so that flooded conduits can exist a few metres above air-filled conduits. If it could be shown be that cave streams and siphons did not leak to the underlying part of the aquifer, then the case against the existence of a water table in karst would perhaps be watertight.

Perhaps the most famous example cited as evidence against the existence of a water table is the surface River Aille in Ireland, which flows just a few metres above the air-filled passage in Doolin Cave (Tratman, 1969). However, an important point that is often missed is that there is leakage downwards of some tens of litres per second from the river into the cave passage, so that the cave passage is in process of capturing the surface river. A more comprehensive example of such leakage is provided by the 69km of passage in Friars Hole System (Worthington, 1984). There are many examples of crossing flow routes, both in the cave, and of surface streams flowing above the cave. In every case the underlying passages receive some leakage, in the form of drips or small streams. The conditions associated with perching is discussed further in Chapter 7.

The pattern of downward leakage from all conduits in caves is widespread, and probably universal. The implication is that the fissure flow will descend to a water table, and will subsequently obey Hagen-Poiseuille flow laws until it reaches a conduit. In the conduit, its behaviour can then be described by the Darcy-Weisbach

equation (Equation 5.2). This can be rearranged to give

$$S = v^2 f / 8gR \quad (5.11)$$

Since g and R are constants with respect to discharge, and f is usually taken to approximate a constant, then S varies directly with v^2 . Since v varies by 10-100 (or more) for most karstic conduits (Figure 5.1; also Table 5.1), then S should vary by $(10-100)^2$, or 100-10000. There has been one detailed study on f , which showed a variation from 0.12-2.3 between minimum and maximum values measured (f_n and f_s , respectively) (Lauritzen et al., 1985). Taking this variation in f into account, it still seems that S should vary by at least 10-100 times.

A partial solution for Equation 5.10 can be obtained at maximum discharge for an equilibrium conduit, for $v_x = 0.2 \text{ ms}^{-1}$, so

$$\begin{aligned} S_x &= (0.2)^2 f / 8gR \\ &= f / 2000 R \end{aligned} \quad (5.12)$$

where S_x is the maximum hydraulic gradient.

Little data has been published on the variation in S with changes in discharge. Table 5.4 shows some examples from the literature, but only two of these, Jordtulla (Norway) and Mill Hole (USA), seem to reflect base-level hydraulic gradients. Jordtulla is a simple, short (500m), high-discharge ($Q_m = 2.5 \text{ m}^3 \text{s}^{-1}$) conduit that has been completely explored by divers. Minimum discharge here is zero in winter, and hence $S=0$ (Lauritzen et al., 1983). Mill Hole-Turnhole Spring has a longer flow route (8km), has not been explored by divers, and there are no discharge records because there are no stream sections in which discharge could be measured (Quinlan and Ewers, 1983).

Further data on variations in hydraulic gradients are available from

observations in wells or caves of the variation in water level. In the Caucasus Mountains, USSR, the variation is often 10-15m, and sometimes 30-50m (Kovalevsky, 1977). Variations of 30m have been recorded in Derbyshire, England (Christopher et al., 1977), over 300m in Yugoslavia (Milanovic, 1981), and 180m in Höllschloch, Switzerland (Table 5.4). But at Grotte de la Luire, France, floodwaters rise 450m to occasionally discharge up to $60\text{m}^3\text{s}^{-1}$ overflow from the cave entrance (Table 5.4).

Many published hydraulic gradients in karst are from dye injection points above thick vadose zones to resurgences. For instance, four long-distance (22-46km) traces to the Fontaine de Vaucluse, the biggest spring in France, have gradients of 0.009-0.023, as measured to the spring from the entrances of the caves where the injections were made (Ford and Williams, 1989). However, one of these four traces was made from the lowest accessible point in Gouffre du Caladaïre, a siphon 668m almost vertically below the cave entrance. Lack of variation in the level of this siphon shows that it is above the water table, indicating a maximum gradient of <0.0028.

In the above discussion, hydraulic gradients in karst have been considered to be linear. However, conduit radius will increase in a downstream direction with increased discharge, and hydraulic gradient is inversely related to radius (Equation 5.11). Thus hydraulic gradients will decrease in a downstream direction. The functional relationship between conduit length and hydraulic gradient is not constant, as the length-catchment area relationship is not constant.

A comprehensive picture of hydraulic gradients in the Mammoth Cave area (USA) has emerged from the dye tracing, well-level and cave passage correlations by Quinlan and Ray (1981). In that area, there is a marked reduction in gradient in a downstream direction. Gradients from 26 flow paths in the ten largest catchments in the area are shown in Figure 5.6. The mean gradient from these flow paths is

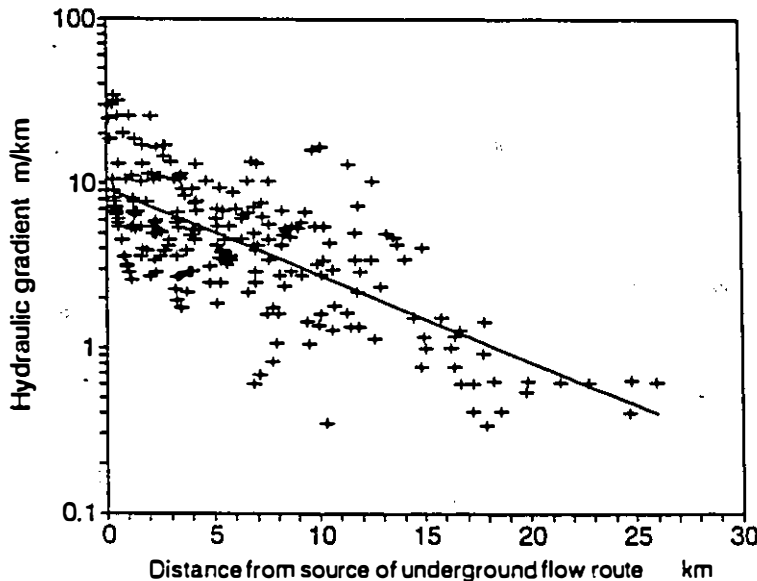


Figure 5.6 Exponential hydraulic gradients of 26 flow paths in the Mammoth Cave area, Kentucky (data from Quinlan & Ray, 1981)

$$S = 0.0092 e^{-0.12l} \quad (n=234, r^2=0.50) \quad (5.14)$$

where l is the distance in kilometres from the beginning of the underground flow path.

Well-documented hydraulic gradients in karst are rare; a search of the literature revealed those listed in Table 5.4. From this, it may be surmised that hydraulic gradients at low stage are commonly <0.001 , and at high stage are commonly >0.001 .

5.3.5 Friction factor

The friction factor can be derived from the Darcy-Weisbach equation (5.2) to give

$$f = 8gRS / v^2 \quad (5.14)$$

Friction factors have sometimes been calculated from scallops in cave conduits (Gale, 1984). Hydraulic calculations involving scallops presume the segment of cave passage where the scallops are measured is representative of the whole conduit. This assumption is valid for discharge calculations because of continuity of flow. However, it is rarely valid for complete flow routes because there is usually a high variance in conduit cross-sectional area. This is certainly true for observations of dry caves, but some constrictions may postdate the active flow history (e.g. ceiling collapse on dewatering). A better source of data is from cave scuba divers. Their dives are frequently terminated by constrictions in otherwise large passages. These appear to be of three types: underwater ceiling collapses (e.g. Malham Cove Rising, England: Round, 1990), U-tube constrictions, where sediment slumps down to almost block the bottom of the U (e.g. the limits of exploration in Swildon's Hole and Wookey Hole, England: Drew, 1975b, Farr, 1980), and low, wide bedding planes (e.g. Keld Head, England: Farr, 1980). In the first two cases it is the small cross-sectional area which increases the friction factor; in the last case it is the increase in wetted perimeter of the conduit which increases it.

Lauritzen et al. (1985) distinguished between the true f (f_t), derived from scallops, and the apparent f (f_a), derived from hydraulic gradients. For practical use in karsts, using the Darcy-Weisbach equation, it is f_a which is of interest. The detailed calculations by Bögli (1980) in Höllloch (Switzerland) have demonstrated this. He calculated friction losses along a 2.6km conduit. Most of this conduit can be visited at low water, but it backs up in flood. The head loss due to conduit roughness along

98% of the passage amounted to only 1.3% of the total; the remainder was accounted for by changes in cross-section (11%), passage bends (1.7%), and a short narrow section (35%) and a section of breakdown (51%). Caves almost always have narrow sections or breakdown, and it is these that give high values to f_s .

A partial solution of the Darcy-Weisbach equation, with respect to f_s may be derived for an equilibrium conduit by rearranging Equation 5.12 to give

$$f = 2000 S_z R \quad (5.15)$$

Some calculated values for f_s , derived from Equation 5.15, or by other methods, are given in Table 5.5. Jordtulla has the lowest values that are likely to be encountered in karst aquifers, for it is essentially a large straight tube with no constrictions. The remaining results illustrate the heterogeneity that is present in most karst systems. These results indicate that average values in karst may usually be in the range 1-100.

Table 5.5 Apparent friction factors for some karst conduits

Conduit	f_s	source
Mill Hole-Turnhole, USA	27*	Equation 5.15
Holloch, Switzerland	104#	Equation 5.15
Castleguard, Alberta	0.87-2.31	Atkinson et al., 1983
Maligne, Alberta	130	see Section 11.2.2
Mendips, England	24-340	Atkinson, 1977a
Jordtulla, Norway	0.116-2.3	Lauritzen et al., 1985
Friars Hole System, USA	46-74	Worthington, 1984c

* with $R=4.8\text{m}$ computed from dye tracing results to Mill Hole, and S (0.000095-0.0028) from Mill Hole to Turnhole Spring (Quinlan and Ewers, 1989)

$R=1.4\text{m}$, $S=0.0006-0.037$ (Bogli, 1980)

5.4 Conclusion

This analysis of karst hydraulics has shown that all karst springs are conduit springs. A dynamic equilibrium phase in conduit development has been identified, which appears to be predominant in the life of a flooded conduit. Most flooded cave passages are in dynamic equilibrium, with silt on the floor and walls. Maximum velocities are about $0.3\text{m}^3\text{s}^{-1}$, and enlargement rates are $<0.001\text{mm/yr}$. The minority of conduits are clean, with higher velocities, and enlargement rates up to 1mm/yr .

The recognition of the existence of conduits in dynamic equilibrium enables conduit velocity and area to be simply calculated. Hydraulic gradients in karst are variable, both within a catchment and between different catchments. Also, seasonal variation is at least one to two orders of magnitude. Dry-season gradients are commonly <0.001 , while wet-season gradients are commonly $0.001\text{-}0.01$. Friction factors in complete conduits are commonly 1-100.

Chapter 6

Flow nets in karst aquifers: morphometrics and initial conditions

6.1. Introduction

The locus of groundwater flow in a karst aquifer has been a topic of academic inquiry since the turn of the century, and this history has been recently summarised by White (1988). The early debate between proponents of flow principally in the vadose zone or the phreatic zone was resolved in favour of the latter. The debate since then has become whether flow was in proximity to the water table, or some distance below it, with a minority arguing against the existence of a water table in karst. Most hypotheses presented a general case, which should have applied to most caves, arguing for deep groundwater flow (e.g. Davis, 1930; Bretz, 1942) or for shallow groundwater flow (e.g. Swinnerton, 1932; Rhoades and Sinacori, 1941; Davies, 1960; Thraillkill, 1968). With the perceived failure of these deterministic theories, more recent ideas have been based on stochastic principles of flow path selection (e.g. Ford, 1971b; Ewers, 1982; Dreybrodt, 1990).

All the above hypotheses were based on the analysis of paleoflow in small fractions (<20%) of the flow routes of the specific aquifers analyzed. With the continual increase in cave exploration and mapping, increasing proportions of paleoflow routes have become available for analysis. For instance, about 20,000 km of cave passages have now been mapped, a fourfold increase in the last twenty years. Of more importance though has been the exponential increase of scuba diving in cave

siphons for lengths of more than 3km and depths of almost 300m (Courbon and Chabert, 1986).

At the same time, the understanding of conduit patterns has been improved by increasingly detailed observations and measurements. Of particular note are the detailed observations of morphological forms by Bretz (1942), studies of the relationship between fractures, flow paths, conduit slope and conduit evolution by Glennie (1950) and Ford (1963), precise levelling by Palmer (1987), and the combination of all these techniques by Jameson (1985).

These explorations have demonstrated that synchronous flow in one geographical area may vary widely in depth below the water table; this finding thus does not support any existing general hypothesis. Mammoth Cave (Kentucky, USA) provides a well-documented example, which may be used to demonstrate the failure of existing hypotheses. It is the longest cave in the world, and has been cited in most hypotheses written by anglophones (e.g. Davis, 1930; Swinnerton, 1932; Bretz, 1942; Davies, 1960; Thraikill, 1968; Ford, 1971; Waltham, 1971; Ford and Ewers, 1978; Palmer, 1984, 1987). In the Mammoth Cave area more than 700km of passages have been explored, but only small fragments of modern flow routes have been penetrated, and less than one third of the distance of any paleoflow route between the recharge area on the Sinkhole Plain and the springs along the Green River has been followed (Brucker, 1989). Most of the cave appears to have been formed less than 2m below the water table, but in recent years examples of depths of more than 15m have been found (Freeman et al., 1973; Quinlan et al., 1983, 1989; Palmer, 1987, 1989; White and Deike, 1989). It thus reinforces the prevailing concept of the last twenty years that conduit flow depth cannot be predicted.

But perhaps the greatest challenge to existing ideas of groundwater flow in karst has been offered by the caves of Mulu, Malaysia. Writing after the mapping of 50km of cave passages in 1978, Waltham and Brook (1980b) described a complex synchronous mix of "water table", "shallow phreatic" and "deep phreatic" cave passages,

and concluded (p138) "it is clear that the caves of Mulu must contribute data to any thoughts on cave genesis.... The great horizontal or sub-horizontal phreatic tubes mostly have an uncertain relationship to their contemporary water table, and raise questions on the distinction between shallow and deep phreatic cave development". Exploration of a further 140km of cave passages since then has not solved the problems (Smart, 1981a, 1984a; Kirby, 1990).

Furthermore, current ideas on groundwater flow in karst offer no systematic explanation for the occurrence of thermal karstic springs, for the predominance of the sulphate ion in some karst waters, or for the occurrence of tiered caves (except by stable base levels through several glacial-interglacial cycles). The lack of a comprehensive model to explain karst groundwater flow has been felt most acutely in Britain. Thus Gunn (1986b, p387) stated "No theoretical models are currently available for water movement in conduit flow systems".

In Alpine countries in Europe, and in France in particular, groundwater flow in karst has often been considered in terms of structure and lithology. While US research has focused on the longest cave, attention in France has concentrated on the deepest caves, where 1000m deep caves have been explored in dipping karstic limestones <500m thick in both the Alps (Jean Bernard, Berger, Miroldo: Delannoy and Maire, 1984) and the Pyrenees (Illaminako Ateak, Pierre Saint Martin, Rivière de Soudet: ARSIP, 1985). In all these caves, the principal passages are perched on aquitards, and flow is simply downdip along the contact, so it is the structure and lithology which control flow patterns in a rather obvious manner. Consequently France, a leading country in cave exploration, has not been a forcing ground for cave development hypotheses.

In recent years, there has been a growing awareness of the importance of tectonics in influencing the direction of cave passages (Renault, 1967; Jameson, 1981, 1985; Worthington, 1984), and an association between fracture stresses and cave passage direction has been demonstrated in several areas (Eraso, 1986; Lauritzen,

1990). It appears that such tectonic control is a major factor for determining flow paths on a local scale (1-100m). However, on a catchment scale (1-100km), hydraulic gradients are of overwhelming importance.

Almost thirty years ago, White and Longyear (1962) argued on hydraulic grounds that general cave genesis hypotheses were irrelevant, and that "discussion of cavern development should be couched in terms of hydraulic gradients and the geologic factors which control it." Soon after, Mandel (1965, p663) suggested that "the most pertinent mathematical model of karstic erosion would consist of the transformation of the flow pattern in a more or less isotropic porous medium to the flow pattern in a strongly anisotropic one". These two approaches will be followed in the following analysis.

In this chapter, the configuration of the initial flow net will be investigated. In the following two chapters, a comprehensive model of conduit development will be tested.

6.2 Morphometric analysis of flow paths

6.2.1 Introduction

There has been little interest in the morphometrics of groundwater flow paths in karst. This is perhaps due to the existing paradigm, which suggests that flow paths are controlled by the unpredictable occurrence of highly transmissive fractures, and thus flow paths are essentially random.

It is argued here that flow paths are not random on a catchment scale, and that morphometric analysis will yield information which will help explain the factors controlling groundwater flow. Six indices which will help characterise flow paths anywhere within a karst catchment will be introduced in the following six sections. In Chapter 7 three further indices will be introduced to describe flow path slopes (initial phreatic drop, terminal phreatic lift) and to describe tributary junctions.

6.2.2 Conduit density

Conduit density is here defined as the total length of conduits (in kilometres) within a unit volume of a karst aquifer (a cuboid, with volume in km^3). Conduit densities from the Rocky Mountains and several other distinctive karsts are given in Table 6.1. Figure 6.1a gives these together with values from the 20 longest and 20 deepest known caves in the world (after Courbon and Chabert, 1986).

These values are all underestimates, based only upon passages which have been mapped. In Yorkshire System, for instance, there are >150 unexplored passages, so the actual density may be an order of magnitude greater than the present value of 27 km km^{-3} . It thus appears that conduit density in limestone aquifers may average of the order of 100 km km^{-3} , and may be 1-2 orders of magnitude greater in narrow aquifers where flow is concentrated, such as the gypsum and marble aquifers listed in Table 6.1.

It is hypothesised here that the conduit densities found in explored caves are broadly representative of the whole areal extent of karst limestone massifs. An alternative hypothesis is that karst aquifers have zones of high conduit density (where explored caves are found), separated by low density zones dominated by diffuse flow. These hypotheses may be readily tested by using data from tracer tests, and the known velocities of diffuse flow and of conduit flow (Figure 5.1). When dye is injected where there is concentrated recharge to a karst aquifer (e.g. dolines or stream sinks), velocities *always* indicate conduit flow (Table 5.1). Since dolines are ubiquitous in mature karsts, this supports the first hypothesis, that the conduit densities found in explored caves are broadly representative of the whole areal extent of karst limestone massifs.

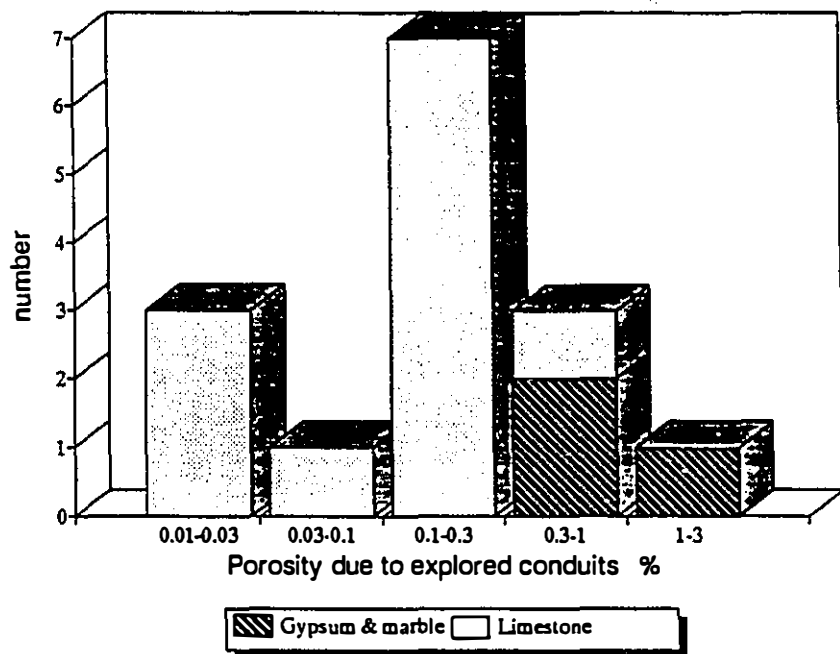
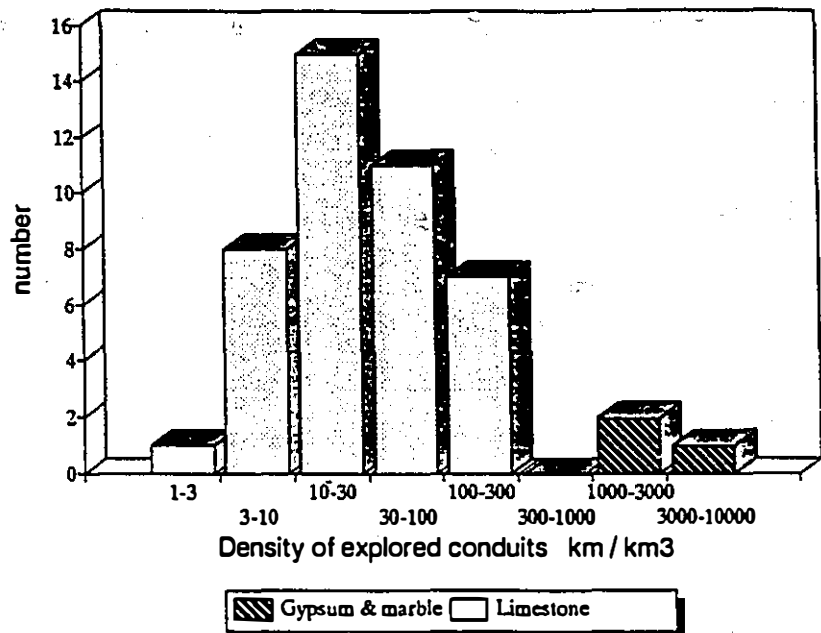
On theoretical grounds, a density of at least 100 km km^{-3} might well be expected, as this only corresponds with one vertical conduit every 100m. Observations of concentrated recharge seen on the surface, and concentrated infiltration seen in caves would suggest a 100m conduit spacing would be a conservative minimum.

Table 6.1 Aquifer porosity due to explored cave passages, and density of passages within karst aquifers

Cave	Volume of rock LxWxH (km) $\times 10^6 \text{m}^3$	Cave Volume# $\times 10^6 \text{m}^3$	Cave Length# km	Conduit Porosity %	Conduit Density km/km ³
Rocky Mountains					
Yorkshire System	2x0.5x0.4	200	0.044	10.6	0.02 27
Gargantua	0.5x0.4x0.3	60	0.096	5.9	0.15 100
Castleguard Cave	6x0.5x0.4	1200	0.12	20	0.01 17
Arctomys Cave	1.5x0.4x0.08*	48	0.054	3.5	0.11 73
Eastern USA					
Friars Hole System	6x2x0.08	960	2.7	69	0.28 72
Mammoth Cave	11x9x0.09	8900	8	550	0.09 62
USSR limestone (Courbon and Chabert, 1986)					
Snežnaja	3x2.5x1.4	10500	1.6	19	0.015 1.8
Klevskaja	0.35x0.09x1	31.5	0.036	1.8	0.11 57
Kujbyševskaja	0.45x0.25x0.74	83	0.81	2.0	0.97 24
Gaurdakskaja	0.85x0.6x0.092	47	0.083	11	0.18 230
Orešnaja	0.7x0.65x0.19	86	0.186	18	0.22 210
USSR gypsum (Courbon and Chabert, 1986)					
Optimističeskaja	1.9x1.5x0.02*	57	0.48	157	0.84 2800
Zoluška	1.7x1.3x0.03*	66	0.59	80	0.89 1200
Sarawak, Malaysia (Brook & Waltham, 1978; Eavis, 1981, 1985; Kirby, 1990)					
Southern Gunung Api	7x2.5x0.4	7000	30	110	0.43 16
Norway (Lauritzen, 1982)					
Pikhaggrottene	0.5x0.02x0.035*	0.35	0.0063	2.0	1.8 5700

* For these caves, H refers to the thickness of the beds within which each cave is located. In all other cases, H refers to the total thickness of limestone.

Volume and length of explored cave. Further exploration may greatly increase volumes and lengths in some cases. Cave volumes were calculated by Soviet speleologists for the USSR caves, and by the author in the remaining cases (where accuracy is probably $\pm 30\%$). Cave lengths were calculated by the compilers of the cave maps. Such lengths commonly have a precision of $\pm 1\text{m}$, and an accuracy of probably $\pm 5\%$.

**Figure 6.1****Conduit porosity and density in karst aquifers**

- Conduit density for the caves in Table 6.1, and for the 20 longest and 20 deepest caves in the world (after Courbon & Chabert, 1986)
- Porosity due to explored conduits in 15 caves (data given in Table 6.1)

Dye tracing at Crowsnest Pass has confirmed conduit flow from ten sinkpoints to Crowsnest or Ptolemy Spring. But it is here presumed that if 1000 sinkpoints were tested, then this would reveal 1000 conduit flow routes. The karst catchments of the Flathead and High Rock ranges exceed 400km^2 (Table 2.2). If they have a conduit density of 100km km^{-3} , then the total cave length is about 20,000 km, which equals the length of all currently known caves in the world.

Such thinking has profound consequences for the way karst aquifers are considered. For instance, Castleguard Cave is the longest known cave in the Rocky Mountains (Section 11.2.2). Cave exploration and dye tracing has shown that there must be a minimum of four major active and fossil components to the conduit drainage of the area (Castleguard 0, 1, 2 and 3, respectively: Ford, 1983b; Smart, 1983a). On the other hand, conduit density calculations show the 20km of Castleguard Cave would comprise <1% of the total cave passage in the area, and thus Castleguard Cave would only have been a minor component of the groundwater drainage of the area. This hypothesis is supported by hydraulic calculations which show that paleodischarge in the cave was only about 5% of the discharge from the modern springs (Section 11.2.2).

6.2.3 Conduit porosity

Conduit porosity is here defined as the porosity (as a percentage) of a karstic rock that conduits contribute. It is often included in the term secondary porosity, which also include fissure porosity (Jennings, 1985; Ford and Williams, 1989).

Only researchers in the USSR routinely calculate cave volumes, so the database is rather small (Table 6.1). As with the conduit density calculations, the figures given may underrepresent reality by an order of magnitude as only some passages within any volume of limestone will have been discovered. Nevertheless, Figure 6.1b shows that conduit porosity commonly exceeds 0.1%, and may average 1%.

6.2.4 Segment length

The following terminology on segments is drawn from the two detailed analyses of conduit segment morphology by Ford (1963) and Jameson (1985). A *segment* is a length of cave passage with a single control. Usually, the segment follows one or more fractures, giving a *structural segment*. This may be a bedding plane, fault or joint (giving a *single-fracture segment*), the intersection of two or more fractures (giving an *intercept segment*), or the segment may develop along closely spaced fracture (giving a *zone segment*). If a segment does not follow any fractures, developing instead by connecting the pores in the rock, then it is a *mined segment*. Mined segments are rare in well-lithified, low-porosity, bedded limestones (Ford, 1963; Jameson, 1985). Conversely, they are presumably common in high-porosity limestones (e.g. the Chalk in Britain and France, tropical Quaternary limestones) and in dolomites.

There have been very few measurements of segment lengths in caves. Table 6.2 gives the results of the studies by Ford (1963) and Jameson (1985). Mean segment lengths (L_s) vary from 5m to 21m. These results would appear to be representative of the range commonly found in caves, and would suggest that the differential initial transmissivities along neighbouring structural segments are the prime controls on conduit location at a local scale (1-100m). On the other hand, the very small ratio of segment length to catchment length (L_c) suggests that it may be hydraulic factors which control conduit location at the catchment scale (1-100km).

6.2.5 Sinuosity

The sinuosity, S , of a flow route along cave conduits may be defined as

$$S = L_c / L_x \quad (6.1)$$

Table 6.2 Conduit segment lengths

Cave	number of segments	L_c mean m	L_s/L_c
Mendips Hills, England (Ford, 1963)			
Swildons Hole	160	13	270
G.B. Cave	121	13	210
St Cuthberts Cave	90	16	200
Cheddar Caves	44	21	580
West Virginia, USA (Jameson, 1985)			
Snedegars Cave	92	4.7	2300

where L_c is the length of cave passage followed by the cave stream, and L_s is the straight-line length of the flow route. For a karst aquifer with an orthogonal joint pattern with two joint sets,

$$S = \sin \chi + \cos \chi \quad (6.2)$$

where χ is the angle between the hydraulic gradient azimuth and the direction of either of the joint sets (Figure 6.2a). This function is shown in Figure 6.2b; it has a maximum of $\sqrt{2}$, and a mean of 1.27. Are such sinuosities seen in caves?

The best data set to investigate sinuosity is from complete and long flow paths through karst aquifers. Table 6.3a lists all known flow paths with straight-line distances $> 5\text{ km}$, while Table 6.3b is a compilation of 19 complete flow paths from autogenic sinkpoint to resurgence, and Table 6.3c is a compilation of 51 complete flow paths from allogenic sinkpoint to resurgence. Horizontal sinuosities of the three data sets in Table 6.3 are 1.57, 1.65 and 1.43, respectively.

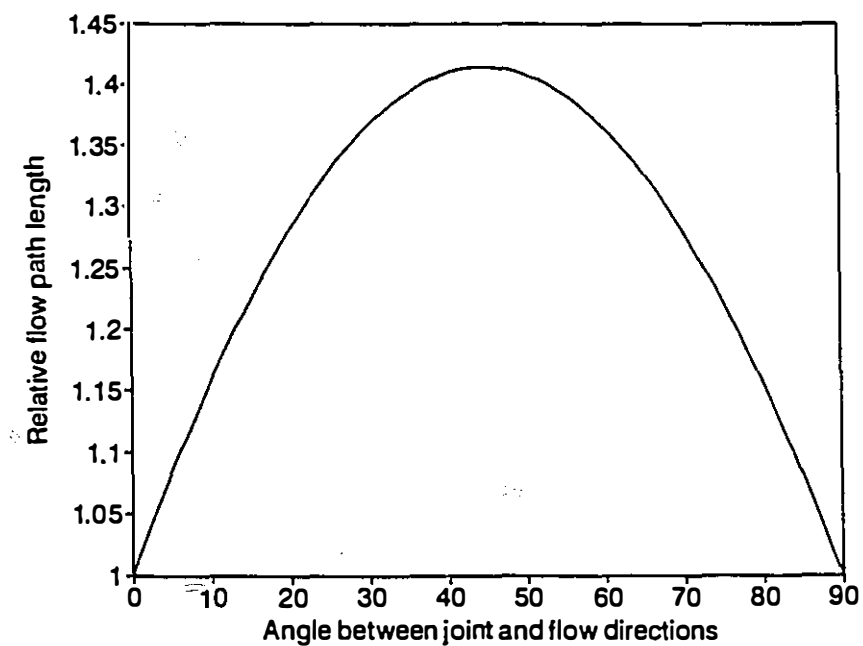
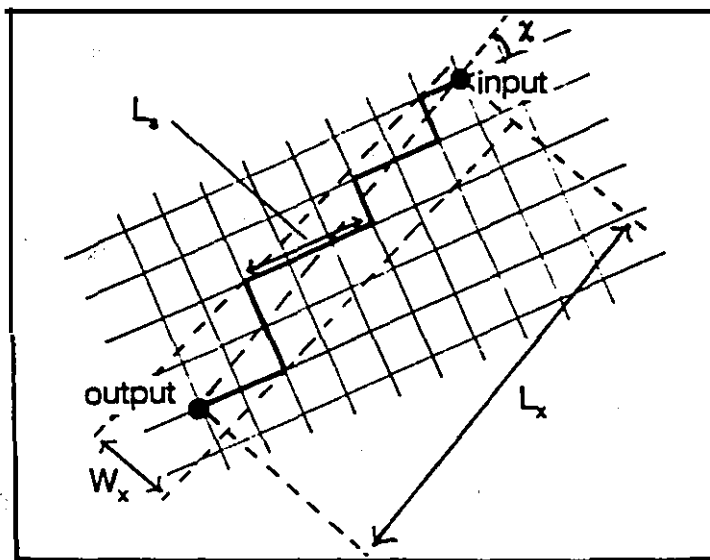


Figure 6.2 Flow paths in an orthogonally-jointed aquifer, using joints or bed-joint intersections
a) terminology (note that this diagram is extremely simplified, and that L_x/L_y is usually >100 .)
b) relative length of flow paths as a function of x

Table 6.3 Sinuosity of flow routes in caves**a) Flow routes with straight-line lengths >5km**

Cave name	Straight-line length			Passage length	S	W _x /L _x	
	XY	Z					
Sistema de Purificación, Mexico	5410	200	6100	1.13	0.043		Sprouse, 1987; Buck, 1990
Rivière du Neuvon, France	7500	30	8700	1.16	0.052		Delance, 1988
Castleguard Cave, Alberta	6510	375	7900	1.21	0.11		Figures 11.2, 11.3
Grotte de Chauvercotte, France	5000	100	6224	1.24	0.18		Minvielle, 1977
Gruto do Padre, Brazil	5000	50	6300	1.26	0.076		Auler, 1988
Grotte de Gournier, France	6400	680	8325	1.29	0.14		Courbon & Chabert, 1986
Great Expectations Cave, USA	5600	415	7300	1.30	0.17		Miller, 1980; Shifflett, 1987
Rio Encantado, Puerto Rico	10850	100	14500	1.34	0.15		Courbon et al., 1989
Réseau des Artes Planétaires, France	5300	587	7500	1.41	0.081		Courbon & Chabert, 1986
Réseau de la Combe aux Prêtres, France	7250	100	10500	1.45	0.20		Delance, 1988
R. l'escalade shunté, Rhar Bou'Maza, Algeria	6100	30	9000	1.48	0.097		Benoit & Collignon, 1988
Gouffre de Padirac, France	5800	230	8581	1.48	0.18		Chabert, 1981; Géze, 1990
Logsdon River, Mammoth Cave, USA	6480	27	9750	1.50	0.15		Coons, in Cl, map of cave
Réseau du Verneau, France	6950	300	10800	1.55	0.040		Couturaud and Aucant, 1990
Blue Nile, Crevice Cave, USA	5050	50	8000	1.58	0.13		Courbon & Chabert, 1986
Red del Silencio, Spain	7540	140	12000	1.60	0.018		Rigal & Boyer, 1989
SC3-Verna, G. de la Pierre St Martin, France	5530	1054	9100	1.62	0.17		Courbon & Chabert, 1986
Cathedral-Falmouth Cave System, USA	5500	39	9250	1.68	0.12		Courbon & Chabert, 1986
Réseau à tout hazard, Rhar Bou'Maza, Algeria	5940	30	10500	1.77	0.16		Benoit & Collignon, 1988
Jaskinia Domica - Baradla Barlang, Czechoslovakia - Hungary							
	5770	90	10500	1.82	0.25		MKB7, 1989
Reinacherstollen - entrance, Höolloch, Switz.	5030	80	9350	1.86	0.13		Bögli, 1980
Torca de los Caballos-Red del Silencio, Spain	5530	498	10600	1.91	0.19		Rigal & Boyer, 1989
Illaminako Ateak, Spain	5550	600	10900	1.95	0.11		Perrette & Maire, 1983
White Nile, Crevice Cave, USA	5100	50	10000	1.96	0.25		Courbon & Chabert, 1986
Réseau de fleurs, Rhar Bou'Maza, Algeria	5420	30	10800	1.99	0.35		Benoit & Collignon, 1988
Siebenhengstehöhensystem, Switzerland	5950	570	12900	2.16	0.14		Jeannin, 1990

b) Complete flow paths in autogenic aquifers

Torca de Hoyu Jondo - Cueva del Valle, Spain	1400	122	1750	1.25	0.10	Rigal & Boyer, 1989
P40 - Guiers Mort, France	1580	623	2130	1.26	0.12	Chevalier, 1951
Torca La Canal - Cueva del Valle, Spain	3700	102	5000	1.35	0.11	Rigal & Boyer, 1989
Arctomys Cave, B.C.	1490	523	2305	1.46	0.25	Thompson, 1976
Sima Tonio - Cueva Canuela, Spain	1265	410	1965	1.48	0.14	Lismonde, 1989
Cueva Oñate - Cueva Tiva, Spain	1800	80	2800	1.55	0.16	Mills & Waltham, 1981
Bull Pot - Keld Head, England	2100	100	3400	1.62	0.17	Waltham & Brook, 1980a
T1 - Cueva de Santa Elena, Spain	1545	558	2800	1.70	0.13	Courbon & Chabert, 1986
Sistema Badalona, Spain	2450	1150	4650	1.72	0.21	Puch, 1989
Sima del Escobal - Cueva del Valle, Spain	1850	102	3200	1.73	0.24	Rigal & Boyer, 1989
Ogof y Daren Cilau, Wales	2980	190	5200	1.74	0.15	Smart and Gardener, 1989
Torca del Sedo - Cueva Tiva, Spain	390	21	700	1.79	0.24	Mills & Waltham, 1981
Tunnel Cave, Wales	480	120	900	1.82	0.14	Coase & Judson, 1977
G. du Bel Espoir-G. de la Diau, France	1720	616	3350	1.83	0.30	Courbon & Chabert, 1986
Gouffre Thérèse - Guiers Mort, France	1060	593	2500	2.06	0.40	Courbon & Chabert, 1986
G. de Cernon-Caborne de Menouille, France	950	120	2000	2.09	0.25	Minvielle, 1977
QS, British Columbia	1190	614	3000	2.24	0.37	Morris, 1984
Windy Link - Quatsino Cave, British Columbia	470	309	1450	2.58	0.13	Morris, 1984
Swinsto Pot - Keld Head, England	950	130	3000	3.13	0.75	Waltham & Brook, 1980a; Farr, 1980; Waltham et al., 1981

Table 6.3c Complete flow paths in allogenic aquifers

Cave name	Straight-line length			Passage length	<i>S</i>	W/L,
	XY	Y	Z			
Sinks of Gandy, USA	780	5		860	1.10	0.06
Gua Payau, Malaysia	1200	10		1400	1.17	0.21
Jordtulla, Norway	495	0.1		580	1.17	0.097
Ogof y Ci, Wales	545	10		640	1.17	0.053
Devils Kitchen, USA	820	15		970	1.18	0.12
Gua Tempurong, Malaysia	970	10		1150	1.19	0.15
Simmons-Mingo-My Cave, USA	4450	140		5300	1.19	0.10
Moira Cave, Ontario	340	2		405	1.19	0.086
Sumidero de Agueyaco, Mexico	340	25		410	1.20	0.13
Sumidero Chicja, Mexico	650	72		795	1.22	0.14
Sof Omar, Ethiopia	970	5		1180	1.22	0.12
Lubang Hijau, Malaysia	1350	180		1660	1.22	0.14
Qiao Ban Dong, China	1800	15		2200	1.22	0.15
Sumidero San Bernardo-Canyon entr., Mexico	520	88		645	1.22	0.16
Ogof Rhyd Sych, Wales	590	10		730	1.24	0.14
Cueva de Cunday, Columbia	450	160		600	1.26	0.23
San Cha He Dong, China	890	15		1120	1.26	0.21
Cueva de Agua Escondida, Guatemala	3370	50		4250	1.26	0.31
Lubang Angin, Malaysia	710	5		910	1.28	0.19
Cochol, Mexico	860	37		1120	1.30	0.22
Grotte de la Roche, France	1210	30		1577	1.30	0.20
Nelson Cave, USA	365	10		480	1.31	0.15
Sumidero del Rio Atima, Honduras	1850	190		2450	1.32	0.11
Rivière souterraine de Bramabiau, France	780	20		1050	1.35	0.28
Sumidero San Bernardo-East trib., Mexico	470	103		650	1.35	0.11
Ren Xiao Dong, China	1500	25		2050	1.37	0.18
The Tunnel, W.A, Australia	430	5		590	1.38	0.35
Tigris Tunnel, Turkey	610	15		865	1.42	0.42
Guan Yan, China	1010	10		1440	1.43	0.21
Raggejavrerge, Norway	885	620		1550	1.43	0.091
C. Veronica del Rio Candelaria, Guatemala	2810	5		4060	1.44	0.12
Gruta del Rio San Jeronimo, Mexico	3830	50		5560	1.45	0.30
Grotte de Saint Casimir, Québec	310	1		460	1.48	0.24
Haphazard Cave - Pitchford's Cave, B.C.	470	20		700	1.49	0.21
Actun Box Ch'ich, Belize	1260	183		1900	1.49	0.11
Sunken Forest Cave, Belize	580	32		880	1.51	0.11
Sleepwalker Series, White Scar Cave, England	1550	105		2360	1.52	0.23
Cueva del Agua-la Cuevona, Spain	855	12		1320	1.54	0.20
Bowden Cave, USA	1010	20		1570	1.55	0.086
Darknight Cave, Belize	320	35		510	1.58	0.28
Kahf Hoti, Oman	2630	260		4300	1.63	0.32
Greenwood Pot - White Scar Cave, England	1610	131		2650	1.64	0.16
G. de Jérusalem-Source du Verneau, France	6500	338		10700	1.64	0.086
Gruta del Rio Chontalcoatl, Mexico	3320	50		5610	1.69	0.44
Grotte de la Vieille Folle-Verneau, France	3550	265		6200	1.74	0.14
Cueva de el Chorreadero, Mexico	1470	334		2695	1.79	0.41
Cueva de Tecolo, Mexico	755	53		1370	1.81	0.43
Réseau de Foussoubie, France	3400	110		6200	1.82	0.21
Broken River Cave, New Zealand	340	20		650	1.91	0.26
Apetlanca, Mexico	1370	139		2740	1.99	0.29
Sumidero San Bernardo-Lower ent., Mexico	890	200		1910	2.09	0.43

Allogenic flow paths are clearly more linear than autogenic flow paths (Figure 6.3). This is because allogenic flow paths usually represent a single linear flow path from sink to spring. Conversely, many of the autogenic flow paths consist of two components: a tributary vector and a principal conduit vector. This is clearly seen in the six longest known flow paths (Figure 6.4). In all six cases the principal conduit is more linear than are tributaries.

It is clear that conduit flow does not follow the shortest single-fracture or fracture-intersection flow paths through an aquifer, for mean sinuosities exceed 1.27. However, the mean sinuosity of 51 allogenic flow paths (the most representative data set in Table 6.3) is only 13% longer than this value. This suggests that hydraulic factors may play an important role in conduit flow path development in karst.

6.2.6 Flow belt width

In plan view, many cave passages appear to be joint-guided, but such passages are often located at bed-joint intersections. If conduit flow routes develop along the most direct joint-oriented paths, then the width of this flow belt, W_x , will be small in relation to L_x .

Using the same data sets as for conduit sinuosity (Table 6.3), width/length ratios (W_x/L_x) of the three data sets are 0.14, 0.19 and 0.20, respectively. The example in Table 6.3 with the greatest non-linearity is Swinsto Cave - Keld Head, with $S=3.1$ and $W_x/L_x=0.75$. Waltham et al. (1981) described this flow path in detail, explaining that there were two components. The tributary section developed in the vadose zone, and is oriented downdip, towards the north-east. The principal conduit section was developed in the phreatic zone, and is oriented to the south, towards the spring. The sinuosity and width/length ratio of the separate components are much more linear than the overall ratios, and are similar to the mean values for allogenic flow paths. They are: $S=1.51$ and 1.64, respectively, and $W_x/L_x=0.15$ and 0.34, respectively. The same holds true for many flow paths with high sinuosities, which are

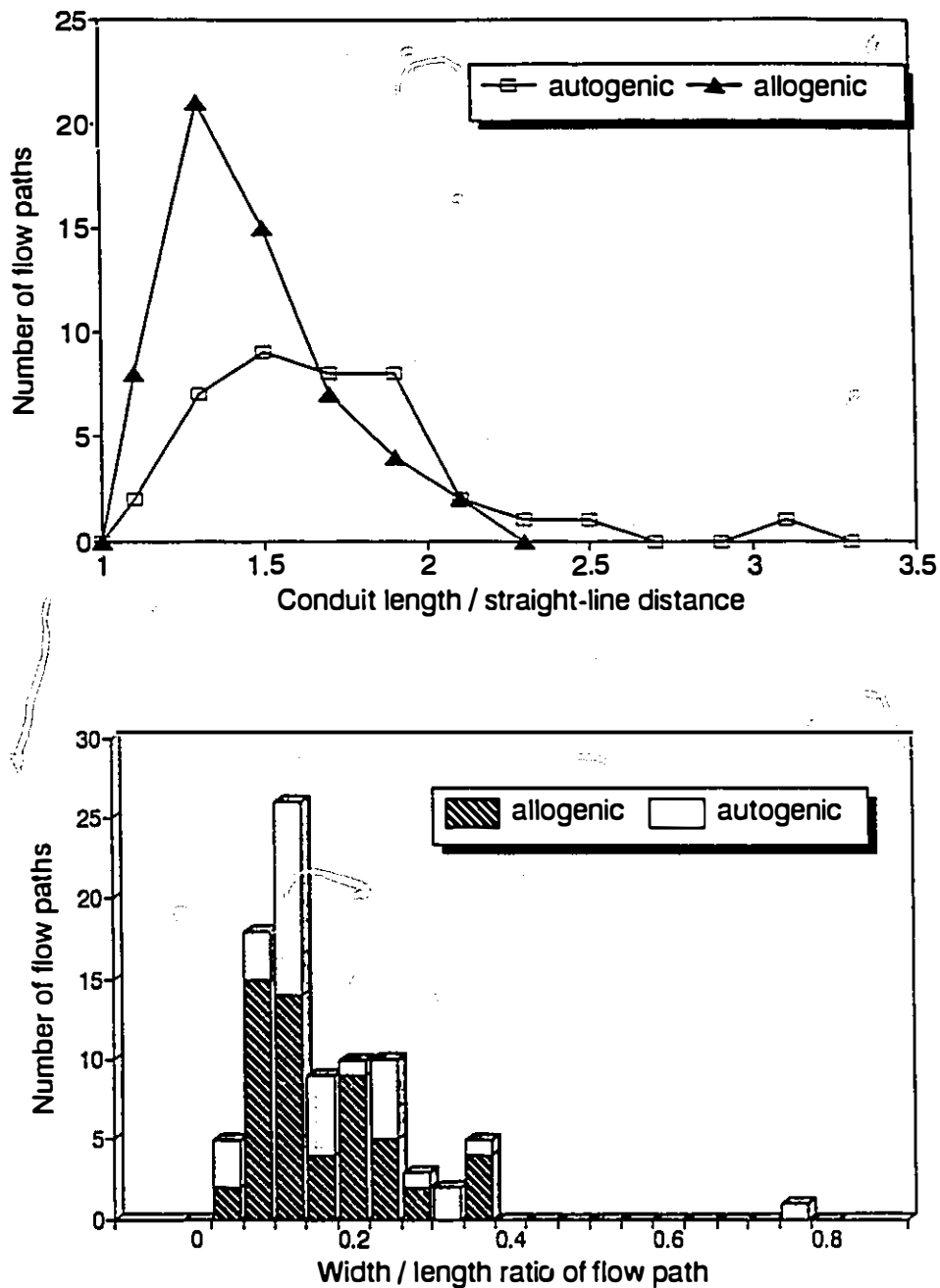


Figure 6.3 Efficiency of flow paths in karst - plan patterns of 57 allogenic and 39 autogenic flow paths (data in Table 6.1)

- sinuosity**
- width/length ratios**

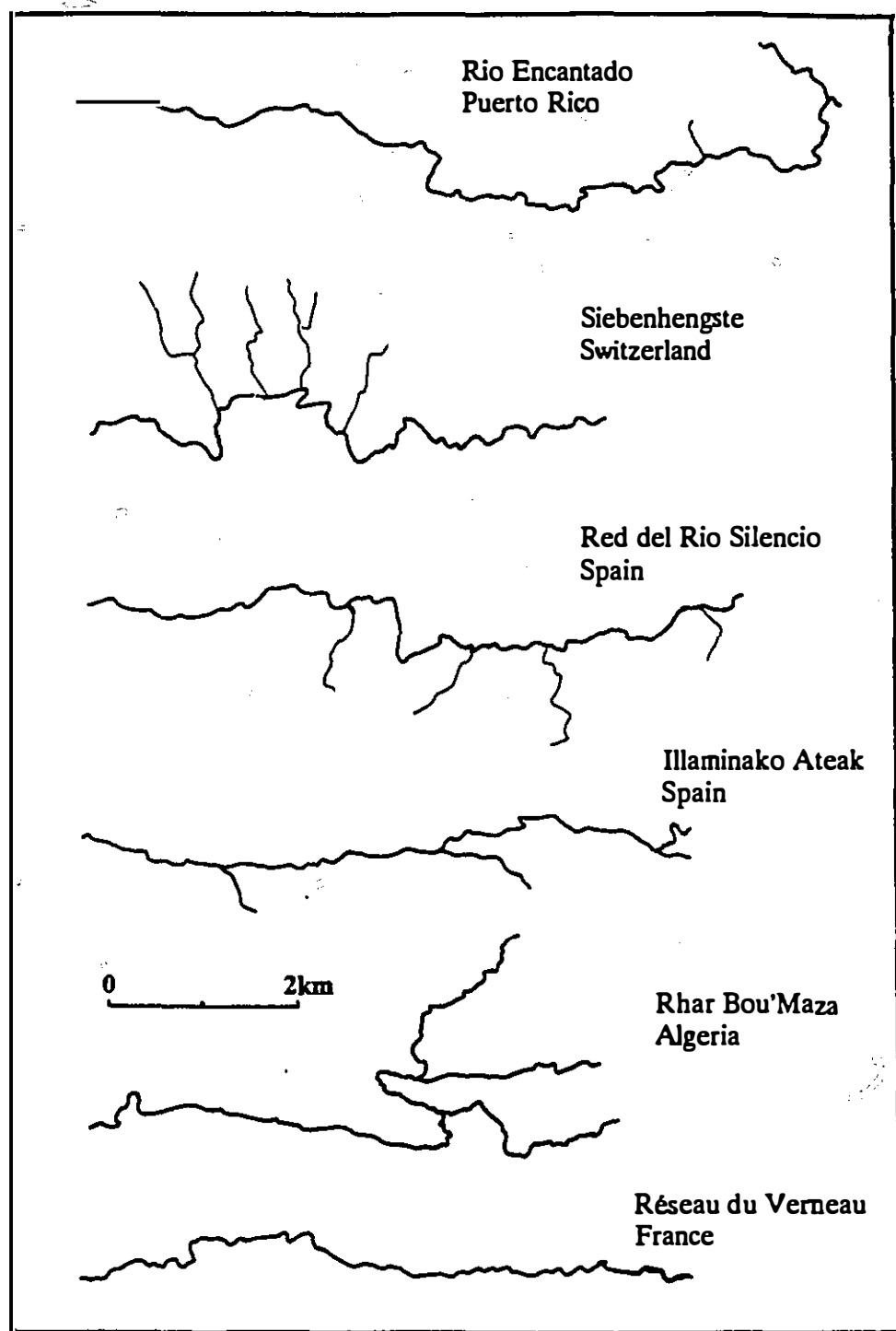


Figure 6.4 Plan patterns of the six longest explored flow paths in karst conduits
(for sources see Table 6.1)

made up of two or more low-sinuosity elements.

6.2.7 Depth of loop crests and bases

The vertical sinuosity of cave conduits is known as looping (Ford, 1965). For each phreatic loop there is a high point and a low point (Jameson, 1985); the high point of a loop has also been called a loop crest (Smart and Christopher, 1989). For clarity and conciseness, the terms *loop crest* and *loop base* are used in this account. For strike-oriented flow along a bedding plane, where there is a regularly spaced orthogonal joint network, then conduits should develop at bed-joint intersections. According to the dominant paradigm of the last thirty years, conduits would develop along favourable fractures or fracture intersections closest to the water table (e.g. Ford, 1971b). In this case:

$$0 < D_c < S_j \cos \lambda \sin \theta \quad (6.3)$$

where D_c is the phreatic depth of a crest, S_j is the spacing between joints, λ is the angle subtended between the strike and a joint direction, where $0 < \lambda < 45^\circ$, and θ is the stratal dip. The depths of the closest adjacent loop base is

$$D_b = D_c + S_j \cos \lambda \sin \theta \quad (6.4)$$

where D_b is the phreatic depth of a loop base. Combining Equations 6.3 and 6.4 gives

$$S_j \cos \lambda \sin \theta < D_b < 2S_j \cos \lambda \sin \theta \quad (6.5)$$

so that

$$0 < D_c/D_b < 0.5 \quad (6.6)$$

with a median value of 0.33.

Equation 6.6 may be tested by using data from both active and fossil conduits. Some well-documented conduits are listed in Table 6.4, and the profiles of

Table 6.4 Crest/base depth for phreatic loops

cave	type	length m	D_x m	D_c m	D_b m	D_c/D_b mean	n of crests and bases	
Doux de Coly, France	p	3180	58	32	42	0.62	8	Figure 6.4a
Holloch: Reinacherstollen-entr.	f	9300	160	83	115	0.73	46	Figure 6.4b
: Schluchtgang - Riesensaal	f	6000	140	59	98	0.60	35	Figure 6.4b
Réseau de Foussoubie, France	a/f	9000	130	68	77	0.89	80	Figure 6.4c
Wookey Hole, England	v/p/f	1300	95	21	37	0.65	34	Figure 6.4d
Swildons Hole (active tier)	v	850	46	30	37	0.81	20	Figure 6.4d
G. Annette-Trou de Glaz, France	f	1600	90	39	57	0.63	18	Figure 6.4e
Yorkshire System: Roller Coaster	f	522	58	33	42	0.78	12	Figure 6.5b
Castleguard Cave, Alberta	f	7900	370	300	325	0.92	6	Figure 11.3
Rats Nest Cave, Alberta	f	900	136	57	82	0.69	16	Yonge, 1990
Grotte de la Mescla, France	p	1510	95	30	59	0.51	18	Tardy, 1990a
Grotte de Paques, France	p	810	50	4.8	19.6	0.24	11	Tardy, 1990b
Grotte des Moulins "C", France	f	150	28	9.6	16.8	0.57	10	Le Pennec, 1989
Grotte du Grenouillet, France	f	520	86	24	45	0.53	16	Houlez, 1988
Grotte de la Doue, France	tp	340	23	5.1	9.7	0.53	11	Colin & Drouin, 1986
Ringquelle, Germany	p	930	23	0.8	21.2	0.51	21	Farr, 1980
Cueva del Agua, Spain								
Grand Circle - Bowling Alley	f	1400	206	72	106	0.78	20	Smart, 1984b
Big rift - Hole in the wall	f	1200	104	65	83	0.77	27	Smart, 1984b
Source du Lison, France	p	802	29	7.7	16.2	0.48	14	Isler, 1981

Notes:

All values for D_x , D_c , D_b , and D_c/D_b are minima; in many cases the water table would have been higher when the passage was formed than can now be ascertained.

Cave types - p = active phreatic

v = active vadose

f = fossil

tp = temporary active phreatic

six are shown in Figure 6.5 and 6.6b.

Perhaps the best example of a currently active phreatic flow path is the world's longest explored siphon at Doux de Coly, Dordogne, France (Figure 6.5a). This is a strike-oriented conduit which maintains a phreatic depth of >30m for over 3km; dye traces have shown the catchment extends at least 8km further along the strike, so that a single strike-oriented loop of 11km may soon be explored (Isler and Magnin, 1985).

A partially drained and partially explored phreatic flow path is found at Wookey Hole, England (Figure 6.5b). The water table has lowered by at least 28m since the present flow path was initiated, but about half the passage explored so far is still submerged. One upstream feeder to Wookey Hole is Swildons Hole. An upper tier of passages was not entrenched before abandonment, but the lower, active tier has seen water levels lower at least 30m since initiation.

Notable fossil examples of phreatic flow paths include Höllloch, Switzerland (Figure 6.5c), Foussoubie, France (Figure 6.5d), Grotte Annette - Trou de Glaz, France (Figure 6.5e), Yorkshire System, Alberta (Figure 6.6b), Tantalhöhle, Austria (Courbon and Chabert, 1986), and Dune Series - Revival in Gua Air Jernih, Malaysia (Waltham and Brook, 1980b).

At Crowsnest Pass, Crowsnest Spring provides the only explored example of active phreatic flow (Figure 6.6a), and Yorkshire Pot is the best example of a fossil phreatic passage (Figure 6.6b). In the latter, the principal initial development was along the Roller Coaster, which meandered up and down, mostly at a phreatic depth of 30 to 45m. Subsequently, tributaries such as Alberta Avenue were formed at greater depths (Figure 6.6b).

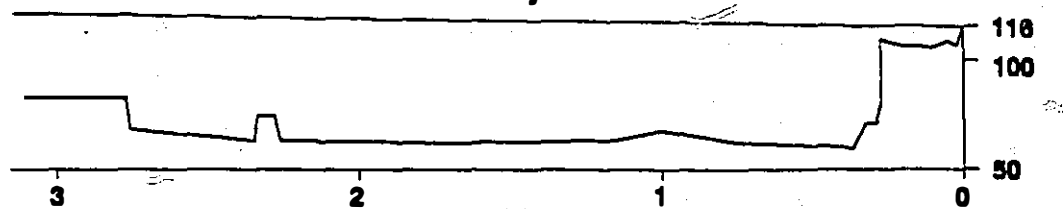
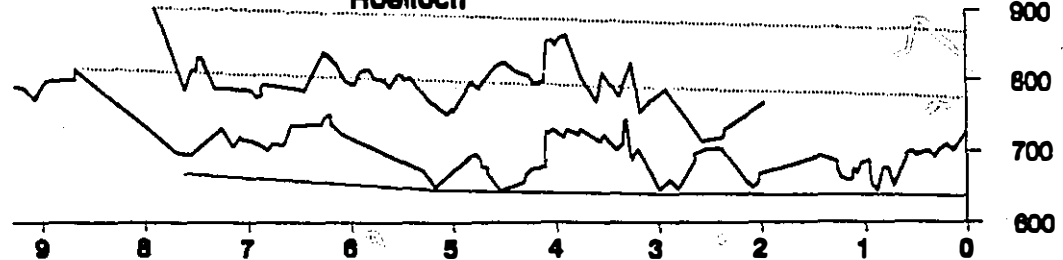
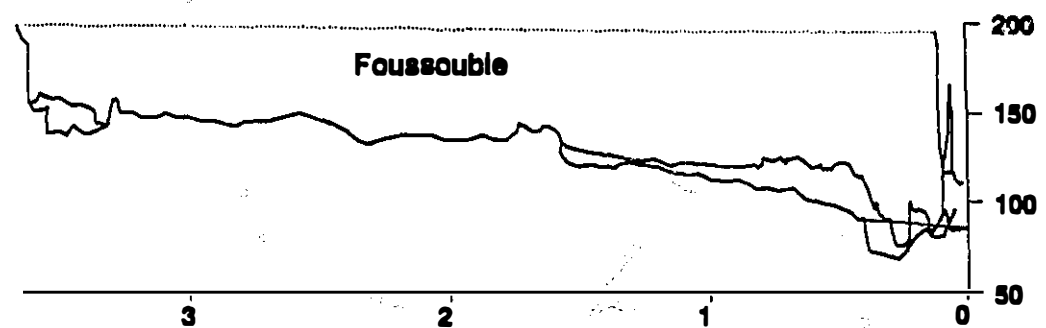
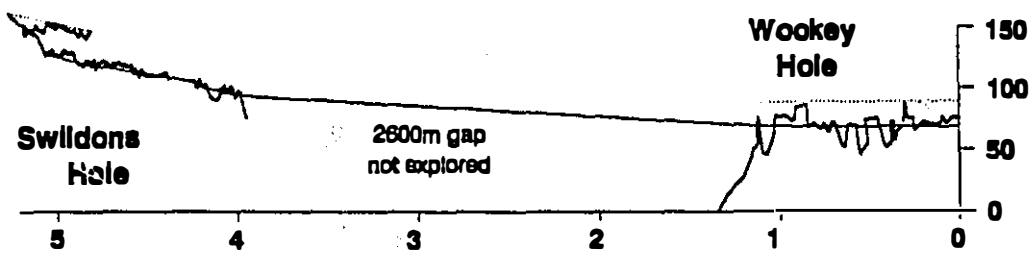
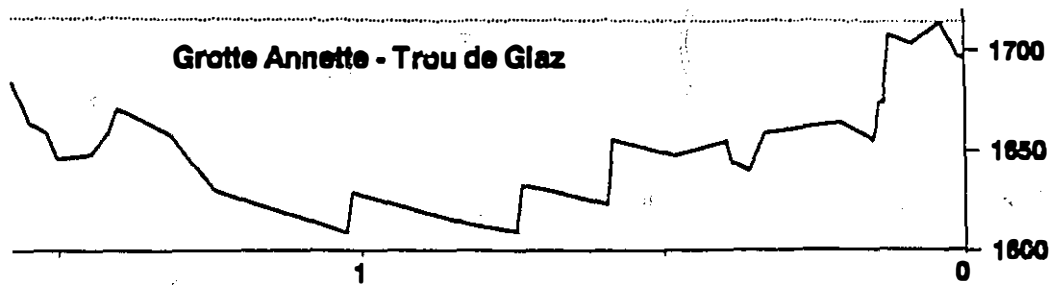
Sixteen of 18 examples in Table 6.4 have $D_f/D_b > 0.5$ (Figure 6.7), and thus do not support the hypothesis of flow along favourable fractures close to the water table. An alternative hypothesis will be proposed in Chapter 7.

Figure 6.5 Profiles of five well-documented phreatic loops

Legend: _____ present low-flow water table
 inferred low-flow paleo-water table

In each case flow is (or was) to the right of the diagram

- a) Extended profile of Doux de Coly, France (after Isler and Magnin, 1985). The cave has developed along the strike in a catchment estimated to be 14km long (Isler and Magnin, 1985). The strata dip gently ($<3^\circ$) to the south, but there is a monoclinal steepening ($4^\circ\text{-}9^\circ$) where the cave is situated. The cave may also be associated with two strike-oriented faults which are located along the axis of the catchment: a 1.5km long fault at Salojour, and the 2.5km long Nadaillac fault (B.R.G.M., 1979).
- b) Extended profile of Höllisch, Switzerland (after Bögli, 1980). The two principal paleoconduits are shown. These passages are developed along the strike on a slickensided bedding plane dipping $12\text{-}20^\circ$. Paleo-water tables shown are assumed to have the same gradient as the present water table.
- c) Projected profile of Réseau de Foussoubie, Ardèche, France (after Le Roux, 1989). There is considerable foreshortening of the profile close to the spring: the passage length from sink to spring is 6.1km. The cave has >50 sumps in low-flow conditions.
- d) Extended profile of Swildons Hole - Wookey Hole, England (after Ford, 1963; Drew, 1975b; Boon, 1977; and Farr, 1983). Note that the 2.6km gap is the straight-line distance. The drainage basin has a length of 8.3km (Drew, 1975a), but Swildons Hole is located only 3.6km from Wookey Hole. It is therefore presumably a tributary to the principal conduit.
- e) Grotte Annette - Trou du Glaz, Réseau de la Dent de Crolles, Isère, France (after Chevalier, 1951). This fossil flow route is now >1700 m above valley level, and the original flow route must have been longer.

Doux de Coly**Hoelloc****Foussouble****Wookey Hole****Grotte Annette - Trou de Glaz**

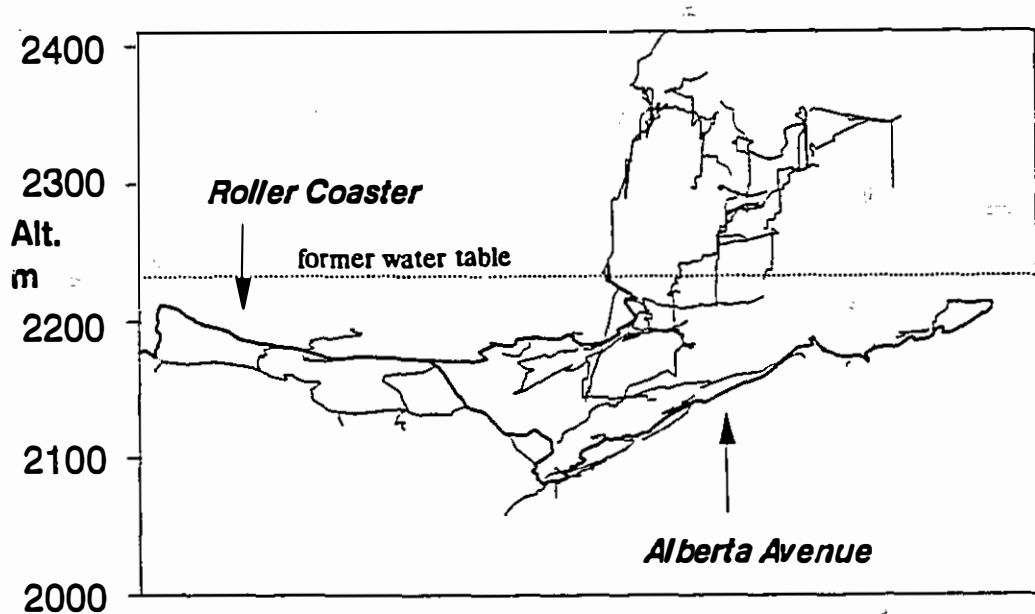
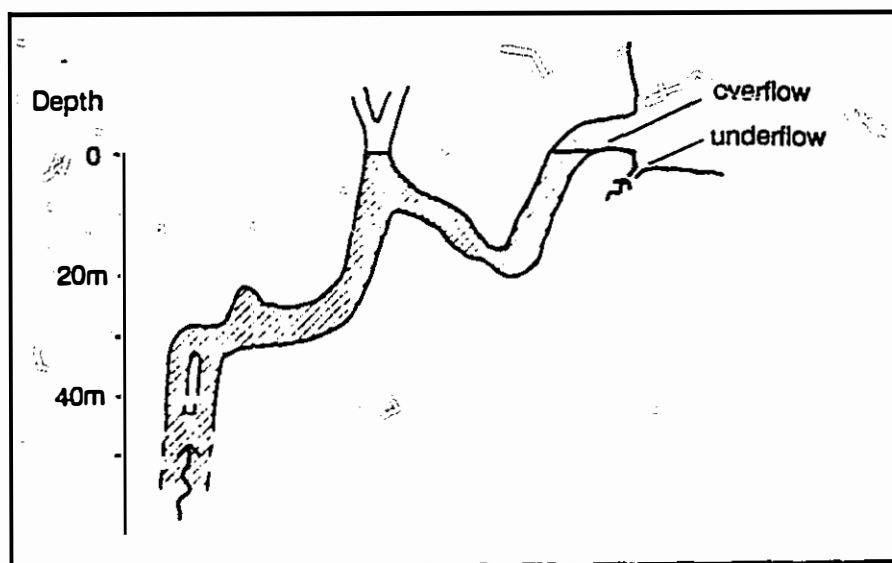


Figure 6.6 Profiles of active and fossil caves at Crowsnest Pass, showing vertical looping
 a) Crowsnest Spring (after Barton, 1981)
 b) Yorkshire System, showing two important passages developed when the water table was at or above 2230m

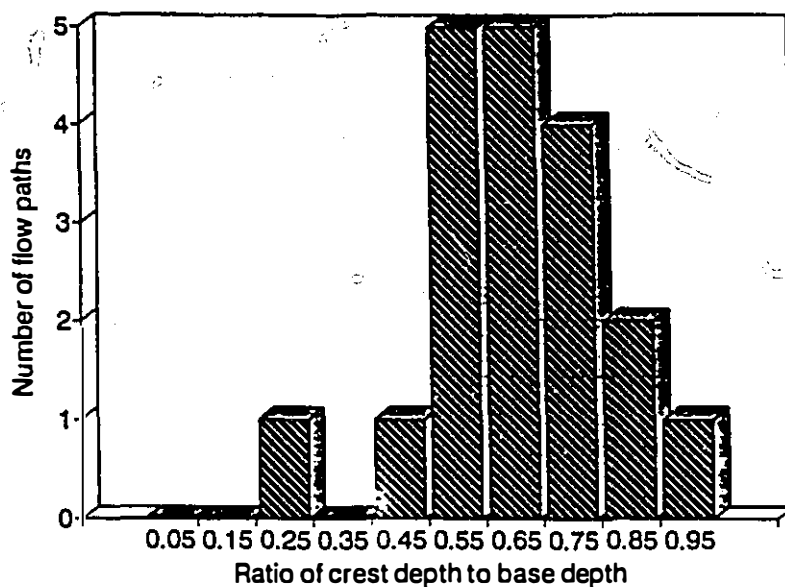


Figure 6.7 Relative depth below the water table of loop crests and loop bases for 19 active and fossil phreatic paths (data listed in Table 6.3)

6.2.8 Conclusion

The development of the six indices in the previous six sections has helped to characterise conduit flow paths. It has been shown that flow paths are made up of many, short structural segments, that flow paths follow efficient paths, and that conduit flow paths are not close to the water table. These findings will be used in Chapter 7 to support a new model of karst groundwater flow.

6.3 Geological controls

6.3.1 Fracture occurrence

Detailed studies of flow paths in well-karstified, bedded limestones have found that almost all conduits are developed along pre-existing bedding planes, joints and faults. Early cave studies considered fracture guidance in terms of a single

variable (e.g. Ford, 1963; Ewers, 1972; Powell, 1977; Charity and Christopher, 1977), but the meticulous studies by Jameson (1981, 1985) showed that conduits frequently form at the intersection of two fractures. Since conduits propagate along such fractures, it follows that the fracture flow net will be distorted by those fractures or fracture intersections with high initial hydraulic conductivities.

Most karst limestones are well-bedded and well-jointed, and the catchment is of large enough size so that the inter-bedding plane and inter-joint distances are insignificant fractions (e.g. <0.001) of the catchment length. In these conditions, if joints and beds were equally favoured for conduit propagation, then the overall hydraulic conductivity would be isotropic, and the flow net would closely resemble a Hagen-Poiseuille or Darcy flow net. On limestone pavements there are often two orthogonal joint sets normal to the bedding, with both joint and bed spacing usually in the range 0.1 - 10m. Thus, the evidence from limestone pavements indicates that there are usually sufficient bed and joint pathways to ensure isotropic conditions on catchment scale. Furthermore, since joints offer two of the three orthogonal planes, then on average they would be utilised by conduits two-thirds of the time. This was the approach used by Bedinger (1966) in an electric analogue study.

Bedding planes are predominantly favoured for conduit development largely because they offer transmissive fractures which are continuous laterally for large distances in both x and y directions (Renault, 1968). Thus a conduit may follow one bedding plane for hundreds, and occasionally for thousands of metres (e.g. Palmer, 1977; Worthington, 1984). Some bedding planes will have higher initial transmissivities than others, and these will be favoured; for instance, in Friars Hole System, USA, two bedding planes, both between lithologically dissimilar limestones, are the locus for some 20km of passage (Worthington; 1984). Furthermore, the lithology of some beds may be particularly favourable for dissolution (Rauch and White, 1970), and minor aquitards may also promote bed-parallel flow, especially in the vadose zone (Waltham, 1971).

On the other hand, joints are neither laterally nor vertically very extensive, and a single joint rarely guides a cave passage for more than a few tens of metres. Furthermore, passages often develop at bed-joint intersections, so that in a horizontal sense they are joint-aligned, but in a vertical sense they are bedding-aligned. This is the case for at least some of the caves in Indiana described by Powell (1976) and for Ogof Ffynnon Ddu, the longest cave in Wales, where one bed is seen in the roof of much of the "joint-oriented" maze of the Top Entrance Series (Charity and Christopher, 1977; Ewers, 1982). The consideration of caves in only two of the three dimensions (x-y) has led some karst researchers to stress the importance of joints in cave development (e.g Trudgill, 1985, p73; Dreybrodt, 1988, p195-198).

Faults are occasionally important for passage alignment. Notable examples are Höolloch, Switzerland (much of the cave along a slickensided bedding plane: Bögli, 1980; Ewers, 1982), and Friars Hole System, USA (more than 10km of passages on bed/fault intersections: Worthington, 1984).

6.3.2 Primary tube development on multiple bedding planes

White and Longyear (1962) found that at the transition from laminar flow to turbulent flow in a conduit, there is a hydraulic jump, with the effectiveness of solution increasing by seven orders of magnitude. This was demonstrated in plaster models by Ewers (1982). He showed how solutional enlargement concentrates in one direction along a bedding plane, producing primary tubes or anastomoses, with the eventual formation of a victor tube. The enhanced hydraulic conductivities along bedding planes will produce equipotential ellipses centred on the victor tube. The development of primary tubes or anastomoses would then decrease exponentially away from the victor tube, and there would be a limit beyond which anastomoses or primary tubes would not form. This equipotential line is called the primary tube limit in Figure 6.8.

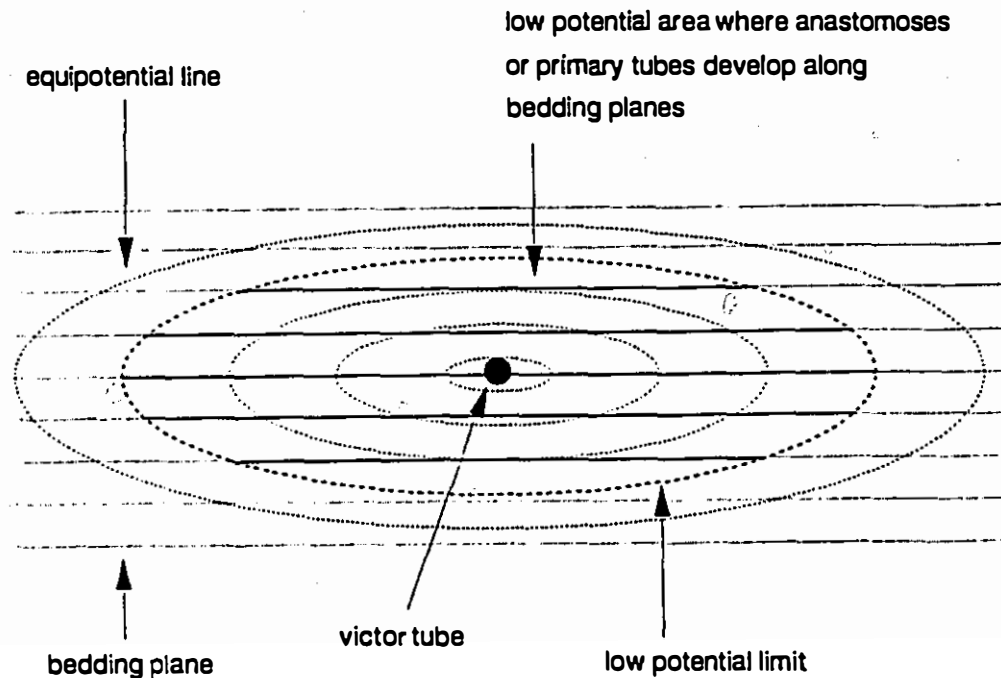


Figure 6.8 Cross-section through the low-potential field surrounding a developing conduit

Unfortunately, there has been little field research on primary tubes or anastomoses. Ford (1971b) found 12 primary tubes in a 360m section of strike-oriented passage in steeply-dipping limestones in Swildon's Hole, England. The tubes were mostly about 20cm in diameter, were oriented approximately downdip, and occurred in two groups; four were spread over a width of 35m, and eight were spread over 90m, with a 150m gap with no primary tubes separating them. Ford (1971) thought that these primary tubes were the earliest conduits of karstic flow, were widespread in the host rock, and were the steep-dip equivalent to anastomoses.

Ewers (1966, 1972) studied anastomoses in several caves in Kentucky where the stratigraphic dip is extremely low ($0.2\text{--}0.5^\circ$). The tubes ranged in diameter from a few millimetres up to about 50cm, with a median diameter of 10-20cm. Ewers (1972) found an exponential decrease in numbers of tubes as passage width increased, as would be predicted from Figure 6.8. The total width of the anastomotic band was commonly less than 5-6m.

Jameson (1985) made a comprehensive study of about 500m of passages in Snedegars Cave (West Virginia, USA), where the dip is 2° . Pre-entrenchment primary tubes had average cross-sectional areas of $0.2\text{--}0.3\text{m}^2$, and few sections of primary tube were not later enlarged by entrenchment.

All three studies confirm that the earliest conduit flow is in small phreatic tubes. Empirical evidence suggests that sometimes in low-dip limestones these may proliferate as anastomotic bands, though there is no theoretical explanation for this. The 12 primary tubes in Swildon's Hole data can be interpreted as developing within two low-potential areas from two separate inputs to the aquifer, with none of the tubes enlarging to full conduit size.

The spacing between low-potential areas (where there are primary tubes or anastomoses) is critical to the subsequent development of conduits, but few measurements have been made. An indirect method is to consider the spacing of inputs to a karstic aquifer. The closest spacing would be expected where there is diffuse infiltration through a permeable, insoluble caprock such as sandstone, or in isolated hills without sinkholes. Palmer (1975) found that 60% of a sample of 260 maze caves which he examined were formed in such situations, with passage spacing typically every 10m. Wider spacing of inputs would be expected where there are dolines, which are typically spaced 100m apart. The approximately 100m spacing in Höolloch and the 200m spacing in Parker Cave of parallel downdip passages were interpreted by Ford (1971b) and Ewers (1982), respectively, as reflecting primary tube

spacing. It is possible that these passage spacings at Höolloch and Parker Cave are similar in each case to doline spacing on the surface.

These examples suggest that the spacing of low-potential areas is related to the spacing of major inputs on the surface, and thus may range from metres to hundreds or thousands of metres. This conclusion could be reached from the plaster laboratory models of Ewers (1982), but it is uncertain to what extent these models may provide an analogue to karstic aquifers.

The model studies of Ford and Ewers (1978), Ewers (1982) and Ford and Williams (1989) predict the establishment of a series of primary tubes 1mm or more in size, which are oriented along the original flow lines along bedding planes. In the case of strike-oriented flow these primary tubes will be essentially downdip close to the sinkpoints, close to horizontal for most of their flow paths, and almost updip near the resurgence. Downdip primary tubes close to sinkpoints were described by Ford (1963), and have been mapped in detail by Jameson (1985), but the complementary horizontal and updip primary tubes have not been described before.

Once one primary tube has extended to connect sink and spring, then it will provide a much lower resistance route for flow than other non-integrated primary tubes. There will be a 10^3 - 10^6 increase in dissolution along this victor tube, and the flow net will be reoriented towards it, so that it may rapidly (10^3 - 10^4 years) become the principal drainage route for the catchment (Ewers, 1982; Ford and Williams, 1989).

Rhoades and Sinacori (1941) envisaged the principal conduit as extending almost horizontally to the spring, while Davis (1966) envisaged the conduit ascending steeply to the spring. Models of fracture flow and the geometry of conduit flow paths will be discussed in Section 6.4, where it will be shown that the latter geometry is more probable.

6.3.3 To what extent are bedding planes favoured as flow routes?

It is now possible to relate hydraulic conductivity (K) in the flow direction along a bedding plane (K_z), normal to x across the bedding plane (K_x), and normal to the bedding plane, along joints (K_y). For an isotropic aquifer

$$K_x = K_y = K_z \quad (6.7)$$

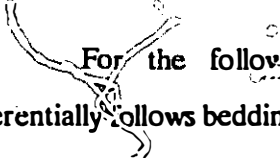
Fracture aquifers are anisotropic, and commonly K_z is about an order of magnitude less than K_x or K_y (Domenico and Schwartz, 1990). In this case, before solutional enlargement a karstic aquifer would have

$$K_x = K_y = 10^1 K_z \quad (6.8)$$

Freeze and Cherry (1979) showed that for a homogeneous, anisotropic medium with principal hydraulic conductivities K_x , K_y and K_z , then equipotential lines can be expressed by a hydraulic conductivity ellipsoid with major axes $K_x^{0.5}$, $K_y^{0.5}$ and $K_z^{0.5}$. For a karstic aquifer the major axes x and z (or y and z) would thus have the ratio of approximately

$$x = y = 10^{0.5}z \quad (6.9)$$

Where the flow path is not along the strike, then the flow cannot follow a single bedding plane, and the situation is somewhat more complicated. Of primary importance is the ratio of bedding plane to joint passages. Waltham (1971, p79) suggested that the ratio "is a function of the difference between the angle of apparent dip and the overall hydraulic gradient of the system". This introduces the concept that the ratio is a predictable function of the geometry of the flow route, but does not take into account the predilection of karst conduits for bedding planes, described in Section 6.2.1. Nevertheless, it is possible to make some predictions of bed/joint passage ratios given certain assumptions.

 For the following analysis it is assumed that groundwater flow preferentially follows bedding planes or bed/joint intersections, that the joint-aligned routes followed between them are normal to them, and that flow will take the shortest route between bedding planes. The validity of these assumptions is discussed at the end of this section.

The ratio (R) of bedding planes to joints utilised by conduits is then

$$R = 1 / (\tan \theta \sin \phi) \quad (6.10)$$

where ϕ is the angle subtended by the strike and the flow direction.

Equation 6.10 refers to the maximum possible bedding plane utilisation in any structural situation. Ford and Ewers (1978) found that >30% of the passages in Swildon's Hole, England followed joints ($R = 1.45$; predicted value from Equation 6.10 is 8). Ewers (1969) found $R = 13$ for some caves in E. Kentucky (predicted $R > 100$). In Jameson's (1985) study of Snedegar Cave, West Virginia, R was 1.1 (predicted $R = 17$). Thus, bedding plane utilisation by conduits is considerably less than the theoretical maximum, but much more than the mean value of 0.5 that would result if joint and bedding plane hydraulic conductivities were equal. These values >0.5 support the contention of greater horizontal K introduced in Equation 6.8.

The maximum bed/joint ratios (Equation 6.10) for different structural situations are shown in Figure 6.9, to which have been added the three caves cited above plus other caves with well-documented geological structures. Most of these caves have predicted R 's >10 , which supports the predominance of bedding planes for conduit flow. Nevertheless, R will be less than 1 in the rare karsts with high dips where the flow is not strike-aligned.

The importance of bedding planes found in studies of cave conduits thus supports the use of bedding planes as guiding fractures.

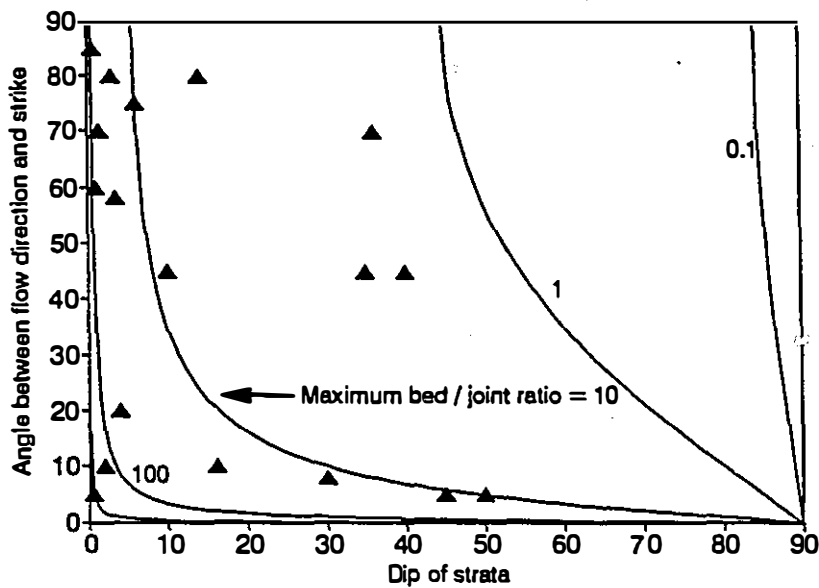


Figure 6.9 Maximum possible use of bedding planes as flow routes as a function of dip and strike
The data points are listed in Table 7.1

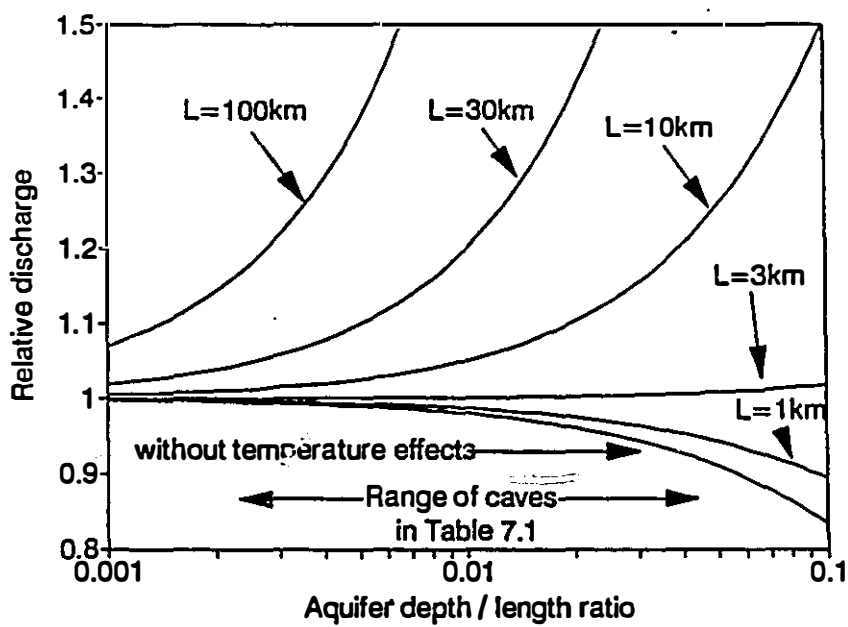


Figure 6.10a Relative discharge of fracture flow paths in an orthogonal flow net, using the Hagen - Poiseuille equation

6.4 Hydraulic controls on conduit development

6.4.1 Flow through fractures

It was explained in Section 6.2.1 that the initial flow through a karst aquifer is largely along pre-existing fractures. This flow is laminar, and may be described by the Hagen-Poiseuille equation (Equation 5.2). Thraikill (1968) used this equation to calculate the relative flow through deep and shallow fractures in simple hydraulic situations. Holding hydraulic gradient and fluid density and viscosity constant, he found that shallow flow paths would carry marginally greater discharge than deeper flow paths. However, both the density and the viscosity are negative functions of temperature, at least between 4° and 100°C, and different results are obtained if these two terms are included. If a geothermal gradient of 25°C km⁻¹ is assumed (Freeze and Cherry, 1979; Hitchon, 1984), then deeper flow paths become more efficient than shallow flow paths in catchments longer than about 3km (Figure 6.10).

Figure 6.10a would suggest that conduits would preferentially form close to the base of aquifers, especially in long catchments. However, the empirical evidence shows that this does not occur. For instance, both Yorkshire Pot (Figure 6.6b) and Castleguard Cave (Figures 11.2, 11.3) formed well above the base of the respective aquifers, and the existence of tiered caves is an even clearer demonstration (e.g. Figure 6.5b,d, 8.2). Instead, flow depth is typically about 1% of the catchment length (Thraikill, 1968; also Figure 6.10a).

It seems reasonable to assume that there is an exponential decrease in permeability with depth in a Hagen - Poiseuille flow field. This could be due to decreasing fracture width and/or numbers with depth, which would be a function of the tectonics and of the flow field forming early conduits within the aquifer. There is some empirical evidence that permeability does decrease exponentially with depth (Milanović, but see Mixon, 1990). Figure 6.10b shows the effect of combining Hagen

158 a

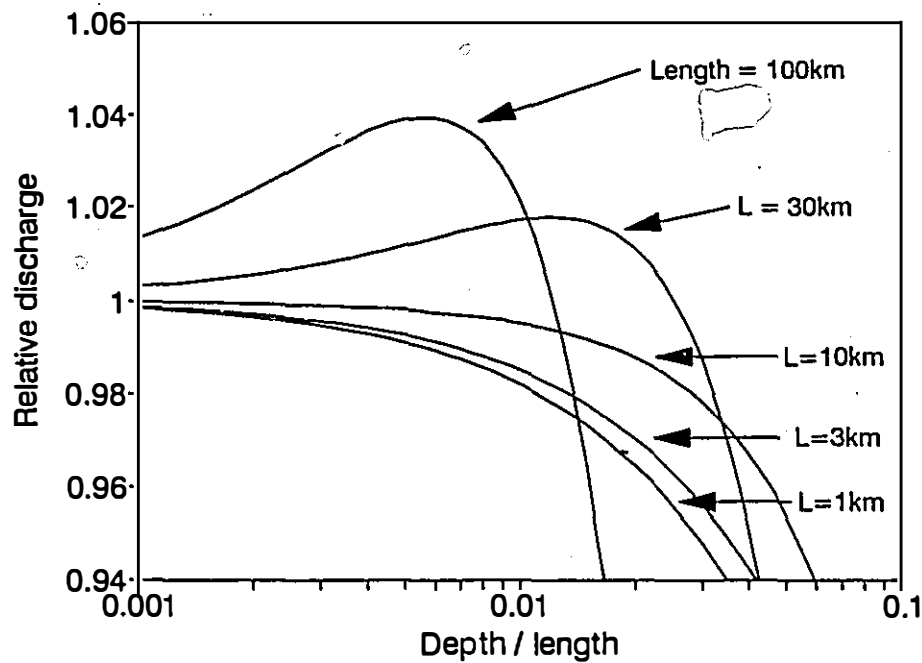


Figure 6.10b Relative discharge of fracture flow paths in an orthogonal flow net, as in Figure 6.10a, but with the addition of decreasing fracture width with depth (with $\omega = 0.0055$)

- Poiseuille flow (Figure 6.10a) with an empirical function (ω) expressing a decrease in relative discharge with depth

$$\omega = e^{-0.0055D} \quad (6.12)$$

where the exponent was selected to ensure maximum discharge for long catchments at a depth/length ratio of about 0.01.

There may also be hydrochemical effects that would influence phreatic flow depth, such as mixing corrosion. These will be considered in Section 7.6.2.

6.4.2 Aquifer inputs

The development of conduits within the fracture flow field is a direct function of solute undersaturation, aperture size, discharge and hydraulic head, and an inverse function of length. An important question concerning the development of conduits in the aquifer is whether flow paths from inputs proximal to the spring develop first, or whether distal ones are favoured.

Two contrasting input situations are common in karst aquifers. The discharge of many karst catchments is dominated by one or more major allogenic inputs, flowing off impermeable rocks and sinking underground close to the limestone contact. The other extreme, such as in the Flathead and High Rock Ranges, is where the inputs are wholly autogenic. The two terrains are known as fluviokarsts and holokarsts, respectively. Early flow paths which might be expected in these two situations are shown in Figure 6.11.

In fluviokarsts, the situation is straightforward, for the conduit will develop between the sinking stream and the spring. On the other hand, in holokarsts there will be many recharge points to the aquifer, as noted above. In holokarsts, there are three important variables have not been well defined in conduit propagation models; they are hydraulic gradient, solute undersaturation, and the topology of the flow net.

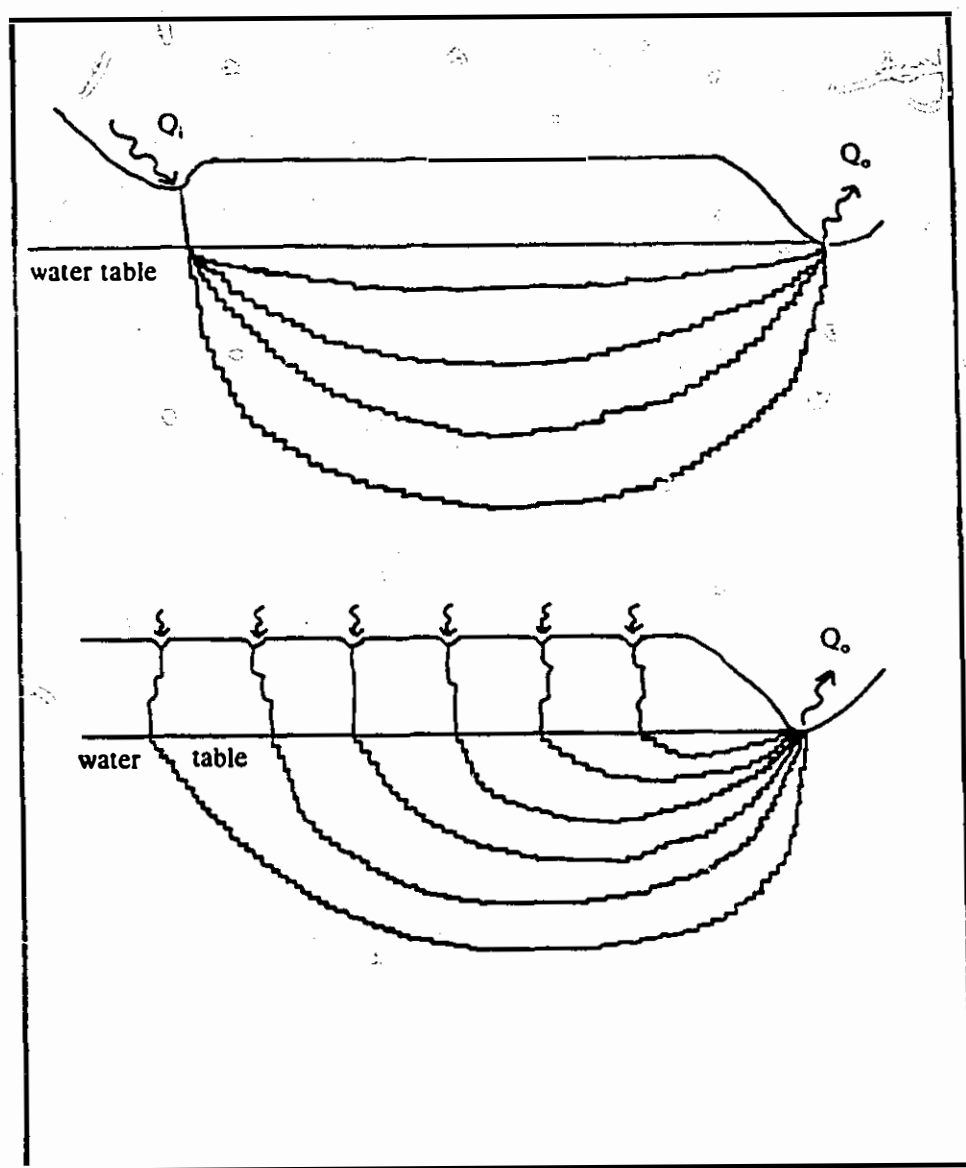


Figure 6.11 Contrasting initial flow paths in allogenic and autogenic karstic aquifers, modelled from the Hagen - Poiseuille equation

6.4.3 Initial hydraulic gradients

Three contrasting hydraulic gradient configurations of a holokarst are shown in simplified models in Figure 6.12. Each has 1000 recharge points in the plane of the diagram: ($I=1$ to 1000), corresponding to concentrated recharge every 10m down joints. For simplicity, only four evenly-spaced input points are shown (I_1 , I_{250} , I_{500} , I_{750}).

The term *initial hydraulic gradient* is defined here as the hydraulic gradient in a karst aquifer when a tier of conduits is being formed. Initial hydraulic gradients may be measured in two situations. First, in fluviokarst it may be possible to identify the original input and output points if there has been little surface denudation since the cave was formed. This is the case, for instance, at the Réseau de Foussoubie (Figure 6.5c), where a dry valley indicates the former surface course of the stream that now sinks into the cave; this shows that the initial hydraulic gradient was <0.003 . Second, in tiered caves (e.g. Figures 6.5b,d, 8.1, 8.2) a lower tier is initiated while there is conduit flow in an upper tier. In both Höolloch and Swildons Hole (Figure 6.5, b and d), the lower tiers were initiated (and also captured all flow) while there was still closed-conduit flow in the upper tier. Measurement of hydraulic gradients in such upper conduits where $r=1-3\text{m}$ (e.g. Lauritzen et al., 1985) and calculations using the Darcy-Weisbach equation show that initial hydraulic gradients are commonly <0.001 .

The uniform head case is the end-member in convex-up water tables, with steepest hydraulic gradients closest to the spring (Figure 6.12a), so that

$$h_1 = h_{250} = h_{500} = h_{750} \quad (6.13)$$

and

$$h_{750}/L_{750} = 2h_{500}/L_{500} = 3h_{250}/L_{250} = 4h_1/L_1 \quad (6.14)$$

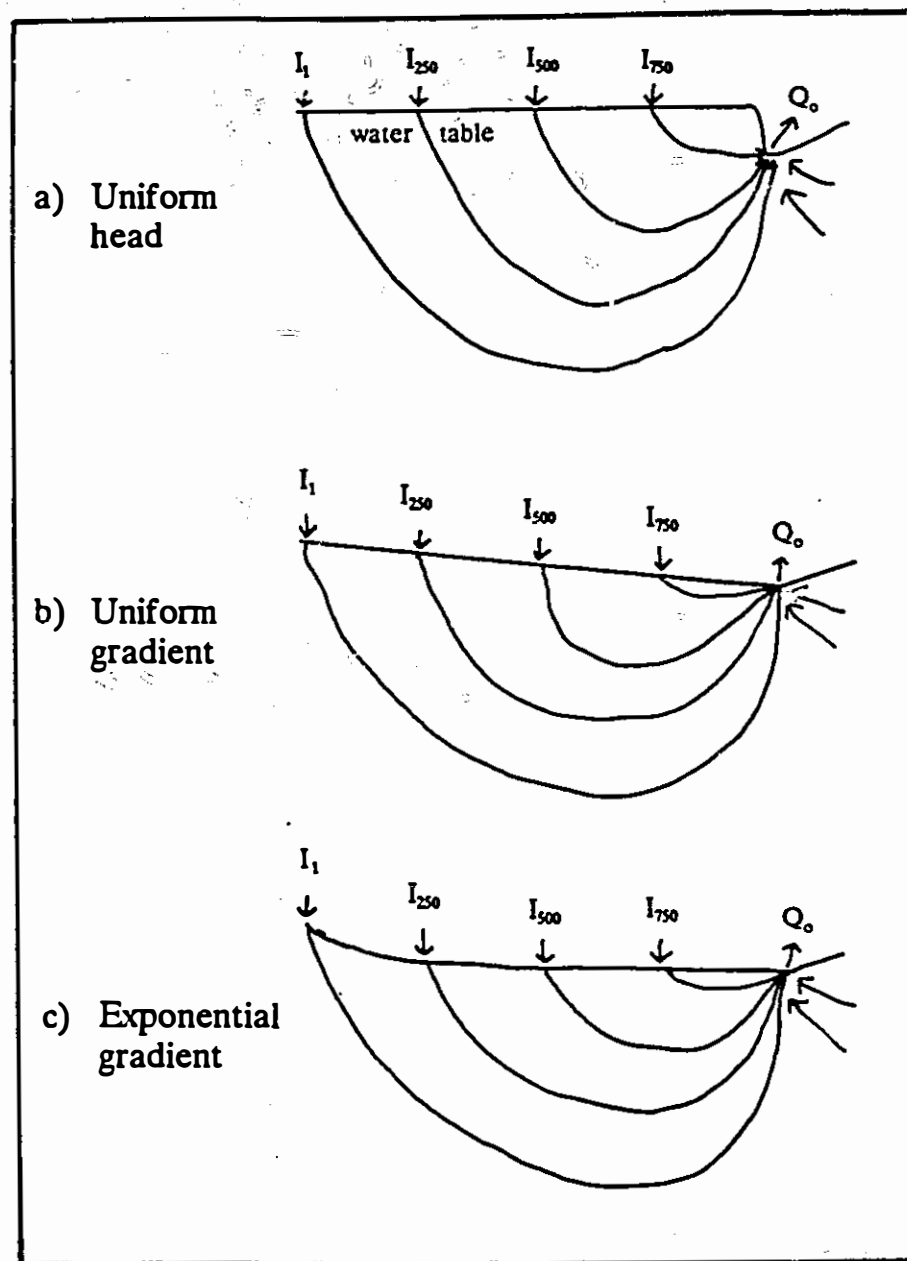


**Figure 6.12 Possible hydraulic gradient configurations in karst
(vertical exaggeration $x \approx 30$)**

where h is the head, L is the length from the input point to the spring, and the subscripts refer to the input points.

The uniform head case may occur where the uplift and/or downcutting rate exceeds the karstification rate. Rapid base-level lowering certainly occurs during glaciations. At Crowsnest Pass, the waterfalls or steep slopes below the orifices of Emerald Cliff Springs, Ranch Spring and Crowsnest Spring show that very steep hydraulic gradients close to springs are possible following deglaciation. However, the spring orifices are not the base of pre-Holocene karstification. This is clearly demonstrated by the 50m+ depth of the conduit feeding Crowsnest Spring (Figure 6.6a). Thus the uniform head model is not applicable at Crowsnest Pass because the bedrock is karstified below the present rejuvenated base level. Furthermore, it is uncertain whether the uplift and/or downcutting rate ever exceeds the karstification rate, so this putative case will not be considered further.

The second case is uniform gradient (Figure 6.12b), where

$$h_1/L_1 = h_{250}/L_{250} = h_{500}/L_{500} = h_{750}/L_{750} \quad (6.15)$$

This would seem to be a more realistic model for initiation of karstification, as it allows a sloping surface, and hence runoff, at the outset.

The third case has a concave-up water table (Figure 6.12c), with a gradient decreasing exponentially towards the spring, so that

$$h_1/L_1 > h_{250}/L_{250} > h_{500}/L_{500} > h_{750}/L_{750} \quad (6.16)$$

It was shown in Section 5.2.4 that conduits have exponentially sloping water tables associated with them. The very first hydraulic gradients in karst would not be concave-up, so the first karstic flow at Crowsnest Pass, about 85 million years ago (Gadd, 1986), might have had a uniform gradient (Equation 6.15). However, if we want to understand the paleohydraulics of the last 84 million years, or the current

hydraulics, then we need to know the hydraulic gradient that existed when a tier was formed. Such initial hydraulic gradients have been exponential for the last ≈ 84 million years. Laminar flow through a fracture flow net is shown in Figure 6.13, using the Hagen - Poiseuille equation and the exponential hydraulic gradient configuration described above. The model assumes uniform initial size in all fractures. The highest discharges are in vertical fractures rising to the spring and in the vertical fractures descending from distal sinkpoints. Empirical evidence for such steep flow paths close to the upstream and downstream limits of karst catchments is presented in Section 7.3.

6.5 Topological controls

The second variable that needs discussing is the topolcgy of the flow paths through the aquifer. One extreme is to assume independent flow lines from input to discharge point, so that

$$N_i = N_o = F \quad (6.17)$$

where N is the number of inputs, the subscripts i and o refer to inputs and outputs, respectively, and F is the number of flow paths in the aquifer. A combination of topographic and geological factors ensure that there is often one most favourable spring position at any time, at the lowest outcrop position of the aquifer, so $N_o = 1$. In a simple fluviokarst, there are likely to be many alternative flow paths, so that Equation 6.18 is far more likely than Equation 6.17.

$$N_i = N_o \ll F \quad (6.18)$$

This arrangement was demonstrated by Threlkill (1968), and is shown in Figure 6.11a.

In the example holokarst of the previous section, where inputs to the aquifer are every 10m, there would be 10^6 inputs in a 100km^2 catchment, so that

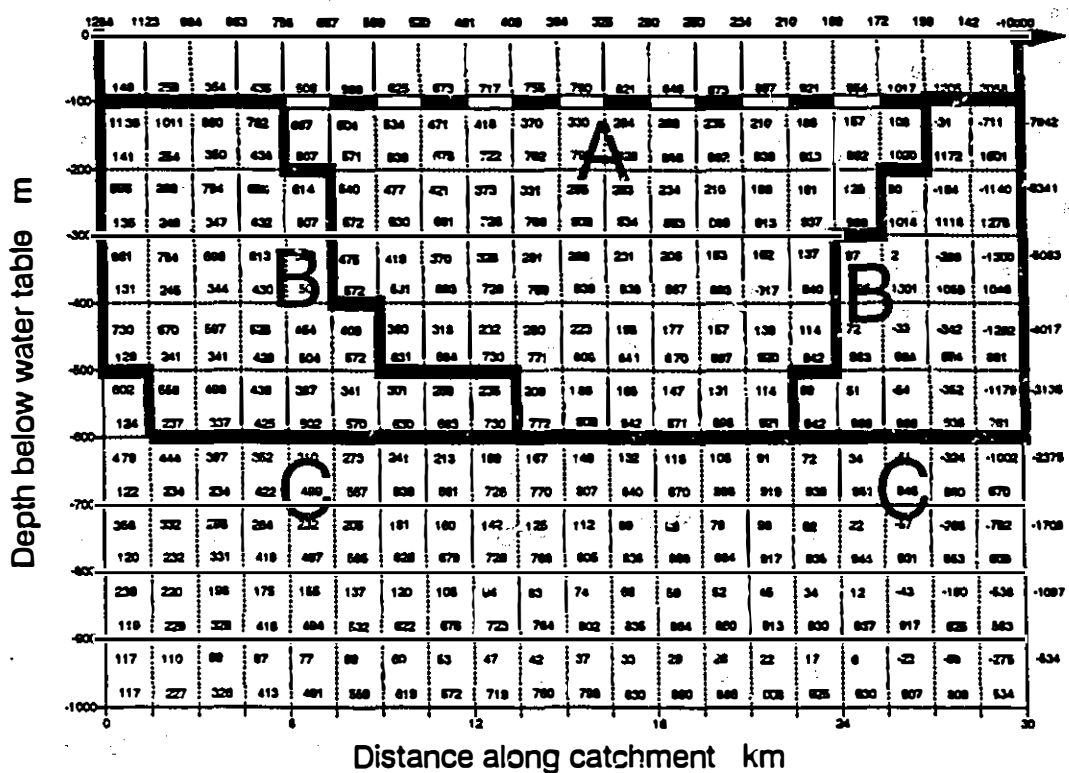


Figure 6.13 Two-dimensional model of Hagen - Poiseuille flow in a karst aquifer.
 Note the vertical exaggeration of 20. Twenty inputs are shown, with discharge being determined by the exponential hydraulic gradient (Equation 5.14). The inputs feed a flow net of equi-dimensional fractures, with discharge of 10,000 units at a single spring. An exponential decrease in fracture width with depth is assumed (Equation 6.12). The upper figure in each rectangle represents flow in the vertical fracture to the left; the lower figure in each rectangle represents flow in the horizontal fracture below. Negative figures represent upward flow. Flow route A (the most shallow) would be the most likely to succeed if $K_x = K_z$. However, Figures 4.3, 6.4, 6.5, 6.6, 7.2 and 7.5 give strong empirical evidence that conduit flow does not follow such paths. If $K_x > K_z$ then flow route C will be favoured, and if $K_x \gg K_z$ then flow route B might be the victor, though this would require a reversal of flow through four elements of the flow net. Note that the requirement for high K_z in flow routes B and C is only for fractures spaced 1500m apart, not for the whole bedrock, and thus does not contradict Equation 6.8.

$$N_i = N_o / n \quad (6.19)$$

where n is 10^6 in this case. The number of flow paths will depend upon the distribution of fractures with large initial apertures (Section 6.4.1).

6.6 Kinetic controls on solution

It has been assumed by almost all karst researchers that the controlling dissolution process is the same in both cave initiation and surface lowering. Bulk rock analyses of limestone outcrops show high CaCO_3 contents (e.g. Table 2.1), so it is logical to assume that carbonic acid is the major agent in surface lowering. However, what initiates cave conduits deep below the surface is open to speculation.

It is commonly assumed that carbonic acid from CO_2 is the agent of conduit initiation. An alternative hypothesis is that sulphuric or hydrosulphuric acid is responsible. The latter hypothesis has been invoked in caves with large deposits of secondary gypsum (e.g. Palmer, 1989, 1991), and has recently been proposed to be more widely applicable (Ball and Jones, 1990).

There are two fruitful ways to consider this question. First, are the waste products of conduit initiation compatible with carbonic acid or with sulphuric/hydrosulphuric acid processes? Second, are the reaction rates compatible with the geological history of karsts?

The waste products of carbonic acid dissolution are Ca^{2+} and HCO_3^- . For sulphuric acid, they are Ca^{2+} , HCO_3^- , and SO_4^{2-} . Clearly, the absence of sulphur in the waste water of conduit initiation would falsify the sulphuric/hydrosulphuric acid hypothesis. The locus of conduit initiation is in the phreatic zone, below existing conduits, so conduit initiation waters will have an elevated temperature due to geothermal heating. It will be argued in Chapter 8 that such waters may be sampled in springs emanating close to the lowest outcrop point of a karst aquifer. Water samples from non-thermal or weakly-thermal springs in such a position, and from

thermal springs commonly have high sulphate/bicarbonate ratios (Table 6.5; also see Section 10.3). The consistently high concentrations of sulphur in these waters suggests that sulphur plays an important role in cave initiation.

The second test is to consider reaction rates. Some of the most widely-quoted experiments on the solution of limestone were performed by Plummer and Wigley (1976), using Iceland spar. They found dissolution rates could be approximated by a second-order equation at low solute concentrations:

$$F = K (c_s - c)^2 \quad (6.20)$$

where F is the dissolution rate, K is a constant that was found to vary by two orders of magnitude between specimens, c is the concentration of dissolved calcite, and the subscript s denotes saturation. Closer to equilibrium, the authors found the reaction varied between a fourth-order process (e.g. experiment 7) and an approximately eighth-order process (e.g. experiment 11). Two specimens of Iceland spar were used in these experiments, the second of which was not as clear as the first. Dissolution rates of the second specimen were markedly slower than the first, and the authors suspected the calcite to have trace inhibitors (Plummer and Wigley, 1976, p197 and Figure 4). Such inhibition close to saturation has been found by several authors (e.g. Terjesen et al., 1961; Berner and Morse, 1974). Plummer and Wigley (1976, p197) concluded that at saturation ratios $> 70\text{-}90\%$, "the data are not sufficient to warrant estimates of rate constants in this region".

Recent modelling of conduit initiation using the carbonic acid reaction has shown that caves can be created in reasonable time periods, but only by assuming high hydraulic gradients (0.02 or more), short flow paths (mostly $< 1\text{ km}$), and very rapid dissolution rates (Dreybrodt, 1990; Palmer, 1991). If mean values are taken from the dissolution experiments of Plummer and Wigley (1976), from empirical data on initial hydraulic gradients (Section 6.4.3), and if reasonable mean catchment lengths are assumed (e.g. 1-100km), then conduit initiation times are in the range 10^6 to 10^{12}

Table 6.5 Sulphate and bicarbonate concentrations in karst springs

Area and spring	n	SO_4^{2-} mg l^{-1}	HCO_3^- mg l^{-1}	$\text{SO}_4^{2-}/(\text{HCO}_3^- + \text{SO}_4^{2-})$ %
Crowsnest (data from Table 3.7 and Figure 3.12)				
Sublacustrine Springs	15	60	148	29
Crowsnest Spring	15	59	110	35
Ptolemy Spring	15	11	75	13
Ptolemy Creek Springs	15	14	105	12
Other Rocky Mountains springs (IWD, 1975; Atkinson et al., 1983; van Everdingen, 1972)				
Maligne Springs	10	31	103	23
Castleguard Red Spring	1(*1)	82	122	40
Banff Hot Springs	25	141	251	36
Miette Hot Springs	6	1116	122	90
Radium Hot Springs	6	281	212	57
Fairmont Hot Springs	8	872	663	57
Darvan, Ain, France (Gibert et al., 1983)				
Grotte du Pissoir	29	14	240	5.5
Grotte du Cormoran	33	6	130	4.4
Basse Cévenne, Languedoc, France (Fabre, 1984)				
Source de Baume Rascasse	?	80	260	24
Emergence de Courlas	?	52	300	15
Source de Carabiole	?	27	280	8.8
Montagne Noire, Hérault, France (Guyot, 1986)				
Source de Poussarou	?	13	200	6.1
Source de Malibert	?	10	165	5.7
Massif de Plate, Haute-Savoie, France (Sesiano, 1989)				
Emergence du Vivier	32	62	180	26
Emergence du Pont	33	30	130	19
Southern Indiana, USA (Bassett, 1976; Krothe & Libra, 1983)				
Pluto Spring	3	1721	278	86
White River Mineral Spring	3	1009	130	89
White River Freshwater Spring	4	382	133	74
Orangeville Rise	3	40	237	14
Orangeville Rise	36	58	200	22
Central Florida, USA (Back & Hanshaw, 1970)				
upgradient groundwater flow	9	14	162	8.0
downgradient groundwater flow	9	186	173	52
Aggtelek, Hungary (Maucha, 1989)				
Miskolc	?(*2)	20	273	6.8
Jósvafo	?(*2)	18	372	4.6
Yucatan, Mexico (Back & Hanshaw, 1970)				
11	90	384	19	
Pennsylvania, USA (Jacobson and Langmuir, 1974)				
19(*3)	22	211	9.4	
Peak District, England (Christopher et al., 1977)				
14(*4)	141	251	48	

(*1) Similar values were obtained in stream and drip samples taken inside Castleguard Cave in April 1979 and April 1980 ($\text{HCO}_3^- = 140 \text{ mg l}^{-1}$; $\text{SO}_4^{2-} = 84 \text{ mg l}^{-1}$; n=27; Atkinson et al., 1983)

(*2) Sampled over a one-year period. Groundwater values are after subtraction of atmospheric inputs.

(*3) Single samples from 19 springs

years. Thus it appears that conduits cannot be initiated by the carbonic acid reaction, unless initial fracture widths exceed the 0.1-0.2mm used in recent modelling (e.g. Dreybrodt, 1990; Palmer, 1991) by at least an order of magnitude.

6.7 Models of conduit development

A realistic model of conduit development in karst aquifers would combine the hydraulic and hydrochemical findings of the previous sections. Specifically, it would combine the following characteristics:

- 1) Mean hydraulic gradients of about 0.001.
- 2) Exponential hydraulic gradients in all tiers subsequent to the first one (in autogenic karsts). Possibly uniform hydraulic gradients to form the first tier in autogenic karsts, and all tiers in allogegenic karsts.
- 3) A large number of inputs (e.g. 10^6) feeding a single output.
- 4) Sulphuric/hydrosulphuric acid reactions so that SO_4^{2-} constitutes a major fraction of the anions.
- 5) If carbonic acid reactions are invoked, then high order kinetics should be used close to saturation.
- 6) A low density of high-permeability fractures combined with a high density of low-permeability fractures, so that realistic width/length and sinuosity ratios are mimicked.

Given the uncertainties at present surrounding many of these parameters, it is not clear from kinetic theory whether conduits are propagated from the input or output end, and whether proximal or distal inputs are the first to achieve breakthrough. For instance, a 10^6 increase in discharge close to a proto-spring could well outweigh the decrease in solution rate along a flow path. Thus conduits could propagate upstream from the discharge point, as suggested by Rhoades and Sinacori (1941).

Although kinetic theory cannot at present give a solution to how conduits propagate, it is possible to investigate the relative time for inputs at different distances

from a spring to achieve breakthrough, using the hydraulic gradients derived from the Darcy-Weisbach equation and from empirical data (Equation 5.14), combined with the exponents for length and hydraulic gradient from the model of Dreybrodt (1990).

Combining these gives

$$T = K L^{1.25} \int_0^L (0.0092 e^{-0.12l})^{-1.3} dl \quad (6.21)$$

where T is the time to breakthrough in the conduit, K is a constant, L is the length of the flow path, and l is the distance from the upstream limit of the catchment. This is shown in Figure 6.14 for a catchment 50km in length. Figure 6.14 shows that the inputs most likely to succeed are either extremely close to the spring (as L approaches zero), or the distal part of the catchment (as the hydraulic gradient increases exponentially, and as deeper flow paths with lower fluid viscosity will be exploited). It thus appears quite possible that distal inputs may be the first to achieve breakthrough.

Three examples will show that short flow paths are not necessary for initiating conduit flow. Mammoth Cave is the longest cave in the world. A distinctive feature of the cave is that most passages are found towards the centre of impermeably-capped ridges, rather than at their peripheries. Several passages take 6km long paths below Flint Ridge; original flow paths below Mammoth Ridge may have been 20km in length. Short flow paths have always been available since cave initiation, but have not been favoured (Palmer, 1981; Quinlan and Ewers, 1989). Second, Friars Hole System is the longest cave in the Appalachian Mountains. The original flow path was 11km in length, below a thick shale cover. Third, the largest karst springs in Mexico are in the El Abra Range (Section 4.4). Flow paths to major springs such as Taninul, Choy, Coy, Santa Clara, and Mante pass beneath the 20km wide shale outcrop in the Valles Valley, despite there being available low-altitude resurgence sites at the upstream margin of the shale (Figure 4.3).

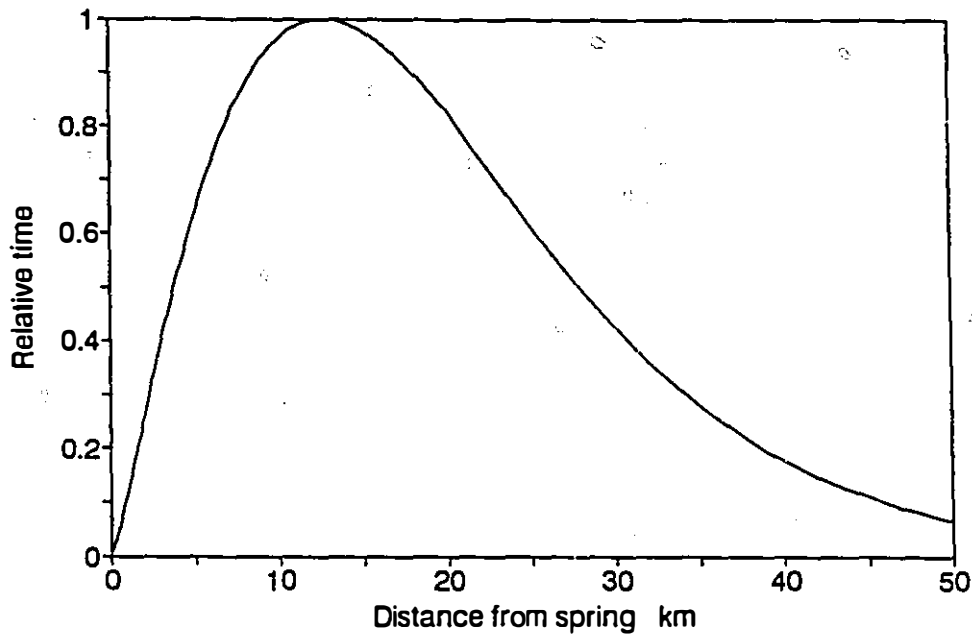


Figure 6.14 Relative times to breakthrough for proximal and distal inputs in a karst aquifer 50km in length, based on empirical length and hydraulic gradient functions. Amalgamation of flow paths, and water density and viscosity variations with temperature are not included.

These three examples clearly show that initial flow paths many kilometres in length are not an obstacle preventing conduit initiation.

Given the highly non-linear evolution from initial flow field to primary tubes to conduits, empirical evidence is more relevant in this context than theoretical models. The hypothesis of distal inputs succeeding first is used in the next chapter, where it is further assumed that the locus of conduit development is a function of the original flow net, and is not dominated by the development of proximal conduits.

Chapter 7

Flow nets in karst aquifers: the locus of flow during one generation

7.1 Introduction

In this chapter a simple model will be described, proposing that flow depth is a function of catchment length and stratal dip and strike. The flow model will be tested in Section 7.2, using a representative data set, drawn from many different topographical, geological and climatic regions.

The model will then be further tested, using data from three other sources. First, the phreatic conduits at the two extremities of a catchment should have steep flow paths. Second, water well yields should be a function of the stratal dip and position along the flow path. Third, tributary conduits should duplicate, on a smaller scale, the patterns found with principal conduits. These three hypotheses will be tested in Sections 7.3, 7.4 and 7.5, respectively. Finally, in Section 7.6, an attempt will be made to falsify the hypothesis, by investigating various hydrological, geological and topographic situations.

7.2 Flow depth as a function of catchment length, dip and strike

7.2.1 Mean flow depth in explored caves (as a function of dip and catchment length)

It was shown in Section 6.7 that the first flow path to achieve breakthrough in a holokarstic catchment will be either a proximal input very close to the spring, or a distal input, from the upstream 10-20% of the catchment. If proximal

inputs were most successful, then it would be expected that conduits below the water would be found aligned along the shallowest available open fractures, with $D_o/D_b < 0.5$ (Equation 6.6). It was shown in Section 6.2.4 that this is not true, and that conduits follow deeper flow paths.

If distal inputs were the most successful, then it might be expected that catchment length L would be proportional to the depth of conduit flow below the water table D . A common situation in a karst catchment, and the easiest to analyze, is where flow is along the strike on a single bedding plane. Following the concepts in Figures 6.7, 6.9 and 6.10, then the flow patterns shown in Figure 7.1 might be expected. The flow paths shown in Figure 7.1a,b and c are broadly similar to those shown in Figure 6.5a, b and c, respectively. Such looping flow paths is also supported by $D_o/D_b > 0.5$ (Section 6.2.4).

Waltham and Brook (1980b) cited the conduit development of Dune Series - Revival in Gua Air Jernih, and of Benarat Walk in Lubang Benarat, Malaysia as inexplicable in terms of present cave formation theories : "there is a problem as to why deep phreatic caves should maintain horizontal courses when there is no geological control adequate to hold them at a given level.... If the horizontality of the trunk passage was due to the influence of the original water table, there seems no reason why the cave should have developed 50 metres below water level" (Waltham and Brook, 1980b, p131). These conduits thus have similar profiles to Doux de Coly (Figure 6.5a), and to Figure 7.1, and are explicable in terms of Hagen-Poiseuille flow fields (Figure 6.13).

If the flow net shown in Figure 7.1 develops along one or more highly transmissive bedding planes, then deeper flow would be found with steeper dips, so it might be expected that

$$D_x = K_1 L_x \sin \theta \quad (7.1)$$

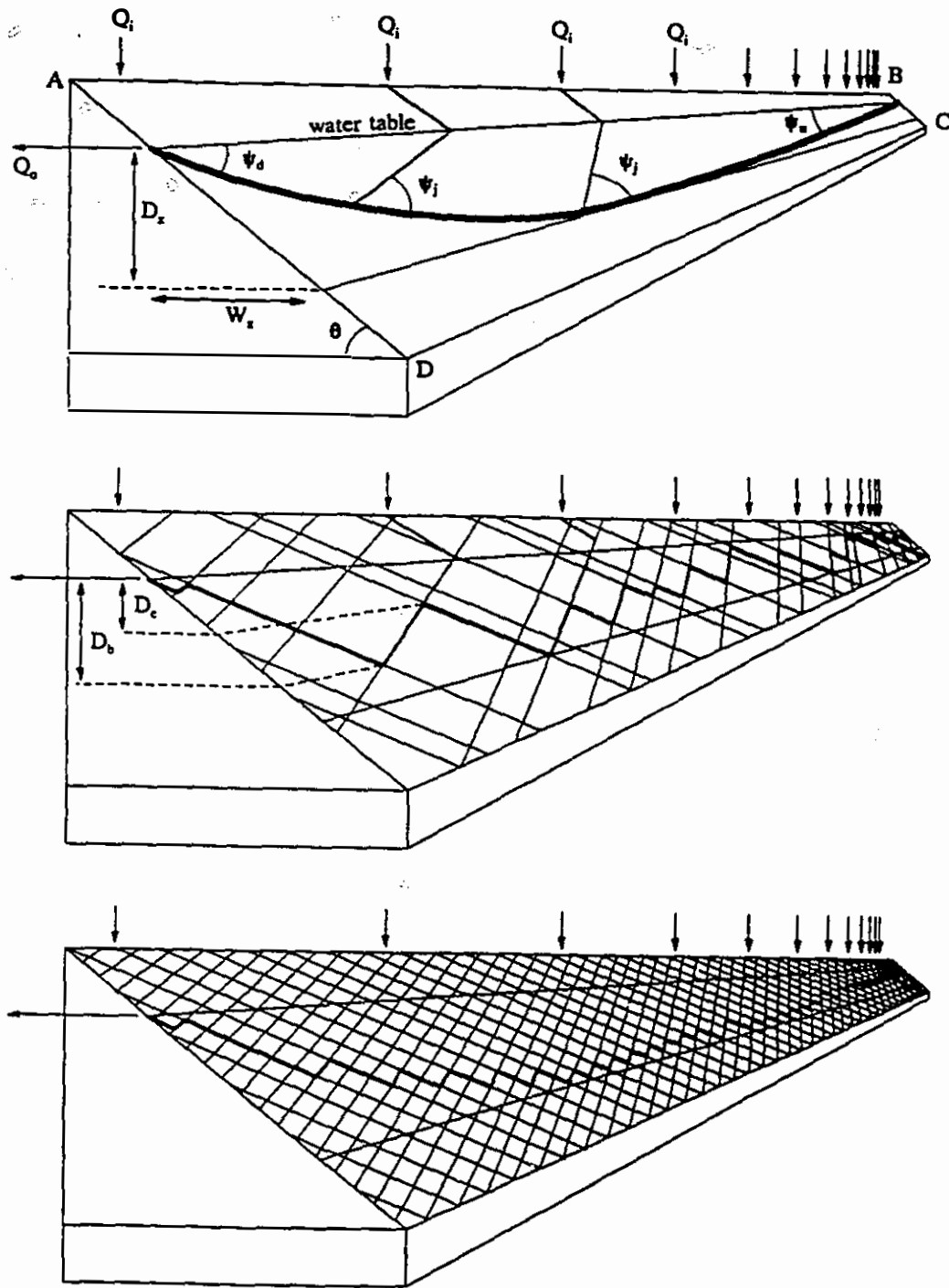


Figure 7.1 Strike-oriented flowlines on a single bedding plane ABCD:

- conduit development with the bedding plane providing structural control
- conduit development at sparse primary tubes or bed-joint intersections
- conduit development at closely spaced primary tubes or bed-joint intersections

where D_x is the maximum depth of conduit flow, K_1 is a constant, L_x is the catchment length, and θ is the dip of the strata. The tendency for steep dips to be associated with deep circulation has been noted by several authors (e.g. Ashmead, 1974; Ford and Ewers, 1978). The easiest way to visualise the relationship of flow depth to stratal dip is to consider flow along a single bedding plane. If the dip of this bedding plane were zero, then the range in depth of flow be zero (and $\sin \theta = 0$). If the dip of the bedding plane were >0 , then any meandering of the conduit would result in a variation of flow depth. The maximum variation in depth would be in the case of a vertical bedding plane (where $\sin 90^\circ = 1$).

In order to test Equation 7.1, the literature was searched for caves where D_x , L_x and θ are known. The caves detailed in Table 7.1 have been drawn from a wide variety of geological, climatic and topographical situations. The data has been compiled not only from the listed primary sources, but also from topographical and geological maps, and from personal knowledge of the caves in most cases.

The depth of flow below the water table has been estimated in four ways (Table 7.1). In four of 16 cases, extensive lengths of siphons have been penetrated by scuba divers (e.g. Figure 6.5a); the depths reached in such cases must represent minimum depths, for there must have been some lowering of water levels since the conduit was formed. In six cases, there are well-identified tiers in the caves (e.g. Figures 6.5b,d, 8.2); each tier was formed while the cave stream was flowing through the next tier above. This again gives a minimum level for depth of flow. In seven cases, the vertical range of looping has been used to establish a minimum depth of flow. This method is the traditional way of estimating flow depth, but may result in considerable underestimates. For instance, two-thirds of the flooded passage in Doux de Coly maintains an almost constant depth of 49-56m (Figure 6.5a); if this were a fossil passage then this horizontality would traditionally be interpreted as being closely associated with a former water table. Similar lack of association between loop crests

Table 7.1 Conduit and catchment characteristics for 16 caves

#	name	L _x km	θ °	φ °	D _v m	D _x m	D _m m	D _x /L _x	Q _u %	L _x /L _s
1	Horseshoe Bay Cave, USA	3	2	90	?	20 ^c	6	0.0067	<10	0.22
2	West Kingsdale, England	2.7	3	90	120	30 ^a	8	0.011	5	0.4
3	Jorcltulla, Glomdal, Norway	0.52	85	0	20	23 ^a	9	0.044	100	1.0
4	Otter-Hole, Wales	3.5	6	10	80	23 ^c	10	0.0066	20	0.38
5	Friars Hole System, USA	11	2.2	5	50	25 ^b	17	0.0022	85	0.35
6	Rfo Encantado, Puerto Rico	9.5	4	20	70	25 ^c	15	0.0026	20	0.8
7	Guanyan, China	6.5	7	?	300	100 ^c	25	0.015	60	0.84
8	Swildons-Wookey, England	6	15	70	100	90 ^a	40	0.015	<1	0.22
9	Demanova, Czechoslovakia	3.2	35	60	200	90 ^b	23	0.028	80	0.8
10	Doux de Coly, France	13.7	6	0	60	56 ^a	46	0.0041	<1	0.21
11	Höolloch, Switzerland	10	16	0	800	190 ^{bc}	100	0.019	<1	0.55
12	Lubang Benarat / Gua Harimau, Malaysia									
		7	45	0	1000	220 ^b	105	0.031	90	0.35
13	Nettlebed, New Zealand	7	50	0	900	150 ^{bc}	120	0.021	<1	0.3
14	Pefia Colorada, Mexico	12	40	45	1000	200 ^c	120	0.017	<1	0.2
15	Nelfastla de Nieva, Mexico	7.4	70	25	400	290 ^b	240	0.039	<1	0.3
16	El Abra, Mexico	150	20 ^a	70	2000	1500 ^d	800 ^a	0.01	<1	*

Notes:

Flow depth measurement by

a scuba diving in flooded conduits

b spacing of fossil tiers

c vertical looping within individual tier(s)

d water chemistry and temperature

* see comments on El Abra caves in Section 4.4

1 Cox (1990)

2 Brook (1974), Waltham & Brook (1980a), Waltham et al. (1981), Farr (1980)

3 Lauritzen et al. (1985)

4 Elliot et al. (1979)

5 Worthington (1984)

6 personal notes; Courbon et al. (1989)

7 Waltham, 1986

8 Ford (1963), Drew (1975a,b), Farr (1980, 1983). Note that the distance from Swildons Hole to Wookey Hole is only 3.5km, but the total catchment length is about 8.3km. The dip is variable, being 10° at Wookey Hole and 19° at Swildons Hole.

9 Droppa (1966)

10 Isler & Magnin (1985), B.R.G.M. (1970)

11 Bögli (1970, 1980), Rouiller & Auf der Mauer (1986)

12 Brook & Waltham (1978), Waltham & Brook (1980b), Eavis (1981, 1985)

13 Pugsley (1979), Ravens (1986), personal notes

14 Stone (1984), Sloan (1985)

15 Worthington (1989), Figure 8.2

16 Fish (1977)

and the water table in seen in Foussoubie and Trou de Glaz (Figures 6.5c and 6.5e, respectively). The fourth method is the use of water chemistry and temperatures of thermal springs to demonstrate deep flow in the El Abra Range (Figure 4.3). This deep flow described by Fish (1977) has been partially validated by a scuba dive at Mante spring to a depth of 280m (Exley, 1988).

Many more caves were rejected because data on the geological structure was not available, because the original drainage basin length was unknown, or because the phreatic flow depth could not be estimated. The overwhelming majority of caves have known straight-line lengths (L_k) that are only a small fraction of the total drainage basin length (L_x), and such small sample sizes would give a poor estimate of mean flow depth, so these were rejected where $L_k/L_x < 0.2$. Many flooded caves have been explored by scuba divers in areas close to sea level, such as Florida, the Yucatan and the Bahamas, but these too were rejected because there is no knowledge of base level (i.e. sea level) at the time the caves were formed.

The caves of Crowsnest Pass also were rejected as examples, despite the fact that the >22km of mapped caves represent the highest concentration of caves in any one area in Canada. There were two reasons: the principal caves were formed when the water table was at least 1km higher, a time estimated as several million years ago by Ford et al. (1981). At that time pre-glacial drainage basins would have been very different, so L_x cannot be estimated for that time. Second, less than 0.5km is known of any flow route, so presumably $L_k/L_x < 0.2$.

It is only possible to measure D_x where a complete flow route is known, and this is the case of only three of the examples in Table 7.1; it is therefore convenient to estimate the mean depth, D_m , as it gives a more stable value from a small sample length, and modify Equation 7.1 to

$$D_m = K_2 L_x \sin \theta \quad (7.2)$$

where K_2 is a constant. Applying this equation to the data in Table 7.1, regressing $L_x \sin \theta$ against D_m gives

$$D_m = 0.11 (L_x \sin \theta)^{0.81} \quad (n=16, r^2=0.95) \quad (7.3)$$

where L_x is the catchment length in metres. The results are shown in Figure 7.2. It should be noted that D_m is not directly proportional to $L_x \sin \theta$; the reasons for this will be pursued in the next section. However, it is clear that conduit flow depth in karst aquifers is principally a function of catchment length and stratal dip.

If a geothermal gradient of 25°km^{-1} is assumed (Freeze and Cherry, 1979), then flow at a mean depth $>200\text{m}$ will become heated by $>5^\circ\text{C}$, the accepted threshold for thermal water. Assuming no heat loss as the water travels up the conduit to the surface, it is possible to define a length/stratal dip field for thermal springs (Figure 7.3). The shortest flow path to produce a thermal spring is 10.4km. Thermal karstic springs will be discussed in detail in Section 8.8.2; all examples discussed there drain catchments which are at least tens of kilometres in length. This association between long catchment lengths and thermal springs further supports Equation 7.3.

7.2.2 Mean flow depth in explored caves (as a function of dip, strike and catchment length)

Most of the caves in Table 7.1 have flow routes aslant the strike, and so in addition to bedding planes they will have to use joints or faults as phreatic lifts or drops (Section 7.2). Nine of the 16 flow routes have essentially strike-oriented paths ($0^\circ < \phi < 20^\circ$), and these give

$$D_m = 0.052 (L_x \sin \theta)^{0.92} \quad (n=9, r^2=0.96) \quad (7.4)$$

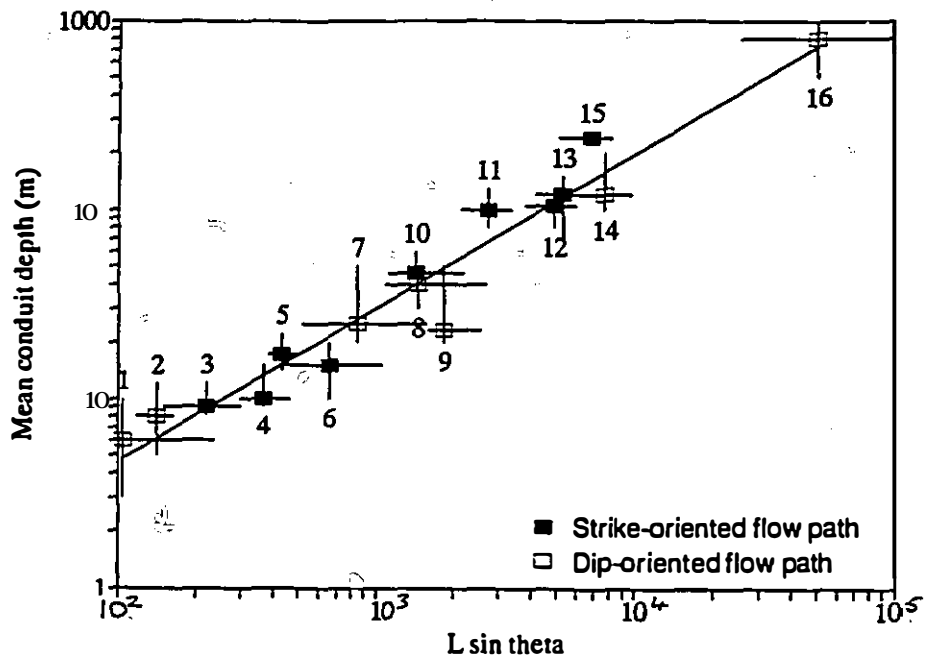


Figure 7.2 Mean phreatic flow depth as a function of stratal dip and aquifer length for 16 karst catchments. Details of these catchments are given in Table 7.1.

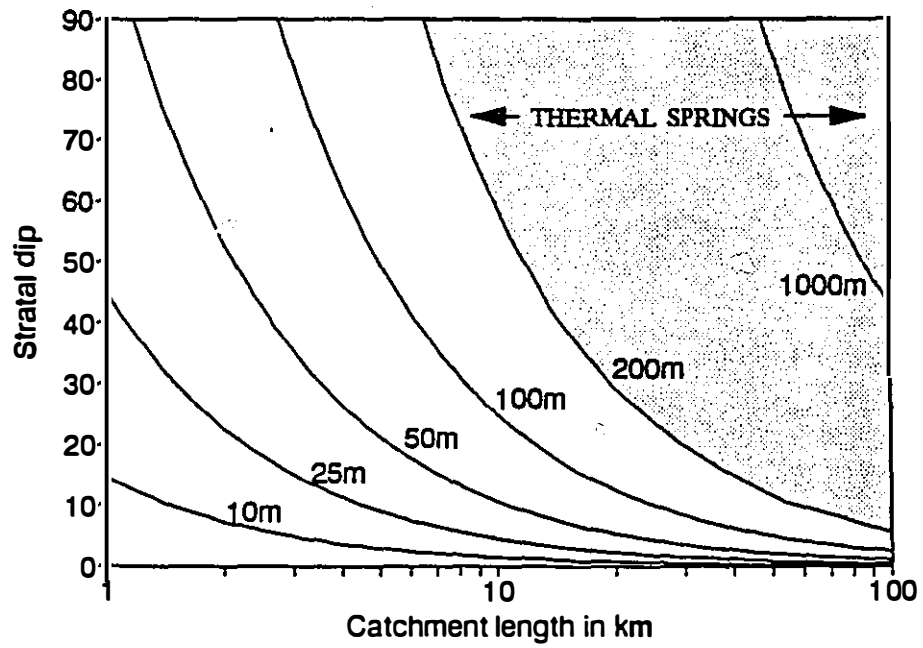


Figure 7.3 Phreatic flow depth and the domain of thermal springs in karst as a function of catchment length and stratal dip

If a dipping bedding plane is considered, with a flow route F aslant the strike, then the path can be divided into a strike-parallel component S and a dip-parallel component P (Figure 7.4). On path S, flow can follow the bedding plane, but on path P joints or faults will have to be utilised to achieve an overall horizontal vector. The utilisation of joints, and hence depth of flow attributable to joints (D_j), will be proportional to the dip-parallel component of flow, P / F . Since P is normal to S, then F is a hypotenuse, and

$$D_j \propto \sin \phi \quad (7.5)$$

where ϕ is the angle subtended between S and F. It follows from Equations 7.1 and 7.4 that

$$D_m = K_1 L_x \sin \theta + K_3 L_x \sin \phi \quad (7.6)$$

where K_3 is an empirical constant. Optimisation of this equation by varying K_3 , using the data in Table 7.1, gives

$$D_m = 0.061 (L_x \sin \theta + 0.034 L_x \sin \phi)^{0.87} \quad (n=14, r^2=0.91) \quad (7.7)$$

The near-linear form of Equations 7.4 and 7.7 suggest that any effects favouring shallow phreatic flow close to the water table are almost balanced by the viscosity effect favouring deeper flow (Section 6.4.1).

7.3 Phreatic lifts and drops

7.3.1 Initial phreatic drops (ψ_i)

Where conduit flow is not along the strike, then alternating bedding plane and joint paths are utilised. This is particularly striking in low-dip situations, where the joint paths are often near vertical. Such steep flow paths were described by Chevalier (1951), and are known as phreatic lifts (Forsell, 1971) or drops (Jameson, 1985).

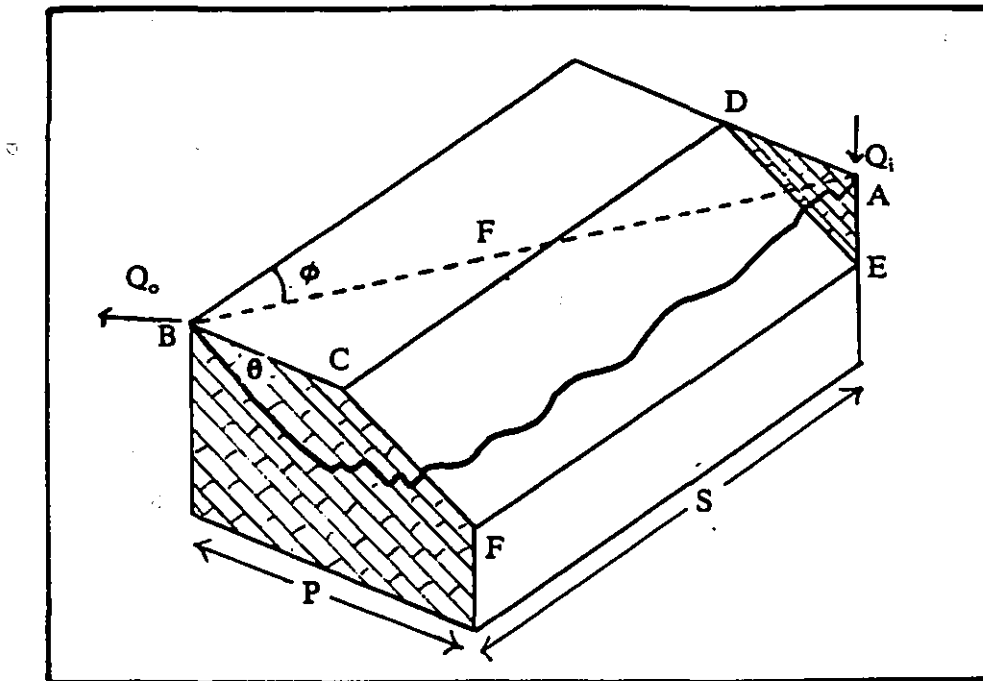


Figure 7.4 Flow routes aslant the strike following fractures

Lifts or drops may occur at any position along the flow path, but drops are more common close to the beginning of a flow path, and lifts are more common close to the end of a flow path (Figure 6.5, 6.12, 7.1). These latter two cases will be termed *initial phreatic drops* (ψ_i) and *terminal phreatic lifts* (ψ_o), respectively. In strike-oriented flow, they may occur along one bedding plane (Figure 7.1), but otherwise they may use beds, joints or faults, either singly or in combination. *Medial lifts* and *medial drops* refer to the central part of the flow path, which will consist of most of the flow route. Initial drops and terminal lifts in excess of 100m will be described in the following section, but the vertical magnitude of medial lifts and drops are usually in the range of only centimetres to tens of metres.

Initial phreatic drops have rarely been recognised in the literature. Probably the most spectacular descending phreatic conduits are at Gouffre Touya de Liet and the nearby Gouffre de la Consolation, France (Courbon and Chabert, 1986), where phreatic tubes up to 10m in diameter follow the 50° bedding downdip for up to 600m. The syngenetic flow depth may be much less, but probably exceeds 300m (Table 7.2). A second major example is Castleguard Cave. Paleohydraulic calculations show that the present entrance of Castleguard Cave was at least 370m below the water table when it was formed (Section 11.2.2). The upper 80% of the cave was apparently formed along a single bedding plane, and thus can be considered morphologically as an initial phreatic drop of 350m (Figure 11.3).

7.3.2 Terminal phreatic lifts (ψ_o): vauclusian springs

Spring conduit slopes are known for several of the great springs of the world, and some major active and fossil springs are listed in Table 7.2; the mean conduit slope of the eleven examples is 45°. Such steeply ascending springs are commonly called vauclusian, after the type locality in France, the Fontaine de Vaucluse. The 11 examples occur in a variety of geological situations, with the upward flow being at least partially guided by faults or joints in at least four of the cases (Vaucluse, Mante, Choy and Ceiba), and being along bedding planes in at least four cases (Crowsnest Spring, Hijau Lubang, Ira Tem, and Salzgrabenhöhle); the remaining three examples are in bedded limestones (Zimapán) or marble (Pearse and Nettlebed), where the structural controls are less certain.

Such steeply ascending flow paths have also been documented from boreholes, such as at the Wujiandu dam site, China, where there are steeply ascending flow paths below the valley-bottom discharge area, with a discernible flow at a depth of 1000m below river level (Li, 1981).

Trombe (1952) defined a vauclusian spring simply as the outflow from the ascending branch of a siphon, and described it (p81) as the most common type of

Table 7.2 Notable initial phreatic drops and terminal phreatic lifts**Fossil sinks**

name	Ψ_i	Ψ_o	L_x km	D_x m	Q $m^3 s^{-1}$	note
Touya de Liet, France	50	-	8.2	>200	-	1,8
Castleguard Cave, Alberta	4	-	6.6	>370	<0.3	9

Active springs

Fontaine de Vaucluse, France	-	51	65	>308	20	1
Nacimiento de Mante, Mexico	-	58	150	>270	12	2,5
Cueva del Nacimiento del Río Choy, Mexico	-	80	100	>120	5	5
Pearse Resurgence, N.Z.	-	90	7	>24	2	3
Crowsnest Spring, Alberta	-	38	20-90	>49	0.67	4,8

Fossil springs

Hoya de Zimapán, Mexico	-	41	100	>295	-	5
Hijau Lubang, Malaysia	?	40	6	200	-	6
Cueva de la Ceiba, Mexico	-	63	100	>195	-	5
Ira Tem, P.N.G.	-	19	>3.3	>120	-	7
Nettlebed Cave, N.Z.	?	50	7	95	-	3,8
Salzgrabenhöhle, Germany	20	20	5	90	*	1,8
Grotte de la Luire, France	-	-	8	450	*	10

* flood overflow: flooded during spring snowmelt

1 Courbon and Chabert (1986)

2 Exley (1988)

3 Pugsley (1979)

4 Chapter 3, Barton (1981)

5 Fish (1977): see Section 4.4

6 Brook and Waltham (1978), Smart (1981)

7 Worthington, 1980

8 personal notes

9 Section 11.2.2, Figure 11.2, 11.3

10 Delannoy, 1984

resurgence. The term has been used in the same sense by other writers (e.g. Sweeting, 1973; Mangin, 1974; Bögli, 1980; Bonacci, 1987), though Bögli (1980, p124) added that vauclusian springs "have an outflow the size of a river". However, other writers have defined vauclusian springs as being analogous to artesian springs, or as being controlled by synclinal folds and/or faults (e.g Jennings, 1985; White, 1988; Ford and Williams, 1989). Because of the importance of the term vauclusian spring in the present discussion, the hydrogeologic conditions of the type example are worth describing. The following analysis is drawn from Margat (1980), Drogue et al. (1983), Michelot and Mudry (1985), Courbon and Chabert (1986), and Puig (1987).

The Fontaine de Vaucluse has been the deepest known springs since 1878, when it was dived to a depth of 23m; a submersible has now descended to a depth of 308m. A cave 40km away from the spring (Gouffre de Caladaïre) has been descended to 112m above the spring without reaching the water table, showing that the high-flow hydraulic gradient is <0.0028 . The mean discharge of the spring is now considered to be $19\text{-}20\text{m}^3\text{s}^{-1}$, though earlier estimates were some 50% greater; nevertheless, it is still the largest spring in France, and one of the largest in the world. The spring itself is in well karstified Urgonian (Lower Cretaceous) limestones 6km north of the east-west axis of a broad synclinal structure, and on a minor fault 500m east of the faulted western margin of the structure.

It used to be thought that there might be an artesian component to flow at the spring, but dye-tracing never confirmed this hypothesis, and the recent budget study by Puig (1987) has shown that runoff from the known non-artesian catchment is sufficient to account for all the discharge at the spring (Figure 7.5). This non-artesian catchment is the Vaucluse Plateau, 1200km^2 of karstic Urgonian limestones, which forms the northern limb of the syncline, with a southerly dip of 3° . Dye tests from Gouffre de Caladaïre and four other locations on the Vaucluse Plateau have confirmed flow routes of 20-46km to the spring (Figure 7.5). It appears that the Fontaine de Vaucluse is not a full-flow spring. The Source de la Folie lies a few

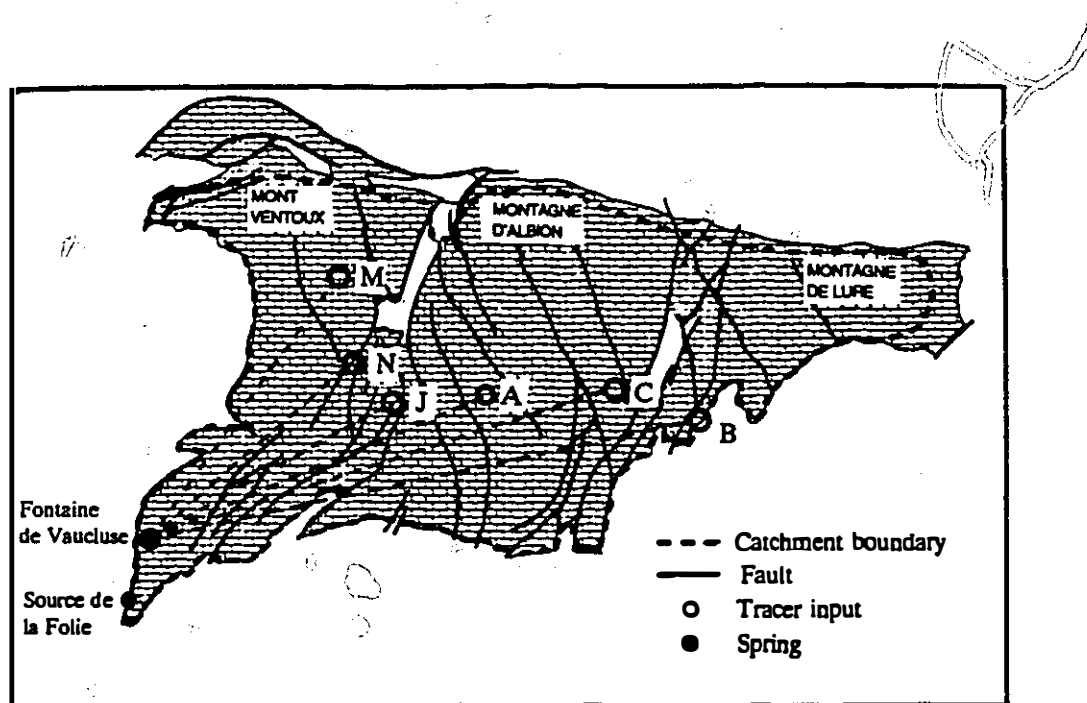


Figure 7.5 Catchment area for Fontaine de Vaucluse, France (after Drogue et al., 1983, Michelot and Mudry, 1985, and Puig, 1987)
 B = La Belette, A = Aven du Chateau, C = Aven du Caladaire, J = Aven Jean Nouveau, N = Nesque, M = Les Melettes

kilometres to the south of Vaucluse (Figure 7.5), and it ceases to flow when the discharge at Vaucluse is $<13 \text{ m}^3 \text{s}^{-1}$ (Michelot and Mudry, 1985).

Thus there is no proven component of artesian flow at the Fontaine de Vaucluse, so it is inappropriate to equate artesian and vauclusian flow. Nor is the spring a result of synclinal structure, as the Vaucluse Plateau is homoclinal.

Predicting the mean depth of the conduit feeding the Fontaine de Vaucluse, using Equation 7.3 or 7.6, will be imprecise, as the flow paths to the spring are likely to be partially fault-guided, as they are known to be at the spring itself (Figure 7.5). If half the flow path is fault-guided, then Equations 7.3 yields a mean flow depth of about 250m.

None of the springs in Table 7.2 are confined in an artesian situation, which would force deep groundwater flow. On the contrary, their deep flow paths can be explained by Equation 7.1; the long flow paths are associated with large catchments, which result in the high discharges typically associated with vauclusian springs. Hence, most of the large karst springs in the world are vauclusian. This includes the largest karst springs of France (Vaucluse), Mexico (Frio: Fish, 1977), USA (Silver: Faulkner, 1976), USSR (Mchishta: Dublyansky et al., 1989), and Yugoslavia (Trebišnica: Torbarov, 1976).

It is concluded that the steep slopes and great flow depths of vauclusian springs are primarily a function of the original flow paths in the aquifer, and that flow depths of several hundred metres may be expected for some of the world's largest springs.

7.4 Prediction of water well yields

The probability of a water well intercepting a flooded conduit in a karst area is low. For example, the areal coverage of the 10km of conduits of Yorkshire System is about 2.10^4 m^2 , under a surface area of 500m by 1km. Thus the probability of a well intercepting a conduit would be 0.04. At any one time, it is likely that less than a quarter of these conduits would have been both developed and flooded, so the probability of intercepting a flooded conduit in Yorkshire System would have been a maximum of 0.01. Away from this concentration of caves, the probability might be less. Consequently, since very few water wells will intercept karst conduits, in general well levels indicate the level of the karst water table, and their yields provide information on fissure flow in the aquifer.

Siddiqui and Parizek (1971) studied water yields from 80 wells in Pennsylvania, finding a range in productivity of over four orders of magnitude. Higher productivities were associated in particular with fracture traces, low dip, dolomite rock type, and with valley bottom locations. From the description above of

flow fields, it would be expected that there would be higher yields at fracture traces and at valley bottom locations, which would be close to discharge points. As the hydraulic conductivity ellipsoid is extended along the x and y axes (Equation 6.9, Figure 6.7), the mean depth of the ellipsoid is a function of the dip of the strata, so that

$$K \propto 1 / \sin \theta \quad (7.8)$$

so an inverse relationship between well yield and dip would be expected. This relationship is shown in Figure 7.6, together with the Pennsylvania well data. The good correlation supports the theoretical empirical findings of Section 6.3.3, that K is greater along bedding planes than orthogonal to them.

7.5 Tributary junctions

It was described in Section 6.3.2 that once one primary tube has connected sink to spring, then flow paths in the aquifer will be redirected towards this victor tube. The reoriented tributary flow fields would then resemble the catchment-scale initial flow field (Figures 6.18 and 7.1), though on a smaller scale as L_x would be less. The victor tube, now enlarging rapidly, would substitute for the spring as a target for the flow field. Evidence for the targeting of tributary flow fields should be forthcoming from cave networks considered in both the horizontal and vertical aspects.

In the horizontal aspect, the junction between a tributary and a principal conduit should be an acute angle, with the angle (ψ_j) being a function of the hydraulic gradient of the principal conduit (S_p) and the tributary conduit (S_r). This is shown graphically in Worthington, 1984, p100) and in Figure 7.1a, but may also be expressed mathematically

$$\psi_j = \arccos (S_p/S_r) \quad (7.9)$$

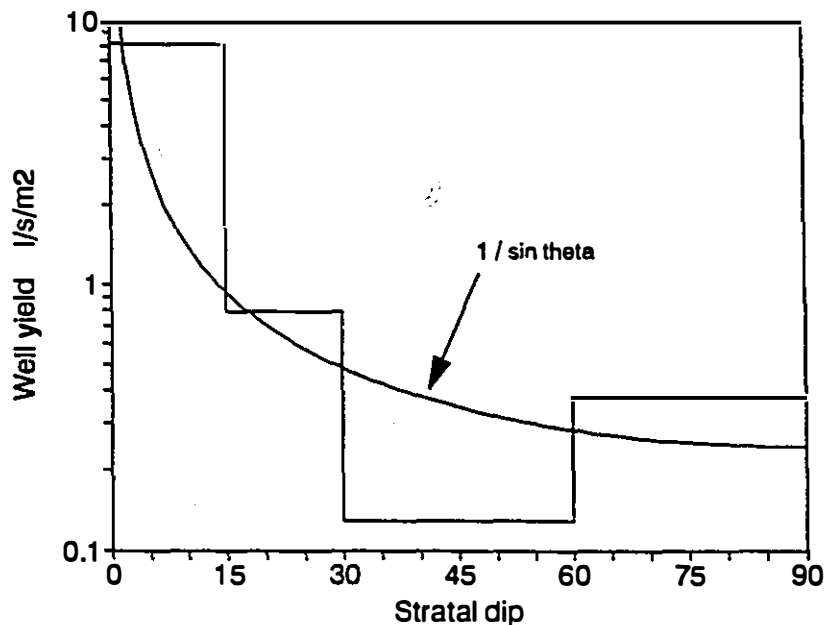


Figure 7.6 Measured well yield from Pennsylvania as a function of stratal dip (after Siddiqui & Parlizek, 1971), compared to the predicted relationship from Equation 7.3

The dendritic conduit networks in the Mammoth Cave area deduced by Quinlan and Ray (1981) from the elevation of the water table in wells and cave passages strongly supports Equation 7.1. In that area, $\psi_j = 63^\circ \pm 25^\circ$ ($n=84$).

An alternative method was used in Friars Hole System. Worthington (1984) measured ψ_j at 53 junctions of tributary phreatic passages with main passages, finding $\psi_j = 79^\circ \pm 25^\circ$. No significant relationship was found between the azimuth of ψ_j and either major joint azimuths or fault azimuths (Worthington, 1984, p29 and 100). The detailed study of one part of this cave by Jameson (1985) shows a similar result ($\psi_j = 79^\circ \pm 13^\circ$, $n=4$).

The null hypothesis is that junction angles are not a function of the hydraulic gradient, and that the orientation of ψ_j is random. An alternative hypothesis is that passages tend to follow orthogonal joint patterns. In either of these cases the mean value of ψ_j would be 90°. The evidence from the three above studies shows that ψ_j is less than 90° in all cases. This supports the hypothesis that tributaries develop in response to flow fields which have a main conduit as the low-potential output point.

In the vertical aspect, the flow field towards the conduit will be a function of the depth of the conduit below the water table. If the conduit is close to the water table, then the flow field should be similar to that shown in Figure 7.1, and tributaries will tend to connect by terminal phreatic lifts.

However, if the conduit is deep below the water table, such as may occur along much of its flow path, then the flow field in Figure 7.7 will result. If there were even infiltration and an isotropic flow field, then the tributary slope towards the conduit will have a gradient

$$\psi_t = 180 L_t/L_w - 90 \text{ } (\circ) \quad (7.10)$$

where L_t is the distance normal to the main conduit between an inflow point to the phreas and the conduit, L_w is the distance normal to the conduit between it and the furthest inflow point (Figure 7.7), and ψ_t is the slope of the terminal part of the tributary, which is defined here for practical purposes as being the last 100m (horizontal distance) of the tributary.

The most notable tributary junction in Yorkshire System is where the tributary of Alberta Avenue has a terminal lift of 82m to join the main passage, the Roller Coaster, with the junction being 52m below the contemporaneous water table (Figure 6.5b).

Active examples of terminal phreatic lifts in tributaries have been forthcoming from recent diving in the phreas of the Three Counties System, Britain's

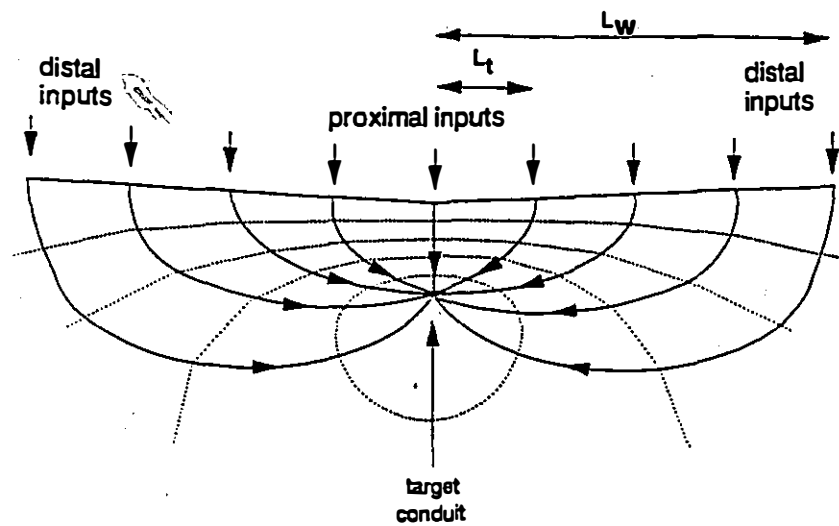


Figure 7.7 Tributary flow fields towards a target conduit, showing equipotential lines

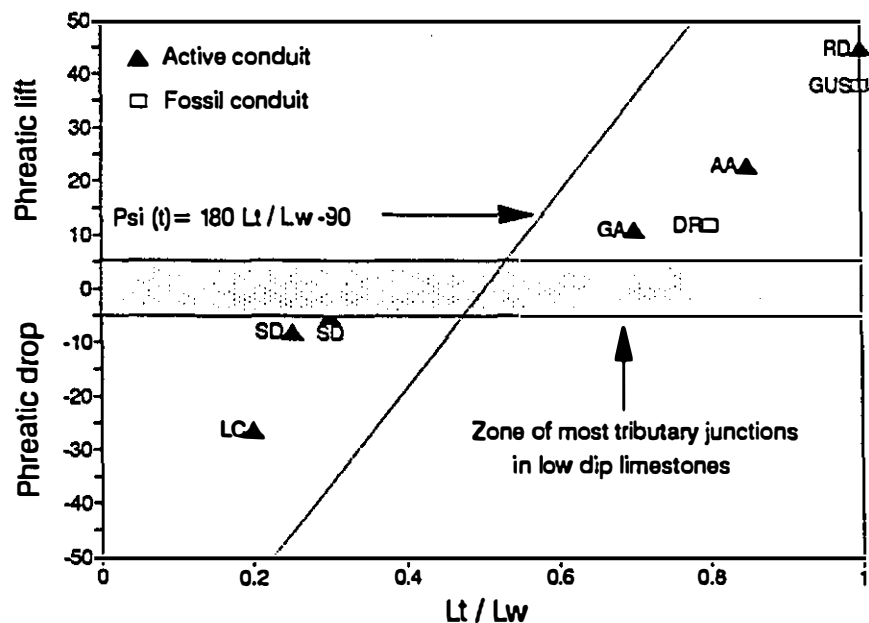


Figure 7.8 Terminal phreatic lifts and drops of selected tributary passages

RD = Ronnie's delight (Eavis, 1981), GUS = Gavel upstream sump (Walther & Hatherley, 1983; Anon., 1989a), AA = Alberta Avenue (Figure 6.5a), DR = Deep rising (Brook, 1974), GA = Grotte Annette (Figure 6.4e), SD = Sheepdip (Worthington, 1984), LC = Lyle Caverns (Walther, 1974)

longest cave, where more than 7km of submerged passages have now been explored. Two tributary passages there have terminal phreatic lifts, which are the deepest points explored in the phreas so far, with the exception of the terminal lift of the whole drainage system (Brook, 1974; Waltham and Brook, 1980a; Waltham and Hatherley, 1983; Palmer, 1986; Anon, 1989a, 1989b).

Data from these tributary lifts, together with several other notable fossil terminal tributary lifts and drops are shown in Figure 7.8. It should be noted that the error margins of these data are considerable, as L_t/L_w is poorly known in most cases. Nevertheless, the data clearly support Equation 7.10.

A fuller analysis of tributary flow fields, which will not be undertaken here, would include the effect of the distortion of flow along bedding planes (Section 6.3.3). However, such analysis would be difficult, as the secondary flow field in which a tributary is formed is less predictable than the primary flow field because it is less isotropic; this is due to the anisotropic development of permeability associated with the primary flow field.

Tributary passages were termed subsequent passages by Ford (1968), who recognised regular forms (not utilising primary tubes) and irregular forms (utilising primary tubes). The descriptions of Ford (1968) and Ford and Williams (1989) concentrated on strike-oriented tributaries utilising portions of dip-oriented primary tubes. However, primary tubes may have any orientation with respect to the geological structure, and so may tributaries.

7.6 Factors possibly modifying the initial flow net

7.6.1 Long vadose paths

So far, the total length of the catchment, L_x , has been considered. This can be measured on the surface. However, a more accurate formulation of Equation 7.3 or 7.6 would utilise the phreatic flow path L_p , where

$$L_x = L_v + L_p \quad (7.11)$$

L_v being the vadose flow path. A major disadvantage of using L_p is that it is much more difficult to measure than L_x .

In most cases D_v (the depth of the vadose zone) is small in relation to L_x (i.e. <0.1: Table 7.1). It was shown in Section 5.2.4 that $\psi_v \approx 45^\circ$, so that $L_x \approx L_p$. Additionally, in aquifers with strike-oriented flow, the vector L_v is usually approximately downdip, in which case $L_x = L_p$. Only in aquifers with dip-oriented flow in conjunction with low dip or high D_v/L_x will L_p substantially differ from L_x . Thus in only a few cases will the use of L_x rather than L_p cause substantial errors in using Equations 7.3 or 7.6.

7.6.2 Effects favouring shallow phreatic flow

Thrailkill (1968) investigated flow paths in the eastern USA, where flow had been considered usually to be just below the water table. On hydraulic grounds, he argued that a karst flow net should approximate a Darcy flow net (Figure 6.1a), as had been suggested by Davis in 1930. To explain the preponderance of shallow phreatic flow, he proposed three ways in which solution would be maximised close to the water table.

This could be caused by the increased aggressivity of cooling infiltration water, the mixing corrosion effect by mixing infiltration and conduit water, and by the lower CaCO_3 concentration in floodwaters. On the other hand, he noted that there is a slight increase in solubility with hydrostatic pressure, which would to some extent favour the longer flow paths at depth.

Thrailkill (1968) noted that it is difficult to test the efficacy of any of these methods by hydrochemical means as most karst waters reach saturation within a few metres of the surface, and the degree of undersaturation once a karst conduit is reached is usually less than the measurement error. In the last twenty years, there

has been much speculation on the possible importance of shallow phreatic boosting effects, as many caves appear to follow shallow paths below the water table. However, the hypotheses of Thraikill (1968) have never been tested.

The three effects boosting shallow phreatic solution (Thraikill, 1968) would be most pronounced where the influx of surface water occurred at frequent intervals along the length of the catchment (Figure 6.11b). This situation corresponds to a karst catchment with autogenic recharge. The converse is shown in Figure 6.11a, where a single stream input subsequently flows beneath an impermeable caprock, so there is no autogenic recharge. In fact, most catchments are intermediate in function between these end members of autogenic and allogenic recharge.

The relationship between flow depth and percentage of autogenic recharge for the caves from Table 7.1 is shown in Figure 7.9. An inverse relationship is not apparent, as would be expected from the shallow phreatic boosting effects of Thraikill (1968). Thus it is concluded that hydrochemical shallow phreatic boosting effects such as mixing corrosion are of little importance in determining conduit flow paths. On the other hand, the shallow flow paths in the eastern USA karst can be explained in terms of a combination of low dips and short catchment flow paths (Equations 7.3, 7.6).

It was explained in Section 6.4.1 that there must be some mechanism promoting flow at shallow depths, or flow in karst would concentrate at the base of the aquifer, where viscosity is minimised. It was suggested the cause might be greater initial fracture width at shallow depths.

7.6.3 Distortion of hydraulic conductivity ellipse by impermeable strata

So far, it has been assumed that the karstic catchment was of infinite extent. It is obvious that impermeable strata will distort flow fields, and an interesting test of the ideas in this chapter is provided by the caves in Norway developed in thin marble bands between schists.

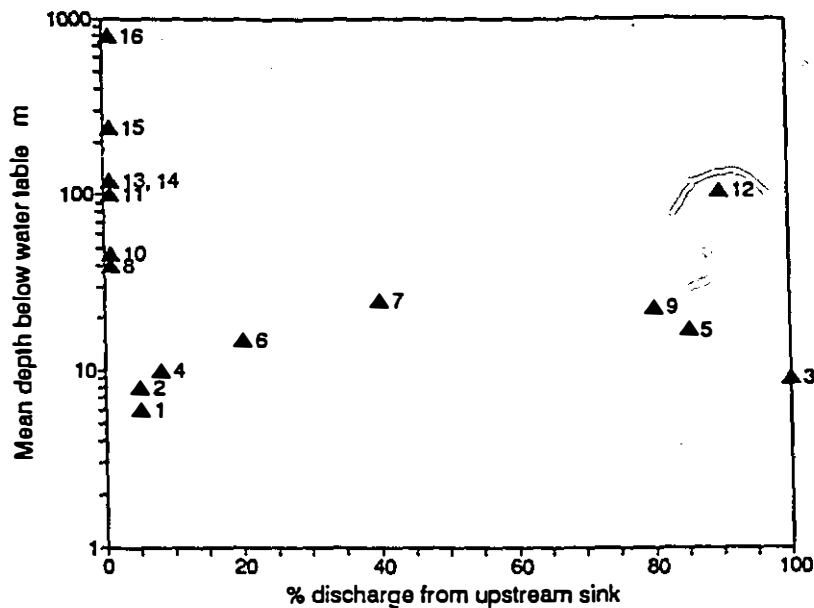


Figure 7.9 Mean phreatic flow depth for allogenic and autogenic karsts
The data points are listed in Table 7.1

Jordtulla is a flooded cave, which has been explored by divers (Lauritzen, 1985). Most of the cave is at or is close to the upper contact between the marble and the overlying mica schist. The fossil cave of Pikhåggrottene is found six kilometres further north, where the marble outcrop has thinned to 20m. Lauritzen (1982) found that most passages developed at foliation/fracture intersections. Sirijordgrotten is a fossil cave developed in a marble band at least 50m thick (Faulkner, 1980; St Pierre and St Pierre, 1980).

Predicted mean flow depths for these three caves are similar to observed values (Table 7.3), so it is concluded that flow nets in these narrow marble bands were not seriously distorted by the narrow aquifer.

Table 7.3 Phreatic flow depth for caves in narrow karst aquifers in Norway

	passage length m	L_x km	dip of contact	D_{obs} m	D_{cal} m
Jordtulla	670	0.52	25	9	8
Pikhåggrottene	>2000	>0.7	70	20	>21
Sirijordgrotten	1380	1.1	81	9	32

* from Equation 7.3

7.6.4 The influence of topographic relief

A relationship between topographic relief and phreatic flow depth has been noted by many authors, and this is supported by the data in Table 7.1. However, this does not establish a causal relationship, for most areas of low relief have low-dip strata, while high relief is often associated with folded and hence high-dip strata. Linear regression of depth against $L_x \sin \theta$ and against topographic relief for the data in Table 7.1 yields correlation coefficients of 0.995 and 0.323 respectively, while multiple regression against the two variables yields a negative relationship between relief and depth, though this is not statistically significant.

Thus it is concluded that there is no causal relationship between phreatic flow depth and topographic relief.

7.7 Conclusion

In the conclusion of their ground-breaking paper on cave hydraulics, White and Longyear (1962, p167) stated "When [hydraulic gradients and controlling geologic factors] are understood, it should be possible to write down the geologic boundaries and immediately deduce the extent and pattern of the cave which should

result". This chapter has shown that catchment length and stratal dip and strike are the principal controlling factors in determining the depth of formation of karst conduits below the water table. Thus for the first time, some characteristics of cave conduits may be predicted from surface measurements. The proposed model is supported by data from water well yields, cave profiles, base/crest depths of phreatic loops, and from vauclusian springs. The validity of the model is also shown in single input, narrow karst outcrop, and in both autogenic and allogenic situations.

The development of conduits in subsequent generations will be analyzed in Chapter 8.

Chapter 8 Flow nets in karst aquifers: response to a falling water table

8.1 Introduction

In the two previous chapters, flow fields have been discussed in terms of a static water table. A falling water table relative to cave conduits is the result of base level lowering and/or uplift, and is visible within most karst aquifers in the form of fossil conduits.

A model for the development of conduits in response to a falling water table is presented in Figure 8.1. This model represents an extension of the findings of the two previous chapters, where it was shown that conduits develop in response to the structurally influenced flow fields found in karst aquifers. The model provides the first holistic karst groundwater flow model. It is holistic for two principal reasons. First, it can describe flow at any time in the life of a karst aquifer (such as when a new conduit has recently been formed, or a million years later while it is still being used). Second, it can describe (and predict) the spatial occurrence of low- and high-discharge variability springs, of low- and high-sulphate springs, of low- and high-temperature springs, and of low- and high-CVH springs.

This model is based on nine hypotheses:

- 1) The locus of cave conduits below the water table is primarily a function of aquifer length and stratal dip.
- 2) Phreatic conduits describe a single loop below the water table at the time of formation.
- 3) A synchronous tier of active conduits is active for a considerable period (e.g. 3×10^5 - 10^7 years).

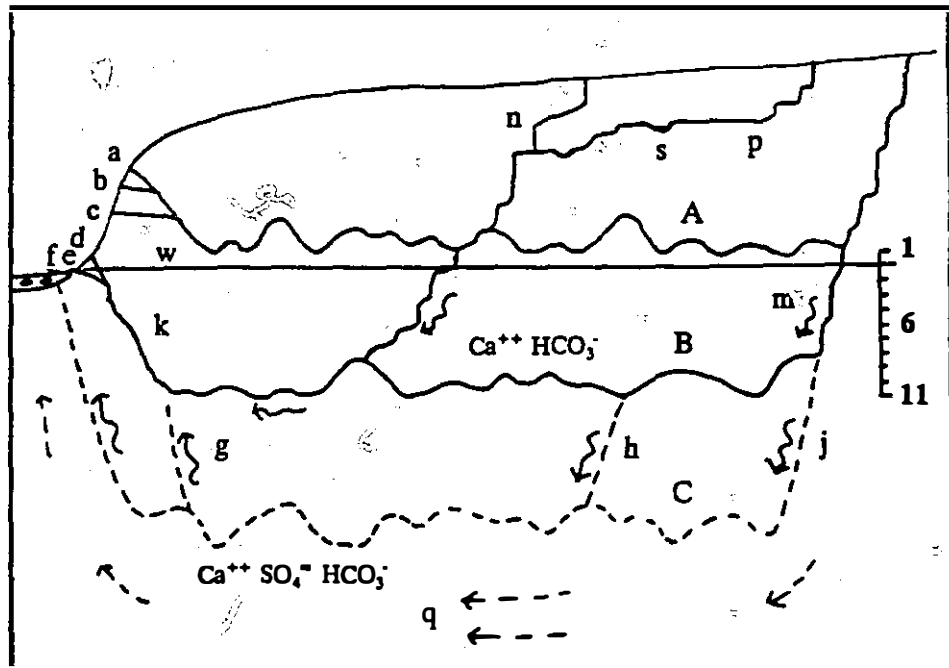


Figure 8.1 Sequential development of conduits in a karst aquifer, shown soon after abandonment of conduit A in favour of conduit B.

Note: the vertical exaggeration is about x20

- A Fossil conduit
- B Dynamic phreatic conduit handling >99% of the discharge from the catchment
- C Proto-conduit C with non-phreatic flow, developing at the locus of maximum discharge through the fracture flow net active below conduit B
- a,b,c Underground delta (fossil) for conduit A
- d Active overflow vauclusian spring
- e Active underflow vauclusian spring
- f Sulphate-rich sub-thermal or thermal spring emanating from alluvium in valley floor
- g Sulphate-rich feeder to conduit B
- h,j Feeders to proto-conduit C
- k Terminal phreatic lifts
- m Initial phreatic drop
- n High-gradient vadose inlet
- p Low-gradient vadose inlet with perched sumps (s)
- q Hagen-Poiseuille flow field, active as far down as the base of the aquifer
- s Perched sumps in the vadose zone
- w Water table
- 1-11 Water table levels

- 4) Active conduits are mostly flooded.
- 5) As base level lowers, the first conduits to emerge above the water table are at the input and output ends of the aquifer.
- 6) There is a developing flow field beneath existing conduits. When this captures flow from the upper conduit will determine whether the upper conduit is left as an unentrenched phreatic tube or a vadose canyon.
- 7) There may be flooded conduits and low-gradient cave streams in the vadose zone, at considerable elevations above the water table.
- 8) Spacing between tiers is equal.
- 9) The flow field beneath existing conduits is characterised by laminar flow, and smaller discharge variation, higher temperatures, and higher sulphate loads than existing conduits.

The empirical evidence that strongly supports the first two hypotheses has already been presented in Chapters 6 and 7 (Equation 7.3 and Figure 7.2 for hypothesis 1; Section 6.2.7 and Figure 6.5 for hypothesis 2). The remaining seven hypotheses will be tested in the following seven sections (8.2-8.8).

8.2 Longevity of flow in conduits within one tier

Successive principal conduits in karst aquifers typically have a vertical spacing of 10-200m (Table 8.1; Figure 6.5b, d; Figure 8.2). The time period that each generation is utilised is usually in the range 0.3-10 million years. (Table 8.2).

Such long occupancy times can be attributed to the large spacing between tiers shown in Figure 8.1, and depends on the locus of new conduit development being at depth below the water table, as was demonstrated in Equation 7.3. The limited data available show that inter-tier spacing is usually much greater than loop amplitude within one tier (Table 8.3). Conduit B in Figure 8.1 will be utilised as the principal conduit from before position 1 to at least position 8, and possibly until position 11. Thus long conduit occupancy is possible without any passage diversions,

Table 8.1 Vertical spacing between cave tiers

Cave	spacing between tiers m	source
Nelfastla de Nieva, Mexico	230, 230	Worthington, 1990b
Hölloch, Switzerland	160, 120	Bögli, 1980
Gua Harimau-Lubang Sakai, Malaysia	120, 90, 110	Eavis, 1985
Nettlebed, New Zealand	65, 90, 60, >65	Ford & Williams, 1989, p122
Ogof Daren Cilau, Wales	40, 27, 48, 63	Smart & Gardener, 1989, p145
Archway-Terikan, Malaysia	35, 35, 30	Eavis, 1981
Demänová, Czechoslovakia	18, 30, 32, 20	Droppa, 1966
Gaping Gill, England	20, 20	Glover, 1974
Friars Hole System, USA	18, 17, 15, 24, 27*	Worthington, 1984
Lancaster-Easegill, England	15, 13	Ashmead, 1974
Carlswark Caverns, England	13.7, 12.8, 12.6	Christopher & Beck, 1977
Mammoth Cave System, USA:		
main tiers	20, 19, 16	Palmer, 1987
Historic Section	9,5,5,1.3,2.4,12,2.7,2.8,3.8	White, 1988, p86

* The prime control on the upper passages is bedding, which dips at 2°; the prime control on lower passage is fractures associated with thrust faults, which have dips of 10-60°.

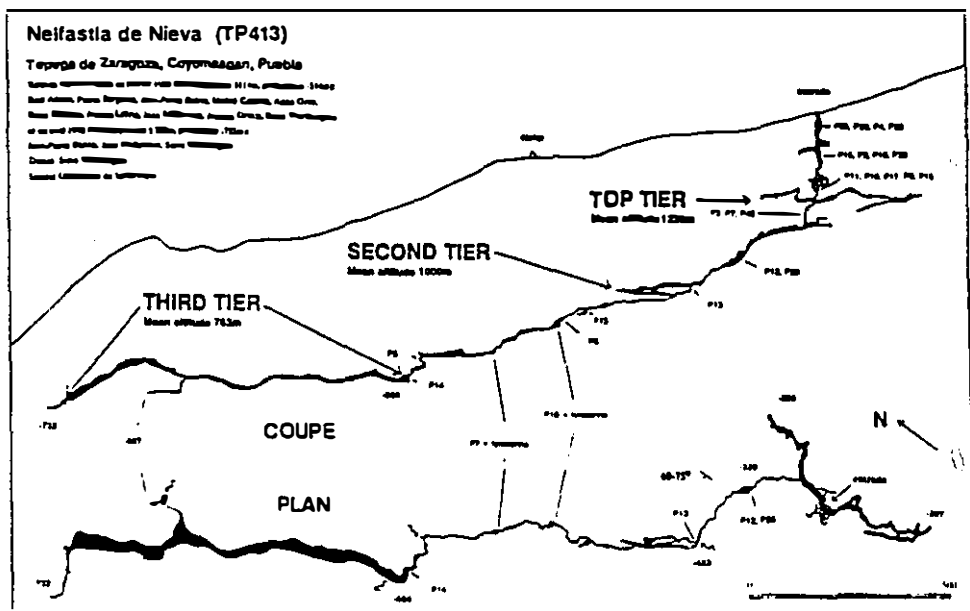


Figure 8.2 Tiers of cave passages in Nelfastla de Nieva, Mexico

Table 8.2 Occupancy times of cave tiers, based on radiometric and paleomagnetic dating, and on denudation rates

Cave	Occupancy time years	Method	Source
Friars Hole System, USA	300,000 - 700,000	U, P	1
Mammoth Cave System, USA	350,000 - 500,000	U, P	2
Crowsnest Pass caves, Alberta	1 - 10 million	U, P, E	3
West Kingsdale System, England	>300,000	U	4
Nelfastla de Nieva, Mexico	2.5 - 4 million	E	5

U = Uranium Series dating; P = Paleomagnetic dating; E = Erosion rates

1 Worthington (1984)

2 Schmidt (1982)

³ Slaymaker & McPherson (1977), Ford et al. (1981), Section 10.4

4 Gascovne, Ford & Schwarcz (1983)

5 Worthington (1989, 1990)

Table 8.3 Loop amplitude and tier spacing

Cave	Loop amplitude	Tier spacing	Spacing	Inter-tier
	mean m	mean m	/loop amplitude	spacing m
Nelfastla de Nieva, Mexico	30	230	8	200
Holloch, Switzerland	100	140	1	40
Swildons Hole, England	8	20	2	12
Nettlebed Cave, New Zealand	20	70	3.5	50
Sótano de Jápones, Mexico	5	32	6.4	27
Friars Hole System, USA	5	17	2.4	12
Mammoth Cave System, USA	1?	18	18?	17

For sources see Tables 7.1 and 8.1

except close to the spring.

8.3 Active conduits are mostly below the water table

Evidence to support the hypothesis that active conduits mostly lie below the water table can be found in several data sets, such as the deepest explored caves, the longest explored caves, the largest springs of the world, and repeated tracer tests.

Of the 100 deepest caves in the world (Courbon and Chabert, 1986), none has been followed to the principal base-level conduit of the aquifer. The closest perhaps is in Sistema del Trave, where a 400m section of streamway was explored to siphons (Yves-Bigot, 1989). However, the gradient of 0.1 to the springs indicates this cannot be a true base level (see Table 5.4). Of the remaining 99 caves, most end in perched siphons above base level, but 15 (all in France) reach geologically-perched trunk conduits. The 15 French perched trunk conduits bias the sample because deep caves in such geological situations can be easily explored. Geological evidence

suggests that only a few percent of groundwater flow systems of the world are geologically perched.

Of the 25 longest caves in the world (Courbon and Chabert, 1986), only three have base-level conduits that are not siphoned for long distances. Of the 26 largest karst springs in the world (Ford and Williams, 1989), at least half are vauclusian, and only one (Matali, PNG) is known to the author not to emerge from a siphon. Repeated tracer tests to determine aquifer conditions were discussed in Section 3.3.1, and results are shown in Figures 3.6 and 5.2. The six flow routes tested so far (3 in England, plus Maligne Spring, Crowsnest Spring, and Ptolemy Spring in Alberta) are all almost wholly phreatic.

Thus four contrasting data sets show that principal conduits in karst aquifers are indeed almost always flooded. However, there are two cases in which open trunk conduits can be expected.

First, in areas of low dip or small aquifer length, the phreatic depth of conduits would be small (from Equation 7.3). In this case only a small amount of downcutting or variation in the water table level between low and high discharge would produce long sections of passage with lakes and low airspaces. This is exactly the case in Whigpistle Cave and Hidden River Complex, both in Kentucky (USA), where the dip is about 0.25° (Quinlan and Ewers, 1989).

The second exception is where there has been considerable vadose downcutting, which will remove flooded sections. Almost all the great high-discharge, low-gradient vadose caves are found in wet tropical areas. The probable reason for this is that the high vegetative activity and high runoff produce high solution rates. This allows vadose downcutting to keep up with base-level lowering, and produces lofty low-gradient stream or river passages. By contrast, almost all high-discharge conduits in temperate areas are flooded, terminating almost always in vauclusian springs.

Some examples of low-gradient river caves are shown in Table 8.4. With the exception of Sof Omar, all are in humid, tropical areas. No examples in temperate or alpine areas are known to the author, despite the fact that most caves explored so far have been in the latter areas. There is a surface analogue to river caves, which is the flowing of alloegenic rivers across karst outcrops. In both cases the river is able to entrench fast enough to prevent capture to a lower path below the river bed. Notable examples hundreds of metres deep include the Nahanni canyons (NWT), the Verdon gorge (France), the Vicos and Samaria gorges (Greece), the Petlapa and Santo Domingo gorges (Mexico), and the Strickland gorge in Papua New Guinea.

8.4 Response at initial phreatic drops and terminal phreatic lifts to base level lowering

As base level lowers, the first passages to emerge above the water table are at the input and output extremities of the aquifer. In the former case the simple response is vadose entrenchment. This response was described by Ford (1971b) as drawdown vadose entrenchment. Clear examples are seen in Swildons Hole (Figure 6.4d) and Nelfastla de Nieva (between the second and third tiers: Figure 8.2).

In the case of vauclusian risings, the simplest response to falling base level is truncation of the ascending passage. This is seen for instance at Doux de Coly, Høolloch, and Trou de Glaz (Figure 6.5), and Castleguard (Figure 11.3). In other cases, there is the formation of distributaries close to the spring. This is known as an *underground delta* (French: *delta souterrain*; Renault, 1967). Crowsnest Spring (Figure 6.5a) is a simple two distributary example. It has a constricted underflow conduit which discharges baseflow, and an overflow conduit which discharges snowmelt. Some more spectacular examples are shown in Figure 8.3 and Figure 4.2. Other examples are shown in Figure 6.5c and d.

Table 8.4 Vadose incision in major low-gradient river caves $(Q_m > 1 \text{ m}^3 \text{s}^{-1}, L > 1 \text{ km})$

	mean passage height (m)	reference
Sof Omar, Ethiopia	20	1, 2
Sistema del Río Candelaria, Guatemala	30	3
Conjunto São Mateus - Imbira, Brazil	15	4
Gua Air Jernih, Malaysia	70	5
Gua Payau, Malaysia	90	5
Sistema del Río Camuy, Puerto Rico	40	1, 6
Chiquibul Cave System, Belize/Guatemala	25	7
Grutas San Jeromino y Chontalcoatlán, Mexico	30	8
San Cha He Dong, China	90	9
Gebihe, China	60	10
Atea Kananda, Papua New Guinea	15	1, 11
Cueva Fun Fun, Dominican Republic	15	1, 12
Fulon Dong, China	45	13

1 personal notes

2 B.S.E.E., 1973

3 Courbon and Dreux, 1976

4 Karmann, 1990

5 Brook and Waltham, 1978

6 Gurnee and Gurnee, 1974

7 Miller, 1986

8 Coons, 1976

9 Waltham, 1986

10 Collignon, 1990

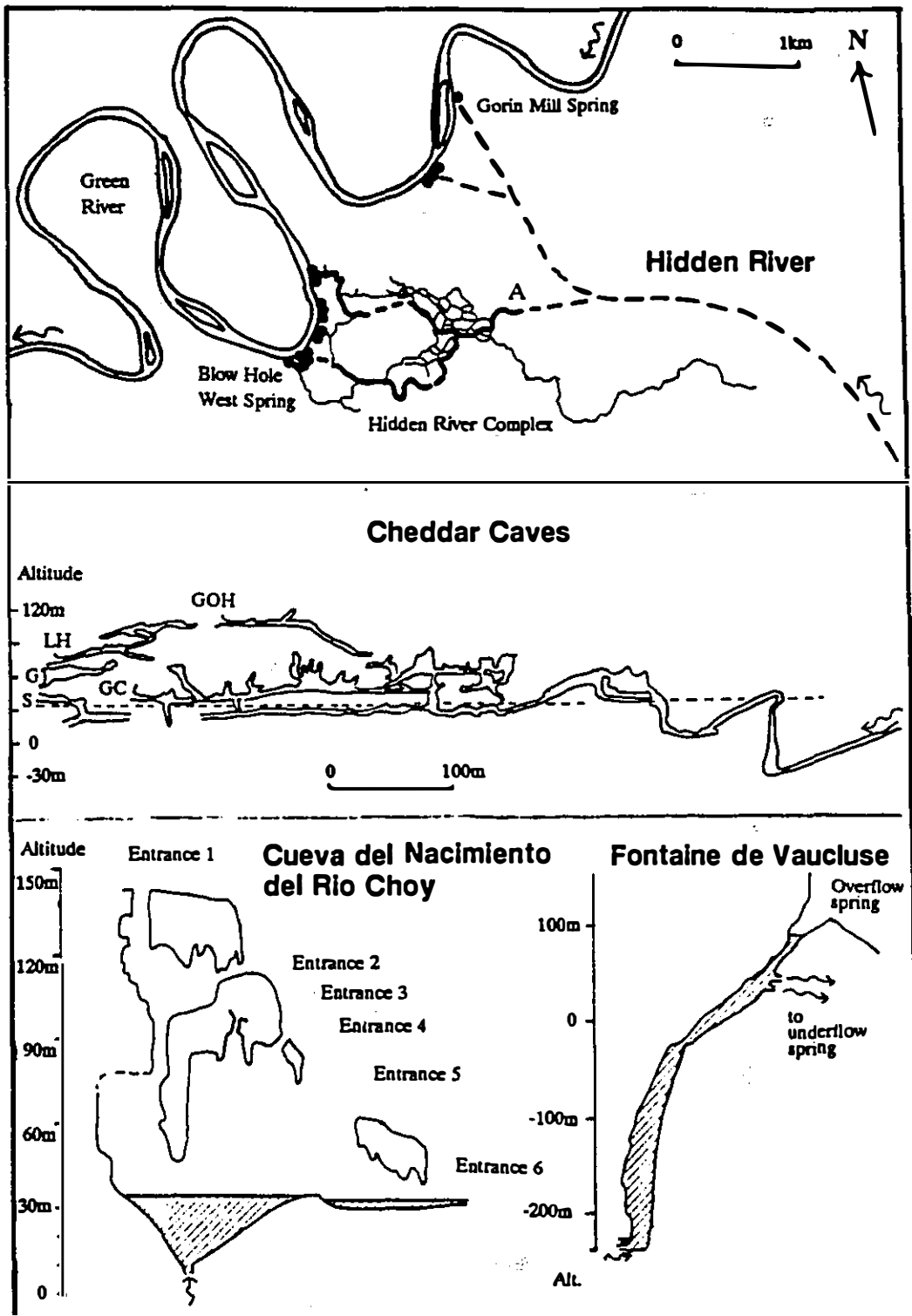
11 James and Dyson, 1980

12 Yonge, 1987

13 Gill et al., 1990

Figure 8.3 Examples of underground deltas

- a) Plan of Hidden River underground delta, Kentucky, USA. Most (and sometimes all) of baseflow is to Gorin Mill Spring. Along an 8km stretch of the Green River between Gorin Mill Spring and Blowhole West Spring there are 45 overflow springs from the Hidden River at 15 locations. In the 31km long Hidden River Complex waters enters by a 17m phreatic lift at A, and diverges at baseflow into two distributaries. All but one of the major groundwater catchments in this area have underground deltas (after Quinlan & Ewers, 1981, 1989; Quinlan et al., 1983).
- b) Extended profile of the Cheddar caves, England. A single conduit appears to have fed a series of distributaries at Great Oones Hole (GOH), Long Hole (LH), Gough's Old Cave (G), Gough's Cave (G), Saye's Hole (S), and now at two resurgences at a lower altitude (after Ford, 1965; Drew, 1975b; Anon., 1988).
/1
- c) Projected profile of Cueva del Nacimiento del Rio Choy, Mexico. Earlier spring flow rose vertically to emerge from the higher entrances (after Fish, 1977).
- d) Extended profile of Fontaine de Vaucluse, France. The main entrance is an overflow, active when total discharge at Vaucluse is $>22.5\text{ m}^3\text{s}^{-1}$. There are also overflow springs at La Folie, 5km south of Vaucluse, which are active when the discharge at Vaucluse is $>13\text{ m}^3\text{s}^{-1}$ (after Michelot & Mudry, 1985; Courbon & Chabert, 1986; Lefalher & Sanna, 1990).



8.5 Hydraulics of existing and developing conduits

Davis (1930) observed that there must be a flow field beneath cave conduits. For instance, in Figure 8.1 while there is flow through conduit B there is also a flow field below it. With time solutional erosion will produce a new conduit, C, which will eventually capture the flow from conduit B. The primary tubes of conduit C develop during the period when conduit B is active, when base level is being lowered from position 1 to position 8. During this period the fissure will enlarge in diameter by about two orders of magnitude (White and Longyear, 1962). From the Hagen-Poiseuille equation (4.2), then discharge will increase $(10^2)^4$ times, which is shown in Figure 8.4 as an increase in Q_C/Q_B from 10^{-11} to 10^{-3} . When the transition from laminar to turbulent flow occurs, there will be an increase in conduit enlargement rates of as much as seven orders of magnitude (White and Longyear, 1962). This threshold is represented in Figure 8.4 as an order of magnitude increase in conduit discharge. Once flow in conduit C becomes more efficient hydraulically, then it will quickly capture the flow from conduit B, which then becomes abandoned.

As the water table drops below position 7, there are four gradational mechanisms which will affect the conduit. These are paragenesis, loop entrenchment, loop base bypassing and loop crest bypassing, and they serve to diminish the vertical amplitude of phreatic loops over time during a single generation flow path. The classic example of all four mechanisms is the Swildon's Hole - Wookey Hole stream, England (Figure 6.5; Ford, 1965; Drew, 1975; Farr, 1980). Paragenesis is also well supported by other studies (e.g. Renault, 1968; Pasini, 1975), and there are examples of loop entrenchment in Yorkshire System and Gargantua, and elsewhere.

Loop base bypassing has previously been known as loop bypassing (Ford, 1965). It is the development of a conduit to bypass the base of a loop as it becomes filled with sediment. Loop crest bypassing is the development of a conduit to bypass the crest of a loop. Smart and Christopher (1989) suggested that it occurs where hydraulic gradients are high, such as when the water table drops so that the crest of

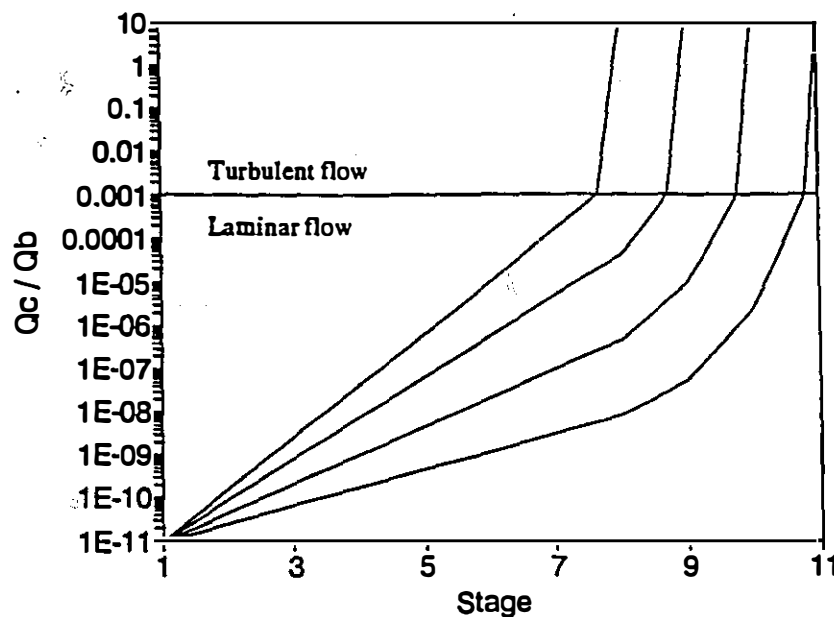


Figure 8.4 Ratio of discharge in developing conduit C to discharge in existing conduit B for four growth rates, corresponding to capture at stages 8, 9, 10 and 11 in Figure 8.1

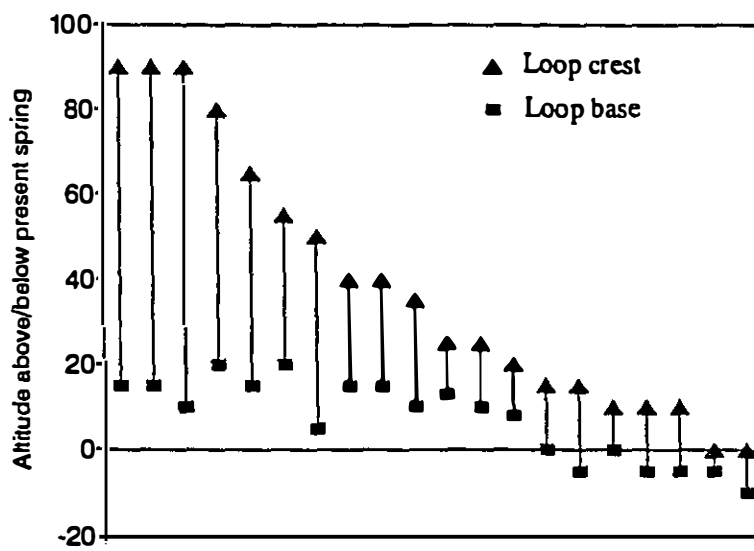


Figure 8.5 Altitude range of phreatic loops in Ogef Ffynnon Ddu I, Wales (after Smart and Christopher, 1989)

a loop becomes vadose. In Ogof Ffynnon Ddu I (Wales) the falling base level has been accompanied by a diminishing loop height (Figure 8.5), which has resulted in most of the stream now being vadose. This has reduced the flow path of the cave stream by over 40% (Glennie, 1950). There is a similar response in Yorkshire Pot, where there are a large number of loop crest bypasses (Figure 8.6). These four gradational mechanisms all operate on a small scale, usually within the range of metres to tens of metres.

Many examples can be found in caves supporting abandonment of conduit B at position 8 or before (phreatic loops unmodified by vadose entrenchment), position 9 (minor entrenchment of crest), position 10 (major entrenchment, with a few loop bases remaining), or position 11 (low-gradient river cave). At Crowsnest Pass, the major phreatic conduits in Yorkshire System, Little Moscow and Gargantua received only minor entrenchment before abandonment.

Positions 8, 9, 10 and 11 in Figures 8.1 and 8.4 broadly correspond with states 1 to 4, respectively, of the "four state model" of Ford and Ewers (1978). The present model differs from Ford and Ewers (1978) in considering the differences between these four water table positions to be due to entrenchment during the development of one tier, rather than an attribute pertaining to the whole tier. Possible enlargement paths for Conduit C are shown in Figure 8.7. During the long period during which the water table is dropping from position 1 to position 8 in Figure 8.1, the discharge through the flow field below Conduit B will be minimal (Figure 8.4). As the base level drops further to position 9, the crests of some phreatic loops become exposed to vadose flow. The higher gradients of these vadose sections then increase the overall hydraulic gradient in the aquifer, including proto-conduit C. The discharge in C then increases rapidly, which leads to the draining of conduit B.

White (1989) and Dreybrodt (1988) suggested on theoretical grounds that caves can form in $<10^4$ years, and such a rapid rate is supported by field evidence from formerly glaciated areas and from Upper Pleistocene limestone (Mylroie and

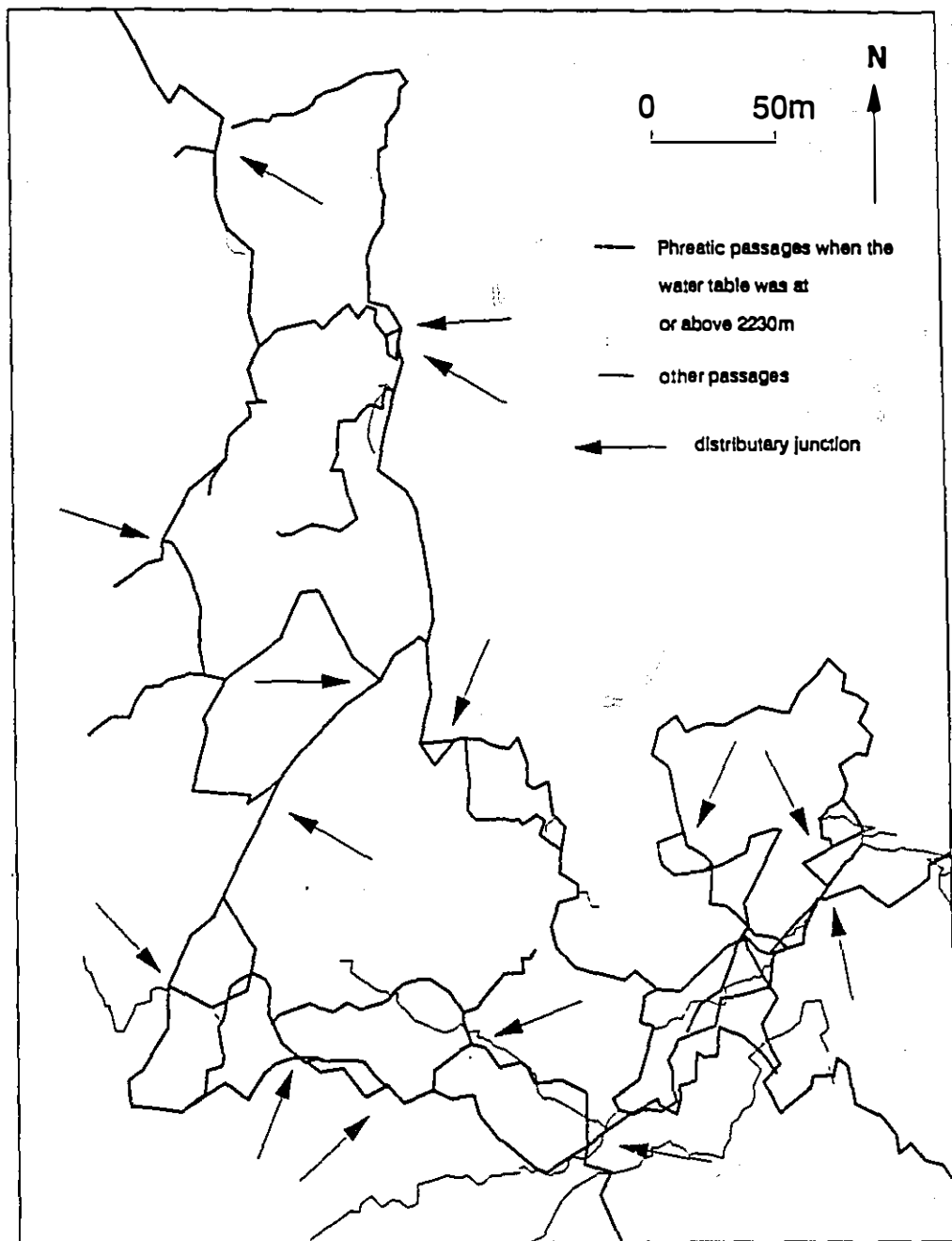


Figure 8.6 Contemporaneous distributary junctions (arrowed) in part of Yorkshire System when the water table was at or above 2230m

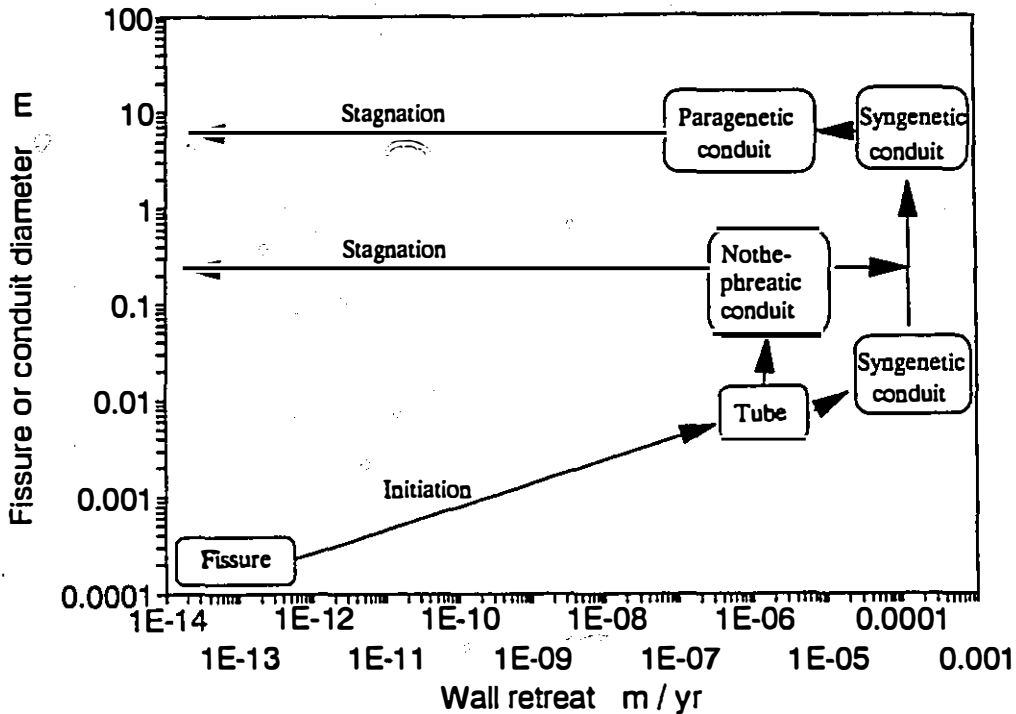


Figure 8.7 Conceptual model of phases in the life of a karst conduit

Carew, 1987). However, in the former case, it may be that the initiation phase had already been proceeding for 10^4 - 10^6 years. The latter case is in a recent high-porosity ($>30\%$) limestone, with the porosity (and hence hydraulic conditions) being many times higher than the $<3\%$ found in most post-diagenetic limestone (Bonacci, 1987).

Thus it may be that the minimum time for the conduit initiation phase (in post-diagenetic limestones) always exceeds 10^5 years at the catchment scale.

From the flow net shown in Figure 8.1 and the conduit utilisation time in Table 8.2, it would appear that times of 10^5 - 10^6 years are normal for the evolution from Hagen-Poiseuille flow net to conduit with turbulent flow. But the development of conduits is a function of velocity and undersaturation of the water, which is only partially a function of base level lowering rates. For instance, the deglaciation 10^4

years ago imposed high hydraulic gradients on many alpine karst aquifers. Some aquifers have responded with new, lower conduit paths. However, the presence of karst springs in cliffs (e.g. Mt Robson, Alberta, and Ice Fall Brook, B.C.) or waterfalls flowing off limestone cliffs into U-shaped valleys (e.g. Lauterbrunnen valley, Switzerland) shows that some karsts have not produced new conduits yet since deglaciation, despite infinite hydraulic gradients ($dh/dl = x/0 = \infty$).

The slow end of the spectrum of conduit formation times is exemplified when a new, lower conduit develops, but the upper conduit remains active. This also could be a product of deglaciation, for the 100m rise in sea level must have reduced hydraulic gradients and reactivated previously abandoned conduits in many karst aquifers. In this case, the lower conduit would experience laminar flow for an extended period.

Eventually, flow becomes more efficient in the lower conduit (C in Figure 8.1) than in the upper conduit, and there is rapid expansion in conduit C. This is the enlargement phase. The initiation, enlargement, equilibrium, stagnation and erosion phases in the life of a conduit were described in Section 5.2.1. One additional phase, the *nothephreatic phase*, will be introduced now.

Jennings (1985) argued that there were two distinct domains of phreatic flow, which he termed *nothephreatic* and *dynamic phreatic*, respectively. Nothephreatic flow is characterised by very slow velocities, and creates such morphological forms as anastomoses, pendants and spongework. Anastomoses represent flow in conduits with diameters typically of a few centimetres, but pendants and spongework are found in conduits with diameters of metres. The spatial and temporal occurrence of retarded flow velocities in large high- K passages with pendants and spongework has hitherto been an unresolved problem. The second domain of phreatic flow, dynamic phreatic flow represents most phreatic conduits, and is characterised by high flow velocities (10^{-3} to 10^0 m s^{-1}).

In Figure 8.1, conduit C will experience low- K conditions for a considerable period of time, during which it may develop to a diameter of some metres, with pendants and spongework. Wells drilled in karst areas provide evidence for this, for karst cavities are often drilled into at depths of hundreds, and sometimes thousands of metres below the water table (Bogli, 1980, p110 cites several examples; Li, 1981). As conduit C captures all the flow from conduit B, it enlarges rapidly, and in so doing removes the evidence for early notephreatic flow. Only occasionally where there was no dynamic phreatic enlargement would pendants and spongework be preserved.

The notephreatic phase may be absent, or present and followed by either conduit enlargement or by stagnation (Figure 8.7).

The discussion so far has been concerned with those fractures that become conduits within the endokarst. These typically have spacings of 10-100m, horizontally and vertically. Other fractures (the vast majority) are less competitive because their initial fracture width is less. These may only develop to conduit width in the subcutaneous zone. These are the grikes of limestone pavements, spaced typically 1-10m apart. Such joint spacing is not just a surficial feature (e.g. as a function of unloading), for Deike (1989) found similar joint spacing 80m below the surface in Mammoth Cave, USA.

8.6 There may be flooded conduits and low-gradient streams in the vadose zone

The water table defines the top of the flooded zone. It may vary considerably with time, since hydraulic gradients in karst conduits vary with the square of the discharge (Equation 5.3). Palmer (1986) demonstrated that this relationship can be used to determine whether cave siphons are located at base level. This methodology can be used for examples from the Rocky Mountains. It shows that the

siphons in Yorkshire Pot and Castleguard Cave do not represent base level, but Medicine Lake fills in response to a rising water table (Figure 11.1).

In the vadose zone three patterns of vadose passages may be distinguished (Figure 8.8). Vertical shaft development (Figure 8.8a) correlates with horizontal bedding, prominent fracturing, pure lithologies and high runoff. Examples >300m deep have been found in humid tropical countries (Mexico, Papua New Guinea, Venezuela) and in alpine ranges (France, Austria, Spain, Italy, Greece). In the Canadian Rockies, the deepest shaft is 280m (Close to the Edge), but most shafts are less than 50m deep. Perhaps the best example is the Astraka Plateau (Greece), where three near-vertical shafts >400m deep have been found (Epos, Epos II, Provatina: Courbon & Chabert, 1986).

Stair-step shaft development (Figure 8.8b) correlates with inclined bedding, impure lithologies and lower runoff. The sub-horizontal sections are typically downdip along the bedding. This is the predominant type of vadose zone conduit development: it was explained in Section 5.2.4 that a sample of deep caves had a median gradient of 48°. The best examples are found in mixed lithologies with low dips, where impure limestone cause perching. Mamo Kananda (Papua New Guinea) is perhaps the best example, where much of the 52km of cave passage is found in eight tiers. Each tier is perched upon an impure limestone (James, Warild et al., 1980). Many Appalachian caves also provide fine examples of stair-step development.

Retarded vertical development (Figure 8.8c) is characterised by long (e.g. 1km) low-gradient (<1°) stream passages which are well above the water table. Such streams are commonly cited to demonstrate that the water-table concept is of limited relevance to karst, but it was argued in Section 5.2.4 that they merely demonstrate the anisotropy of karstic limestones. It is possible that a cave stream may flow sub-horizontally for 1km and only cross joints which will take $>10^6\text{-}10^7$ years to develop into conduits. However, three examples will show that such slow development may be retarded for good reasons.

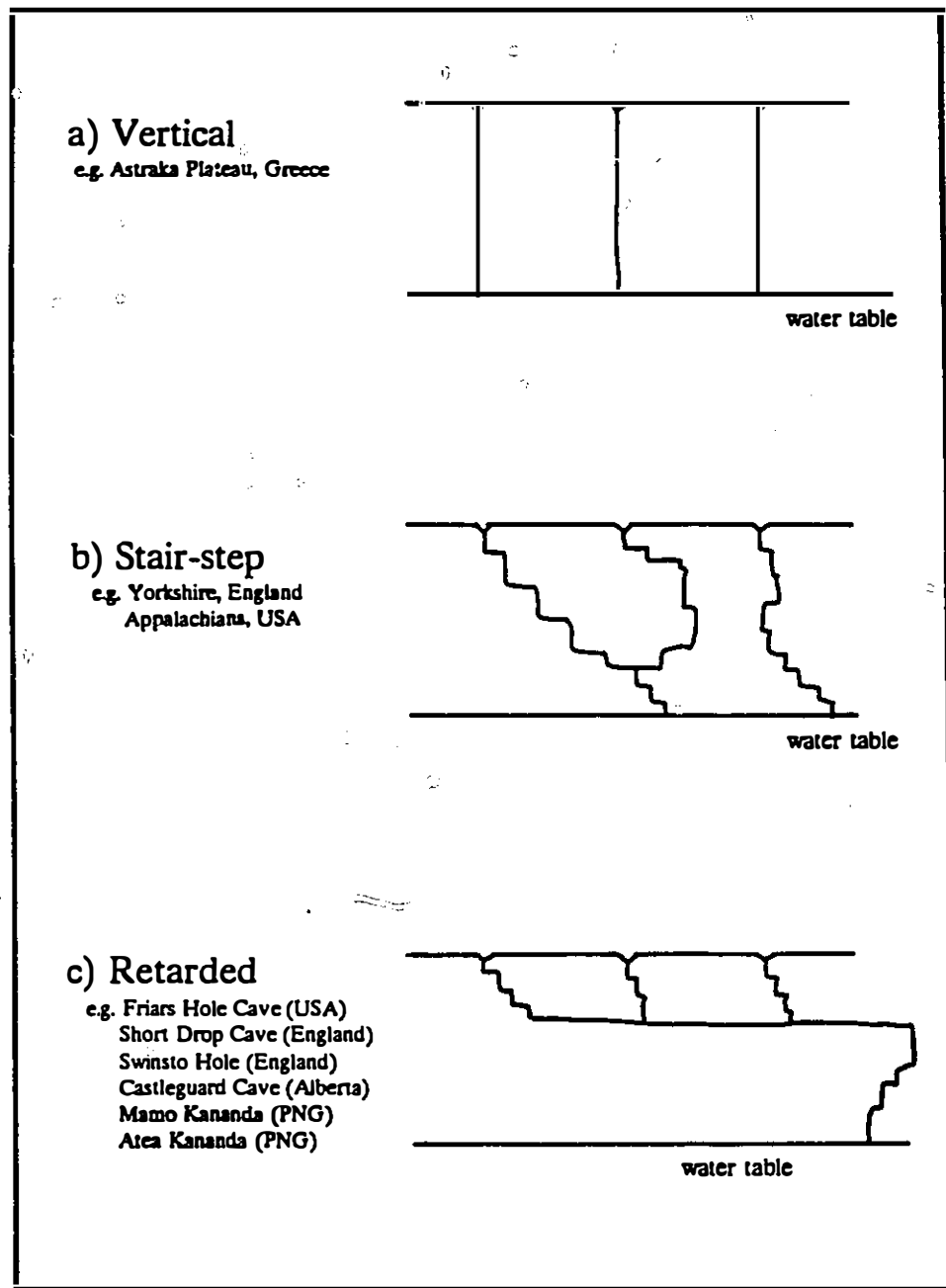


Figure 8.8 Patterns of vertical shaft development in the vadose zone

Castleguard Cave, Alberta (Figure 1.1, Section 10.2.2) has a subhorizontal flood overflow conduit, which emerges at the entrance. This is in a steep hillside, 300m above permanent valley-floor springs. The flood overflow conduit has been explored for 1200m, the last 150m being a permanent siphon (Sawatsky, 1987). Another 500m of passage siphons when the cave floods, which is 0-30 days per year, with maximum discharges of $5 \text{ m}^3 \text{ s}^{-1}$ (Smart and Ford, 1986). Smart (1983b) showed that the cave stream is not an overflow hydraulically related to the Big Springs, and he concluded that it was probably an overflow from an englacial conduit in Saskatchewan Glacier. Since water only flows in the conduit for about 4% of the time, thus solutional erosion is greatly retarded.

Friars Hole Trunk, Friars Hole System, USA is a low-gradient (0.5°) passage at least 50m above the local water table. It has an underfit stream, which meanders over siliciclastic sediments for all but 10m of the 1400m of passage (Worthington, 1984). Interstitial flow in similar sediments was found to be almost three orders of magnitude lower than stream velocities (Williams and Hynes, 1974). Thus the water in contact with the limestone below the armoured stream bed is almost stagnant, so solutional erosion is greatly retarded.

Short Drop Cave, England has a 1km long, low-gradient stream flowing over bedrock. One hundred metres directly below it is another vadose stream in a second cave (Lost Johns). Both caves flow along the axis of a syncline (Waltham, 1974; Waltham and Hatherley, 1983). In this case, compressive forces in the synclinal axis are probably responsible for reducing fracture width, and hence solutional erosion of joints in the bed of the Short Drop stream is retarded.

In all three of the above cases, there are low-gradient vadose streams at considerable heights above the water table. In all three cases there is no relationship between the low-gradient reaches and the water table.

From the foregoing discussion, it is possible to define the mean time for conduit initiation (Figure 8.9). The time depends on the scale considered. Initial

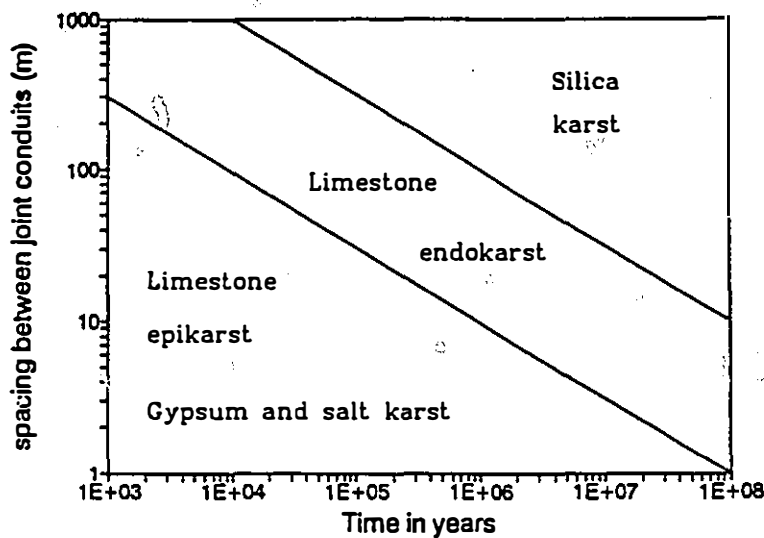


Figure 8.9 The domain of karst in terms of horizontal spacing between joint-aligned conduits

pathways may develop in $<10^4 - >10^6$ years, but it takes considerably longer for most joints to be enlarged to where turbulent flow may occur. In fact, it is an essential attribute of karst that such development only takes place within a few metres of the surface. More rapid development would produce a Darcy flow, porous aquifer. Slower development is shown for example by silica karst. Solution is so slow in this case that silicate rocks are normally considered impermeable. Only in very stable Gondwanaland surfaces is silicate karst conspicuous (White et al., 1966; Jennings, 1985).

8.7 Cave tiers are equidistant

8.7.1 Previous studies

Many caves have stacked "levels" of cave passages. Because such passages are frequently not level, the term tier has sometimes been used (e.g. Ford, 1965; White, 1988), which avoids the unfortunate connotation of horizontality.

It has been generally thought that cave tiers form in response to an exogenetic process: the falling of base level of local or regional rivers. Cave tiers have been correlated with local erosion surfaces and fluvial terraces in several countries (eg. Sweeting, 1950; Ek, 1961; Wolfe, 1964; Droppa, 1966; Miotke and Palmer, 1972; White and White, 1974). The downward shift from one base level to the next was accomplished by nick-point recession (Warwick, 1960), periglacial streams (Ford, 1965) or glacier erosion (Atkinson et al., 1978). There were often two to five tiers in a cave, so the most plausible correlation was one tier per glaciation (Ford, 1965; Ashmead, 1967; Brook, 1974; Bögli, 1980).

This simple and elegant explanation has in recent years been shown to be deficient in three ways. More detailed studies of some of the classic tiered caves have failed to substantiate the postulated horizontal levels of tiers; in addition stratigraphical and sedimentological control have also been shown to produce levels (Waltham, 1970; Pasini, 1975; James et al., 1980; Quinif, 1989). Second, speleothem dating has now shown that phase-fitting resulted in great underestimation of the true ages of tiers (Gascoyne et al., 1983; Waltham, 1983), and that some caves with well-developed tiers date from the Tertiary (Schmidt, 1982; Worthington, 1984). Third, it has been shown there have been possibly twenty or more glaciations, rather than four or five (Shackleton and Opdyke, 1973; Ford et al., 1984).

The present picture of cave tiers is that each was utilised for flow for a period of several hundred thousand years, and thus several glaciations (Table 8.2). Thus the exogenetic model suggests usually two to six rapid base level lowering episodes in the Pleistocene, with stable base levels in the intervening 10^5 - 10^6 years.

This bears little correlation to the known 100m changes in sea level during the Pleistocene, which has a periodicity of 10^5 years in the Late Pleistocene.

The assumption of exogenetic control is thus challenged. The two recent major books on karst (White, 1988; Ford and Williams, 1989) tacitly acknowledge this by not presenting any detailed examples of correlation between cave tiers and external base level, and White (1988, p85) states that "one of the tasks of cave origin models is to explain why" cave tiers sometimes form.

8.7.2 The endogenetic model

It was shown in Section 8.2 that a single cave tier is responsible for discharging most of the flow from an aquifer for an extended period, in the range $3.10^5 - 10^7$ years. During this time, the flow field developing beneath the conduit will have fixed boundary factors, and will develop according to Equation 7.3.

In a homoclinal aquifer of constant length, then Equation 7.3 could be applied to any generation of flow route. If the base level for the propagation of flow paths for the new conduit is the old conduit rather than the water table at one particular time, then the distance between old and new conduits will be constant, and hence

$$V \propto D_m \quad (8.1)$$

where V is the vertical spacing between successive generations of conduit in an aquifer. This cannot be directly tested, for the argument is circular, as V has been used to define D_m in Table 7.1.

However, the model can be simply tested against the exogenetic model in three ways. Do tiered caves have a constant spacing between tiers as long as aquifer length remains constant (the endogenetic model), or is the spacing random (the exogenetic model)? Are the levels of tiers in separate drainage basins in one area uncorrelated (the endogenetic model), or the same (the exogenetic model)? Are

currently active tiers at various depths below current base level (the endogenetic model), or are they closely related to it (the exogenetic model)?

To test the first question, some examples of spacing between tiers is given in Table 8.1. The regular spacing in almost all examples strongly support the endogenetic model. The one exception in Table 8.1 is the Historic Section of Mammoth Cave. However, the nine tiers are not continuous throughout the cave. The section was taken <1km from the downstream end of the cave, and the passages seem to be part of an underground delta, as has been found with almost all modern drainage routes (Quinlan and Ewers, 1981; also Figure 8.3).

The second test concerns the correlation of tiers between adjacent catchments. Possibly the most studied cave area where regional base levels have been hypothesised is the Yorkshire Dales in England. Sweeting (1950) suggested that there were two main tiers of caves, at 380m and 290-305m, and that these correlated with a widespread erosion surface, and valley erosion surfaces, respectively. With further cave exploration and more careful surveying of caves, the main tiers of caves are now known to be at 250m, 265m and 278m in Lancaster-Easegill (Ashmead, 1974), 220m and 280m on Leck Fell (Waltham and Hatherley, 1983), 260m and 335m in Kingsdale (Brook, 1974; Waltham and Brook, 1980a) and 290m, 310m and 330m at Gaping Gill (Glover, 1974). It appears that each drainage system has its own well-developed tiers, and they do not fit any regional base level. A similar lack of correlation is shown at Mulu (Table 8.1), and in the Mendip Hills, England, where Ford (1965) postulated former water table at 330m, 225m, and 135m in the Cheddar caves, but at 290m at Wookey Hole. The lack of correlation between adjacent catchments supports the endogenetic model.

The third test concerns the relationship of active tiers to base level. Much evidence has only recently become available with the increased popularity of cave diving. The seven kilometres of siphons now explored in the Three Counties System, England were discussed in Section 7.2. Conduit depths below current base level vary

greatly, with a maximum of 64m³ (Waltham and Brook, 1980a; Waltham and Hatherley, 1983; Palmer, 1986). The Doux de Coly (Figure 6.7a) has two kilometres of near-horizontal siphon, currently at a depth of 49-56m. Mammoth System has many kilometres of near-horizontal conduits that were thought to have developed just below a static base level (Palmer, 1981, 1987). However, further research has shown that some of these fossil conduits developed up to 23m below base level (Palmer 1989a), and an active phreatic lift of 17m in bedrock has also been found (Quinlan and Ewers, 1989, p77). These three examples show that active tiers show little correlation with current base level, which supports the endogenetic model. Thus all three tests support the endogenetic model.

The model was recently tested in a Mexican cave, Nelfastla de Nieva. Previous exploration has revealed two tiers, with a vertical separation of 220m between the mean altitude of the two tiers (Worthington, 1989). In 1990 a third tier was found, with a mean altitude 237m below the tier above it (Figure 8.2). This provides strong supporting evidence to the endogenetic model, that the development of cave tiers is a function of original flow net development within the aquifer.

8.8 Hydrochemical characteristics of the flow-field beneath active conduits

8.8.1 Expected hydrochemical characteristics

The flow field beneath an active conduit will be characterised by low-radius proto-conduits (Section 8.5). Flow velocities will be very low, as velocity varies with the fourth power of conduit radius (Equation 5.2). The multiplicity of flow paths, together with the low velocities, ensure high water-rock interaction. If there is pyrite or gypsum present in the rock, this will be leached out preferentially as the equilibrium solubility of sulphate is an order of magnitude higher than that of bicarbonate. Additionally, the deep flow paths should ensure geothermal heating of the water.

A young vauclusian spring (e.g. when the water table is at position 1 in Figure 8.1), may be the discharge point for all the water from the deep flow field. In this case, distinguishing different hydrochemical components may only be possible if high-quality data is available (e.g. Crowsnest Spring; Figures 9.17, 10.4). However, with base-level lowering to position 8 in Figure 8.1, the vauclusian spring may be at some distance from the lowest outcrop point of the aquifer, and some of the discharge from the deep flow field may now rise closer to the lowest outcrop point. This hypothesis that warmer, higher-sulphate springs than the main springs will be found at lower altitude than the main springs may be tested using two data sets. The first data set consists of thermal karstic springs. The second data set comprises spring pairs where both sulphate and bicarbonate were measured.

8.8.2 Thermal karstic springs

Thermal springs occur in two principal hydrogeological environments. They may be associated with vulcanism, in which case the heating of infiltrating meteoric water is easily explained. The second environment is in karst, where the groundwater flow paths are poorly understood. Some thermal karstic springs are found in areas of enhanced geothermal gradients (e.g. Black Hills, USA; Budapest, Hungary; Ford and Williams, 1989), but this is not true for most thermal karstic springs. For instance, it is known that the karstic hot springs in the Rockies are associated with thrust faults, and it has been suggested that flow is from local sources (van Everdingen, 1972). But any transect across the Rockies will cross up to 40 thrusts, suggesting that hot springs might be extremely common, which they are not. In England, there are several thermal springs on the perimeter of the karstic limestones of the Peak District (Edmunds et al., 1969; Edmunds, 1971; Christopher et al., 1977), but none of these papers suggest why this should be so. Only in artesian situations such as the area around Bath, England, does the geological structure

provide a convincing structural mechanism (artesian flow) which would necessitate deep groundwater flow (Edmunds et al., 1969; Atkinson and Smart, 1977).

The hypothesis of a deep flow net below existing conduits would explain the existence of thermal karstic springs in areas of normal geothermal gradients. Five examples of non-artesian thermal karst springs in areas of normal geothermal gradients were found in the literature. They are in the area immediately north of the Canadian Rockies (the Mackenzie Mountains), El Abra (Mexico: described in Section 4.4), Ljubljana (Yugoslavia), Mulu (Malaysia), and the Peak District (England). Do they support the hypothesis of warmer, higher sulphate water emerging downstream of the main spring(s)?

There is a major hot spring which emerges in the alluvium of the South Nahanni River, in the Mackenzie Mountains at 61°N. It is known as Nahanni or Krause Hot Spring, and has a discharge estimated at several hundred litres per second (Schroeder, 1990). Some 10km upstream, there is a large karst spring studied by Brook (1976), and known as White Spray. This spring is located at an altitude of 270m, and had a high-flow discharge of $5\text{m}^3\text{s}^{-1}$, and a temperature of 4.5°C on July 4th, 1973 (Brook, 1976). Krause Hot Springs are located very close to the lowest outcrop point of the karst aquifer on the South Nahanni River, at an altitude of 230m. Moreover, they are at the lowest outcrop point of this aquifer in the Mackenzie Mountains, the next lowest being at 350m on Mountain River at 65°N and at 380m on Keele River at 64°N. This suggests that Krause Hot Springs drain a regional aquifer some hundreds of kilometres in length.

The Ljubljana karst springs were described in Section 4.3. In addition to the springs described, there is Ljubljana Thermal Spring (#1.46). The discharge of this spring is evidently minor, for it was not monitored during the tracer tests of Gospodarić and Habić (1976). The Thermal Spring is the lowest of all the springs at Ljubljana, and appears to be close to the lowest outcrop point of the limestone. The low tritium values in 1974 indicated that some 98.5% of the water pre-dated

atmospheric nuclear tests. The low deuterium (-62‰) suggested a high-altitude source remote from the spring (20-50km: Moser et al., 1976). These authors gave no temperature details, but application of Equation 7.3 suggests a flow depth of at least some hundreds of metres.

The Hot Water Spring at Mulu is in a small inlier of the karstic Melinau Limestone (Laverty, 1980). The inlier is the lowest outcrop of limestone along the Melinau River (Rose, 1982). The main springs are several kilometres upstream, where many kilometres of spectacular caves have been explored (Brook and Waltham, 1978; Eavis, 1981, 1985). The Hot Water Spring is sulphidic, with hardness values much greater than any other karst waters at Mulu (Ca^{2+} 213 mg l⁻¹, Mg^{2+} 50 mg l⁻¹: Laverty, 1980). The position of the spring, and its high temperature and high dissolved solids suggests this spring too has a deep flow path as in Figure 8.1. For a strike-oriented flow path of 35km from the furthest surface exposure of limestone, and a dip 30°-70° (Webb, 1982), Equation 7.3 gives $D_m = 300\text{-}500\text{m}$.

The limestone of the Peak District, England is an inlier 37km in length and up to 21km in width. Thermal springs occur on the eastern, western, and northern margins of the dome. The heat flux (F) derived from geothermal heat may be calculated by

$$F = Q (T_h - T_c) \quad (7.2)$$

where T_h is the water temperature of the thermal water, and T_c is the water temperature of normal groundwaters of the area. An average spring temperature value from 73 non-thermal karst sites in the Peak District (Christopher et al., 1977, p202) gives $T_c = 7.7^\circ\text{C}$. This reveals that 96% of the thermal water emanates from the limestone in the neighbourhood of Matlock (Table 8.5). This is the lowest outcrop point of the limestone in the Peak District. It is not possible to apply Equation 7.3 in this case, for it is not possible to predict how much of the fracture control of flow would be on the several near-vertical often-mineralised faults, and how

**Table 8.5 Heat fluxes of thermal springs in the Peak District, England
(data from Edmunds, 1971)**

Thermal centre	source	T °C	Q l s ⁻¹	Heat flux* J s ⁻¹
Buxton	St Anne's Well	27.5	10.6	880
Bradwell	Bradwell Spring	12.4	0.7	14
Stoney Middleton	Stoney Middleton Spring	17.7	1.3	54
	Stoke Sough	11.6	1.3	21
Bakewell	British Legion	11.6	9.3	150
Matlock	Fountain Bath	19.7	11.8	590
	New Bath Hotel	19.8	6.3	320
	East Bank of Derwent	17.4	0.5	20
	Ball Eye Quarry Borehole	13.6	1.5	30
Beresford Dale	Meerbrook Sough	15.3	790	25,000
	spring	13.8	1.7	43
	Lower Dimindale	11.5	4.2	67

* from Equation 8.2; $T_c = 7.7^\circ\text{C}$

much would be on low-dip bedding planes. The thermal springs have high sulphate concentrations (Table 6.4). Low tritium values (<10TU) measured in 1968-1969 showed that most, if not all, of the spring water at Buxton, Bradwell, Stoney Middleton, Bakewell and Matlock (New Bath Hotel) had flow-through times of at least 15-20 years (Edmunds, 1971). This indicates mean velocities of $<10^4\text{ms}^{-1}$ over a 37km catchment length, which indicates non-phreatic flow.

Thus the evidence from non-artesian thermal karst springs in the North West Territory, Mexico, Yugoslavia, Malaysia and England support the hypothesis of warm, high sulphate springs occurring close to the lowest outcrop points of karst aquifers. All these thermal springs drain extensive aquifers, with putative flow paths of tens to hundreds of kilometres. Where the water chemistry has been measured, the thermal waters have high sulphate values, and high sulphate/bicarbonate ratios. Equation 7.3 would indicate deep flow paths in each case sufficient to cause geothermal heating, and Figure 8.1 suggests these are non-phreatic underflows associated with proto-conduit development.

8.8.3 Sulphate / bicarbonate ratios

Six data sets were located in the literature, where pairs of springs were monitored for both sulphate and bicarbonate. The results are shown in Table 8.6, and they support the hypothesis. Additionally, it was found that higher sulphate/bicarbonate ratio spring in five of six cases had lower discharge variability.

8.8.4 Implications of high sulphate values in the deep flow net

Cations are more commonly measured in water samples than anions because of the greater ease of measurement, and it is usually logically assumed that in a karst water the source of calcium would be CaCO_3 , as this is the dominant mineral in limestone outcrops. Analyses of karst waters for anions from a number of areas were found in the literature, and these are presented in Table 6.3. They show

Table 8.6 Contrasts between high and low sulphate/bicarbonate ratios and high and low temperature springs

Name of higher SO ₄ /HCO ₃ spring	Name of lower SO ₄ /HCO ₃ spring	Attributes of higher SO ₄ /HCO ₃ spring		
		Lower Altitude	Lower Q _s /Q _a	Higher Temperature
Crowsnest Spring	Ptolemy Spring	Yes	Yes	Yes
Grotte du Pisseoir	G. du Cormoran	Yes	Yes	N.R.
Source de Baume Rascasse	two springs	N.R.	Yes	N.R.
Source de Poussarou	Source de Malibert	Yes	No	N.R.
Emergence du Vivier	Emergence du Pont	N.R.	Yes	Yes
Pluto Spring	Orangeville Rise	N.R.	Yes	N.R.

Name of higher temperature spring	Name of lower temperature spring	Attributes of higher temperature spring		
		Lower Altitude	Lower Q _s /Q _a	Higher SO ₄ /HCO ₃
Krause Hot Spring	White Spray	Yes	N.R.	N.R.
Ljubljanica thermal sp.	(1)	Yes	N.R.	N.R.
Mulu Hot Spring	Gua Air Jernih	Yes	N.R.	Yes
Meerbrook Sough	(2)	Yes	N.R.	Yes
Coy spring	Agua Clara	Yes	Yes	Yes
Mante spring	Santa Clara	Yes	Yes	Yes

Note: data sources and spring locations are given in Sections 4.3, 4.4, and 8.8.2, and in Table 6.5

N.R. = not recorded

(1) There are 15 higher altitude springs on the Ljubljanica River

(2) There are several major springs in the White Peak. All are at higher altitudes and have lower temperatures, and almost all have lower sulphate/bicarbonate ratios than Meerbrook Sough

that sulphate concentrations are a significant proportion of bicarbonate concentrations, indicating that commonly 5-30% of the host rock being dissolved is not limestone.

Three possibilities come to mind to explain the high sulphate values in general in karst springs, and in the Rocky Mountains in particular.

- 1) Anhydrite makes up 10-30% of the stratal thickness in the karst succession. Non-phreatic circulation preferentially removes the soluble anhydrite, totally removing thick anhydrite beds. In outcrop, there may be no indication that 10-30% of the succession has been removed, except by comparison with the stratal thickness and succession in well logs.
- 2) The high sulphate values measured in karst springs represents preferential removal of this sulphur due to rejuvenation thanks to the work of Pleistocene glaciers. Thus the pre-glacial concentration of sulphate in karst springs and regional rivers would have been much lower. Sulphate is derived from pyrite or anhydrite disseminated in the bedrock, or from anhydrite concentrated along bedding planes, in concentrations up to a few percent. Solution of these is partly responsible for producing the porosity observed in the limestone (Murray, 1960). For instance, it is possible that Crowsnest Pass was created by a glacier that lowered base level by >1km. There would also be additional sulphur from shales (e.g. Exshaw Shale at Crowsnest Pass), from fertilisers (Langmuir, 1971), and deposition from the atmosphere (Krothe and Libra, 1983).
- 3) The high sulphate values measured in karst springs represent the removal of sulphur not only from the outcrop area of limestones, but also from the extensive subcrops of these strata. Migration of sulphur would be down the hydraulic gradient as a solute, but could be up-gradient as a gas (H_2S). In the Rocky Mountains, deep groundwater flow in carbonates is demonstrated by the existence of hot springs. These have high sulphate concentrations, and concentrations of several parts per million H_2S have also been found (Table 6.3, van Everdingen, 1972). There are also high H_2S concentrations (up to >90% of the gas phase) in Devonian and Mississippian

carbonates in the petroleum reservoirs of the Rocky Mountain Foothills. These are interpreted to have formed by thermochemical reduction of aqueous sulphate by hydrocarbons at temperatures $>90^{\circ}\text{C}$ (Krouse et al., 1988). The presence of several mg l^{-1} of H_2S in thermal springs in the Rockies (van Evergingen, 1972) suggests that H_2S may be of some importance in the Rockies both for cave formation and for providing a sulphate source.

The westward-dipping thrust plates of the Rocky Mountains have extensive subcrops, which extend to depths of $>5\text{km}$ (Price and Fermor, 1985). Hydrogen sulphide from thermochemically reduced sulphate from this subcrop might migrate updip, reacting in an oxidizing environment to produce sulphuric acid and subsequently sulphate (Palmer, 1989; Ball and Jones, 1990). However, it seems probable that this might be of only minor importance in providing a sulphate source.

The second hypothesis has been generally invoked on individual cases, but does not satisfactorily explain the widespread high values of sulphate in karst spring waters, so the first and third hypotheses may have some validity.

High sulphate/bicarbonate ratios are present in Crowsnest Spring and Sublacustrine Springs in winter. Here, they are associated with low spring altitude, low Q_s/Q_n , and higher temperatures (in Crowsnest Spring, at least). The same correlations are found in thermal springs in the Rockies and elsewhere (Section 8.8.3), and also in non-thermal karst springs, though sulphate is rarely measured in karst springs, so the data set is not large (Tables 6.4, 8.6).

These associations suggests that deep-circulating karstic waters preferentially remove the sulphur (from gypsum and/or pyrite), and indicates that sulphuric acid speleogenesis may be as common or more common than carbonic acid speleogenesis in the early stages of cave formation. Such a mechanism has recently been proposed by Ball and Jones (1990), who suggested that cave passages in South Wales are preferentially developed in impure sulphidic limestones.

8.9 Conclusions

This chapter demonstrated that there is strong supporting evidence for the nine hypotheses upon which Figure 8.1 is based. The explanations for tier spacing and for the location of thermal and high-sulphate karstic springs are radical, yet follow from the precepts of the model, and provide further support for it. The model provides a comprehensive description of how and where in an aquifer karst conduits are formed, and a comprehensive model that is able to predict much of the discharge, chemical and temperature variations found in karst springs.

Chapter 9 Catchment delineation of the springs at Crowsnest Pass

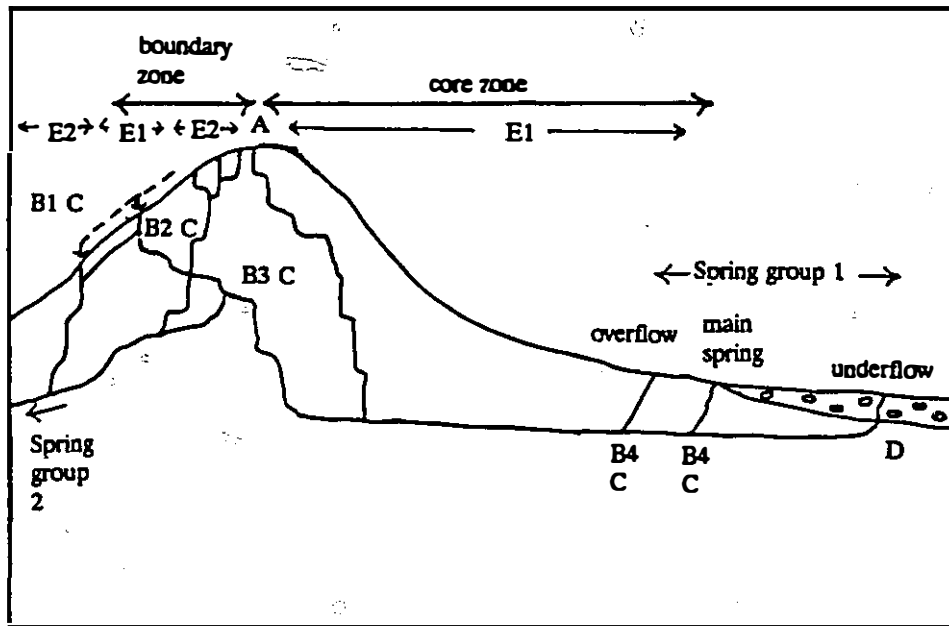
9.1 Problems of catchment delineation in karst

9.1.1 Introduction

Catchment delineation is usually the first step in any hydrological study. Delineation normally relies on the notion that discrete catchments with definable, perennial boundaries may be identified. This assumption has often been made in karst studies, but there is strong evidence that it is unwarranted. There are five distinct problems encountered in catchment delineation in karst. They are shown in Figure 9.1, and will be discussed in the next five sections.

9.1.2 Groundwater boundaries do not coincide with topographic boundaries

It was explained in Section 5.2.4 that hydraulic gradients in karst are not a subdued reflection of the ground surface, as is usually the case in Darcy-flow aquifers. There is thus no reason why karst groundwater boundaries should follow topographic divides in a holokarst (Figure 9.1: A). The lack of correlation has been shown by many tracer studies, including the present study, where dye tracing showed that karst groundwater crosses the topographic continental divide (Figure 3.2). The precise delineation of groundwater divides requires extensive water tracing or cave exploration. For instance, in Central Kentucky, >500 traces were used to supplement data from 1400 water wells and >700km of cave passage to define catchments and flow paths in an area of 2000km² (Quinlan and Ray, 1981; Quinlan and Ewers, 1981, 1989).



- A Groundwater boundaries do not coincide with surface catchment boundaries
- B Distributary flow feeds different springs
- B1 Surface creek sinking at different locations
- B2 Distributary flow in subcutaneous zone
- B3 Distributary conduits
- B4 Underground delta
- C Flow route varies with stage
- D Unmonitored underflow spring
- E1,E2 Non-contiguous components of catchments E1 and E2

Figure 9.1 Problems of catchment delineation in karst

9.1.3 Flows may branch to two or more springs

Branching may occur by underflow from a surface river or glacier (e.g. Trebišnjica River: Section 4.3; Saskatchewan Glacier: Smart, 1983a,b), by lateral spreading in the subcutaneous zone (e.g. Mendip Hills: Friederich and Smart, 1981), in the main part of the aquifer, or close to the springs (Figure 9.1: B1-B4, respectively). The latter two cases have been particularly well demonstrated by Quinlan and Ewers (1989). Discharge from the Three Springs Basin ($\approx 100\text{km}^2$) bifurcates into two flow routes at a point about 10km from the resurgences. Much closer to the springs there is an underground delta, so that the water discharges at 52 springs (Figure 8.3a). In the Rockies, distributary flow has been demonstrated at Castleguard (≈ 80 springs: Smart and Ford, 1986) and at Maligne (>60 springs: Brown, 1970; Kruse, 1980; Smart, 1988a; Ford, 1991).

9.1.4 Flow route may vary with stage

The varying of flow route with stage is normally the addition of overflow routes at high stage (Figure 9.1: C). The bifurcation may occur on input to the aquifer, such as the baseflow of Hills Creek (West Virginia, USA) flowing 17km to the south-west to Spring Creek, while flood overflows are routed to Locust Spring, 2km east of the sinkpoints (Coward, 1975; Williams and Jones, 1983). The bifurcation may also occur within the aquifer, and many examples of flood overflow conduits are known. At the output end of the aquifer, the six Emerald Cliff overflow springs provide a notable example (Section 2.2.2).

9.1.5 There may be unmonitored underflows

Unmonitored underflows may constitute the majority of discharge from a karst aquifer (Figure 9.1: D). In Section 4.2, such a situation was described in the White Peak (England), White Ridges (B.C.), and Dorvan (France). The Rocky

Mountains also have substantial unmonitored underflows (see Chapter 10 and 11). In Ontario, there are notable unmonitored underflow springs in the Lake St Clair delta (Pugsley, 1986) and Georgian Bay (Buck, 1990).

9.1.6 A catchment may have non-contiguous components

The crossing of flow paths in the vadose zone is common and well-documented, and usually operates on a scale of tens to hundreds of metres (Section 5.2.4). In these circumstances, stream catchments will have non-contiguous components (Figure 9.1: E). On a larger scale, Mangin (1975) showed that the Fontestorbes catchment (Ariège, France) had two components, separated by a tongue of overlying impermeable strata >2km wide.

9.1.7 Conclusion: do springs have definable catchments?

In the light of all these distinctive characteristics of karst groundwater flow, it is pertinent to ask whether karst springs have definable catchments. The evidence from dye tracing would suggest that the answer is a qualified yes.

It seems clear from the analysis in Chapter 4 that a karst catchment should be defined at the output end in terms of the spring group rather than the individual spring. A spring group may be loosely defined as a series of springs in geographical proximity which have a common catchment area. Such a group will have underflow and overflow members, and tracer injections will often be recovered at more than one spring in the group. Underflow members of a spring group are likely to have higher solute concentrations and higher temperatures than overflow members because of nonthe phreatic flow. The Ljubljanica Springs (Section 4.3) and the 46 springs of Bear Wallow Basin (Figure 8.3a) are both well-researched examples of spring groups. The hydrogeology of such aquifers can only be understood by studying the spring group, rather than individual springs.

At the input end, Smart (1976) advocated defining catchment boundaries as the point where tracer injected would be shared evenly between adjacent catchments. Such tracing needs to be carried out at the highest and the lowest discharges, and the catchment boundaries weighted by discharge.

At a large scale, it would seem to be unlikely that one karst catchment could be distinguished by a simple perennial boundary from adjacent catchments. Instead, it may be better to think in terms of catchments having core and boundary zones. A *core zone* is the area which drains to a single spring group. A *boundary zone* is an area which drains to more than one spring group.

The width of a boundary zone is a function primarily of the depth of the vadose zone. From observations of vadose flow routes in Yorkshire Pot (Figure 5.3) and elsewhere, it may be surmised that the width of the boundary zone averages about half the depth of the vadose zone.

9.2 Catchment area model for Crowsnest Pass

9.2.1 Model design and validation

Due to the limited possibilities in using tracers to delimit catchment size (Section 3.3.2), a discharge budget model was developed to estimate specific runoff. As Crowsnest Pass occupies the lowest elevation incision into the karst aquifers in the Flathead and High Rock Ranges, there is the possibility for springs there to drain the limestones of the whole of the Flathead and High Rock Ranges (Section 3.3.2). However, initial discharge budget calculations suggested that the northern limit of drainage to the springs at Crowsnest Pass is some 20km to 50km.

The data used in the discharge model comprise the discharge data collected by the Inland Waters Directorate for the period September 1985 to August 1986 for nine gauged catchments, four of them in B.C. and five of them in Alberta (Figure 9.2). The data sets from the subcatchments of Kilmarnock Creek, Upper Fording River, Line Creek, Crowsnest River (at Crowsnest Lake) and the springs

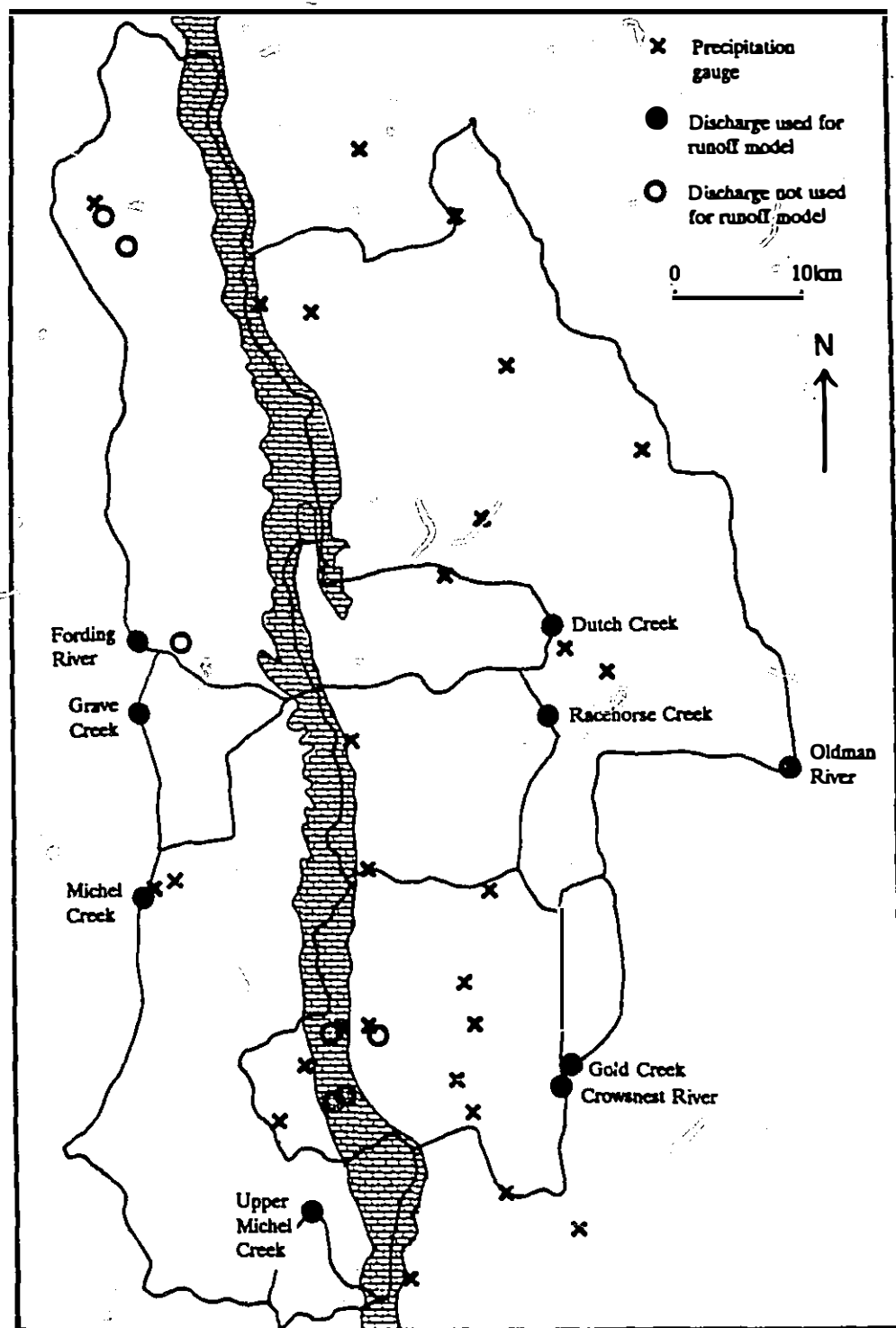


Figure 9.2 Catchments and precipitation gauge locations used for development of the runoff model

gauged during the study were rejected, as the high fraction of karst in these catchments meant there was likely to be a low correlation between the topographic and real catchment areas. Also, Castle River was rejected as the discharge was anomalously high (reflecting the anomalously high precipitation noted by Curry and Mann (1965): see below). Discharge data from Squaw Creek (draining the western flank of the southern Flathead Range) would have been pertinent, but the only data available are from a gauge on the Flathead River at the U.S. border, far to the south.

Five of the nine catchments used have complete records for 1985-1986; the four remaining gauges (Racehorse Creek, Dutch Creek, Upper Michel Creek, Gold Creek) have no records for 4 to 5½ months over the winter (October/November to March/April). Discharge data for the missing months were estimated by extrapolating from existing data and by comparing with gauged sites during the appropriate months. For these four sites the missing data were estimated to represent only 11% on average of the annual discharge, so an error in estimation of 20% would only affect the annual discharge by 2%.

The centroid and mean altitude of the nine basins were regressed against basin discharge, which gave

$$Q = 0.810A - 5.99E - 4.27N - 132 \quad (r^2=0.914) \quad (9.1)$$

where Q is discharge in mm per unit area, A is altitude in metres, and E and N are eastings and northings respectively, in kilometres from an origin 100.3km grid south of, and 70.4km grid west of Crowsnest Spring. Model data and results are shown in Table 9.1.

The trend surface expressed in Equation 9.1 indicates a reduction in runoff to the east and to the north, together with a strong altitude effect. These results were checked independently by means of precipitation data from the 25 stations in and immediate surrounding the nine catchments (Figure 9.2). The stations vary in altitude from 1128m to 2256m. In the Sixties there were 21 Sacramento storage

Table 9.1 Runoff model catchments and results

Catchment	Area km ²	Mean Altitude m	Discharge		
			gauged ls ⁻¹	mm	model mm
Crowsnest River	285	1705	2830	313	323
Gold Creek	63.6	1785	639	317	326
Racehorse Creek	221	1842	2990	426	386
Dutch Creek	156	1867	1698	343	379
Oldman River	1080	1859	9140	267	256
Upper Michel Creek	36.1	1868	680	595	622
Lower Michel Creek	592	1785	10700	568	509
Grave Creek	81.3	1776	1070	415	439
Fording River	608	1881	7900	410	418

gauges in the area, but this number now has been reduced to nine. To maximise areal coverage, the earlier data were used when no data were available for 1985-1986 (Dept of Transport, 1970). Corrections to precipitation data were made to allow for a 16% underrecording of Sacramento gauges, as found by Curry and Mann (1965) in a study of the same area. Further corrections were made to allow for differences between 1985-86 and 1967-1969, using the 15 gauges that were operating during both periods; the mean difference was 3%. Curry and Mann (1965) found the area from the Castle River catchment southwards was distinctly wetter than further north, so this area was excluded from the calculations as it is only of peripheral interest to this study.

Regression of the precipitation data gave

$$P = 0.673A - 3.60E - 4.59N + 525 \quad (n=25, r^2=0.65) \quad (9.2)$$

where P is the precipitation in mm. This result confirms the trend surface found in Equation 9.1.

The difference between Equation 9.1 and 9.2 is evapotranspiration (E), which by subtraction is

$$E = -0.14A + 2.4E - 0.32N + 660 \quad (9.3)$$

It was observed during field work that cloud cover was greater at altitude, and greater further west, and Equation 9.3 confirms this, though the accuracy of this residual calculation is not high. However, the altitude component does correspond fairly closely to the value of $-0.19A$ derived from the Thornthwaite equation.

9.2.2 Model use

The discharge model was used to estimate runoff from 27 catchments for which some discharge data were available. These catchments were subdivided into non-karst and karst fractions, and the karst fractions were further divided between eleven topographic blocks (Table 2.2). This gave a total of 72 subcatchments (Figure 9.3). Hypsometric curves were prepared for each subcatchment; and model discharge derived from Equation 9.2.

Results for 16 catchments with measured discharge are shown in Figure 9.4. Confidence limits of 20% are shown, and ten catchments lie within these limits. This suggests that the true catchments in ten cases are close in size to the topographic catchments.

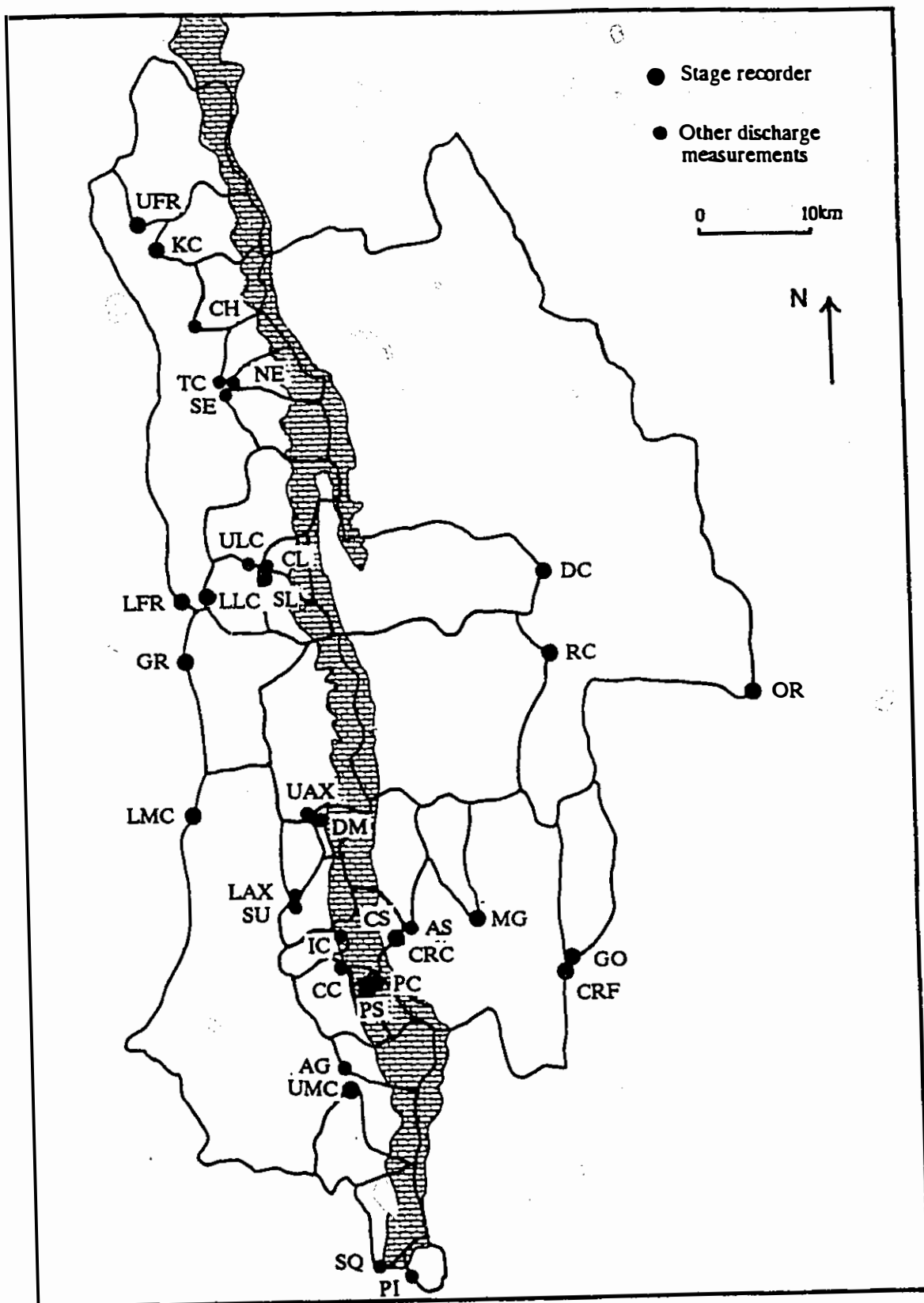
Three catchments have a model discharge more than 20% greater than the measured discharge, but each catchment has a substantial limestone area, and the data suggest that the hydrological catchment is much smaller than the topographic catchment in these cases.

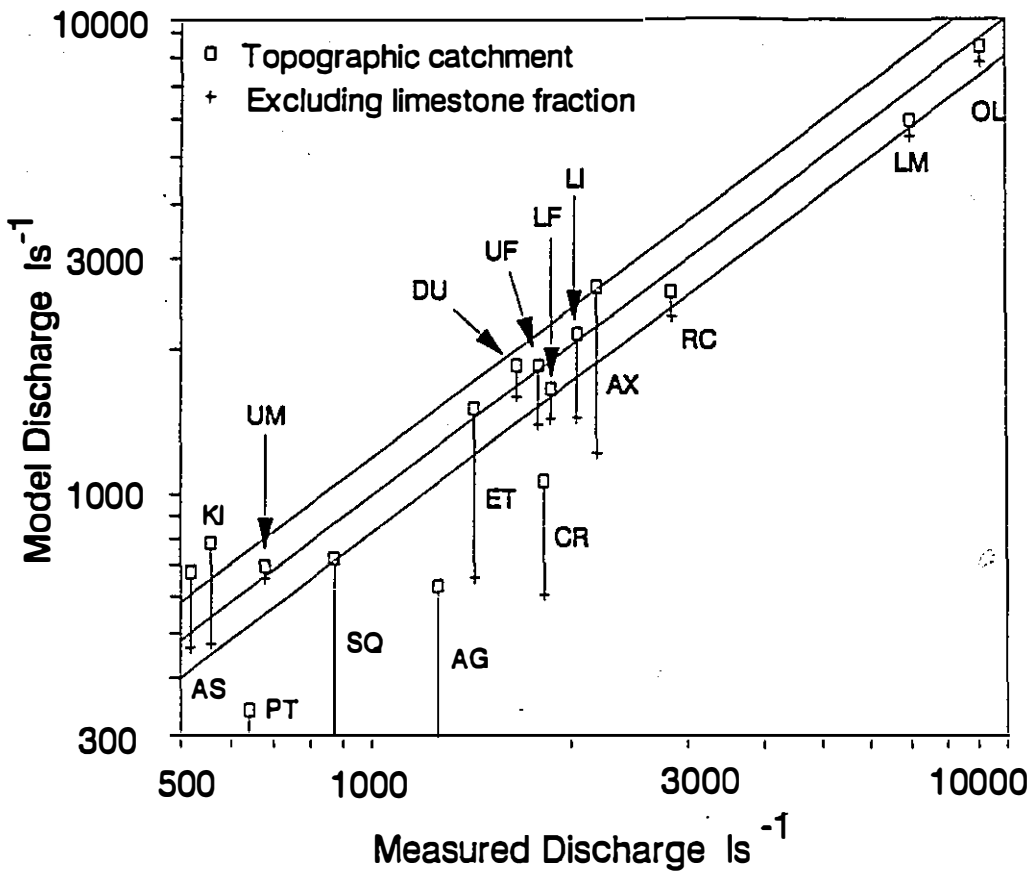
Figure 9.3 Subcatchments used with the runoff model**● Continuous discharge measurement (stage recorder)**

UFR	Upper Fording River	KC	Kilmarnock Creek
LFR	Lower Fording River	LLC	Lower Line Creek
GR	Grave Creek	LMC	Lower Michel Creek
UMC	Upper Michel Creek	PS	Ptolemy Spring
PC	Ptolemy Creek	DC	Dutch Creek
RC	Racehorse Creek	MG	McGillivray Creek
GO	Gold Creek	OR	Oldman River
CRF	Crowsnest River at Frank		
CRC	Crowsnest River at the outlet of Crowsnest Lake		

• Occasional discharge measurement

CH	Chauncey Creek	TC	Todhunter Creek
NE	North Ewin Creek	SE	South Ewin Creek
ULC	Upper Line Creek	CL	Line Creek Centre Fork
SL	Line Creek South Fork	UAX	Upper Alexander Creek
DM	Deadman Creek	LAX	Lower Alexander Creek
SU	Summit Creek	IC	Island Creek
CC	Crowsnest Creek	AG	Andy Good Creek
SQ	Squaw Creek	PI	Pincher Creek
AS	Allison Creek		





- AS Allison Creek
- KI Kilmarnock Creek
- PT Ptolemy Creek
- UM Upper Michel Creek
- SQ Squaw Creek
- AG Andy Good Creek
- ET Ewin and Todhunter Creeks
- UF Upper Fording Creek
- LF Lower Fording Creek
- LI Line Creek
- AX Alexander Creek
- RC Racehorse Creek
- CR Crowsnest River (at Crowsnest Lake, excluding Ptolemy Ck)
- DU Dutch Creek
- OL Oldman River
- LM Lower Michel Creek

Figure 9.8 Model discharge for topographic catchments

The remaining three catchments shown in Figure 9.4 have a measured discharge more than 20% greater than the model discharge. This fulfils expectations for Ptolemy Creek and Crowsnest River, as substantial karst springs were gauged in these catchments. The model also predicts substantial a large hydrological catchment for Andy Good Creek. The karst springs of this creek have yet to be located. Thus the catchment areas implied by the discharge model correspond in each case with observations and measurements.

Using the above model surpluses and deficits, together with geological structure (Section 2.1.2), other measured discharges (Section 3.2) and the tracer results (Section 3.3.2), the karst catchment areas of the Flathead and High Rock Ranges were redistributed to optimise the fit to measured discharge. A conservative approach was used, minimising transfers between blocks. The only inter-block transfer incorporated in the model was from Allison Block southwards to Crowsnest Pass.

The results are shown in Table 9.2 and Figure 9.5. The model discharge from Darrah Block is somewhat low (resulting in deficits for Squaw Creek, Andy Good Creek, Upper Michel Creek, and particularly for Lower Michel Creek). It was noted in Section 9.2.2 that the precipitation, and hence discharge, in the adjoining Castle River catchment (in Alberta) is anomalously high with respect to the discharge model, and the lack of calibration data in the Squaw Creek catchment in B.C. means that Darrah Block discharge is poorly defined. Thus it seems probable that the high precipitation in the Castle River catchment is reflected by high precipitation on the west side of the divide too.

North of Racehorse Pass, a deficit was found in the large Oldman River catchment, which has a large fraction of its catchment in the marginal Foothills, and in the Racehorse Creek catchment, where higher than model precipitation values would account for the difference. Otherwise, surpluses are found in most catchments. The surpluses (totalling 500ls^{-1}) could be accounted for by transfer southwards

Table 9.2 Areas of karst catchments draining the Flathead and High Rock Ranges

Catchment	Topographic Area		Measured	Model	Model Area km²
	Total km²	Non-Karst km²	Q ls⁻¹	Q ls⁻¹	
Catchments south of Racehorse Pass					
Squaw Creek	33.7	11.3	874	819	36.5
Andy Good Creek	31.1	9.9	1270	1170	50.1
Upper Michel Creek	36.1	34.6	680	711	34.6
Lower Michel Creek	390	373	7110	5700	373
Ptolemy Creek	19.8	0.1	642	608	29.3
Crowsnest River (at Crowsnest Lake outlet, excluding Ptolemy Creek)					
	83.9	56.1	1880	1850	129
Deadman Creek	14.5	1.3	192	192	10.8
Alexander Creek (excluding Deadman Creek)					
	156	89.1	2090	2080	129
Allison Creek	50.3	39.6	520	513	41.1
Catchments north of Racehorse Pass					
Line Creek	133	99.4	2120	2370	140
Ewin Creek and Todhunter Creek					
	82.6	47.3	1450	1680	89.2
Kilmarnock Creek	43.2	30.8	560	592	35.0
L. Fording River	244	234	1930	1930	254
U. Fording River	106	84.8	1840	1880	106
Racehorse Creek	221	209	2990	2600	216
Dutch Creek	156	146	1700	1720	150
Oldman River	1080	1050	9140	8440	1060

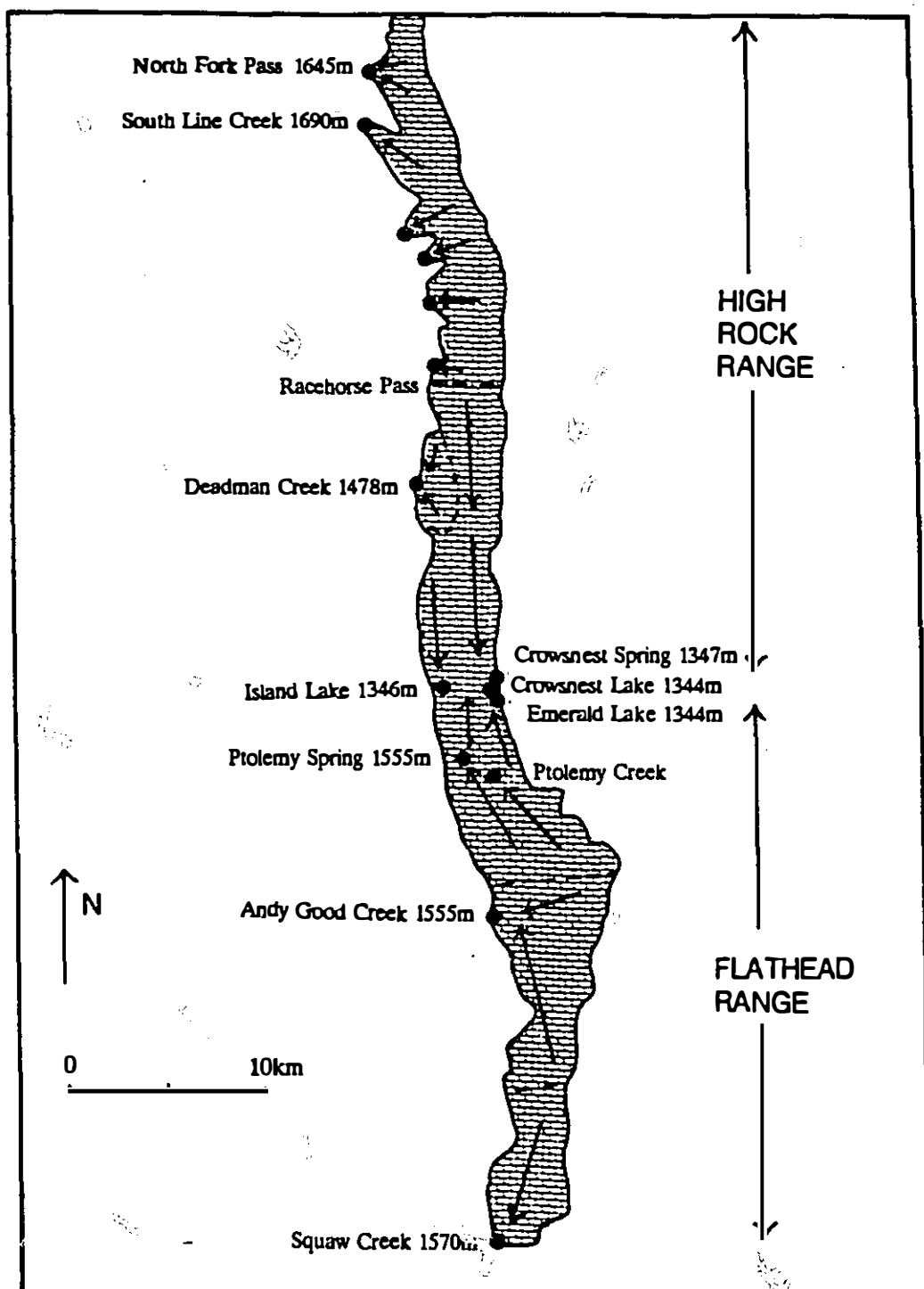


Figure 9.5 Mean catchments in the karst of the Flathead and southern High Rock Range, derived from the runoff model. The major groundwater flow vectors are shown. In winter, there is an underflow to Crowsnest Pass from all of the karst outcrop shown (as in Figure 2.2). During the snowmelt season, there is considerable surface runoff from the karst.

towards Crowsnest Pass, but this assumption is not justified from these data alone, as the surplus lies within the error margin of the results.

An excellent fit could be made between model and gauged discharge from the Ptolemy, Phillipps and Allison Blocks (discharge to Ptolemy Creek, Crowsnest River, Deadman Creek, Alexander Creek and Allison Creek). However this required substantial inter-catchment transfers to be postulated, some of which has been proven by tracer tests.

The principal finding of the model is that 84% of the drainage from Ptolemy, Phillipps and Allison Blocks is to Crowsnest Pass. Ptolemy Creek has a hydrological catchment almost 10km² bigger than its topographic catchment; much of this extra area was confirmed by tracer tests to Ptolemy Spring. The catchment gain for Crowsnest Spring and Sublacustrine Springs is 44km²; tracer tests only partially defined the Crowsnest Spring catchment, and no testing was attempted to Sublacustrine Springs.

Also of importance in helping to define the karst catchments at Crowsnest Pass are the peripheral karst catchments to the south and north. To the south, Darrah Block is drained almost exclusively by Andy Good Creek and Squaw Creek. To the north of Racehorse Pass, there are several spring-fed creeks, of which the most important are at Line Creek and Ewin Creek. The results show that there is a net transfer from scarp slope to dip slope catchments, and from high areas to deeply incised valleys such as Crowsnest Pass and Andy Good Creek. The model results for the Crowsnest Pass springs will be used in the next section, where seasonal differences in infiltration patterns are examined.

9.3 Underflow and overflow regimes

9.3.1 Underflow and overflow in surface creeks

Underflow, full-flow and overflow springs were introduced in Chapter 4.

It was shown that many karst spring hydrographs could be explained in these terms,

rather than in terms of aquifer differences. Examples of these three flow situations in the field area are shown in Figure 9.6.

Kilmarnock Creek and Upper Fording River have adjacent catchments on the western flank of the High Rock Range to the north of Crowsnest Pass (Figure 9.1). The two catchments have similar hypsometric curves (mean altitudes: Kilmarnock Creek 2150m, Upper Fording River 2130m), and similar proportions of limestone (Kilmarnock Creek 27%, Upper Fording River 18%). However, much of the discharge from the limestone fraction of the Kilmarnock Creek catchment is lost to groundwater, so that Q_u/Q_g over the gauged six summer months of 1986 is more than double that of Upper Fording River, which has a full flow regime. By contrast, Q_u/Q_g for Crowsnest River, which has a substantial underflow contribution from karst springs, is much lower than Upper Fording River.

The best fit between the discharge values of Kilmarnock Creek and Upper Fording River is achieved (Figure 9.7a) if the groundwater loss from Kilmarnock Creek is assumed to be

$$q_u = 0.095 + 0.4 Q \quad (9.4)$$

where q_u is the underflow loss from Kilmarnock Creek to groundwater and Q is the gauged discharge from Kilmarnock Creek. This gives a mean underflow loss from Kilmarnock Creek of $0.53\text{m}^3\text{s}^{-1}$ for the summer period. Underflow losses are estimated to be almost one third of the total runoff (Figure 9.7b).

Similar responses are seen in other karst catchments in the field area, and there are many small catchments with no surface runoff except during the snowmelt peak (Section 2.2). All surface creeks flowing on karst in the Flathead and High Rock Ranges can be defined as seasonal overflows in their upper reaches (Figure 4.1 - type 2).

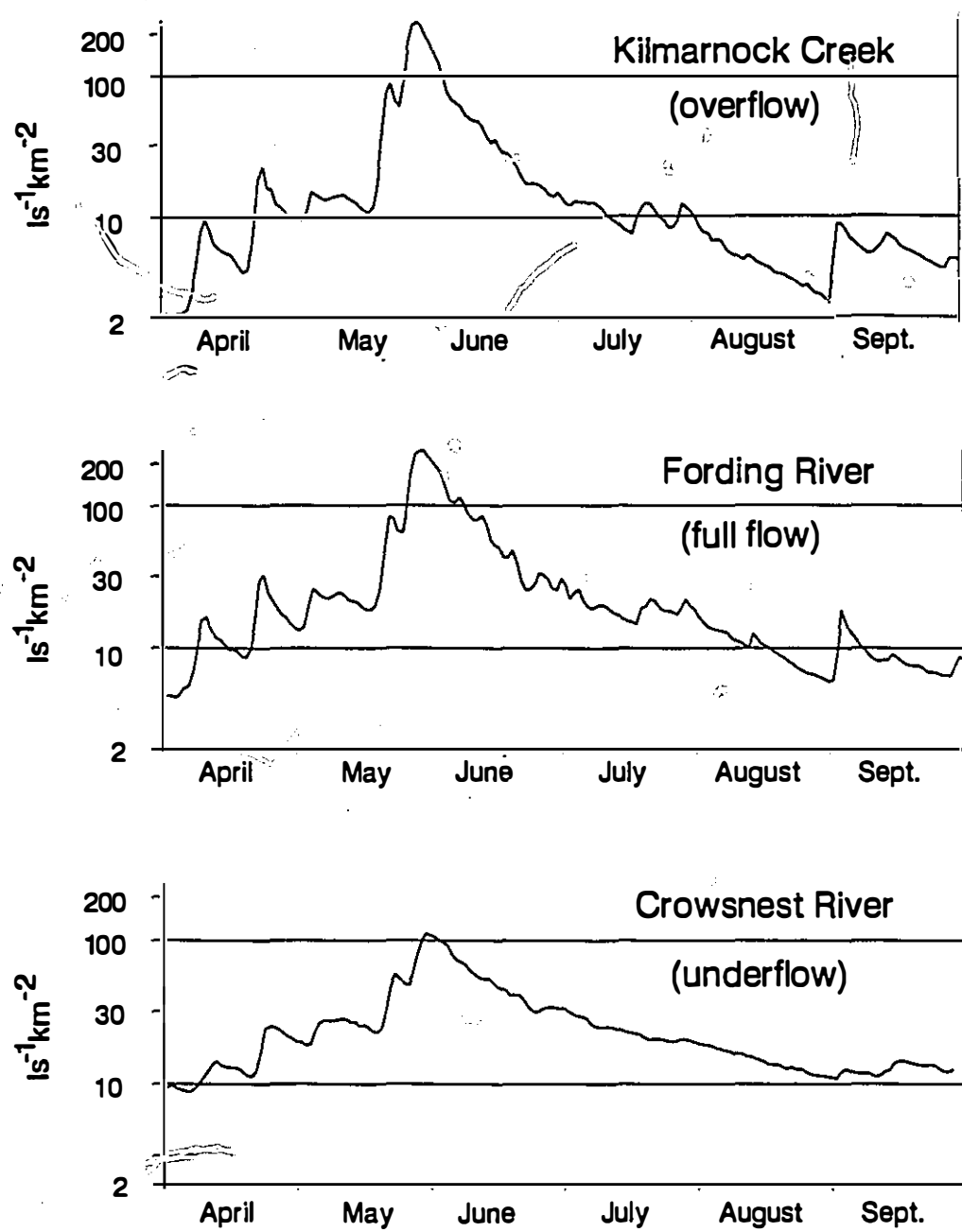
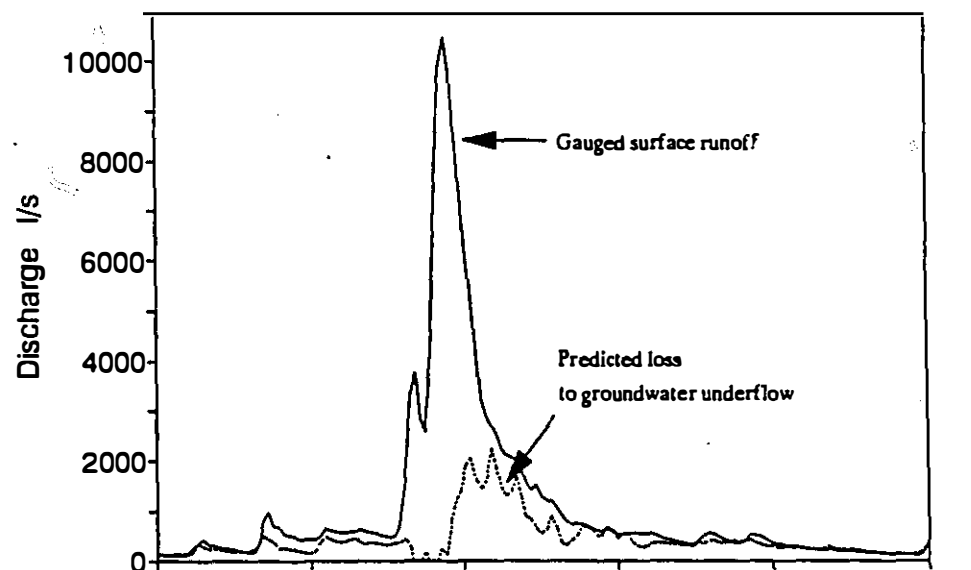
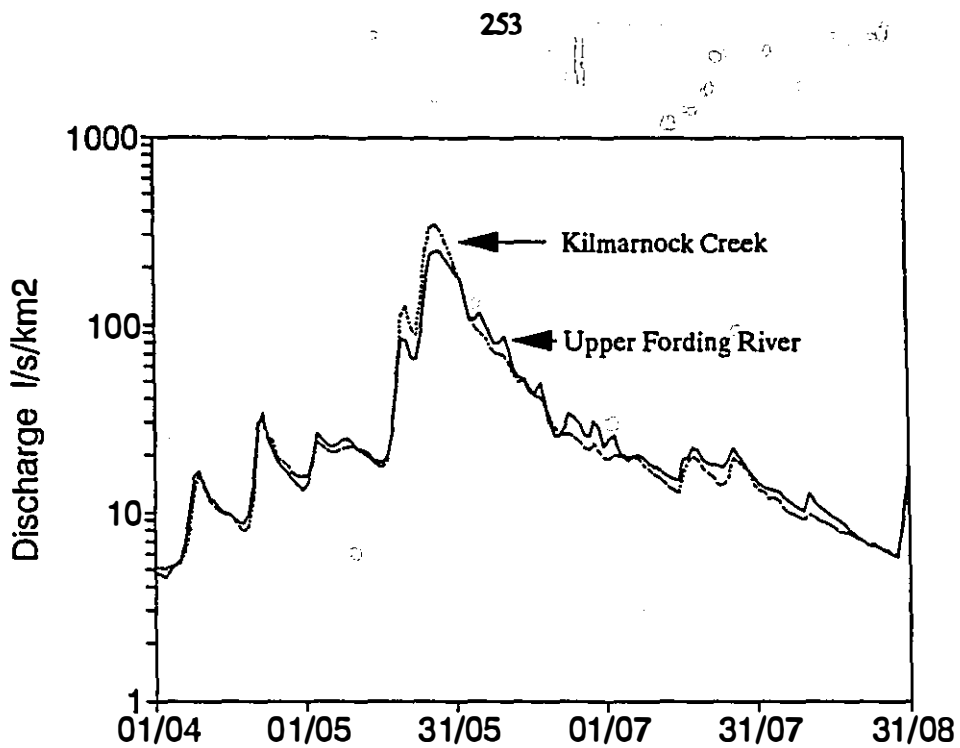


Figure 9.6. Examples of overflow (Kilmarnock Creek), full flow (Upper Fording River) and underflow (Crowsnest River) regimes in the Front Ranges



9.3.2 Overflow springs

There are a large number of overflow springs at Crowsnest Pass. These include not only all high-altitude springs, but also springs as little as a few metres above base level (Table 3.4). When monitored for short-term periods, the overflow nature of these springs may not be apparent. For instance, Figure 9.8 shows the very similar responses of Parrish Spring and Ptolemy Spring to precipitation events in August 1985. The overflow nature of Parrish Spring is only revealed by the fact that it dries up for at least seven months. A second example is Ptolemy Creek, which is fed by Parrish Spring, Ptolemy East Cirque Lake Spring, and other karst springs in addition to surface runoff. In summer, the regime is similar to Ptolemy Spring (Figures 3.8 and 9.9), but in winter all high-level springs cease flowing, and the discharge of $10\text{--}20\text{ l s}^{-1}$ emanates from alluvium in the valley bottom in the lower part of the catchment, below 1505m (Table 3.3).

The complementary underflow to these overflow springs must be accounted for, and this component can be found in the regimes of Crowsnest Spring (Section 9.3.4) and Sublacustrine Springs (Section 9.3.5).

9.3.3 Ptolemy Spring: a full-flow regime

It would be expected that the underflow losses from surface creeks in the Flathead and High Rock Ranges would be complemented by gains in catchments such as Andy Good Creek and Crowsnest River (Table 9.2). Underflow springs were characterised in Chapter 4 by low Q_x/Q_n , perennial flow, a low proportion of quickflow, and by low values for α .

Daily discharge data for Ptolemy Spring and Crowsnest Spring are shown in Figure 9.10. Monthly discharge data for Sublacustrine Springs (with Crowsnest Spring and Ptolemy Spring for comparison) are shown in Figure 3.5; separation of quickflow from baseflow is not possible using monthly data.

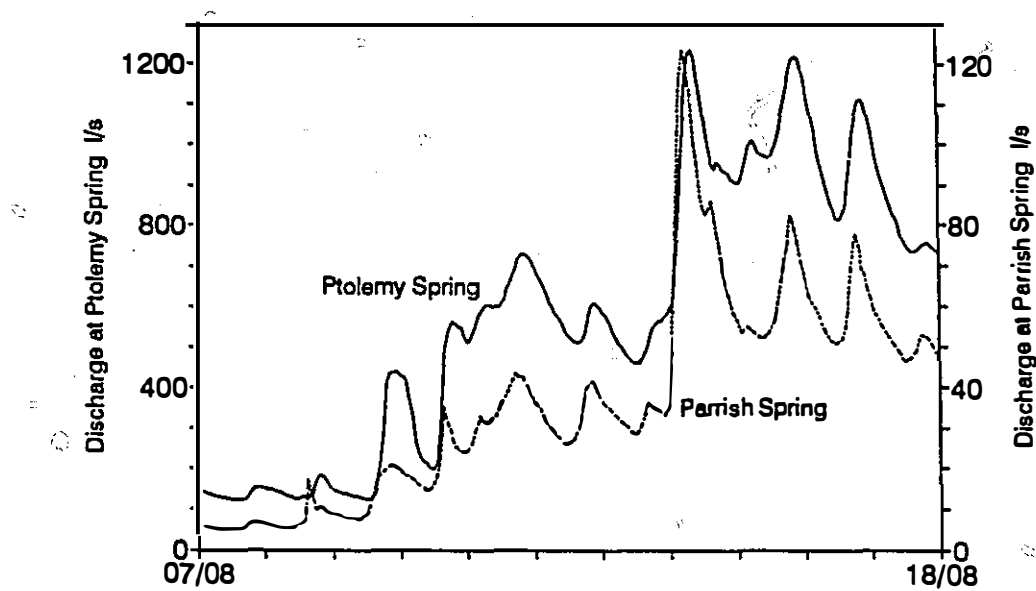


Figure 9.8 Discharge at Ptolemy Spring and Parrish Spring during August 1986, showing the greater variability at Parrish Spring

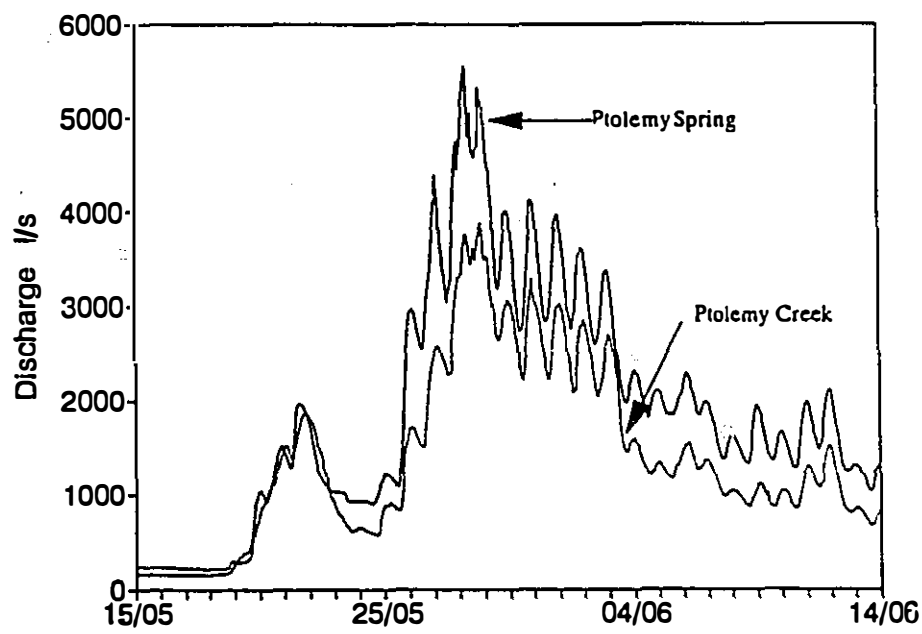


Figure 9.9 Instantaneous discharge of Ptolemy Creek and Ptolemy Spring during the snowmelt peak in 1986

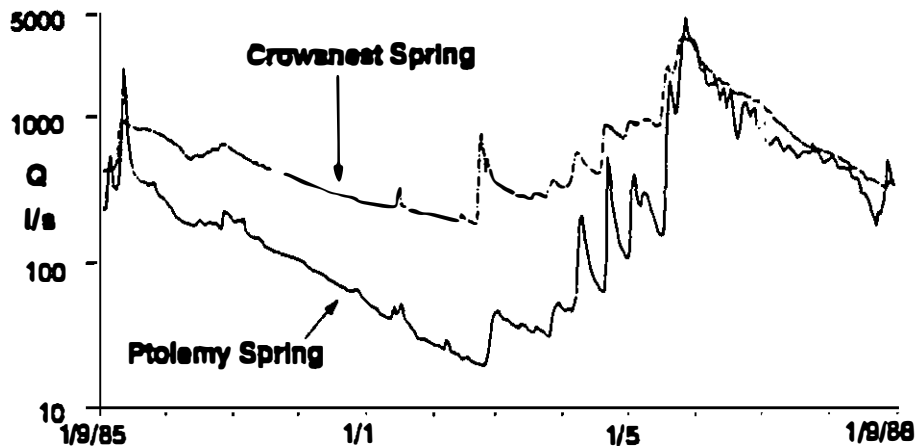


Figure 9.10 Discharge of Ptolemy Spring and Crowsnest Spring from September 1985 to September 1986, showing contrasts in exponential recessions

There is a marked contrast between the behaviour of Ptolemy Spring on the one hand and Crowsnest Spring and Sublacustrine Springs on the other hand (Table 9.3). Ptolemy Spring has a regime similar to those of the surrounding surface creeks with catchments of similar size and altitude, with quickflow contributing a substantial proportion (24%) to discharge. On the other hand, Crowsnest Spring and Sublacustrine Springs have underflow regimes.

Table 9.3 Discharge characteristics of the principal springs at Crowsnest Pass

Spring	Q_u	Q_x/Q_m	Perennial	Quickflow
Ptolemy Spring	390	280	Yes	24%
Crowsnest Spring	670	21	Yes	5.3%
Sublacustrine Springs	890	17	Yes	≈5-7%

The catchment of Ptolemy Spring, based on dye tests and discharge calculations, is shown in Figure 9.5. Of the calculated 18.6km^2 catchment, some 10km^2 is holokarstic, never having any surface runoff. Of the fluviokarst fraction, over half lies within the Ptolemy Creek topographic catchment, and so surface overflow would augment Ptolemy Creek, which would then have a greater discharge variation than Ptolemy Spring. This would be similar to the contrasting responses of Kilmarnock Creek and Upper Fording River (Figures 9.6 and 9.7).

The discharges of Ptolemy Creek and Ptolemy Spring at the time of maximum runoff in 1986 are presented in Figure 9.9. The response of Ptolemy Spring is greater than that of Ptolemy Creek at the snowmelt discharge peak, indicating no significant loss to underflow to Ptolemy Creek at high stages.

The exponential recession of Ptolemy Spring in winter (Figure 9.7) suggests that there is no significant loss to underflow at low stages. Thus at a first approximation, Ptolemy Spring may be considered a full-flow spring.

9.3.4 Crowsnest Spring: an underflow regime

Identification as an underflow regime

Q_s/Q_n of Crowsnest Spring is an order of magnitude less than that of Ptolemy Spring, quickflow is much less important (Table 9.3), and α diminishes markedly during baseflow (Figure 9.7). All these factors indicate that Crowsnest Spring has a major underflow component (see Section 4.2). The magnitude of that component may be assessed by comparison with Ptolemy Spring.

Two conditions need to be fulfilled to make this comparison. First, differences in spring response should be due to boundary rather than aquifer conditions. Tracer tests showed that flow velocity in the main conduits of the two catchments is similar (Figure 3.6), and the similar lithology, structure, relief and geological history suggest that the aquifers should be similar. The second condition

is that Ptolemy Spring should be a full-flow spring. This was demonstrated in the previous section.

The underflow character of Crowsnest Spring may be demonstrated by analyzing the discharge response to major rain and snowmelt events. The recession indices for all major discharge peaks at Crowsnest Spring and Ptolemy Spring were calculated. A major peak was defined as a maximum satisfying two criteria; first, the continuous rise from the previous minimum to the peak be greater than 50%; second, there be a continuous recession following the peak of at least 24 hours. Because of these limitations, diurnal snowmelt peaks were eliminated, but eleven events at each spring satisfied these criteria. At Ptolemy Spring (Figure 9.11, top), the eleven events fitted the relationship

$$\alpha = 0.0681 Q^{0.64} \quad (n=11, r^2=0.77) \quad (9.5)$$

where Q_s and Q_{s+1} represent peak discharge and the discharge one day later respectively. At Crowsnest Spring (Figure 9.11, bottom), the recessions are much more varied, but three seasonal arrays are apparent

January - February	$\alpha = 0.39 - 0.80$
April - June	$\alpha = 0.049 - 0.13$
September - October	$\alpha = 0.013 - 0.014$

Such striking seasonal differences at Crowsnest Spring, not reflected in any significant seasonal variation at Ptolemy Spring, can hardly be explained by differences in catchment altitude (Ptolemy Spring 1610m to 2814m; Crowsnest Spring 1350m to 2644m). Furthermore, there is no firm evidence to support the hypothesis that these contrasts are due to aquifer differences (Section 3.6). However, they can be explained by surface overflow from the Crowsnest Spring catchment.

The winter floods at Crowsnest Spring are characterised by recessions that are somewhat more rapid than the general annual trend at Ptolemy Spring. Winter

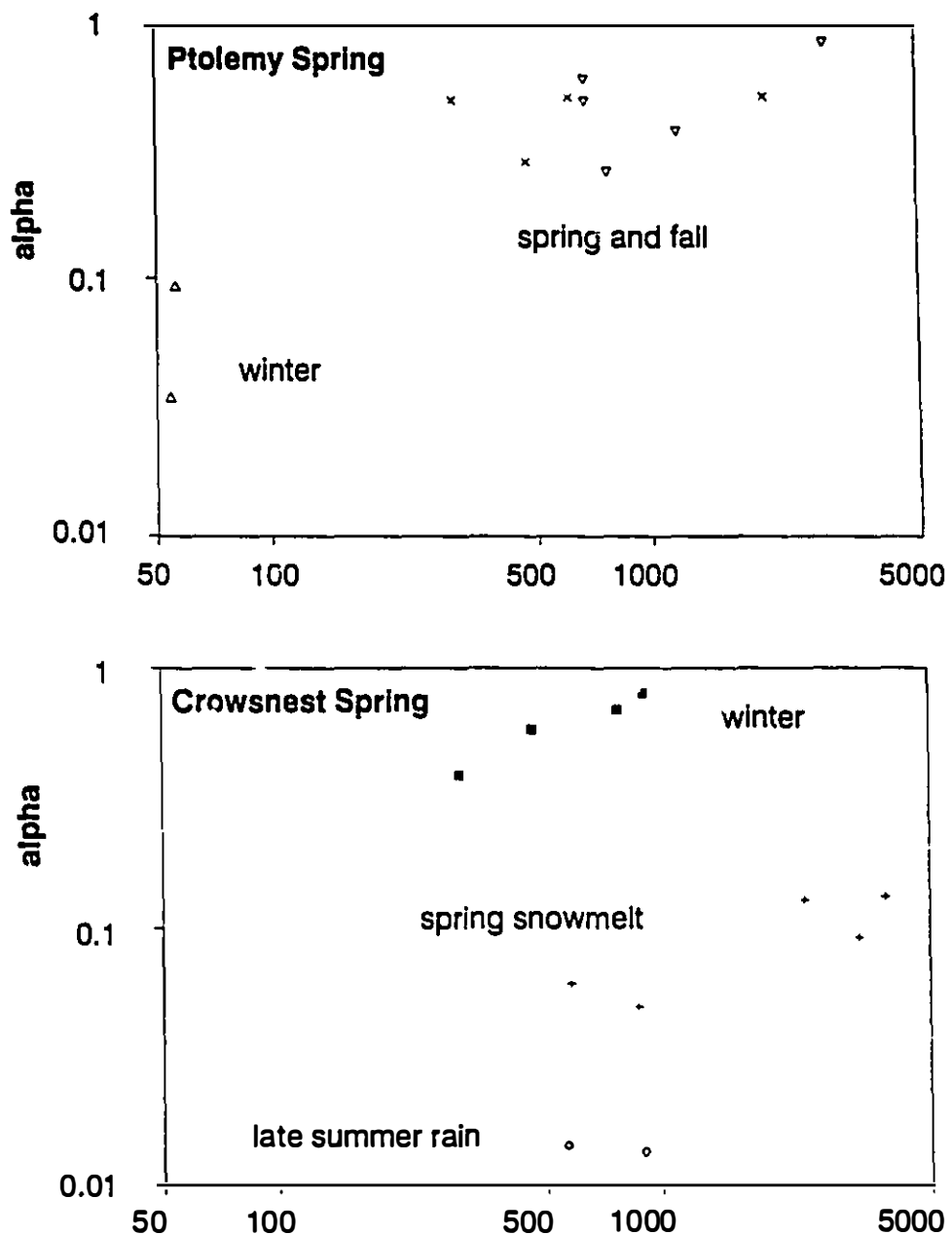


Figure 9.11 Recession coefficients for first 24 hours after major flow peaks at Ptolemy Spring and Crowsnest Spring

discharge peaks at these springs are shown in Figure 9.12, together with daily precipitation and temperature minima and maxima recorded at Sentinel, 4km east of Crowsnest Spring. The two greatest runoff peaks are associated with rain-on-snow events. Such events are highly altitude-dependent, owing to the higher cold content of the snowpack and deeper snowpack at altitude, and to precipitation falling as snow there rather than rain. The result is that there will be substantial runoff at low altitude (rain plus melted snowpack), but above a critical altitude there will be no runoff (snowpack not ripened). This is apparent from the spring runoff. The two events cause rises of 140 l s^{-1} and 660 l s^{-1} , respectively, at Crowsnest Spring (altitude 1350m), but of only 9 l s^{-1} and 28 l s^{-1} , respectively, at Ptolemy Spring (altitude 1610m) (note the order of magnitude difference in the discharge scales in Figure 9.12). From these data it is concluded that there was insignificant runoff above 1600m. The runoff to Crowsnest Spring would have been from the low altitude proximal part of the catchment, principally from Crowsnest Ridge and Phillipps Pass. Surface runoff from Crowsnest Ridge and Phillipps Pass is very rare, so the rapid recessions are due to full flow from a small portion of the Crowsnest Spring catchment. The major spring snowmelt recessions are seven times less rapid than the winter recessions (Figure 9.11) at Crowsnest Spring. This fits the hypothesis of surface overflow, which should be at a maximum during high runoff. The hypothesis is confirmed by the substantial surface overflow observed at this time leaving the limestones of the Phillipps and Allison Blocks and the well-developed stream beds.

The late summer rain or rain on snow events (Figure 9.11) have extremely gradual recessions. These were not observed, but may possibly be due to intense precipitation events overflowing down surface streambeds, or to an unripe snowpack causing delayed infiltration. Alternatively, they may be an indication of flow or storage differences between the two aquifers.

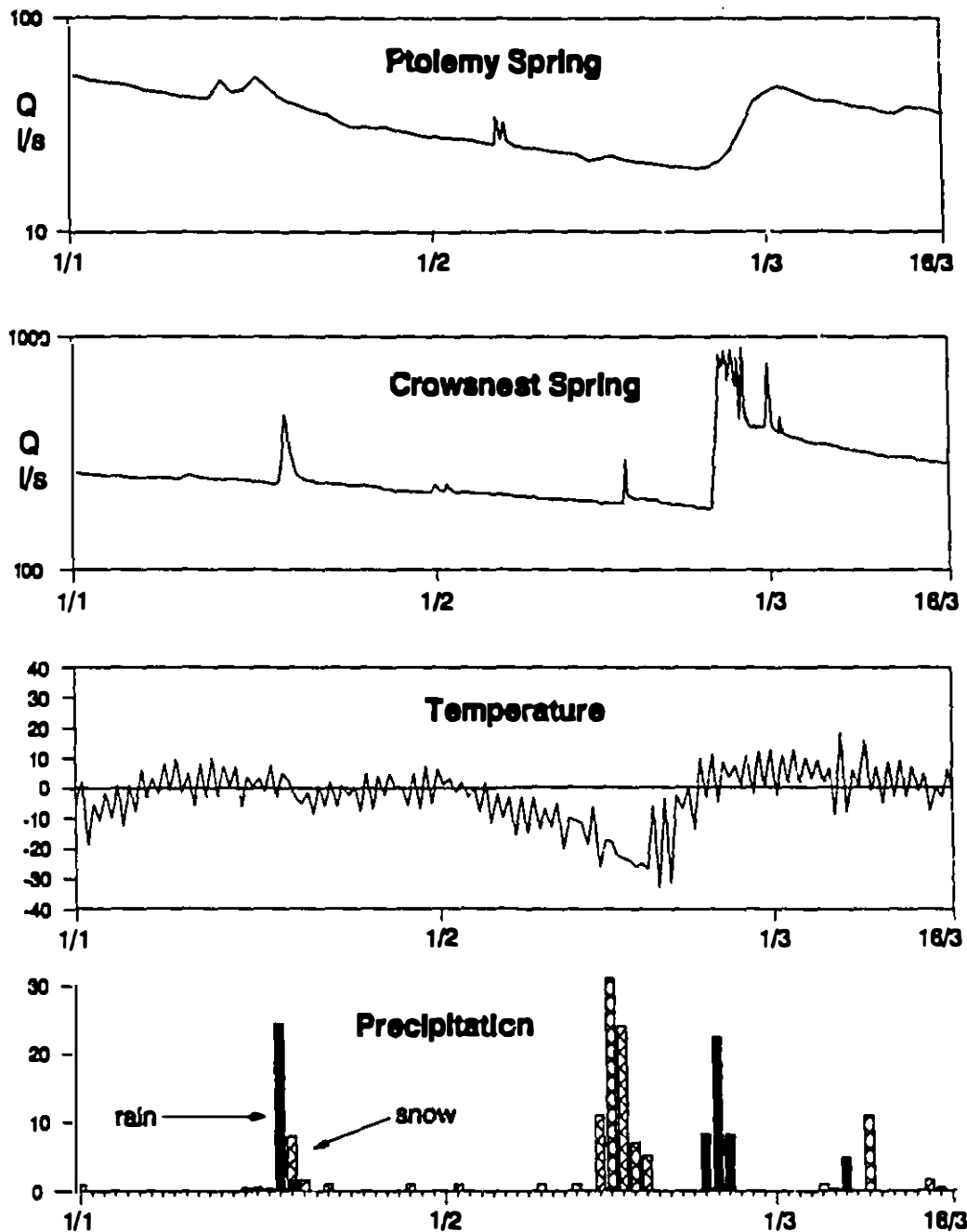


Figure 9.12 Response of Ptolemy Spring and Crowsnest Spring to precipitation events and temperature changes, January - March 1986

Quantification of the underflow component

None of the surface overflow creeks in the Phillipps or Allison Blocks were gauged. It would be a formidable task to gauge the overflow, as there are a multitude of creeks draining the limestone, each with a different overflow regime, with some only flowing for a brief period on May 28th, 1986, the peak runoff day. An alternative, simpler, method is to assume the specific runoff for the Crowsnest Spring catchment is similar to the Ptolemy Spring catchment, which was shown above to exhibit full flow characteristics. This should be broadly true, as the catchments are of similar altitude, exposure and geology, and velocities in the conduits leading to both springs are almost identical (Figure 3.6).

The simplest way to model the regime of underflow is to approximate it to a constant discharge (Drake, 1974), so the underflow fraction will be greatest, and most easily identified, at low stages. Accordingly, a constant discharge component was subtracted from the discharge data of Crowsnest Spring, and the residual was regressed against the Ptolemy Spring data, using the 150 day period from September 27, 1985 (after the last major runoff peak) to February 27, 1986 (the end of the winter recession). The result was

$$Q_C = 2.18 Q_P + 150 \quad (\text{ls}^{-1}) \quad (r^2=0.98) \quad (9.6)$$

where Q_C and Q_P are the discharges at Crowsnest Spring and Ptolemy Spring, respectively.

Using the estimated catchment area of 18.6 km² for Ptolemy Spring, the catchment for Crowsnest Spring is 41 km², with the addition of the area contributing to the 150 ls⁻¹ underflow (Figure 9.13). This underflow component can be equated with the lower flow path (proto-conduit C) in Figure 8.1. This contention is supported by the fact that Crowsnest Spring is close to the lowest outcrop point of the aquifer, has a thermal component (Section 9.4.2), has a high sulphate to bicarbonate ratio (Sections 7.6.3, 9.3), and a low discharge variation (Sections 7.6.3,

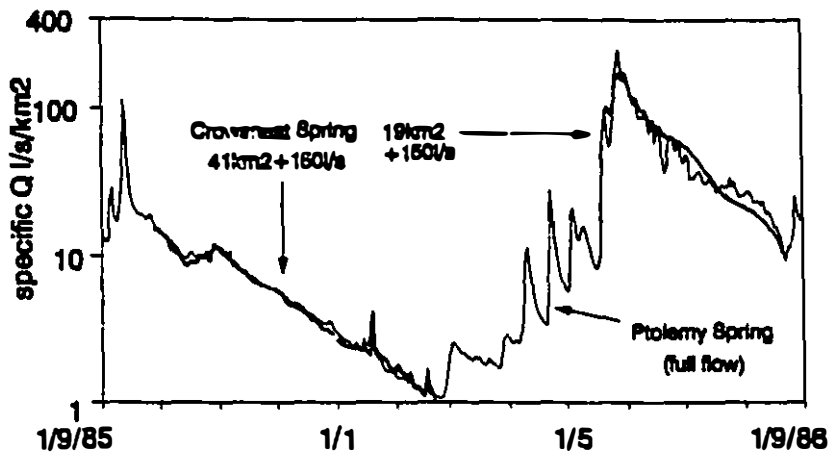


Figure 9.13 Specific discharge from Ptolemy Spring and Crowsnest Spring during the winter and summer recessions, assuming differences to be due to aquifer boundary conditions

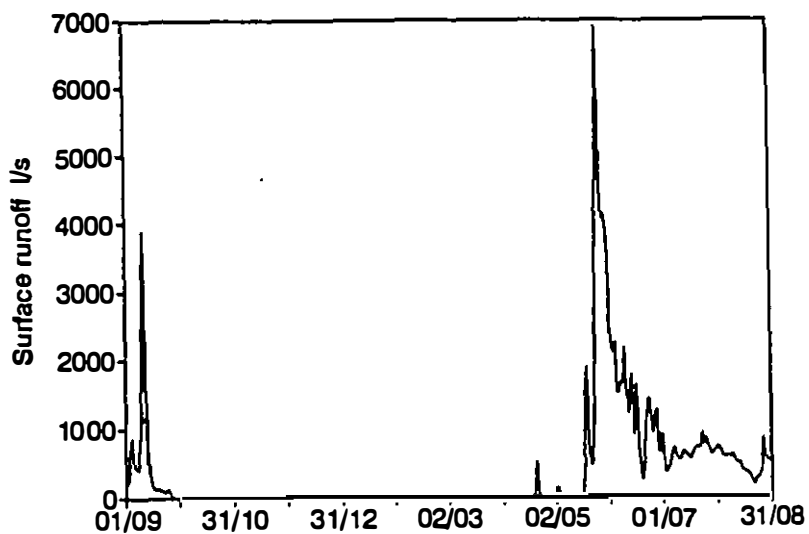


Figure 9.14 Predicted surface overflow runoff in 1985-1986 from a 41 km^2 Crowsnest Spring catchment assuming identical specific discharge to Ptolemy Spring

9.3, Table 9.1). Using the calculated 41 km^2 catchment for Crowsnest Spring, the surface overflow during high stages (Figure 9.14), and the area drained by Crowsnest Spring (Figure 9.15) at any time can be estimated.

Four contrasting responses can be distinguished in Figure 9.15. The winter recession indicates 41 km^2 , as discussed above. Following this is an 81 day period in which a greater drainage area is indicated (February 28 - May 19); this is due to the advanced snowmelt season at Crowsnest Spring due to its lower altitude than Ptolemy Spring. The mean surplus of 134 l s^{-1} must be allowed for in the succeeding snowmelt peak and recession (May 20 to August 29), which suggests a mean catchment of 19 km^2 during this period (Figure 9.15). The fourth period is from late August to the end of September, when the contrasting responses of the two springs to rain-on-snow events is reflected in the greatly varying area indicated in Figure 9.15. The poor fit obtained in the May to September period (Figure 9.11) partly reflects the inadequacy of daily discharge data at springs which respond in only hours to melt or precipitation events, when Crowsnest Spring lags Ptolemy Spring by several hours. It may also be partly due to aquifer differences.

The observed surface runoff at high stages, the seasonably variable recession indices, and the success in modelling discharge in winter as a two-component system all support the contention that the regime of Crowsnest Spring has a strong underflow component. The modelling suggests that the contributing area to conduit flow at the spring varies from 19 km^2 in summer to 41 km^2 in winter, with an additional underflow component of 150 l s^{-1} .

9.3.5 Sublacustrine Springs: an underflow regime

The hydrochemistry and rapid response to runoff of Sublacustrine Springs suggest that these are karstic springs similar in nature to Crowsnest Spring (Section 10.1), and the analysis of the catchment size will be made in the same way as for Crowsnest Spring.

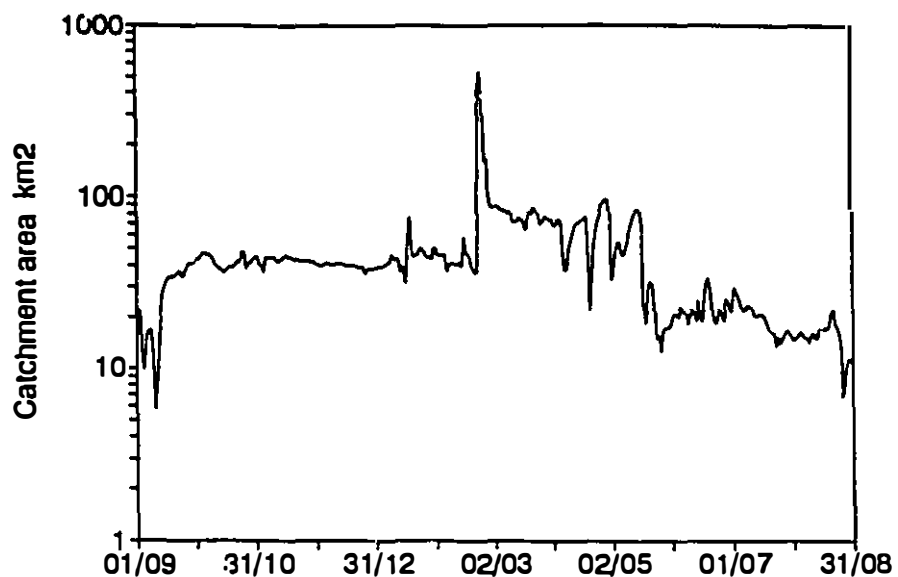


Figure 9.15 Calculated catchment area for Crowsnest Spring, assuming identical specific discharge to Ptolemy Spring

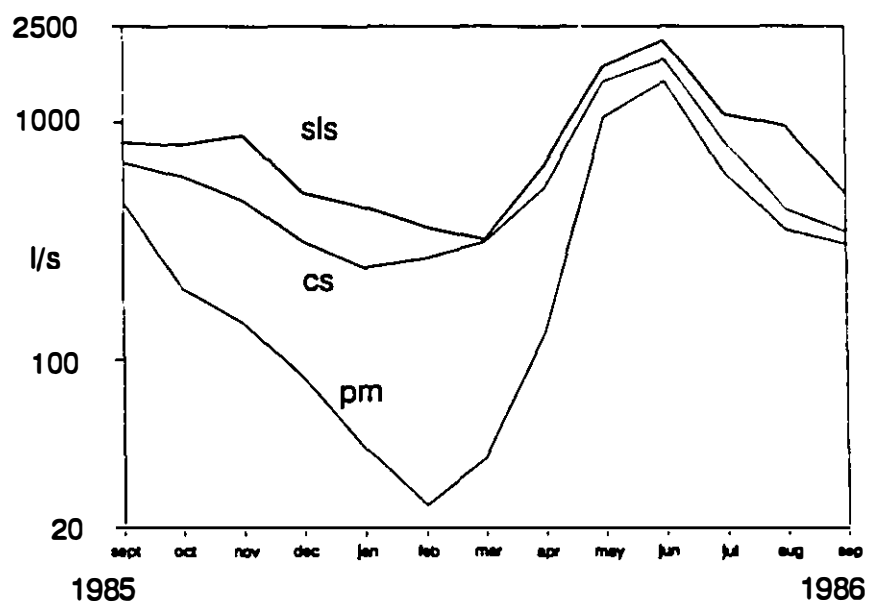


Figure 9.16 Mean monthly discharge for Sublacustrine Springs, Crowsnest Spring and Ptolemy Spring

As only monthly discharges are available for the whole year (Figure 9.16), it first needs to be established whether this data set is sufficiently detailed to allow catchment calculations. A simple test is to use the monthly averages from Crowsnest Spring, and compare to the results obtained using daily averages. The specific discharge and catchment of Crowsnest Spring, calculated in the previous section (summer 19km², winter 41km²) are shown in Figure 9.15. High correlation for both the four winter months of October to January ($r^2=0.99$) and the four summer months of May to August ($r^2=0.98$) justify the approach of using monthly data to calculate catchment areas.

The best fit ($r^2=0.96$) when regressing the four winter months of November to February at Sublacustrine Springs against Ptolemy Spring gives a constant (underflow) component of 330ls⁻¹. However, the winter recession of Sublacustrine Springs continues through March, and this month can be used additionally in extrapolation of an exponential recession (Figure 9.17). This gives an upper constraint on the underflow component of 260ls⁻¹ and a catchment area of 73km² ($r^2=0.94$). For summer, the five months from May to September give an area of 25km² ($r^2=0.94$).

The above calculations suggest that Sublacustrine Springs, grouped together, have a similar flow regime to Crowsnest Spring, with considerable losses to surface overflow in summer and a substantial underflow component.

9.4 Catchment altitude

There are altitude effects associated with many hydrological parameters, which can be used for helping to define catchments. Possibly the four most useful which can be monitored at a spring are freezing and thawing effects, differences in limestone solute concentrations and spring temperature, and isotopic differences. Of course, tracer tests and cave exploration provide irrefutable evidence of flow routes between specific points. However, these techniques are only sufficient to adequately

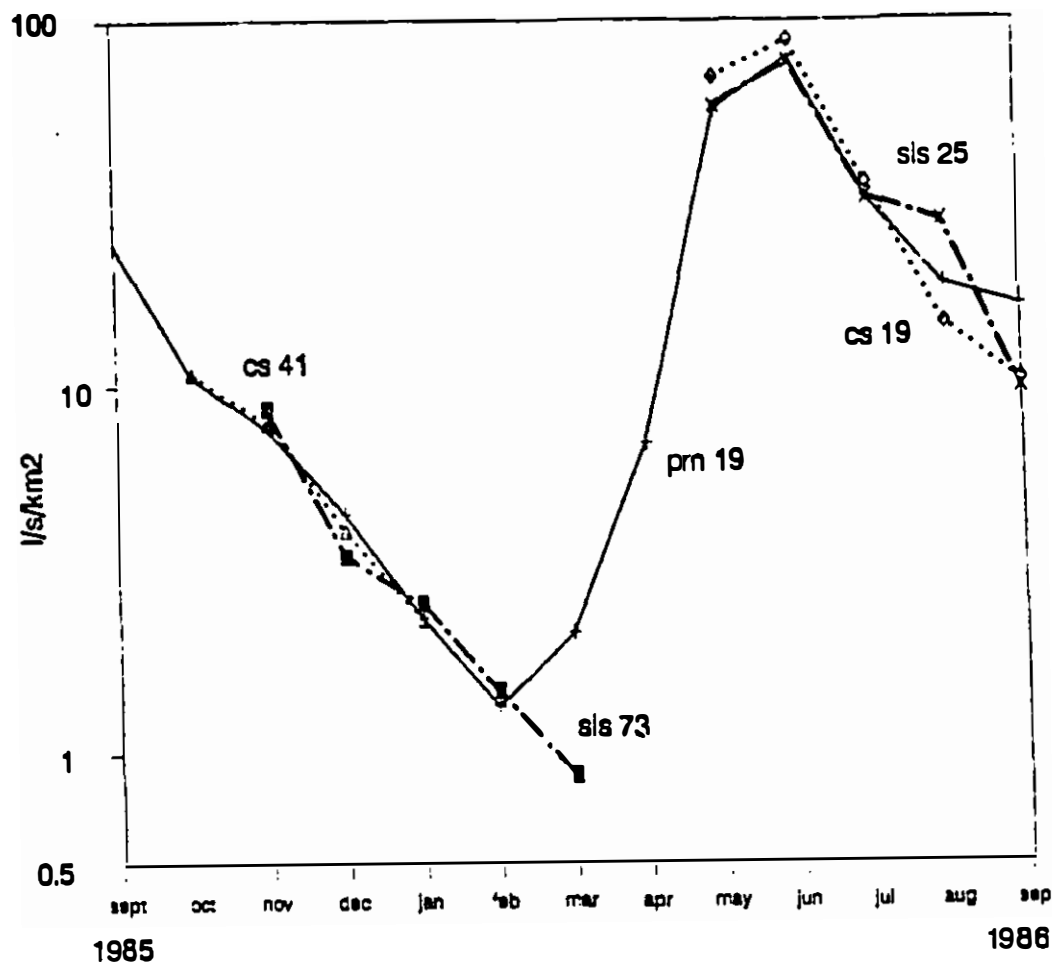


Figure 9.17 Catchment areas of Sublacustrine Springs and Crowsnest Spring as a function of season, assuming the same specific discharge as Ptolemy Spring

define a catchment in a holokarst if most of the cave streams are accessible, which is almost never the case, or if one is prepared to make tens or hundreds of tracer tests (c.g. Quinlan and Ewers, 1989).

9.4.1 Freeze-thaw effects

The most fundamental altitude effect is the phase change of water between liquid and solid phases. Alpine river regimes are dominated by the spring snowmelt (Figure 3.5), and the timing of snowmelt will give an indication of catchment altitude. The snowline progressed upward in 1986 from 1500m in April to 2000m in early June to 2500m in July.

The snowmelt season of 1986 was dominated by a period of hot weather at the end of May (Figure 3.1). This caused heavy runoff from the altitude range of 1700m to 2200m, which resulted in almost simultaneous discharge peaks at Ptolemy, Crowsnest, and Sublacustrine Springs, with exponential recessions thereafter (Figure 3.5).

The early part of the melt season is more instructive (Figure 9.18), as it shows that the low-altitude fractions of Crowsnest Spring and Sublacustrine Springs are similar, and substantially exceed the low-altitude fractions of Ptolemy Creek and Ptolemy Spring. Overall, Figure 9.18 suggests that the mean altitudes of Sublacustrine Springs and Crowsnest Spring are similar, ^{and} are higher than Ptolemy Creek, but lower than Ptolemy Spring.

9.4.2 Spring temperatures

At Crowsnest Spring, 36 spot readings of temperature throughout the year were supplemented by continuous measurements with a submersible recorder for short periods in summer. A range from 3.9 to 5.8°C was recorded, with a discharge-weighted mean of 4.3°C. The mean annual air temperature at Sentinel (altitude 1366m) was 3.5°C for September 1985 to August 1986. All spring temperatures at

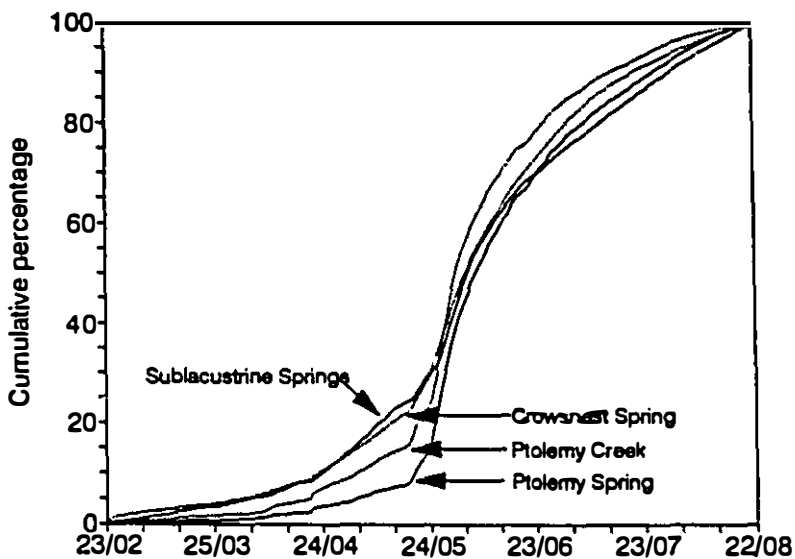


Figure 9.18 Cumulative discharge of Ptolemy Spring, Crowsnest Spring, Ptolemy Creek and Sublacustrine Springs over the snowmelt season in 1986 from snowmelt and rainfall, excluding extrapolated baseflow recession from Fall 1985

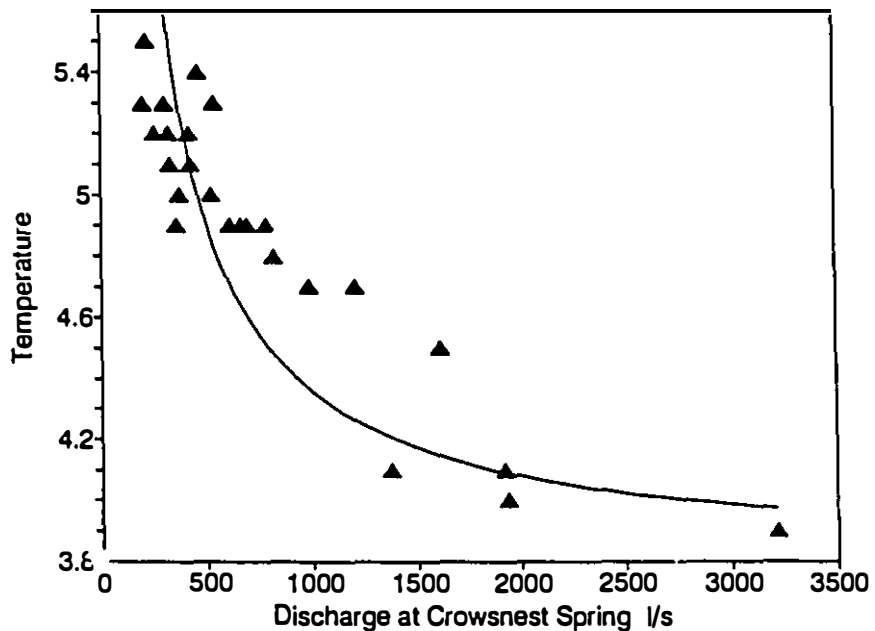


Figure 9.19 Relationship between temperature and discharge at Crowsnest Spring. The equation line assumes two flow components: a fixed discharge component (150 l/s^1 , $T=7.5^\circ\text{C}$), and a variable discharge component ($T=3.8^\circ\text{C}$)

Crowsnest Spring are above this. They show a seasonal variation, but this is related to spring discharge rather than surface temperature, with maximum spring temperature occurring in February (Figure 9.19).

Ptolemy Spring has difficult access in winter, and no readings were made at the spring itself during the winter months. Continuous submersible recordings for short periods (totalling 40 days) between May and September give a range of 2.2 to 2.7°C.

Summer discharge is dominated by snowmelt, and infiltration from snowmelt is likely to be only slightly warmer than 0°C, with no correlation to altitude. Thus the differences between the temperatures of Crowsnest Spring and Ptolemy Spring cannot be used to estimate altitude.

9.4.3 Solute concentrations

The solubility of limestone is primarily dependent upon the availability of carbon dioxide in the soil zone, and whether there are coincident or sequential conditions (Drake, 1984). In a study of the relationship between limestone solution and soil type and depth, Drake (1983) noted that the Southern Canadian Rockies waters expressed the lower concentrations of sequential conditions, when the enhanced levels of coincident conditions might have been expected. In that study, Drake related concentration to mean annual temperature, but since temperature is a function of altitude, concentration can equally be related to altitude.

Eight data sets of alkalinity measurements are available from springs and creeks at Crowsnest for the six month summer period in 1986. This period includes 74% of the annual discharge of Crowsnest River at Crowsnest Lake, but 88% for Ptolemy Spring, due to its high-altitude source (Table 3.3). Discharge-weighted estimates of annual alkalinity averages only differ by a few mg l^{-1} from the six month averages, so the summer data set gives a valid approximation for annual averages.

Additionally, there are one or two measurements from each of three high-altitude springs taken during July. The July measurements at the low-altitude springs and creeks averaged 11% more than the six-month average, but for the three highest-altitude sets, the average was 2% less than the six-month average. Thus it was reasoned that July measurements above the tree line at Crowsnest Pass approximate the discharge-weighted annual mean.

The bedrock geology of the five highest-altitude data sets is limestone, while the remaining six are dominated by shales and sandstones, with lesser proportions of limestone and dolomite. However, tills are common at lower elevations, and colluvium at higher elevations (Alberta Environment, 1980), so that coincident system solution could be expected.

For the eleven data sets, a linear relationship between alkalinity and mean catchment altitude was found:

$$K = 424 - 0.161 H \quad (r^2=0.94) \quad (9.7)$$

where K is the alkalinity in mg l^{-1} , and H is the height above sea level in metres.

This relationship can be related to the empirical coincident and sequential solution relationships developed by Drake (1984) by using the environmental temperature lapse rate (ELR). This was estimated from the difference between daily temperature maxima and minima in the west cirque of Andy Good Peak and Crowsnest Lake, 670m lower, over four months in the summer of 1986. The ELR was found to be $0.0067^\circ\text{C m}^{-1}$, which is close to the global average of $0.006^\circ\text{C m}^{-1}$. However, considerable variability was found; in August, for instance, the calculated ELR was only $0.0046^\circ\text{C m}^{-1}$.

The altitude (or temperature) dependency of solute concentration at Crowsnest of $0.16\text{mg l}^{-1}\text{m}^{-1}$ (Figure 9.20) is much greater than the model of Drake (1983; $0.03\text{mg l}^{-1}\text{m}^{-1}$) or of the subarctic study in Scandinavia by Lauritzen (1981; $0.06\text{mg l}^{-1}\text{m}^{-1}$). Drake (1983) used mean air or groundwater temperature, but noted

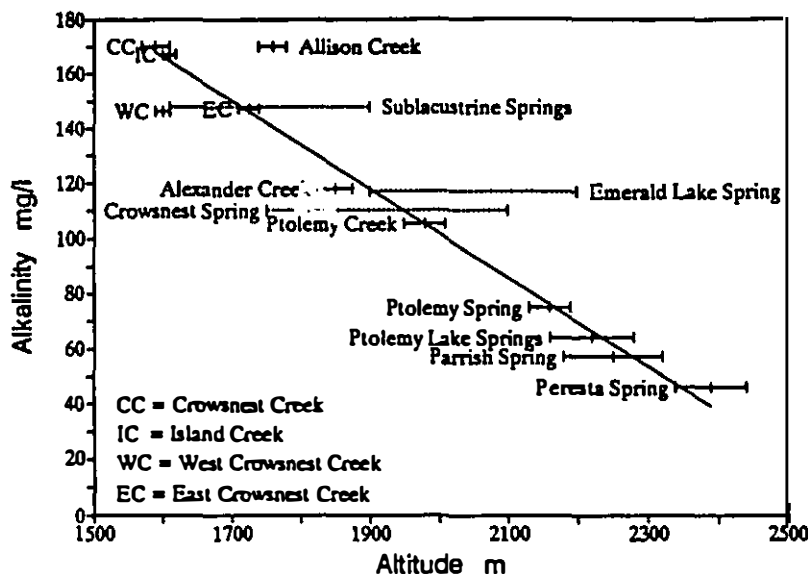


Figure 9.20 Relationship between alkalinity and altitude at Crowsnest Pass

the problems when aquifer recharge is seasonal, and stated that it might be more pertinent to use a mean aquifer recharge temperature, rather than the mean annual temperature. This is certainly true at Crowsnest, where the 0°C isotherm is at about 1900m, yet much of the field area is above this altitude.

Other probable causes for the high altitude-dependence of solution are the thin or absent soils at high altitude, so there is both a lack of soil CO_2 -boosted solution and a lack of coincident solution conditions, and depleted atmospheric partial pressure of CO_2 at high altitude.

The altitude of the Ptolemy Spring catchment is fairly well defined by the peripheral Crowsnest Creek (to the east), Andy Good Creek (to the south) and the upper contact of the karst aquifer (to the west). The catchments for Sublacustrine Springs, Crowsnest Spring, and Emerald Lake Springs are much more poorly defined

(Figure 9.20). The mean altitudes of these three catchments, from Equation 9.8, are 1610m, 1970m, and 2040m, respectively.

9.4.4 Isotopes

The isotopic ratios of H and O offer a great potential for catchment delineation, as there is a strong altitude effect. However, the rapid flow and differential flow velocities in karst aquifers create a rapidly changing signal at the springs, which cannot be adequately monitored using existing resources. The problems are discussed in Section 3.4.3.

9.5 Geology of catchments

If there were differential enrichment of trace elements or of isotopes between water percolating through the Palliser, Banff and Rundle formations, then these differences could be used to help define source areas for spring waters. However, results with trace elements were inconclusive (Section 3.4.2). Sulphate is a major ion which varies between different karst springs, but it seems to correlate poorly with lithology (Section 10.3).

9.6 Definition of catchments at Crowsnest Pass

The findings about karst catchment areas at Crowsnest Pass are summarised in Table 9.4. The runoff model indicated that karst catchment area at Crowsnest Pass is about 102km². This is more than double the topographic area for the karst catchments. This area includes most of the Ptolemy, Phillipps and Allison blocks (Figure 9.4). However, there is surface runoff from the karst during high-discharge periods, which reduces the effective catchments at such time to 73km².

Table 9.4 Karst catchment areas at Crowsnest Pass

catchment	topographic area km ²	winter area km ²	spring area km ²	notephreatic component l s ⁻¹	mean area km ²
Ptolemy Creek	19.7	10.7	10.7	0	
Ptolemy Spring	-	18.6	18.6	0	
Crowsnest Spring	-	41	19	150	
Sublacustrine Springs	-	73	25	260	
Crowsnest River (1)	47.6	143	73	410	
Crowsnest River (2)	47.6				102

- (1) from underflow and overflow calculations at each spring (Section 9.3)
 (2) from runoff model (Table 9.1)

During the winter, there is a modelled catchment area of 143 km², plus the area from which 410 l s⁻¹ is derived. Minimum discharges in surface catchments in the vicinity of the field area average about 3 l s⁻¹ km⁻² between January and March. For instance, the Oldman River catchment (1440 km²) has 2.6 l s⁻¹ km⁻², Elk River (1870 km²) has 2.9 l s⁻¹ km⁻², and Michel Creek (637 km²) has 3.3 l s⁻¹ km⁻² (Figure 3.3). Similar values are found in other catchments in the Rockies, most of which have large fractions of karstic limestones (Table 1.1).

One interpretation is that the 410 l s⁻¹ underflow derives from a catchment area of about 140 km², giving a total winter karst catchment for Crowsnest Pass of about 280 km². This is somewhat less than the 390 km² calculated in Section 2.3.2 for the case where Crowsnest Pass is the focus for all underflow from the High Rock and Flathead Ranges. However, continued discharge in winter at higher springs such as on Andy Good Creek show that the karst cannot be considered as a simple aquifer with uniform planar hydraulic gradients.

An alternative interpretation is that the "underflow" component is simply a function of high aquifer storativity in the Sublacustrine and Crowsnest Spring catchments. This explanation seems unlikely as this component is not seen in higher-altitude springs such as Ptolemy Spring, Parrish Spring, and Ranch Spring.

Thus it seems likely that hydraulic gradients are oriented towards Crowsnest Pass from all of the High Rock and Flathead Ranges (Figure 2.2), but that local semi-autonomous drainage exists to creeks such as Andy Good Creek. While the catchment of Ptolemy Spring is fairly well-defined, this is not true for Sublacustrine Springs and Crowsnest Spring (Figure 9.5). On the other hand, the mean altitude of all catchments is fairly well-defined (Figure 9.20).

The nature of the karst aquifers at Crowsnest Pass will be discussed in the next chapter.

Chapter 10

Karst groundwater flow at Crowsnest Pass

The hydraulics, hydrochemistry and flow vectors in the karst at Crowsnest Pass can now be summarised, using the results from Chapters 3 through 8.

10.1 Karst spring hydraulics

10.1.1 Discharge

The principal springs at Crowsnest Pass are Sublacustrine Springs, Crowsnest Spring, and Ptolemy Spring (Table 3.4). The karstic origin of Sublacustrine Springs is not obvious, as they are hidden below the three lakes (Section 3.2). A comparison of the discharge of Sublacustrine Springs with the other two springs is shown in Figure 10.1.

The discharge for Sublacustrine Springs is subject to some inaccuracy as it is a residual from five discharge measurements plus change in lake storage (Equation 3.3), and there are lag effects between these measurement points. Three of the five discharges were measured continuously for 15 months, but there were only weekly measurements for seven months for the remaining two creeks. However, the more than threefold increase in discharge in four days at the end of May (Figure 10.1) is very similar to the response at Crowsnest Spring, and can only be attributed to flow from an aquifer with well-developed fracture or conduit porosity. At Crowsnest Pass, this can only be the karstic limestones.

Underflow and overflow behaviour plays an important part in spring regimes. Crowsnest Spring and Sublacustrine Springs are the lowest springs at Crowsnest Pass, and both have important underflow components (Section 9.3).

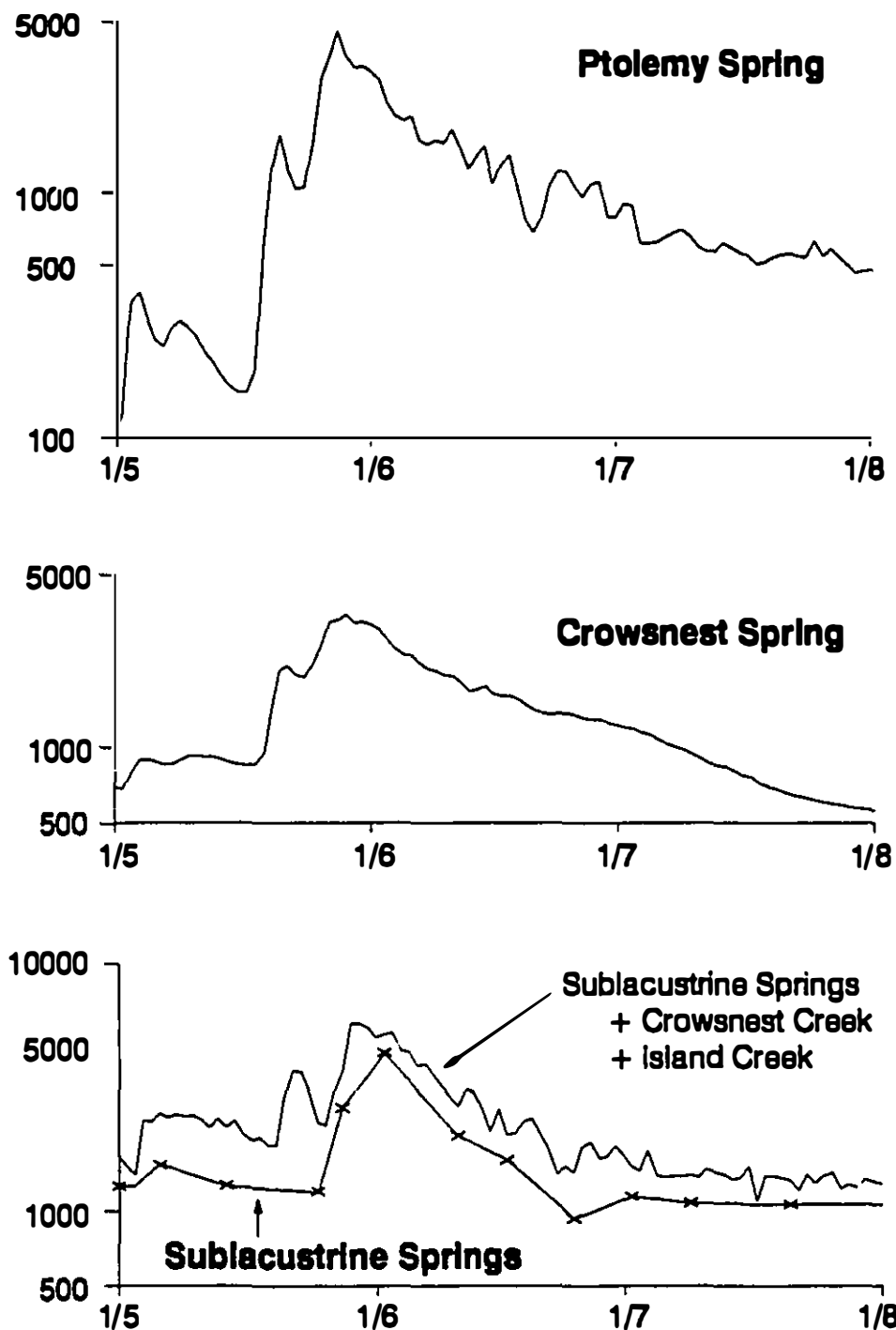


Figure 10.1 Mean daily discharge for Ptolemy Spring and Crowsnest Spring, and calculated discharge for Sublacustrine Springs from May to August 1986, showing karstic response of Sublacustrine Springs

However, Crowsnest Spring has an upper and a lower orifice, and these give overflow and underflow behaviour, respectively (Section 2.2.2, Table 3.4).

Ptolemy Spring closely approximates a full-flow spring, but it is 150m above Ptolemy Creek, up a steep hillside. Therefore, it is in an overflow position, and the high hydraulic gradients in the limestone below the spring must ensure that there is some underflow. However, underflow behaviour is not apparent from the hydrograph, and it is probably only a few litres per second at most.

There are many overflow springs at Crowsnest Pass that flow for variable periods. The lowest of these are only a few metres above Crowsnest Lake, but most are in obvious overflow positions, up steep slopes, or in cliffs (Section 9.3.2).

10.1.2 Velocity

Velocity measurements through the conduits leading to Ptolemy Spring and Crowsnest Spring were presented in Figure 3.7. It was shown in Section 5.2.1 that these are both equilibrium phreatic conduits. Dye peaks at Ptolemy Spring are unimodal, but there are bimodal peaks at high discharges at Ptolemy Spring (Figure 10.2). This indicates that a minority of the flow goes through a less efficient conduit on its path to the spring. Such bifurcations have been demonstrated by dye tracing before (e.g. Smart and Ford, 1986), but dye tracing cannot fully reveal the complex branching that may be present in karst conduits (see Figure 8.6).

10.1.3 Area of conduits

The cross-sectional area of the conduits feeding Crowsnest Spring and Ptolemy Spring may be estimated in several ways. Direct exploration of the first 100m of the flooded conduit at Crowsnest Spring has shown that the cross-sectional area varies between 7m^2 and 22m^2 (Figure 6.5a).

A second method of determining conduit cross-sectional areas is from the water displaced in a conduit between dye injection and recovery (Table 3.4). The

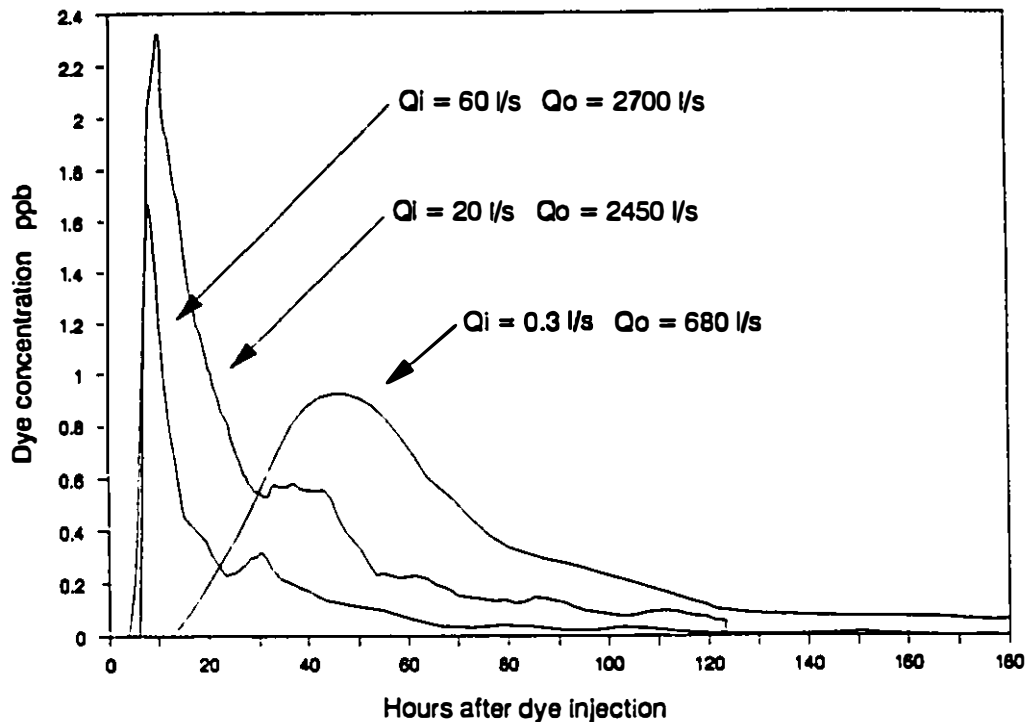


Figure 10.2 Bimodal dye peaks at Crowsnest Spring from Phillips Pass injections

standard method is to use

$$A = Q_o / v_s \quad (10.1)$$

This gives estimates of 47m^2 for Crowsnest Spring, and 51m^2 for Ptolemy Spring. These are maximum estimates, and two factors must be allowed for. First the method assumes that there is negligible delay before the dye reaches the main conduit, and that there is no increase in discharge along the main conduit. This is only true for a simple alloigenic karst where $Q_i = Q_o$. Second, the sinuosity of the conduit will give a true length on average 60% longer than the straight-line distance (Table 6-3). Allowing for these two factors gives conduit cross-sections in the range $15\text{-}20\text{m}^2$ for

Ptolemy Spring and Crowsnest Spring. This range thus corresponds with the larger sections of conduit explored in Crowsnest Spring.

10.1.4 Hydraulic gradients

It was shown in Section 5.2.4 that hydraulic gradients in karst conduits should vary seasonally by at least 10-100 times. The following discussion will make the simplification of assuming linear hydraulic gradients; in fact their form is exponential (Section 5.2.4). Minimum hydraulic gradients can be estimated from the catchment area calculations, which show there is substantial underflow oriented towards Crowsnest Pass (Section 9.6). This method gives a maximum value of 0.005 (Figure 2.6).

Maximum hydraulic gradients in conduits may be estimated from the positions of overflow springs. However, these gradients apply with respect to the conduit distance, and not to the straight-line distance. For instance, the main overflow spring emerging on Emerald Cliff has a local hydraulic gradient of infinity down the vertical cliff, but the head at the spring is operating ineffectively through the low-porosity limestone. Instead, the head is operating through the conduit system, driving the flow out of the underflow spring(s), which is probably located at the bottom of Emerald Lake. Overflow spring positions suggest that maximum hydraulic gradients must be in the upper range of those cited in Table 5.7, or about 0.02-0.05.

An alternative method of calculating hydraulic gradients is by using scallops. Scallop lengths have been measured in passages in the Yorkshire System and Gargantua, and these give a dominant-discharge hydraulic gradient of <0.0015 (Section 10.2). These fossil passages are similar in size to the principal passages feeding both Ptolemy and Crowsnest Springs (Figure 6.7a, Section 10.1.3).

Lauritzen et al. (1985) investigated the discharge responsible for scallop development at a site in Norway, and found this dominant discharge to be in the upper 4% of discharges, rather than the mean discharge. The highest discharges at

Crowsnest are the most aggressive (Figure 3.13), so it follows that the dominant discharge for scallop formation at Crowsnest also is much greater than the mean discharge. Thus maximum hydraulic gradients in the main conduit feeding Crowsnest Spring are probably in the range 0.001-0.005; minimum hydraulic gradients would be at least 1-2 orders of magnitude less than this (Section 5.2.4). Maximum hydraulic gradients in the Ptolemy Spring conduit must be higher than this, as the resurgence is blocked by boulders.

The order of magnitude difference of maximum hydraulic gradients shows the range that can occur in karst between unobstructed conduits and those with major blockages such as obstruction of the spring by boulders or by alluviation. Furthermore, the karst groundwater is not fully integrated, and semi-autonomous high-level springs occur. These can largely be attributed to the low aggressivity and limited flow periods of high-altitude waters, combined with the short period since deglaciation.

10.1.5 Friction factors

Friction factors in the conduits feeding Ptolemy Spring and Crowsnest Spring can be calculated, using Equation 5.12. Given $r=2.5\text{m}$ (Section 10.1.3), and $S_x=0.02-0.05$ (Section 10.1.4), then friction factors are in the range of 50-125. These values are consistent with the upper part of the range found in Section 5.2.5.

10.2 Aquifer characterisation from paleohydrology

The past hydrology of the karst at Crowsnest Pass is recorded in the fossil caves there. In most of the caves only tantalisingly short sections of paleoflow routes have yet been found, but the two most extensive caves, the Yorkshire System and Gargantua (Figure 2.5), offer a somewhat better record. In these caves, ancient flow paths of 1km in length have been followed. In Yorkshire System, the major paleoflow was in the Roller Coaster, Alberta Avenue and Bloodstone Passage (altitude 2080-

2230m), with flow to the north-west. On the other hand, in the major passages in Gargantua (Big Dipper, Interprovincial Way, the Canyon and G.B. Passage: altitude 2260-2480 m) paleoflow was to the south-east (Thompson, 1976).

Scallops measured by Ford (1971c) at four sites in the Big Dipper, Interprovincial Way and the Canyon give discharges of 0.8-2.2m³s⁻¹. Scallops in Alberta Avenue, the largest passage in Yorkshire System, give discharges in the range 1-2.5m³s⁻¹. These dominant discharges (Section 10.1.4) in two caves are of the same order as the present discharge from Ptolemy Spring, and thus indicate catchment areas probably >10km².

Paleohydraulic gradients can also be calculated, given $v_m = 0.11 \text{ ms}^{-1}$, $r_m = 2\text{m}$, and an estimated $f=1$. Using Equation 5.11, this gives a dominant discharge hydraulic gradient of 0.0015.

One of the most notable features of the caves at Crowsnest Pass is the upward and downward looping of such passages as Alberta Avenue and the Roller Coaster, where there is a vertical range of at least 150m (Figure 6.7b). Given the mean stratal dip of about 35° in the Ptolemy Block (Figure 2.2), this indicates flow paths of 5-10km (Equation 7.3), which similar to modern flow paths in this area.

The evidence from the principal fossil conduits in the caves at Crowsnest Pass thus indicates that they are analogous to the principal active conduits.

10.3 Aquifer characterisation from hydrochemical evidence

The most marked seasonal trend in total hardness at Crowsnest Spring and Ptolemy Spring is the inverse relationship with discharge during the summer snowmelt season (Figure 3.7). This is common in karst springs, is principally a function of residence time, and has been noted before in the Rockies (Drake and Ford, 1974). This dilution by low-residence time snowmelt water is true for bicarbonate concentrations at both springs. The response of sulphate is very different, with

Crowsnest Spring showing a strong dilution response, but this is much diminished at Ptolemy Spring (Figure 3.8).

Total hardness at Ptolemy Spring describes a marked hysteresis loop with respect to discharge (Figure 10.3a). This reflects the behaviour of bicarbonate (Figure 10.3b), and can be explained by a flushing out of the pre-flood high-hardness water by the low-hardness snowmelt water (Ashton, 1966). The hysteresis is less obvious with sulphate, but the minimum of 6mg l^{-1} coincides with the end of the low bicarbonate values. The dilution by snowmelt is exemplified by the high variations in solute fluxes at Ptolemy Spring: $54 \pm 46\text{gs}^{-1}$ for alkalinity, and $8.3 \pm 7.0\text{gs}^{-1}$ for non-alkaline hardness.

Total hardness at Crowsnest Spring exhibits no hysteresis effect (Figure 10.4a), but in fact this is masking two contrasting loops (Figure 10.4b). The bicarbonate loop shows a similar effect to that at Ptolemy Spring, but the sulphate loop is reversed (i.e. counter-clockwise), with the high-sulphate water occurring on the hydrograph recession. The sulphate concentration is inversely proportional to discharge over the period studied, while the inverse relationship of bicarbonate is much weaker. Thus the sulphate flux is $53 \pm 17\text{gs}^{-1}$, while the bicarbonate flux is $121 \pm 62\text{gs}^{-1}$.

In Section 9.3.4, it was shown that the discharge regime of Crowsnest Spring was similar to that of Ptolemy Spring, if the former had an underflow component of 150l s^{-1} . The sulphate concentrations reinforce this evidence. The reverse hysteresis loop described by sulphate can then be explained. The flow path of the underflow through the aquifer was substantially different from that used by the snowmelt water, or the underflow was displaced into storage by it. An underflow with a substantially different flow path corresponds to the concepts of Hagen - Poiseuille flow nets, notephreatic flow, and conduit evolution which were developed in Chapters 6, 7 and 8 (see Figure 8.1). The inverse relationship between temperature and discharge at Crowsnest Spring also supports this contention, with geothermal heat

raising the temperature of the underflow component above local mean annual temperatures (Figure 8.17).

There is no accurate information on changing solute concentrations with time in Sublacustrine Springs, because of the large storage volume and imperfect mixing in the three lakes overlying the Springs. However, the mean concentration can be calculated from the total measured solute fluxes into and out of the three lakes. The results indicate that mean sulphate concentrations in both Crowsnest Spring and Sublacustrine Springs are almost identical (Table 3.5), while the higher bicarbonate can be associated with a lower-altitude catchment (Figure 8.18). The underflow components of Crowsnest Spring and Sublacustrine Springs are proportionally similar (24% and 29%, respectively, of Q_m), which supports the concept of a high-sulphate ($\approx 150\text{-}200\text{mg l}^{-1}$) underflow component at Sublacustrine Springs.

Drake (1974) found that sulphate represented 36% of the anions in solution in the Athabasca and North Saskatchewan catchments, and suggested that gypsum beds in Mississippian Mt Head Formation and the Triassic Spray River Group might be major sources for this. In the Flathead and High Rock Ranges, little gypsum has been found in either of these formation, yet concentrations of sulphate in Crowsnest River are high, providing 26% of the anions in Crowsnest River (Table 3.7). Sulphate represents at least 10% of anions in all springs and creeks monitored regularly at Crowsnest Pass (Table 3.5). There are particularly high concentrations in Crowsnest Spring and Sublacustrine Springs (associated with underflow) and also in Crowsnest Creek, where values up to 880mg l^{-1} were recorded in the leachate from coal spoil heaps.

The high sulphate values in limestone springs are confusing, for the abundance of sulphur in geological samples is sufficiently low ($<<1\%$) for it not to have been analyzed for separately (Table 2.1). However, there is a solution breccia in the Palliser Formation, and another breccia in the Upper Livingstone, which may represent a solution breccia, but it is difficult to see how such beds could yield such

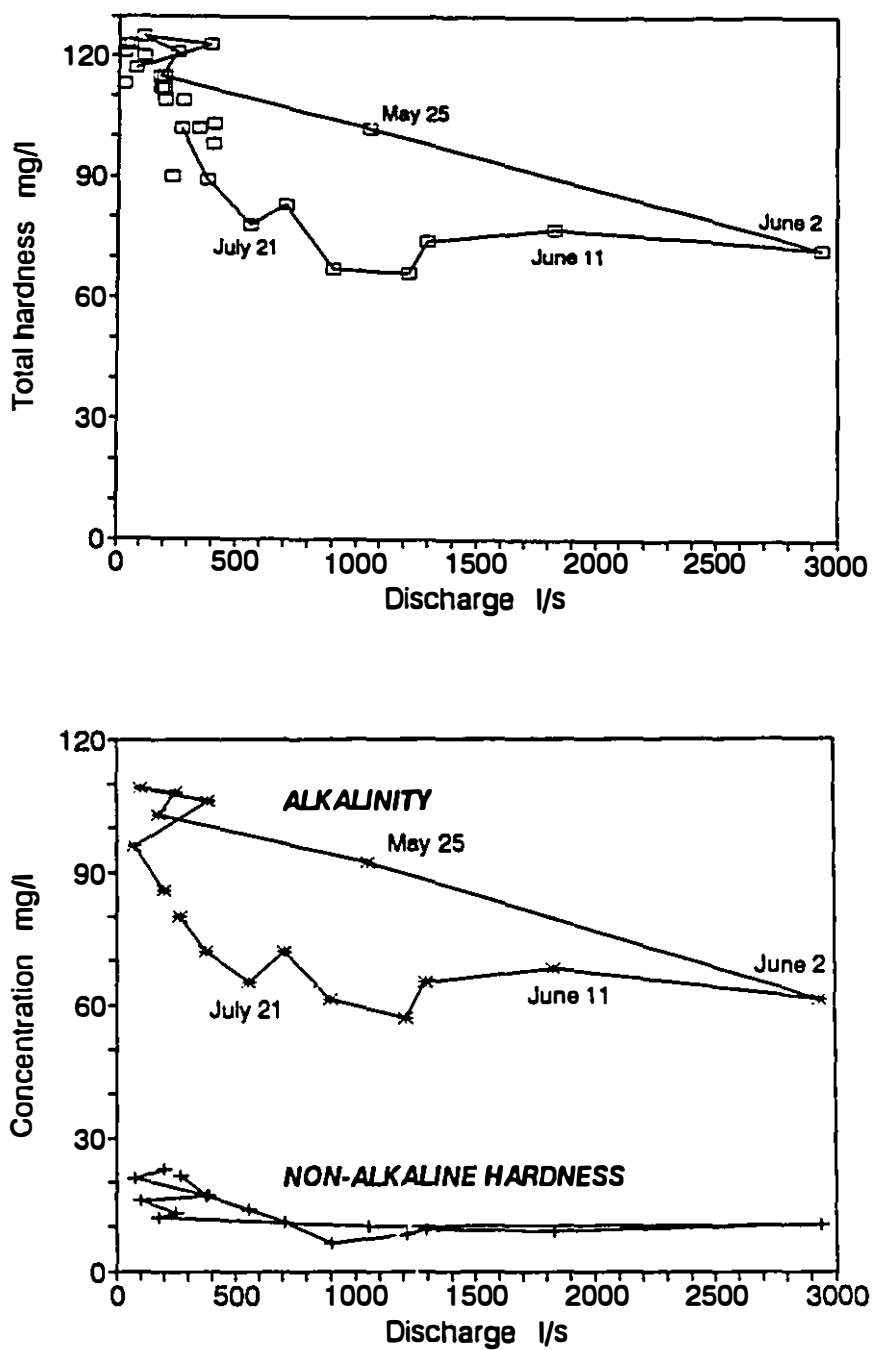


Figure 10.3 Chemograph variation at Ptolemy Spring

- a) Total hardness from September 1985 to September 1986
- b) Alkaline and non-alkaline hardness 15/4/86 - 20/9/86

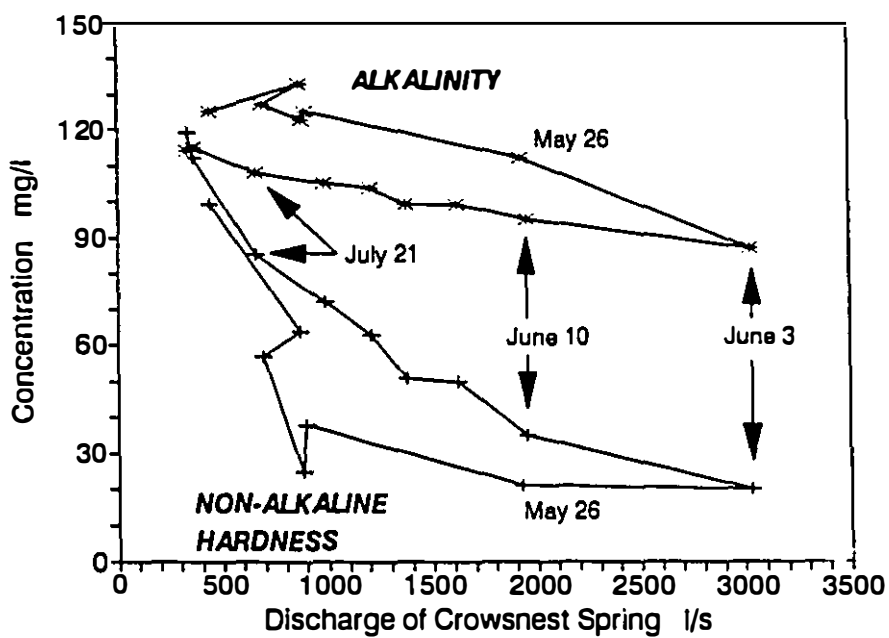
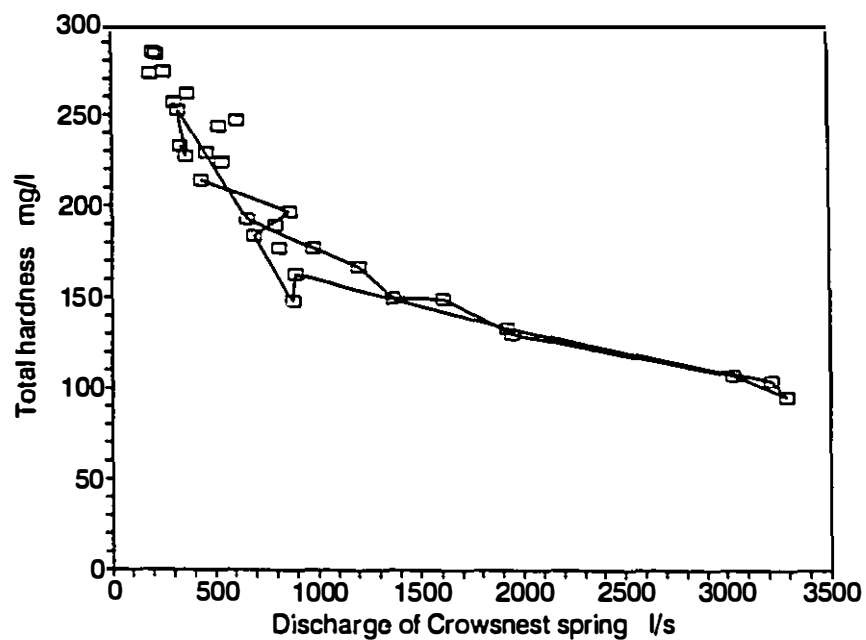


Figure 10.4 Chemograph variation at Crowsnest Spring
a) Total hardness from September 1985 to September 1986
b) Alkaline and non-alkaline hardness 15/4/86 - 20/9/86

a high proportion of solutes in karst springs. The problems were further discussed in Section 8.8.4.

10.4 Aquifer characterisation from flow model

The depth of flow in the aquifers at Crowsnest can be estimated from Equation 7.3. The mean stratal dip in the Ptolemy Spring catchment is about 35° (Price, 1962a,b), and the southern boundary is constrained by the low-altitude Andy Good Creek, which gives $L_x=7\text{km}$. These limits give an estimated mean conduit depth of 90m below the water table.

To the north of Crowsnest Spring, the mean stratal dip is 46° in the Phillipps Block, and 41° in the Allison Block (Price, 1962a,b). The aquifer length is imprecise as the furthest tracer test is from 4.4km. The lower limit can be estimated from discharge budget calculations, which gives the mean catchment area as extending the 16km to Racehorse Pass (Figure 9.5, but see Table 9.5). The upper limit is about 80km (Sections 2.3.2 and 9.6), over which the mean stratal dip is about 40°. From Equation 7.3, these estimates give a mean conduit depth of 210-770m below the water table.

The deep flow to Crowsnest Spring has been partially confirmed by diving, with a depth of almost 50m being attained so far in this vauclusian spring (Figure 6.5). The maximum temperature of Crowsnest Spring (in February) is 2°C higher than the local valley-bottom air temperature (Section 9.4.2), and about 4-5°C higher than the mean recharge temperature, which can be little over 0°C. This confirms that there is some geothermal heating of the spring water. Assuming the spring water has a constant discharge nothephreatic component of 150 l s^{-1} (Section 9.3.4) and a variable discharge dynamic phreatic component, the nothephreatic component has a temperature of 7.5°C (Figure 9.19). This water is thus classified as thermal, being $>5^\circ\text{C}$ warmer than local surface meteoric water.

The flow model presented in Figure 8.1 implies that the lowest springs at Crowsnest Pass (i.e. Sublacustrine Springs) should have the highest geothermal heating. This hypothesis has not been tested yet, as not even the location of Sublacustrine Springs within the three lakes has yet been determined.

The estimated mean depths for the conduits feeding Crowsnest Spring and Ptolemy Spring are comparable to the depths of ancient phreatic conduits, which have been found in the caves high above Crowsnest Pass, where depths have exceeded 150m (Figure 6.5b, Section 10.2).

10.5 Reasons for the contrasting regimes of Ptolemy Spring and Crowsnest Spring

It was explained in Section 3.6 that the discharge and hydrochemical contrasts could not be rationally explained using existing hypotheses of karst aquifer development and flow. Using the ideas developed in Chapters 4 and 6, these contrasts can now be explained as being due to two principal factors.

The principal contrasts in discharge are because Ptolemy Spring is essentially a full-flow spring, while Crowsnest Spring is an underflow spring (Section 10.1.1). The greater catchment length, deeper flow paths, and low altitude produce a significant underflow component at Crowsnest Spring; it is this nonphreatic underflow component which causes the principal differences in the hydrochemistry of the two springs (Section 10.2).

10.6 Flow vectors in the Flathead and High Rock Ranges

The principal vectors of flow from the karst can be estimated, using the catchment delineation results (Chapter 8). The total discharge from the karst of the Flathead and High Rock Ranges is about $7\text{-}8\text{ m}^3\text{s}^{-1}$ (Table 8.2), of which $2.17\text{ m}^3\text{s}^{-1}$ were gauged at Crowsnest Pass (Table 3.3).

The most obvious flow vector to a surface water hydrologist would be the surface runoff, utilising the fluvial network which drains 97% of the Flathead and High Rock Ranges (Figure 2.3). There is an almost 50% reduction in catchment area for the Crowsnest Pass springs in the snowmelt season due to surface runoff (Table 8.4), over the period that 65-75% of the runoff is discharged (Table 3.3). This suggests that about 35% of the runoff from the karst is on the surface.

The most obvious flow vector to a karst hydrologist would be the flow from visible springs. However, spring discharge includes both visible and aggraded springs. The visible springs at Crowsnest Pass include Crowsnest Spring, Ptolemy Spring, Parrish Spring and several smaller springs, and account for about $1.15\text{ m}^3\text{s}^{-1}$ (Table 3.4). The aggraded springs include Sublacustrine Springs, Ptolemy Lake Springs, and other ungauged springs along Ptolemy Creek; these total about $1.0\text{ m}^3\text{s}^{-1}$ (Table 3.4). Therefore at Crowsnest Pass, about 47% of the spring discharge from the karst is via aggraded springs. This amounts to about 31% of the total discharge from the karst.

Spring discharge at Crowsnest Pass has been divided into dynamic phreatic and nothephreatic components (Table 8.4). The nothephreatic component is only present in Crowsnest Spring and Sublacustrine Springs, and is characterised by steady discharge, high sulphate/bicarbonate ratios and high temperature (Section 10.2). It was concluded in Section 8.6 that the underflow of $0.41\text{ m}^3\text{s}^{-1}$ probably reflects drainage from all of the Flathead and High Rock Ranges, and so is unlikely to be found in higher-altitude springs in the Flathead and High Rock Ranges. It thus accounts for only about 5% of the total runoff from the Flathead and High Rock Ranges. While the flow paths of the underflow component may be as long as 80km (Figure 2.2, Section 8.6), most karst springs reflects much more local flow, with paths rarely exceeding 10km.

The final flow vector to consider is dip-oriented regional flow to springs in the Rocky Mountain Trench. Such putative flow paths are discussed in detail in

the context of the Rocky Mountains as a whole in Chapter 10, where it is concluded that they account for <1% of the runoff from karst.

A summary of the karst runoff vectors in the Flathead and High Rock Ranges is given in Figure 10.5.

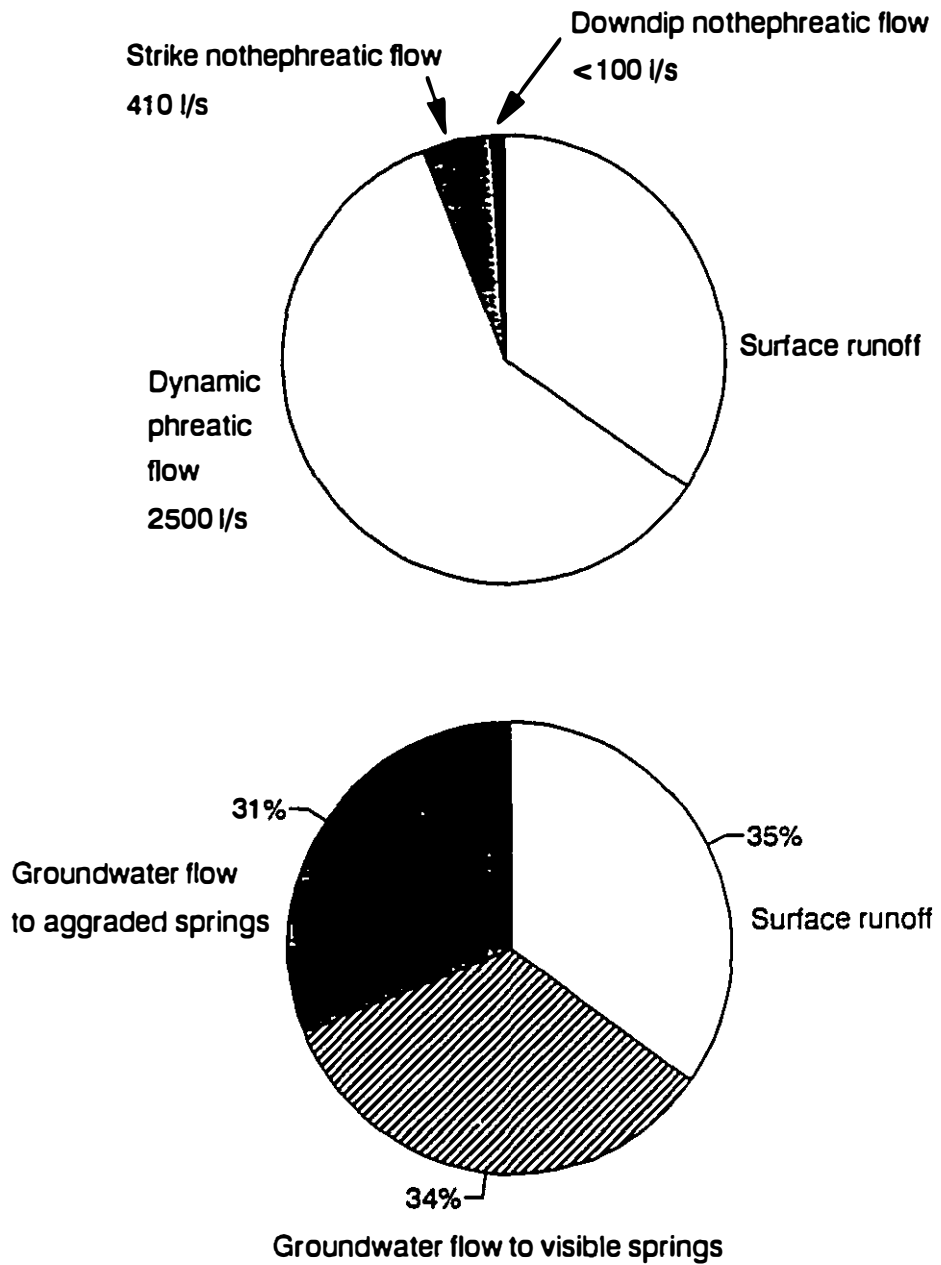


Figure 10.5 Runoff vectors from the karst of the Flathead and High Rock Ranges

Chapter 11

Karst groundwater flow

in the Rocky Mountains

11.1 Introduction

In the previous chapter, the character of groundwater flow to Crowsnest Pass was described. It was shown that hydraulic gradients are very variable, that there is an important underflow component to aggraded springs, that flow paths exceed 100m in depth below the water table, and are up to tens of kilometres in length. In this chapter it will be determined if these findings are applicable in general to Rocky Mountain karst aquifers.

11.2 Hydraulics

The information that can be deduced on the hydraulics of karst groundwater flow in the Rockies is rather limited, and this is impeded in particular by the lack of measurements of water table levels. However, at two sites, Medicine Lake and Castleguard Cave, there is sufficient information to be able to calculate friction factors and hydraulic gradients.

11.2.1 Maligne karst

The Maligne Springs are the largest karst springs in the Rockies (Table 11.1). The cave behind the springs has yet to be entered as there are constrictions at the sink and resurgence points, though dye traces have shown that the intervening

Table 11.1 Major gauged karst springs of the Rocky Mountains

	# of springs	mean monthly discharge m^3s^{-1}			I.W.D. (1989a), Smart, 1983a Table 3.3
		Q_n	Q_m	Q_x	
Maligne Springs	>60	2.2	15.2(1)	39.3(1)	I.W.D. (1989a), Smart, 1983a Table 3.3
Castleguard River springs	~80	<1	(4-6)	(20)	Table 3.3
Sublacustrine Springs	several	0.32	0.88	2.2	Table 3.3
Crowsnest Spring	2	0.32	0.66	1.83	Table 3.3
Ptolemy Spring	1	0.025	0.38	1.48	Table 3.3

(1) excludes summer surface overflow from Medicine Lake

Data in parentheses are estimates

cave is of considerable size (Brown, 1974; Kruse, 1980; Smart, 1988a). There have been eleven positive dye traces from sinks in Medicine Lake to Maligne Canyon, 16km away and 420m lower, and these traces have enabled velocity calculations to be made. Smart (1988a) suggested that the karst system that drains Medicine Lake may be filled at high discharges, and he calculated a friction factor of 130, if this were the case.

The hypothesis that the karst system fills up may be tested, using the Darcy-Weisbach relationship between discharge and head (Equation 5.10). The simplest assumptions about the filling of Medicine Lake are that it is caused by the constrictions at the sinks into the cave, or at the resurgence from the cave, or both. In the former case, it then follows from Equation 5.10 that

$$Q^2 \propto h_i \quad (11.1)$$

where h_i is the head above the input constriction. If the filling of Medicine Lake is caused by output constriction, then

$$Q^2 \propto h_o \quad (11.2)$$

where h_o is the head above the output constriction. A plot of Q^2 against head for four years of Medicine Lake levels (Figure 11.1) shows that the discharge is a function of input constrictions (Equation 11.1) at low discharges, so that

$$Q^2 = 830 h_i$$

and

$$h_i = Q^2 / 830 \quad (11.3)$$

However, once the level rises to 1429m, with $Q=41.2 \text{ m}^3\text{s}^{-1}$, then the cave becomes water-filled, and discharge responds to the head above the output constriction, so that

$$Q^2 = 4.46 h_o$$

and

$$h_o = Q^2 / 4.46 \quad (11.4)$$

These results demonstrate that high-flow hydraulic gradients as high as 0.025 can occur in the Rockies when associated with aggraded springs.

11.2.2 Castleguard Cave

Castleguard Cave is the longest explored cave in the Rockies. A detailed map of the 20.1km of known passage in the cave has recently been completed (Figure 11.2, 11.3). The map shows that the vertical range of the cave is 386m, which is 76m more than the estimated depth of the previous sketch-map of the cave, which was known to be in error (Thompson, 1976). The 8900m of passage from the entrance to the ice plug 225m below the surface of the Columbia Icefield provides an exceptionally long linear traverse in a cave, and so the cave has been used to test

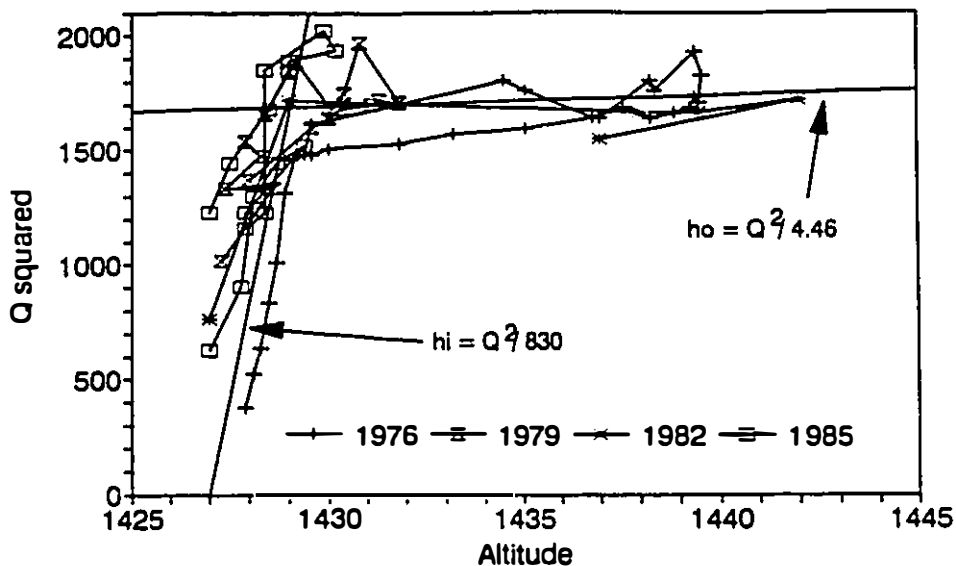


Figure 11.1 Water level in Medicine Lake as a function of head above the flow constriction at the lake bottom (at low discharges) and above Maligne Springs (at high discharges)

hypotheses on aspects of cave climates, radon movement, and sediment deposition (Ford, 1983b).

Speleothem dating has enabled the cave to be partially dated. A reversed magnetised speleothem in the Corridor indicates that the cave first emerged above the water table >730ka B.P., and another speleothem shows that deposition of calcareous silts terminated before 144ka B.P. (Gascoyne et al., 1983b).

Some paleohydraulic parameters of the cave can be calculated using scallops. Scallops in early phreatic passages such as Twinkle Alley were >0.2m in length, indicating velocities <0.12ms⁻¹. In a later phase of development, scallop length in passages such as Holes in the Floor and the Grottoes was 0.75-1m, indicating velocities of 0.02-0.03 ms⁻¹ (see Muir and Ford, photos 78, 82, 84, 85).

These scallops represent discharges of $0.1\text{-}0.3 \text{ m}^3\text{s}^{-1}$ and $0.2\text{-}0.3 \text{ m}^3\text{s}^{-1}$, respectively. These discharges probably represent flood discharges, with mean discharges possibly an order of magnitude less than this (see discussion in Section 9.2). These discharges show that the catchment for Castleguard Cave was much smaller than the catchment for the present Castleguard Valley springs, where $Q_m = 3\text{-}6 \text{ m}^3\text{s}^{-1}$.

The hydraulic gradient of the cave can be calculated from the Darcy-Weisbach equation (5.11). The present Darcy-Weisbach friction factor of the cave was calculated by Atkinson et al. (1983) to be in the range 0.9-2.3, based on air flow measurements. This includes the high friction in narrow sections caused by silting (e.g. lower end of Subway) or boulder chokes (e.g. end of Schoggistollen), and during active expansion of the cave it was probably lower than this. In the early phreatic phase, with $r=0.8\text{m}$, $v=0.05\text{-}0.12 \text{ m s}^{-1}$, and $f=0.1\text{-}1$, then $S=0.000008\text{-}0.0005$. Thus the drop in the level of the water table over the 6.5km length of the cave was $<3\text{m}$. This means that a now-eroded passage must have risen $>370\text{m}$ from the present entrance passage to reach spring level, which indicates a vauclusian rising.

The formation of the cave was described by Ford et al. (1983). The completion of the detailed map of the cave since then has increased the known length of passages in the cave by 50%, and has enabled a more detailed history of the cave to be proposed.

The hydraulic history of the cave can be divided into four principal phases, though these may only represent a fraction of the total history of the cave:

1) Early phreatic phase. Water table lies above 2390m. Phreatic tubes up to 3m^2 develop downdip along bedding planes (e.g Boon's Blunder - Entrance Passage, Mini Holes - Twinkle Alley: Figure 11.2), along intersections between one bedding plane and the $140\text{-}150^\circ$ joint set (e.g. Slickenslides, Holes-in-Floor, Corridor, Subway), or along the intersection between the bedding plane and igneous dikes (e.g. parts of the Grottoes). Almost all the cave utilises just one bedding plane in one large phreatic

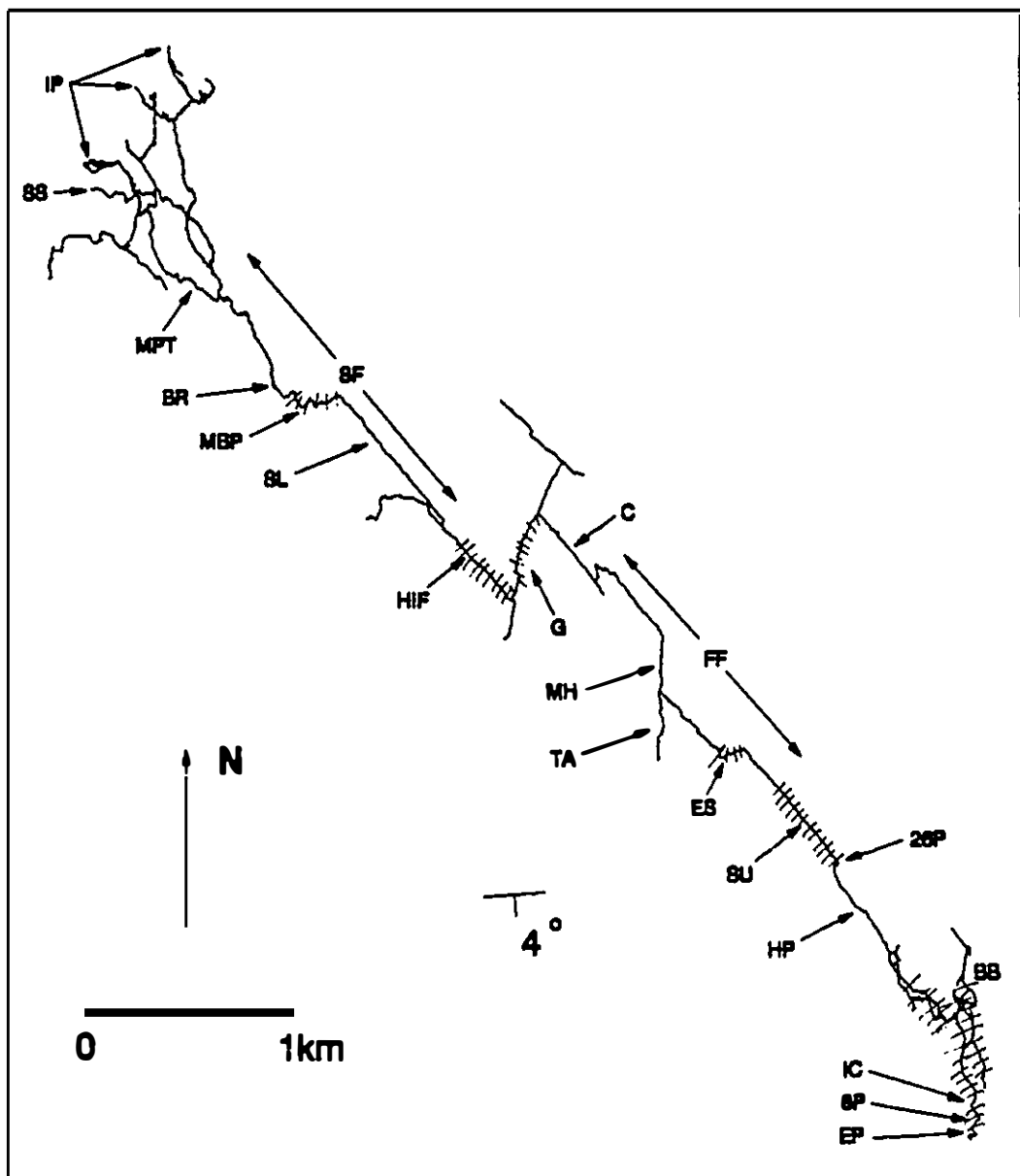


Figure 11.2 Plan of Castleguard Cave

IP	Ice plugs	SS	Schoggistollen
MPT	Munchkin Peon Trail	BR	Big Room
SL	Slickenslides	SF	Second Fissure
MBP	Mud Bank Passage	HIF	Holes in the Floor Passage
G	The Grottoes	C	The Corridor
FF	First Fissure	MH	Mini Holes
TA	Twinkle Alley	ES	Easy Street
SU	The Subway	26P	26m pit
HP	Helictite Passage	BB	Boon's Blunder
IC	Ice Crawl	8P	8m pit
EP	Entrance Passage		

III Phreatic passages during second phase of cave development

Note that the Big Room is shown to scale, but the width of all other passages is exaggerated

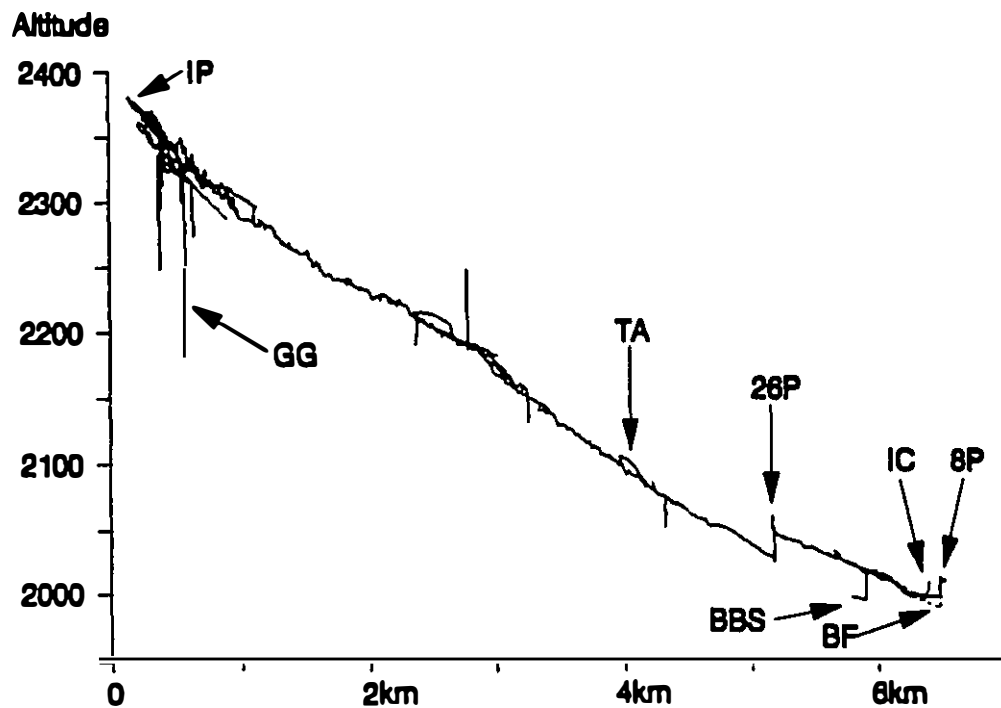


Figure 11.3 Profile of Castleguard Cave, viewed along the strike of the strata

IP	Ice plugs	GG	Grande Gueule
TA	Twinkle Alley	26P	26m pit
BBS	Boon's Blunder Sump	IC	Ice Crawl
BF	Hypothesised bedrock floor beneath Ice Crawl before paragenesis		

drop, but near the entrance there are two phreatic lifts, each of 26m, to two higher bedding planes. These are from the Subway to Helictite Passage, and from the paragenetic Ice Crawl to the Entrance Passage (Figure 11.3).

2) Main expansion phase. Water table drops to <2020m. The cave becomes vadose, and a small stream erodes the deep, narrow (width = 0.3-3m; height/width ratio 4-30) canyons which are characteristic of much of the cave (First and Second Fissures). Phreatic sections (height/width ratio = 0.2-3) averaging 10m² remain in several locations where flow is up dip (e.g. Mud Bank Passage, Grottoes, Corridor/First Fissure junction, Easy Street) or up the two major phreatic lifts (Figure 11.2).

3) Silt deposition phase. Water table rises to >2390m. Deposition of calcareous silts throughout the cave from the Headward Complex to Helictite Passage and Boon's Blunder in a low-velocity environment. These silts may have been deposited under full glacial conditions, with the raised water table being due to the presence of a glacier (Schroeder and Ford, 1983). Alternatively, they may be interglacial or preglacial, deposited when flowing water was more abundant at the high altitude of Castleguard Cave (Smart, 1984). The presence of high carbonate concentrations in the silts does not necessarily imply glacial flour, as high concentrations are found today in autogenic cave sediments (see Section 5.3.1). The rise in water table could have been caused by blockage during an interglacial period of the drain at the bottom of the 370m+ phreatic lift by valley aggradation. Aggraded karst springs in the Rocky Mountains are very common in the present interglacial period (Section 11.5).

4) Modern phase. Water table drops to <2000m. Small vadose streams ($Q = <0.01 \text{ m}^3 \text{ s}^{-1}$) incise trenches in silts at most locations. Large floods ($Q_s = 5 \text{ m}^3 \text{ s}^{-1}$; Smart, 1983b) almost completely remove silts from the Entrance Series, but transport coarse sediments that enable 15m of parogenesis to create the 300m long bedding-transgressive Ice Crawl. (An alternative explanation is that there was no parogenesis. In this case there would have been a series of minor phreatic lifts totalling 15m.)

11.2.3 Conclusions

It has been shown that the Darcy-Weisbach equation can be used to gain insight into the both ancient and modern hydraulic conditions in Rocky Mountain karsts. The order of magnitude differences in hydraulic gradients and friction factors between Castleguard Cave and Maligne exemplify the range of hydraulic parameters that can occur in the Rockies. This also shows the disruption caused when springs become aggraded. The >370m flow depth in Castleguard Cave is similar to the putative present flow depth of Crowsnest Spring (Section 10.4).

11.3 The water balance

The area of the Rocky Mountains, as shown in Figure 1.1, is about 145,000 km². Calculations from outcrop areas on Geological Survey of Canada maps show that karst rocks outcrops in about 33,000 km², or 23% of this area. These calculations are consistent with an earlier calculation of 17,500 km² for karst outcrops in the Rockies and Foothills of Alberta (Ozoray, 1977).

The mean discharge from the Rockies is about 2600 m³ s⁻¹ (Inland Waters Directorate, 1989a,b), so the discharge from the karst fraction should average 600 m³ s⁻¹. There is some surface runoff from karst, which would diminish groundwater flow. However, this is probably more than compensated for by the fact that limestones and dolomites are resistant to erosion; hence they cover a disproportionate amount of the higher ground, where runoff is much higher than in the valleys (see Chapter 9). So the estimate of 600 m³ s⁻¹ is considered to be a conservative minimum of mean karst groundwater flow in the Rockies.

Major gauged karst springs in the Rockies are listed in Table 11.1. In addition to these, Borneuf (1983) catalogued 165 more springs within the Alberta Rockies, but the aggregate discharge of these springs was only 8 m³ s⁻¹. Presumably many of these springs were only gauged once, in summer, but a single gauging in summer is unlikely to underestimate the mean discharge. In addition, another ten or

so karst springs with peak discharges $> 1 \text{ m}^3 \text{s}^{-1}$ have been found in the central Rockies (Figure 1.1, Section 1.2). The combined discharge of all these springs account for about 10% of the estimated discharge of the Alberta Rockies, and less than 2% of the estimated discharge of the B.C. Rockies.

In order to comprehend the karst hydrology of the Rockies, there must be some understanding of the flow paths of the ungauged 90% of karst discharge in Alberta, and the ungauged 98% in B.C. In Chapter 9, it was shown that about one third of the discharge from the karst at Crowsnest Pass is from aggraded springs, which are not easy to detect without careful discharge measurements. A further third of the runoff from the karst at Crowsnest is surface flow, and the remaining third is to visible springs. It was shown that the most productive springs, Sublacustrine Springs and Crowsnest Spring, are close to base level. These springs have a high-sulphate component of 410 l s^{-1} which probably represents regional underflow of $1.2 \text{ l s}^{-1} \text{ km}^{-2}$ from all of the Flathead and High Rock Ranges. Are these findings applicable in general to the karst of the Rockies? Surface flow and aggraded springs will be discussed in the two sections, and then underflow springs will be discussed in the following three sections.

11.4 Surface runoff from Rocky Mountains karst

It was explained in Section 2.2.1 that karst groundwater flow in the Flathead and High Rock Ranges is not obvious to the casual observer. The surface drainage net is almost intact, draining 97% of the limestone (at the 1:50,000 topographic map scale). Only detailed observation reveals that most runoff sinks into the karst, and the fluvial nets are but rarely used, being maintained by high-magnitude runoff events from the snowmelt peak.

The same situation is broadly true throughout the Rocky Mountains, with extant surface channels on probably >90% of karst rock outcrops, but with underground flow accounting for most of the discharge.

11.5 Aggrated karst springs

Most Rocky Mountain valleys have thick (>10m) glaciofluvial and alluvial deposits which form wide flood plains. These deposits are composed of sands, gravels and boulders, and are highly permeable (Barnes, 1978; Shaw and Kellerhals, 1982). Barnes (1978, p15) noted that "large point discharges do occur in recent colluvial and alluvial valley fill at the edge of many valleys underlain by carbonates. The large flow rates and localised nature of these discharge points make it inconceivable that the water is derived from the gravel deposits. Therefore it is thought that these discharge points are located over buried karst springs."

Aggrated springs play an important role at the two largest known spring sites in the Rockies, at Castleguard and Maligne. Smart (1983b) found that most of the karst spring discharge into Castleguard River is from aggrated springs. The karst outcrop along the Castleguard River extends downstream for some 5 km below the largest visible spring, Big Spring, and about 80 springs have been found in this reach, most of them being aggrated (Smart, 1983a,b). In winter, the higher springs are dry, but some tens to hundreds of litres per second was observed by the author from a helicopter in early April 1987 flowing further down Castleguard River, and this is probably derived from the Castleguard karst aquifer.

At Maligne, a majority of the discharge in winter is from the lower, aggrated springs along Maligne River, and the flow from these springs rises to an estimated $6 \text{ m}^3 \text{s}^{-1}$ in summer (Brown, 1970). In addition, there may be unquantified aggrated springs along Athabasca River.

In the Mount Robson area, karst is developed in the 300m thick Cambrian Mural Formation, which has upper and lower aquifers, separated by a thick shale unit. There are some resurgences hundreds of metres above valley level (e.g. Stump Cave, Middle Risings, a spring on the west face of Mt Robson), but the steeply-dipping limestones continue down to major valleys where aggrated springs are found (e.g. two

large springs in Small River valley, resurgence in Moose River valley for Arctomys Cave) (Thompson, 1976; Lowe, 1983; Yonge and Worthington, 1984; Huntley, 1990).

These examples demonstrate that aggraded karst springs are common in the Rockies, and thus substantiate the findings from Crowsnest Pass, where almost half the flow is from aggraded springs. It is probable that aggraded springs are an important component of almost every karst aquifer in the Rockies. The only exceptions would be where the lowest outcrop point of an aquifer was perched upon impermeable strata above the level of alluvial sediments; no such aquifers have yet been documented in the Rockies.

11.6 Regional strike-oriented underflow in the Rocky Mountains

The existence of regional strike-oriented underflow to Crowsnest Pass has been a major finding of this thesis (see Chapter 8). Is there similar regional underflow to other low-altitude transverse valleys which cross carbonates?

Some other major transverse valleys in the Rockies are the Elk (between Sparwood and Elko), the Bow (at Banff, and below Canmore), the North Saskatchewan (below Saskatchewan Crossing), the Athabasca (below Jasper), the Peace, and the Liard (Figure 1.1). All of these rivers have gauging stations upstream and downstream of the reaches of interest. However, the Bow River has been regulated since before discharge records were started, so these records cannot be used to investigate underflow.

There is a wide range in specific runoff in summer, due to varied patterns of snow- and glacier-melt. On the other hand, in winter there is very little runoff from precipitation as it is almost completely stored as snow and ice. Thus the sustained runoff in surface rivers in winter reflects depletion of groundwater reserves (Drake and Ford, 1976).

Specific discharge in winter for these major rivers is presented in Table 11.2. In every case the specific discharge in the reaches where these rivers cross the

Table 11.2 Winter discharge to some major transverse valleys in the Rocky Mountains

River	Altitude ^a m	Mean specific discharge January to March l s ⁻¹ km ⁻²			topographic catchment of D km ²	approx. underflow gain m ³ s ⁻¹	
		A	B	C			
Crowsnest River (1)	1344	-	-	3.7(2)	7.5(2)	104	1.2
Eik River (3)	730	3.0	-	4.9	8.2	1043	4
North Saskatchewan R. (4)	1400	2.1	-	2.1	3.6	630	1
Athabasca River (5)	1100	2.8	2.3(6)	1.9	4.4	3852	6
Peace River (7)	640	3.6	-	<1(8)	5.0	6300	12
Liard River (9)	340	2.3	2.6(10)	<1(8)	6.3	5130	20

Notes:

- Altitude of the lowest incision point into the aquifer
- A In main river, upstream of gaining reach
- B Tributaries in gaining reach
- C Downstream of gaining reach
- D Gaining reach
- (1) At output of Crowsnest Lake
- (2) Data from January 1986; chinooks in February and March caused extensive low-altitude (<1500m) melting, resulting in high monthly discharges at the downstream gauging point of Frank for both February (85% > average) and March (205% > average)
- (3) Between Sparwood and Elko
- (4) Between Saskatchewan Crossing and Whirlpool Point
- (5) Between Jasper and Hinton
- (6) Maligne River and Rocky River
- (7) Between Finlay Forks and Hudson Hope
- (8) Data not reliable (ice conditions)
- (9) Between Lower Crossing and Beaver River
- (10) Trout, Toad and Grayling Rivers

Sources: Crowsnest River data from this thesis. Remaining data are long-term averages from Inland Waters Directorate, 1989a,b.

major limestone ranges are anomalously high (Table 11.2, column D). Comparison with other river reaches in the vicinity (Table 11.2, columns A-C) suggests that the gain from underflow from outside the topographic catchment amounts to a total in excess of $40\text{m}^3\text{s}^{-1}$ for these six valleys.

The only karst springs in the Rockies that have been gauged by the Inland Waters Directorate are at Maligne. Over the period 1973-1988 the mean of the minimum annual discharges has been $1.94 \pm 0.19 \text{ m}^3 \text{s}^{-1}$, with a remarkably constant discharge in late winter (Figure 11.4; Inland Waters Directorate, 1989a).

These results from the major transverse valleys and from Maligne confirm the findings from Crowsnest Pass, that strike-oriented flow in the limestones to topographic low points is a major component of winter discharge. The magnitude of these flows suggests that the underflow typically travels tens of kilometres, and in examples such as Liard River distances probably exceed 100km. Such long flow paths should have a marked thermal, high sulphate/bicarbonate ratio nontherapeutic component. Banff Hot Springs and Miette Hot Springs represent two examples of such flow.

Banff Hot Springs are located on the southern side of the Bow River, where it crosses a major karst range. The largest spring (Cave Spring) is a few metres above valley level, but the other springs are up to 180m higher. All eight springs issue from the thrusted contact between Rundle Group limestones and Rocky Mountain Formation sandstones on the one hand and Fairholme Group dolomites on the other hand. Local flow paths from Sulphur Mountain (distance 1-10km) have been postulated (van Everdingen, 1972), but Equation 6.20 suggests flow paths of some tens of kilometres. Underflow from the Elk Range (up to 90km to the south) and the Vermilion Range (up to 70km to the north) seems to be likely.

Miette Hot Springs flow from the Rundle Group, where Sulphur Creek crosses the culmination of an anticline. Putative flow paths are from as far as 85km to the south-east, along the strike in the Nikannasin Range.

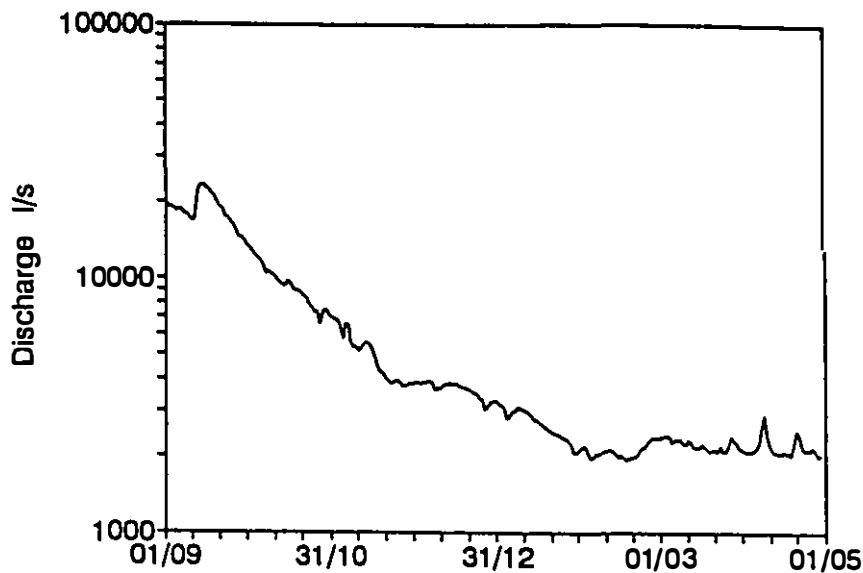


Figure 11.4 Discharge from Maligne Springs from September 1st 1985 to May 1st 1986, showing the nearly constant minimum discharge between February 1st and May 1st

11.7 Regional dip-oriented flow in the southern Rocky Mountains

Though Crowsnest Pass is the local base level of the strike-oriented flow from the Flathead and High Rock Ranges, nevertheless the Pass is on the Continental Divide, and is still 1350m above sea level, so regional groundwater flow away from it may be expected.

The presence of regional flow patterns in the western Canada sedimentary basin (Porter et al., 1982) has been established from hydraulic evidence (Hitchon, 1969a, 1969b) and geochemical evidence (van Everdingen, 1968), and recently the link between geothermal gradients and groundwater flow has been pursued in several papers (e.g. Lam et al., 1981; Hitchon, 1984; Majorowicz et al., 1985). Low geothermal gradients are generally associated with topographic highs, where there are

high piezometric surfaces and hence recharge of cold meteoric water to regional aquifers. High geothermal gradients are associated with topographic lows, and upward flow of warm formation waters (Hitchon, 1984).

None of the papers on the petroleum-rich western Canada sedimentary basin consider in detail the petroleum-poor Rockies, and much less geothermal information is available on this latter area. However, a strong positive geothermal heat anomaly has been found 30km east-south-east of Crowsnest Pass, in the Foothills and centred at Burmis on Crowsnest River. There is a strong reentrant of the 1200m topographic contour to the west along Crowsnest River, which would indicate this would be a groundwater discharge area. This could possibly be a discharge area for flow from the Flathead and High Rock Ranges. However, it is more likely that the Livingstone thrust brings water to the surface here, and that this may be the discharge point for flow from the karstic Livingstone Range.

The role of the many high-displacement (10^2 - 10^5 m) faults in groundwater circulation in the limestones of the Rocky Mountains is disputed. Van Everdingen suggested (1968, p527) that "a zone of faults and high-angle thrusts along the eastern edge of the mountain belt may prevent a large part of the recharge [from the Rockies] from getting into the [western Canada sedimentary] basin". Certainly such faults may impede flow by juxtaposing permeable strata against impermeable strata. However, in many instances springs are located on high-displacement faults. For instance, van Everdingen (1972) found that most of the thermal and mineral springs that he investigated in the southern Rocky Mountains are located on thrust faults. At Crowsnest Pass, Ptolemy Spring is located on, or very close to a thrust (Figure 2.2c). However, the situation at the two largest karst spring sites in the Rockies, at Castleguard and Maligne, is equivocal with respect to flow along faults.

At Castleguard, structural dips steepen from 4° at Castleguard Cave (Figures 11.2, 11.3) to 35° in the valley, where a structural discontinuity across the Castleguard River has been recognised (Smart, 1983a). This has been explained as

a hinge line (Ford, 1983c). However, two normal faults with a displacement of about 1000m, and with the same trend as the Castleguard valley, have been mapped at a location 4km south-east of Castleguard valley (Price and Mountjoy, 1970). These faults may extend along the strikingly linear Castleguard valley, where they would provide paths for groundwater flow to the many springs.

At Medicine Lake, the Maligne River partly sinks into the Side Sinks, which seem to be located on or very close to a thrust fault with a displacement of 200m. And along the same linear trend as the Side Sinks lies Cold Spring, which also may lie on the thrust (Kruse, 1980, Figures 2 and 7). Thus it appears that faults are important in the Rocky Mountains for transmitting water to both thermal springs and major karst springs.

Hydraulic gradients throughout the southern Rockies are much steeper west towards the Rocky Mountain Trench than east towards the Prairies (Table 11.3). Thus, an explanation more in line with the geological structure, the location of thermal and karst springs, and regional hydraulic gradients is that both faults and transmissive beds will tend to conduct water to the west, away from the western Canada sedimentary basin, towards the low-lying Rocky Mountain Trench.

There are several major faults between the Front Ranges and the Rocky Mountain Trench, which makes it difficult to estimate the optimum pathway for groundwater flow, the depth of such flow, and whether there is a pathway using only carbonate rocks. However, the steep dips to the west ensure that groundwater flow would have to rise stratigraphically at least 10km, though this could probably be accomplished using faults (Price, 1962, 1965; Price and Fermor, 1985). Rising flow routes to the Rocky Mountain Trench might be through the 1500m thick Cenozoic silts, sands and gravels in the trench itself (Thompson, 1962; Clague, 1974, 1975), or along faults in Paleozoic bedrock adjacent to the trench.

Van Everdingen (1972) studied the hot springs of the southern Rocky Mountains, and recorded that all eight hot spring groups are located in steeply-

Table 11.3 Regional hydraulic gradients from Rocky Mountain valleys east to the Prairies and west to the Rocky Mountain Trench

from	latitude	east to Prairies	west to Rocky Mountain Trench
Southern Rockies			
Crowsnest Lake	49°38'	0.005	0.010
Bow R at Banff	51°10'	0.004	0.009
Athabasca R at Jasper	52°52'	0.0015	0.004
Monkman Pass	54°33'	0.004	0.009
Northern Rockies			
Pine Pass	55°24'	0.006	0.006
Bedaux Pass	57°46'	0.007	0.005
Gundahoo Pass	58°56'	0.018	0.013

dipping limestones, and that the four major ones (Banff, Miette, Radium, Fairmont) are all located on or close to major faults. Two of these springs, Radium and Fairmont, are located west of the continental divide, and both are located adjacent to the Rocky Mountain Trench. Van Everdingen (1972) calculated that the high spring temperatures (35°-45°C) were due to the spring waters rising from depths in excess of 1200m, and suggested local sources for this hot water.

The analysis in Chapters 6 and 7 associates deep groundwater flow in karst with long travel distances, which points to the Main or Front Ranges of the Rockies as the source for Fairmont and Radium Hot Springs. Updip sources for these springs would then be about 100km north of Crowsnest Pass, but there could be further minor hot springs further south, unrecognised because they percolate up through the Cenozoic sediments of the Rocky Mountain Trench.

The combined discharge of all six groups of hot springs on the west flank of the southern Rocky Mountains is less than 1001 s^{-1} (Table 11.4), so the westward downdip groundwater flow from the karst rocks at Crowsnest Pass to the Rocky Mountain Trench is most unlikely to exceed a few tens of litres per second. Thus for water balance purposes the amount is negligible.

11.8 Regional flow to thermal springs in the northern Rocky Mountains

In the previous section, it was explained how regional hydraulic gradients in the southern Rockies are towards the west, where the low-altitude Kootenay, Columbia and Fraser Rivers are located. This is true as far north as Monkman Pass, which at $54^{\circ}33'N$ is the latitudinal mid-point of the Canadian Rockies (Figure 11.5). North of Monkman Pass, the situation is reversed, with steeper hydraulic gradients being to the east, to the low-altitude Liard and Peace Rivers (Table 11.3).

The location of hot springs in the northern Rockies is at topographic low points to the north and to the east of the mountains (Figure 11.5). This supports the contention that karst hot springs reflect regional flow to the lowest outcrop of the aquifer (Section 8.8.2, 11.6).

The Liard is the lowest river in the whole of the Canadian Rockies, descending from 480m to 340m as it traverses the Rockies. This is considerably lower than the next lowest rivers in the Rockies, the Peace River (455m at Hudson Hope), and the Fraser River (565m at Prince George). Discharge data suggest it has the highest groundwater gain of any of the investigated catchments in the Rockies (Table 11.2), and it has the highest concentration of hot springs in the Rockies (Table 11.4; Figure 11.5). This supports the arguments on regional karst groundwater flow, developed in Chapters 6, 7, and in this chapter.

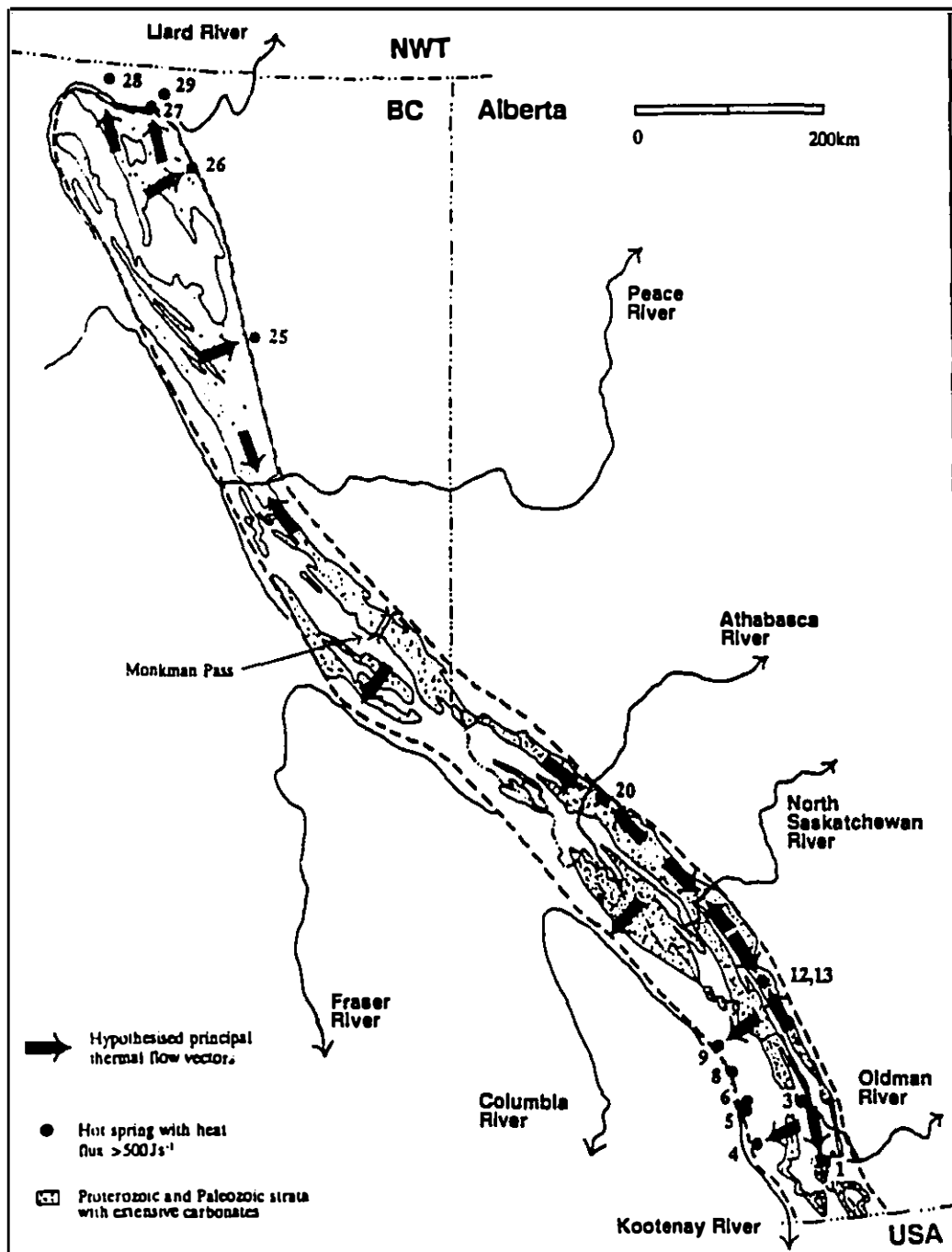


Figure 11.5 Location of major thermal springs of the Rocky Mountains. Names of numbered springs are given in Table 11.4.

Table 11.4 Heat fluxes of thermal and mineral springs of the Rocky Mountains

#	Name	Temperature °C	Q 1s ⁻¹	Valley -bottom temperature (1)	Heat flux (2) J s ⁻¹
1	Crowsnest Spring	7.5	150(3)	4	2200
2	Turtle Mountain	9.1	7.5	4	160
3	Fording Mountain	25.9	7.5	4	690
4	Wildhorse River	28.5	7.3	5	726
5	Ram Creek	36.6	3.8	5	500
6	Lussier Canyon	43.4	3.8	5	610
7	Red Rock	-	-	-	-
8	Fairmont	48.9	37	5	6800
9	Radium	47.7	30	5	5400
10	Paint Pots	10.7	5.5	4	150
11	Canmore Creek	6.1	0.083	3	1.1
12	Banff	33.7	56	3	7200
13	Vermilion Lake	19.7	13	3	910
14	Stoney Squaw	6.5	0.017	3	0.25
15	Mt Fortune	14.0	-	3	-
16	Panther River	3.0	0.75	3	-
17	Forty Mile Creek	-	-	-	-
18	Ink Pots	4.8	30	3	230
19	Canoe River	60.0	0.25	3	60
20	Miette	50.1	13	3	2600
21	Cold Sulphur	9.0	>8.3	3	>210
22	Overlander	-	-	-	-
23	Shale Banks	-	-	-	-
24	Mud Creek	-	-	-	-
25	Prophet River	-	-	-	-
26	Racing River	-	-	-	-
27	Liard River	54.0	40	0(4)	9000
28	Deer River	32.0	73	0(4)	9800
29	Grayling River	>38	>50	0(4)	>8000
30	Portage Brûlé	48.0	0.67	0(4)	130

(1) from Gadd (1986, p250)

(2) from the product of discharge and the difference between spring temperature and valley-bottom temperature (Equation 8.2)

(3) Nonephreatic component: see Figure 9.19

(4) Mean annual temperature is below 0°C, so 0° is used for heat flux calculations
Data from this thesis (#1), Evans (1990: #2), van Everdingen (1972) and Gadd (1986)

11.9 Conclusions

The findings of this chapter suggest that the runoff vectors identified and quantified at Crowsnest Pass are broadly representative of karst throughout the Rockies, with roughly equal proportions of discharge remaining on the surface, flowing to visible springs, and flowing to aggraded springs. The principal groundwater vector is along the strike to local springs, and to regional springs in the major transverse valleys. In the latter case, groundwater flow paths probably exceed 100km in some cases, and the springs will be sub-thermal or thermal. The occurrence of dip-oriented underflow to springs at low topographic positions explains the occurrence of hot springs downdip and west of the southern Rockies, but updip and east of the northern Rockies. However, this may only be a minor discharge component, since gauged hot springs only total $<0.5\text{m}^3\text{s}^{-1}$.

Proportions of bicarbonate and sulphate in overflow, underflow, and thermal karst springs are shown in Figure 11.6. The mixing of these three water types largely explain the high sulphate values found in Rocky Mountain rivers (Table 1.1), though non-carbonate rocks will also contribute to solute loads.

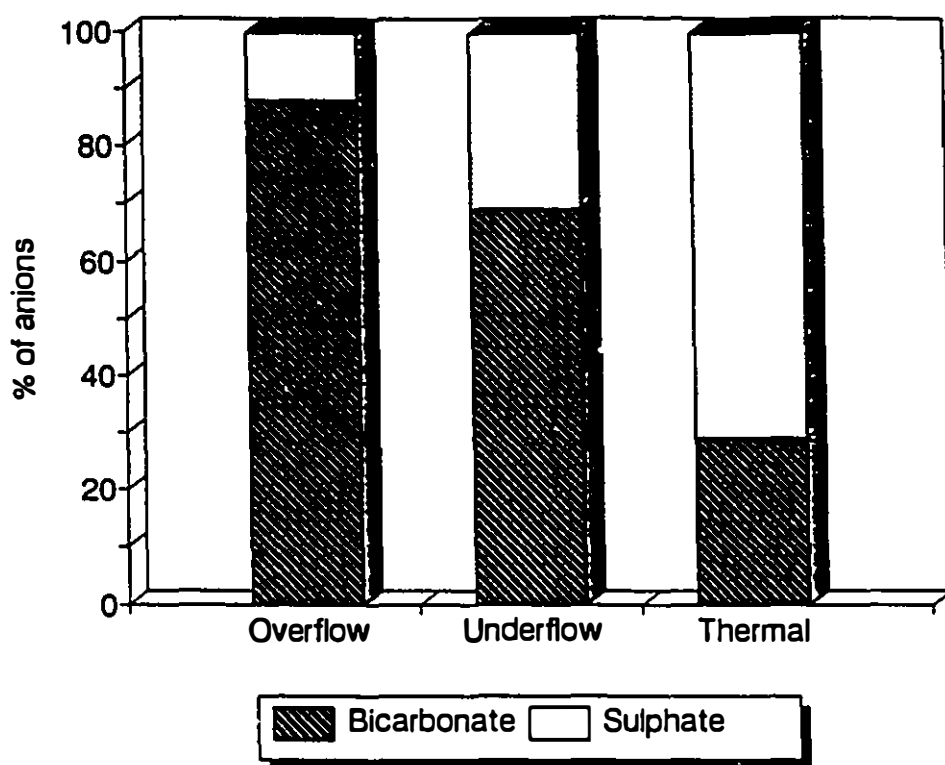


Figure 11.6 Variation in the proportions of bicarbonate and sulphate in overflow springs (Ptolemy Spring, Parrish Spring), underflow springs (Crowsnest Spring, Sublacustrine Spring), and thermal springs (Banff, Miette, Radium and Fairmont Hot Springs) in the southern Rocky Mountains (thermal spring data from van Everdingen, 1972)

Chapter 12

Karst groundwater as a geomorphic agent

Two related topics are discussed in this chapter. First, the relative importance of near-surface dissolution in karst is quantified. Second, the importance of dissolution is compared to other geomorphological processes in modifying alpine karst landscapes.

12.1 The vertical distribution of solutional erosion

Below the soil zone in karst, there is a high porosity zone which has been called the hypodermic zone (Drogue, 1980) or the subcutaneous zone (Williams, 1983; Gunn, 1986a,b). Williams (1983) defined the subcutaneous zone as the weathered zone beneath the soil, and suggested that there could be considerable water storage in this zone.

Most karst areas are soil covered, with soil-filled grikes that diminish in width slowly with depth. The data set in Figure 12.1 shows void space as a function of depth in nine areas. However, the data set is biased towards low soil cover, as 6 of 9 examples are from quarries or roadcuts where little soil cover remains. Nevertheless, the only example in Figure 12.1 with an abrupt transition from soil zone to bedrock is the glacially-smoothed surface in Burlington, Ontario, which has been shielded from dissolution since deglaciation by a carbonate-rich till. Furthermore, in all examples there is greater water storage in the soil than in the bedrock. It used to be thought that soil water in excess of the field capacity drained rapidly, but it has been shown that there is continued exponentially-decreasing discharge from soil after

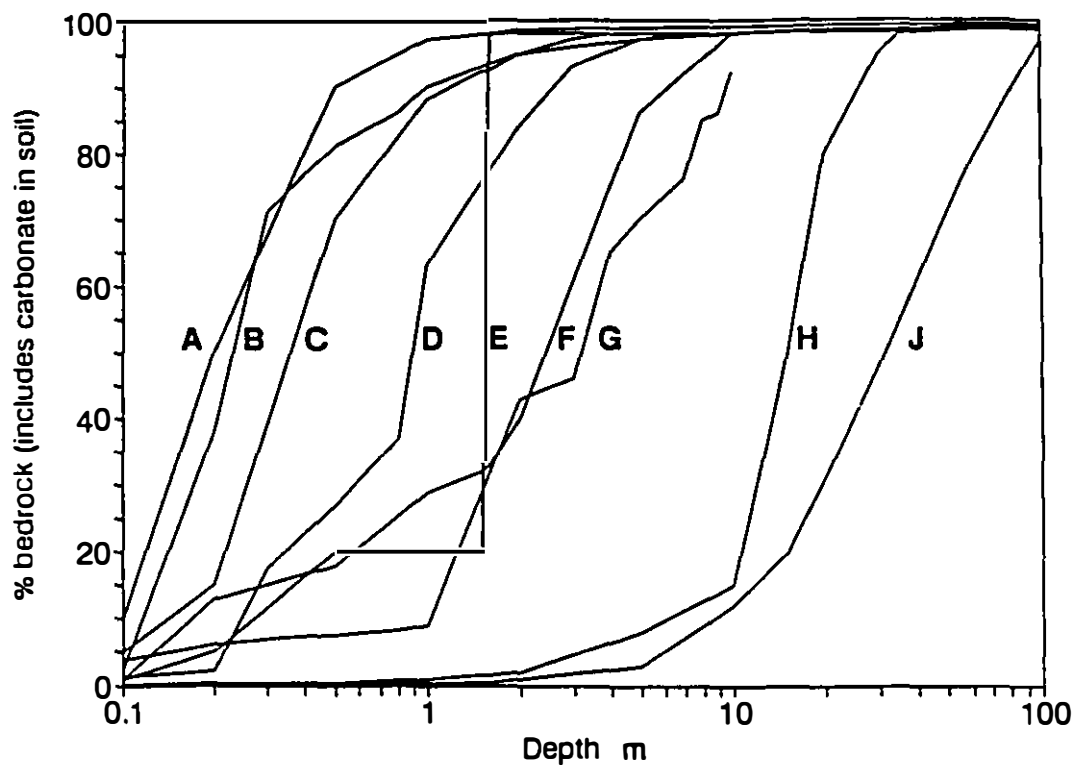


Figure 12.1 Percentage of bedrock removed by solution as a function of depth for 9 karsts

- A marble at Stoney Lake, Ontario
- B limestone in County Clare, Eire (from section in Williams, 1983)
- C dolomite at Crowe's Landing, Ontario
- D marble in Italy (from section in Williams, 1983)
- E dolomite in Burlington, Ontario
- F limestone in Indiana, USA (from section in Ford et al, 1988)
- G limestone in Mammoth Cave area, Kentucky, USA (from section in Williams, 1983)
- H limestone at Cajamar, Brazil (data from Karmann, 1990)
- J limestone in Far West Rand, South Africa (from section in Sweeting, 1975)

the field capacity is reached (Hillel, 1971). Gunn (1986b, p399) considered that "the soil zone has previously been rather neglected by karst hydrologists", and gave examples in New Zealand and England where considerable soil zone storage had been measured.

Thus it is useful to consider the soil and weathered bedrock zones together as a zone of high solutional erosion, and hence of high porosity and high water storage. The surficial zone in karst has also been called the epikarstic zone (Mangin, 1975; Friederich and Smart, 1981; Bakalowicz, 1981). This epikarstic zone, consisting of the cutaneous soil zone and the subcutaneous weathered bedrock zone, contrasts with the endokarstic zone (Bakalowicz, 1981), where near-surface weathering is absent.

It has been generally thought that most solutional erosion in karst is in the epikarst, with possibly 15-50% occurring in the endokarst (Smith and Atkinson, 1976; Gunn, 1986). Such calculations have been based on hydrochemical measurements. However, representative sampling at the base of the epikarstic zone is not possible.

Perhaps the most comprehensive data set yet collected has been that of Gunn (1981b). He sampled karst waters in the Waitomo area, New Zealand, and found that subcutaneous flow, shaft flow and some vadose flow had total hardness values in the same range as cave stream values (Table 12.1). However, vadose seepage hardnesses were lower than shaft flow and some vadose flow values, which contradicts the conventional wisdom that vadose seepage yields the highest hardness values within a karst. Furthermore, vadose flow measurements in the two field areas are very different. These contrasts, together with the large standard deviations for all infiltrating waters, suggest that the standard method of characterising infiltration by taking just a few measurements is wholly inadequate.

From the data in Table 12.1, it is apparent that the epikarstic zone is of predominant importance in solutional erosion. Unfortunately, Gunn (1981b) was not able to estimate the relative importance of the different components of infiltration at

Table 12.1 Total hardness measurements at Waitomo, New Zealand (after Gunn, 1981b)

Component	n	mean mg l ⁻¹	s mg l ⁻¹
Rainfall	26	5	4
Overland flow	6	21	20
Soil water	109	64	10
Throughflow	154	51	14
Subcutaneous flow	139	122	18
Shaft flow	58	122	18
Vadose flow (Mangapohue)	84	130	15
Vadose flow (Glenfield)	99	40	5
Vadose seepage	1714	96	19
Cymru stream (Mangapohue)	59	125	8
SP2 stream	33	126	7
Glenfield stream	59	124	9

Waitomo; in fact, this has not been quantified in any karst. This illustrates the problems of using solute data to quantify the vertical distribution of solution in karst.

However, the vertical distribution of solution *can* be simply calculated, if it is assumed that the present vertical distribution of solution has operated for an extended period. First the present porosity of the rock at different depths needs to be established.

Bonacci (1987, p47) cites the effective porosity (including solution porosity) of well-karstified limestones from 20 locations in seven countries; the mean effective porosity is 2.0%, and the median is 1.4%. Cave exploration has shown that cave passages rarely constitute a void volume >1% (Table 6.1), so it is considered that 1.5% is a representative average for endokarstic porosity, even in areas where

a high density of caves have been explored. Examination of the epikarstic zone in quarry faces indicates that the porosity increases upwards in the subcutaneous zone from about 1.5% at the base to 100% at the ground surface. The soil zone varies in thickness from zero (i.e. exposed limestone pavement) to some tens of metres of residual soils in some tropical karsts (Figure 12.1).

Now consider a unit volume of pure limestone that has now been eroded away, where the unit volume is of sufficient size to be representative of the porosity at that depth below the surface in the limestone. When the unit volume was just below the epikarstic zone, its porosity was (on average) 1.5%. Possibly 0.5% of this was primary porosity, so only approximately 1% of its mass had been dissolved up till that time in the endokarst by meteoric groundwaters. As the surface lowered, the unit volume of limestone was progressively dissolved. At the top of the subcutaneous zone, probably just a few percent of the original volume was left, in the form of rock fragments. After time, these rock fragments are dissolved away. Thus only 1% of this unit volume of limestone was dissolved in the endokarst, while 98.5% was dissolved in the epikarst.

Thus solution in the endokarstic zone is not the 15-50% quoted above, as has been commonly supposed, but at about 1% it is more than an order of magnitude less. This startling result has profound consequences for models of karst hydrochemistry and evolution.

It has previously been assumed that rapidly infiltrating, aggressive waters must make up a substantial proportion of infiltration to account for the presumed 15-50% of endokarstic solution. Such concentrated recharge infiltrates down fissures or shafts at the base of dolines, and has been considered to have low hardness and high aggressiveness (White, 1988, p201). However, the large data set from Waitomo (Table 12.1) has shown that this is not necessarily true. Furthermore, aggressive waters that are found within caves must only contribute <1% of the total spring solute load. There are two possible explanations for why they are so ineffective.

Either they may represent only a small fraction of the total discharge of the karst, or they may pass through the karst without accomplishing much solution.

The high sulphate loads found in underflow springs (Table 8.7; see also Tables 1.1 and 6.3) pose a considerable problem in the context of the 1% of solution (of CaCO_3) taking place in the endokarst. It is difficult to avoid the conclusion that the principal mineral being removed in the endokarst in most (or possibly all) karst areas is not limestone, but anhydrite (Figure 12.2).

12.2 Erosion processes and fluxes in the Rocky Mountains

It is pertinent to a karst hydrogeological study to inquire about the importance of solution and karst groundwater flow in the evolution of the landscape. This is facilitated by the fact that the Rocky Mountains are one of the most visited tourist destinations in Canada, and the mountains (and especially the karstic areas within them) have received considerable attention from geomorphologists.

Erosional fluxes studied in the Rockies include solutes (Drake, 1974; Drake and Ford, 1976), stream sediment yields (McPherson, 1975; Desloges and Gardner, 1984; Gardner, 1986), rockfall and rock slides (Luckman, 1976, 1978b; Gardner, 1979, 1980, 1983b, c), snow avalanches (Luckman, 1977, 1978a; Gardner, 1983a), solifluction (Smith, 1987, 1988), soil creep (Harris, 1973), and even the yield from burrowing by ground squirrels (Smith and Gardner, 1985). In addition there have been reviews on some aspects of erosional fluxes by Slaymaker and McPherson (1977), Luckman (1981), Ford et al. (1981), Gardner (1982), Gardner et al. (1983), and Rutter (1987).

The field studies by Luckman (1976, 1978a,b) focused on Surprise Valley, an enclosed karstic valley in the Front Ranges just south of Maligne (Figure 1.1). Luckman measured the visually-dominating coarse sediment cascade. Gardner, Smith and Desloges also investigated a Front Range carbonate area, in Kananakis Country (Figure 1.1). Studies here concentrated on both coarse and fine sediment cascades

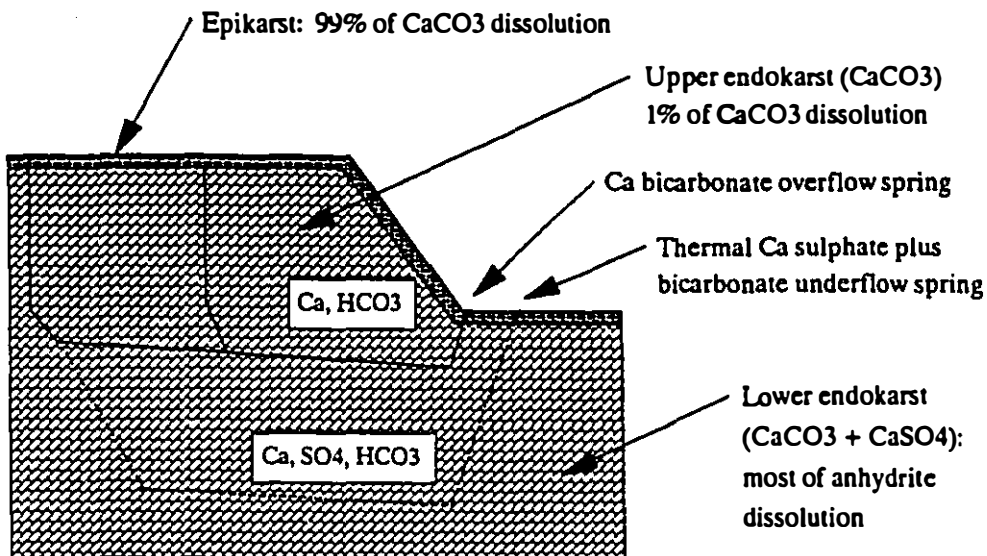


Figure 12.2 Model of the principal solutional erosion zones in karst

(Gardner, 1979, 1980, 1982, 1983a,b,c; Smith, 1987, 1988; Smith and Gardner, 1985; Gardner, Smith and Desloges, 1983).

At the output end of the sediment cascades, Water Survey of Canada data has been used by Drake (1974), McPherson (1975), Drake and Ford (1976), Slaymaker and McPherson (1977), Luckman (1981), and Gardner et al. (1983) to show that solutes are an important flux in all regional catchments, while suspended sediment fluxes vary greatly in both space and time.

The relative importance of the different erosion mechanisms in the mountains is an important factor in determining their geomorphology. Jäckli (1957) and Rapp (1960) pioneered the method of direct comparison by conversion to work done, and this has since been used by Caine (1976, 1986), Barsch and Caine (1984), and Smith and Gardner (1985). However, existing comparisons have only been at the

basin level. There is a great contrast between erosion processes and fluxes at high altitude and at low altitude in the Rocky Mountains, but this has not been quantified before. The description of the relationship between solutes and altitude (Figure 8.18) and the identification of the surficial zone as responsible for 98-99% of solution (Section 12.1) enable the altitudinal variation in solute fluxes to be calculated.

12.3 Erosional fluxes in the Ptolemy catchment

12.3.1 Measurements

The Ptolemy catchment was chosen for the erosion study because it is a well-defined catchment (Section 8.3.3), with a full year's discharge and solute data (Figures 3.8, 3.11, 3.12). Additionally, it is fairly representative of Front Range geomorphology, with an altitude range of 1420-2814m, and both scarp and dip slopes of steeply-dipping carbonates. The hypsometric curve for the catchment is shown in Figure 12.3.

Field mapping identified the areal extent of major geomorphological units (Figure 12.4). The erosion rates for most processes were taken from the literature, but data were collected in the field for the three most important processes of solute and particulate loads in streams, and of rockfall (Table 12.2).

The solution flux of limestone is the product of runoff (direct correlation with altitude) and solution rate (inverse correlation with altitude). Figure 9.20 suggests that solute loads vary linearly with altitude, from 198mg l^{-1} at the outlet of the catchment (altitude 1420m) to 37mg l^{-1} at 2400m. Above the tree line, the high-altitude solute measurements of Ford (1971) are suggestive of an exponential decrease to about 10mg l^{-1} at the altitude of Ptolemy Peak (2815m). Using Equation 9.1 for runoff and Equation 9.7 for solute loads in runoff, solution rates in the Ptolemy catchment vary from 5mm ka^{-1} at Ptolemy Peak to 14mm ka^{-1} at the outlet of the catchment. However, the maximum dissolution rate of 26mm ka^{-1} is at 1900m, just below the tree line (Figure 12.5).

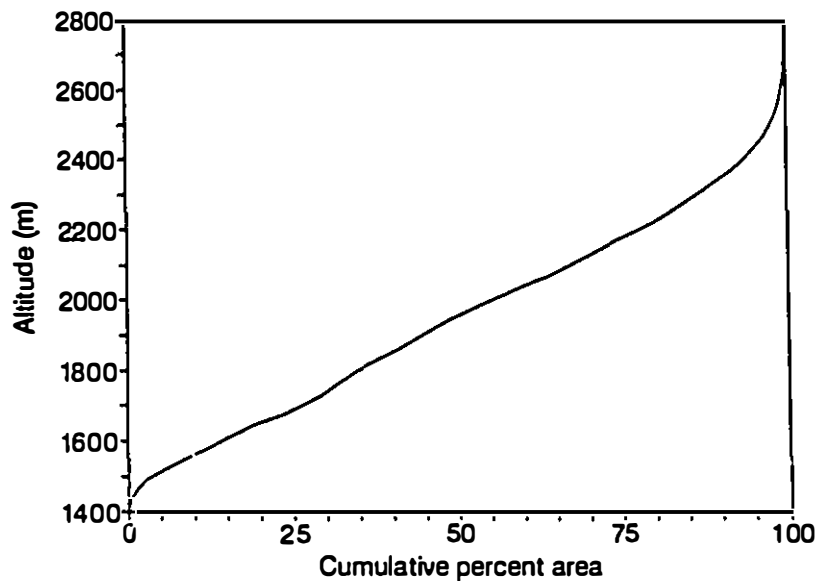


Figure 12.3 Hypsometric curve for the Ptolemy Creek catchment

Table 12.2 Erosion processes studied in the Ptolemy catchment

Process	Data source
solutes	Ptolemy Spring discharge (Table 3.3) Ptolemy Creek discharge (Table 3.3) altitudinal variation of runoff: Equation 8.1 altitudinal variation of solution: Equation 8.18
stream particulate load	Crowsnest Creek alluvial fan study
rockfall/talus shift	Emerald Lake road study Luckman (1978b), Gardner (1980)
soil creep	Harris (1973)
solifluction	Smith (1987, 1988)
snow avalanche	Luckman (1978a)

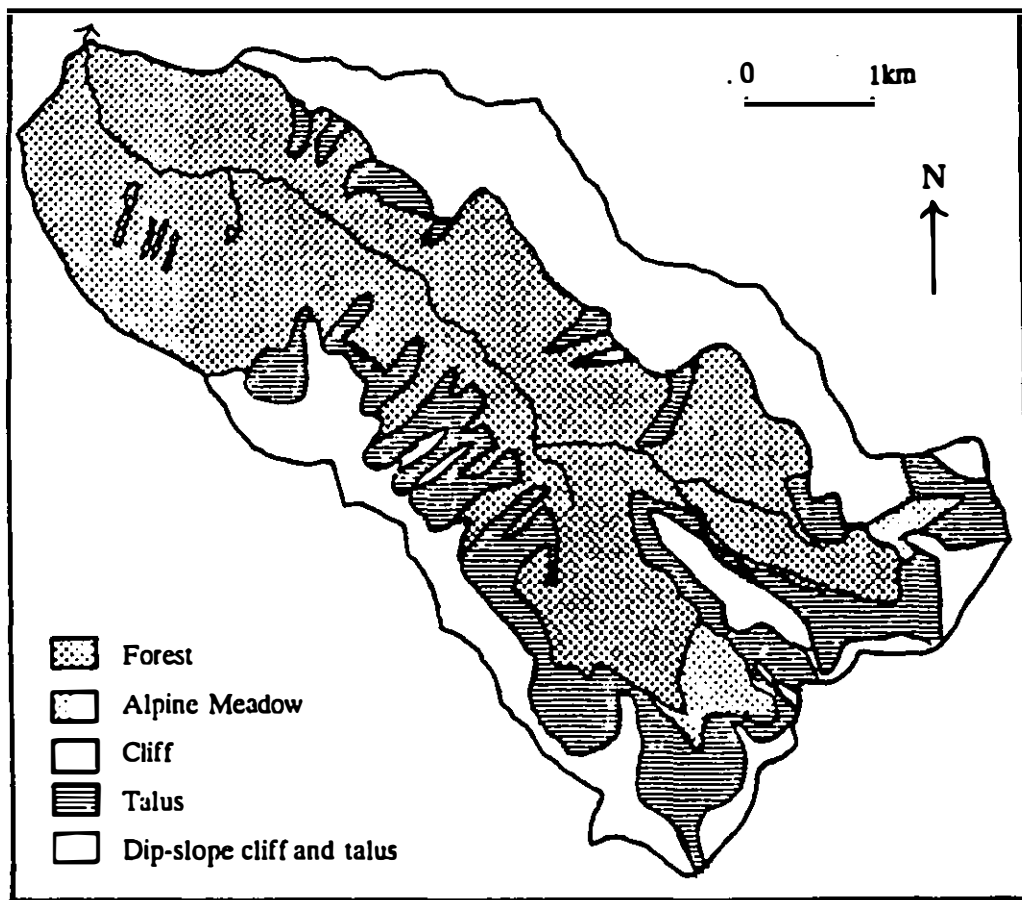


Figure 12.4 Geomorphological units of the Ptolemy Creek catchment

The variation in solution rates recorded here is much greater than in the only other comparative altitudinal study known to the author, that of Bögli (1980). He found that bare karst above the tree line suffered 78% of the solutional loss of tree-covered karst. In the Ptolemy catchment, there is a much higher altitude dependence of solution (Figure 12.5).

In addition, there is the solution derived from anhydrite, as shown by the mean value of 11 mg l^{-1} at Ptolemy Spring and 14 mg l^{-1} in Ptolemy Creek (Table 3.5).

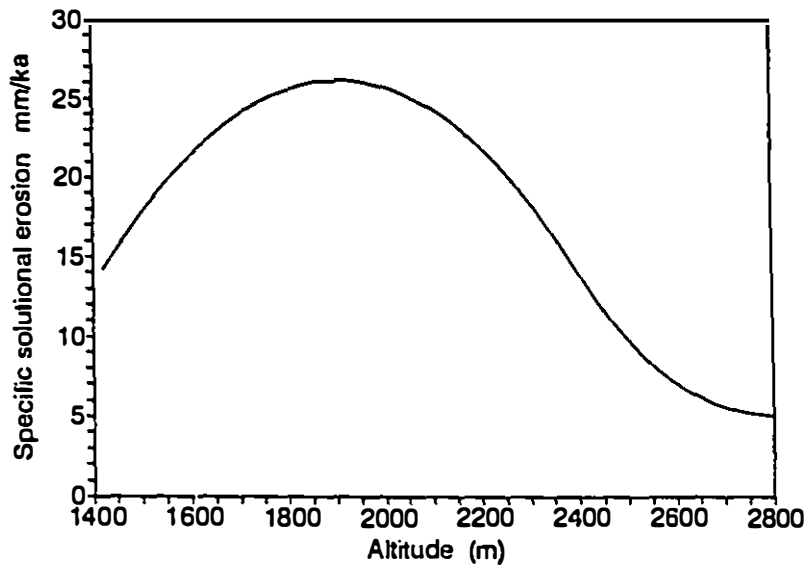


Figure 12.5 Specific dissolution of limestone in the Ptolemy Creek catchment as a function of altitude

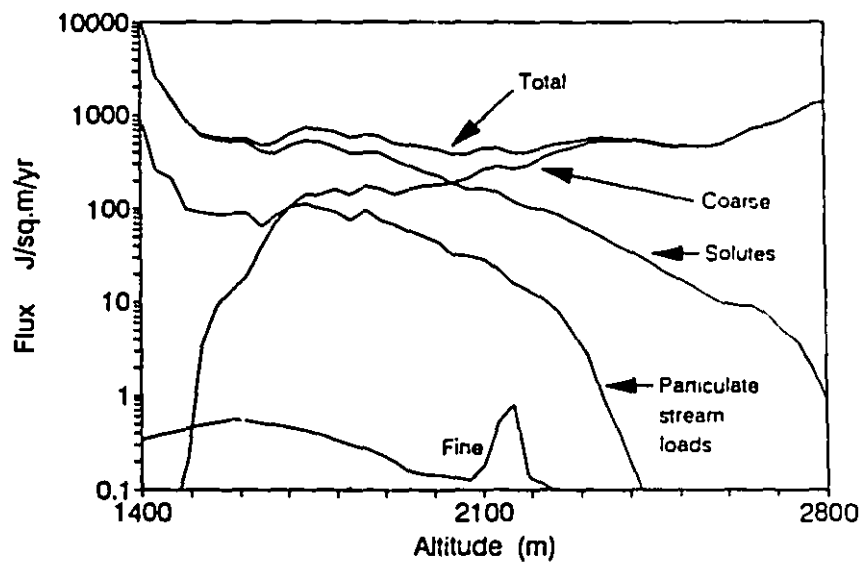


Figure 12.6 Erosional fluxes in the Ptolemy Creek catchment as a function of altitude

It is assumed that the anhydrite has the same solution rate with respect to altitude as limestone; this simplification may not be strictly true, but the possible error has little effect on the magnitude of the total solute flux.

Stream particulate loads in the Ptolemy catchment were estimated from the volume of the alluvial fan which now separates Island Lake from Crowsnest Lake. The alluvial fan has been deposited since deglaciation, 14,000 years ago. Bathymetric readings of Crowsnest Lake indicate a mean depth of 12.6m, and it is assumed that the fan started building into Crowsnest Lake-Island Lake immediately after deglaciation. This gives a volume of $1.32 \times 10^7 \text{ m}^3$ for the 700x1500m deposit, and an annual flux of 1960 tons, assuming a mean specific gravity of 2.6, and a mean porosity in the fan of 20%. Discharge readings in Crowsnest Creek and Ptolemy Creek, turbidity at high discharges, sediment composition in the fan, and channel morphology of the two creeks suggest that each creek delivers about half the total flux. Ptolemy Creek delivers most of the bedload, predominantly as limestone cobbles, while Crowsnest Creek delivers most of the suspended load which is predominantly quartz sand.

A study of rockfall was made on an abandoned paved road beside Emerald Lake. The road was built across a scree slope about 50m long, which terminates in Emerald Lake. A 345m^2 section of road, lying close to the foot of the 150m high Emerald Cliff, was cleared. One year later, 234kg of rock had accumulated, with maximum concentrations 3.8m from the foot of the cliff, and 90% of accumulation occurring within 15m of the cliff foot. The average accumulation rate for the whole scree is 0.2mm yr^{-1} , which is similar to the mean of the studies by Gardner (1983b) and Luckman (1978b).

Studies of rockfall onto scree slopes, and debris movement down the slope, have traditionally used mats to identify accumulation, and painted stones to identify movement (Rapp, 1960; Luckman, 1976, 1978b; Gardner, 1979, 1983b). Gardner et al. (1983, p105) described some of the problems, "Firstly, without direct observations

in the field, the mechanisms by which the material accumulates can only be postulated. Secondly, there is no way of knowing the source of the accreted material. The material could be derived from the upslope points and/or the free face."

The study on the almost-horizontal accumulation surface below Emerald Cliff largely eliminated the problem of debris shift. In so doing, it was able to quantify the longitudinal pattern of accumulation on a scree slope, showing that almost all rockfall is added to the Emerald Cliff scree slope close to its upper limit.

12.3.2 The altitudinal variation in erosional fluxes

Results from the Ptolemy catchment are shown in Figure 12.6. The coarse sediment cascade predominates above the treeline, and the solute cascade predominates below the treeline. The fine sediment cascade is important in restricted areas just above the treeline where there are extensive solifluction deposits.

Particulate stream loads are important at low altitudes on the north side of Ptolemy Creek, where there is considerable surface flow down the dip slope of bare limestone surfaces. On the scarp slope on the south side of Ptolemy Creek, the treeline is much higher, and there is minimal surface runoff, though avalanche tongues succeed in penetrating the treeline and transferring debris downhill.

A comparison with sediment fluxes from other studies is presented in Table 12.3. Solution is the most important flux in the Ptolemy catchment. The coarse sediment cascade is more important than in several other studies, due to the extensive outcrops of cliffs up to 500m high in the Ptolemy catchment. The order of magnitude differences in particulate loads depend on whether the coarse sediment cascade is coupled to stream channels (e.g. Upper Rhine, Mt Rae, north side of Ptolemy Creek), or uncoupled from it by lakes (e.g. Colorado) or by the water sinking underground (e.g. south side of Ptolemy catchment, Surprise catchment: Luckman, 1981).

Table 12.3 Sediment fluxes in high mountain basins

	area km ²	flux in J m ⁻² yr ⁻¹				bedload +suspended	solute
		glacial*	coarse	fine			
Upper Rhine (Jäckli, 1956)	4307	65	730	54	14000	2800	
Karkevagge (Rapp, 1960)	15	0	94	4	ND	91	
Green Lake (Caine, 1986)	2.1	1.7	31	0.42	0.63	4.9	
Williams Fork (Caine, 1986)	1.0	0	34	8.1	ND	3.3	
Eldorado Lake (Caine, 1986)	1.2	0	10	0.3	ND	1.5	
Mt Rae (Smith & Gardner, 1985)	?	ND	37	2.3	3900	860	
Ptolemy (this study)	19	0	200	0.3	61	380	

* including rock glaciers

12.4 Conclusion

In this chapter, it has been shown that the epikarst is of overwhelming importance in karst dissolution, with only 1-2% of the solution of limestone taking place in the endokarst. Solution is the most important erosional flux in the Ptolemy catchment. However, above the tree line, the coarse sediment cascade becomes the most important flux.

Chapter 13

Karst hydrogeology: a new paradigm

13.1 Introduction

This thesis has shown that flow in karst aquifers is primarily a function of the boundary factors of the aquifer. Thus the variance between different karst aquifers is primarily a function of these boundary factors, and only to a small extent to differences in transmission and storage of water within the aquifer. Since aquifer boundary factors can be measured, this new approach is more easily subject to verification by hypothesis-testing than earlier methodologies.

The findings of this thesis amount to a new paradigm for karst groundwater flow. This replaces the existing paradigm, in which boundary factors such as catchment length, stratal dip, and underflow and overflow have been considered to be factors of only minor importance in most karst aquifers.

The principal findings of this thesis are outlined below, with reference to the chapters where these new ideas are discussed.

13.2 Hydrochemistry

- 1) Only some 1% of solution is below surficial zones, not the 20-50% that has been previously supposed (Section 12.1).

- 2) It is extremely difficult to take representative samples of epikarstic or endokarstic waters. Representative samples can only be easily obtained at the catchment level (Section 12.1).
- 3) From the limited number of springs where sulphate concentrations have been measured, it appears that sulphate commonly constitutes 10-30% of the total spring load of anions (Section 9.3).
- 4) The high sulphate concentrations in the deepest flow paths in karst suggest that sulphuric acid and hydrosulphuric acid reactions may be more important than carbonic acid reactions in conduit initiation (Sections 6.7, 8.8.4, 10.3).
- 5) Hydrochemical contrasts between springs are principally due to boundary factors rather than aquifer conditions (Chapter 4).
- 6) The coefficient of variation of total hardness (CVH) of spring discharge is primarily a function of differential mixing of two different water types. Contrasts are greatest when autogenic calcium bicarbonate water mixes either with soft alloegenic water or with highly mineralised deep-circulating thermal non-phreatic waters (Sections 4.6, 9.3).
- 7) The coefficient of variation of sulphate (CVS) and of bicarbonate (CVB) are better indicators of water types than CVH. CVS is a good indicator of mixing of non-phreatic and dynamic phreatic water. CVH may indicate mixing of alloegenic and autogenic flow and/or flow from source areas with different soil CO₂ concentrations (Sections 4.3, 9.3).
- 8) Solutional erosion constitutes only a minor fraction of erosion above the tree line, except on lapiaz. The maximum rate of solutional erosion in alpine karst is just below the tree line.

13.3 Hydraulics

- 1) The Hagen - Poiseuille equation demonstrates that deep flow in most karst catchments ($L > 3\text{ km}$) is more efficient than shallow flow (Section 6.4.1).

- 2) Hydraulic gradients have an exponential form (Section 5.3.4).
- 3) Hydraulic gradients are typically 0.0001-0.05 at maximum discharges, and 1-2 orders of magnitude less than this at low flow (Section 5.3.4, Table 6.1).
- 4) Darcy-Weisbach friction factors vary by >3 orders of magnitude, from <0.1 for unobstructed conduits to >100 for conduits feeding aggraded springs (Section 5.3.5).
- 5) Discharge variability of karst springs (Q_f/Q_n) is typically 10-200 (Section 5.3.2).
- 6) Most active conduits have closed-channel flow (Section 8.3).
- 7) In addition to the previously-recognised initiation, enlargement and stagnation phases in the life of a conduit, it is also possible to recognise that there is a nothephreatic phase of laminar conduit flow in some conduits, and a dynamic equilibrium phase (Sections 8.5, 5.3.1).
- 8) Most active phreatic passages are in the dynamic equilibrium phase. Maximum velocities in these conduits are about 0.2 ms^{-1} , so mean velocities are usually in the range $0.02-0.03 \text{ ms}^{-1}$ (Section 5.3.1).

13.4 Discharge and drainage

- 1) Each overflow spring (or stream) has a complementary underflow spring (Section 4.2).
- 2) Any surface stream on karst gains or loses flow to groundwater, and frequently it does both (Section 4.2).
- 3) Finite hydraulic gradients ensure that at least some groundwater must emerge at the lowest outcrop point of an aquifer, except in coastal aquifers, where the denser seawater will limit freshwater flow depth (Section 4.2).
- 4) Discharge contrasts between springs are principally due to boundary factors rather than aquifer conditions (Chapter 4).
- 5) Most karst springs have underflow and/or overflow components, so full-flow springs are rare. On the basis of recession exponents it is possible in theory to

distinguish full flow, seasonal overflow, perennial overflow, high-stage underflow, low-stage underflow, and overflow-underflow types. In practice, overflow springs are usually only recognised as such if they dry up seasonally, and underflow springs are often aggraded so are missed (Section 4.2).

- 6) Water budget studies have shown that a substantial proportion of runoff from karst flows to aggraded springs, which are not readily apparent in the field (Sections 4.2, 9.6, 10.5).

13.5 Morphometric analysis of conduits and conduit flow

- 1) Bedding planes are the major fractures used in karst groundwater flow in almost all aquifers. The ratio of bedding planes to joints used in any hydrological situation is a function of the relationship between the flow path and the stratal dip and strike (Section 6.3.3).
- 2) The initial primary tubes may have any orientation with respect to the stratal dip, and are simply oriented down the hydraulic gradient (Section 6.3.2).
- 3) Conduit density in karstic limestones is commonly 10-100 km km⁻³ (Section 6.2.2).
- 4) The porosity in karstic limestones attributable to conduits is commonly 0.1-1% (Section 6.2.3).
- 5) Conduit flow paths are commonly 30-80% longer than the straight-line distance (Section 6.2.5).
- 6) The width of a conduit flow belt is commonly 10-20% of the straight-line length (Section 6.2.6).
- 7) Crest/base depth ratios are usually >0.5 (Section 6.2.7).
- 8) Phreatic flow depth is commonly in the range 1/30 to 1/300 of catchment length (Table 6.1,

13.6 A comprehensive model of karst groundwater flow

- 1) The fracture-controlled Hagen-Poiseuille flow field determines where conduits will form in a karst aquifer. Empirical data clearly shows the initial Hagen-Poiseuille flow net in an aquifer determines the positioning of conduits. This contention is supported not only by the high correlation between conduit depth and length/dip, but also by loop crest/base ratios >0.5 , initial phreatic drops and terminal phreatic lifts in main conduits and tributaries, and targeting of tributary flow fields (Sections 6.2.2, 7.2, 7.3, 7.5.1).
- 2) At any stage in the development of a conduit aquifer, it is the Hagen-Poiseuille flow field towards pre-existing conduits and springs which determines the position of the next generation of conduits (Section 8.5).
- 3) Though conduits are formed at depth below the water table, base-level lowering will reduce the flow depth over time. Thus a conduit evolves from "deep phreatic" to "shallow phreatic" to a position above the water table after it is abandoned (Section 8.5).
- 4) Below an active conduit there is a Hagen-Poiseuille flow net. In homoclinal strata with constant catchment length, this net has similar characteristics to the flow net which produced the active conduit. With lowering of external base level a tiered cave is produced, with constant spacing between tiers. Thus cave tiers are endogenetic (Section 8.7).
- 5) The Hagen-Poiseuille flow net below an active conduit is typically active for 10^6 years before the new conduit thus produced is utilised by turbulent flow. It seems probable that laminar flow through the lower conduit produces non-phreatic passage forms such as anastomoses and pendants. These lower flow routes tend to have high sulphate loads for reasons that are not altogether clear, and high temperatures, and resurge at the lowest outcrop points of aquifers, often as aggraded springs (Sections 8.5, 8.8).

- 6) In a tiered cave, the capture of flow to a new, lower flow route is a function primarily of increasing inefficiency of flow in the existing conduit, rather than of increasing efficiency of flow in the new conduit (Section 8.5).
- 7) Dynamic phreatic flow is characterised by calcium bicarbonate plus sulphate water. Non-phreatic flow is characterised by calcium sulphate plus bicarbonate waters (Section 8.8).
- 8) It is not clear from kinetic and hydraulic theory whether conduits should propagate from sink to spring, or from spring to sink (Section 6.7).
- 9) The phreatic depth of conduits is a simple function of catchment length, and the relationship between dip, strike and the flow direction. These three factors account for over 90% of the variance in depth. Factors such as mixing corrosion, fracture spacing and the amplitude of surface topography have a limited or negligible importance. This function explains both fracture flow (in wells) and conduit flow (in caves) (Sections 7.2, 7.4).
- 10) Speleothem dates and vadose passage slopes indicate that even after $>10^6$ years only a small minority of fractures in karst are utilised by conduit flow. Maximum fracture utilisation is only attained in the epikarst, where it is typically 1-3 orders of magnitude higher than in the endokarst (Section 8.6).
- 11) Vauclusian springs are the normal springs for karst aquifers where aquitards do not block the flow. Most of the major karst springs of the world are vauclusian. Their great depths are a function primarily of the great length of their catchments (Section 7.3.2).
- 12) In humid tropical areas vauclusian springs are still common, but cave river incision rates are frequently able to keep pace with base level lowering rates, so tall passages occupied by low-gradient rivers result. Such passages are absent from temperate areas (Section 8.3).
- 13) The formation of an underground delta at a vauclusian spring is a consequence of a falling base level (Section 8.4).

- 14) Tributary conduits join main conduits at large acute angles in plan view (as with tributaries of surface rivers). In a vertical sense, they may join at grade, or as phreatic lifts or drops. Proximal inputs tend to join as drops, and distal inputs tend to join as lifts (Section 7.5.1).

Chapter 14 Conclusions

This thesis has proposed a holistic model of groundwater flow. It incorporates and explains springs with different hydrological regimes (e.g. underflow, overflow), physical characteristics (aggraded, non-aggraded), temperature characteristics (thermal, non-thermal), radioisotope characteristics (dynamic phreatic, non-phreatic), and hydrochemical characteristics (calcium bicarbonate, calcium sulphate).

There are three contrasting types of karst springs in the Rocky Mountains, calcium bicarbonate non-aggraded springs with high discharge variance, calcium bicarbonate plus sulphate springs with low discharge variance, and thermal springs. These have not previously been integrated into a unified groundwater flow model.

The new model explains all three types of spring as part of an evolving groundwater flow net. Thermal springs are one end member. They represent the earliest manifestations of conduit flow, with deep, slow-moving, laminar flow through fissures and proto-conduits producing high-sulphate thermal water; the integrated flow is then delivered rapidly up better-developed conduits to the surface. These springs represent more the removal of anhydrite from the aquifer than of limestone and dolomite. Thermal springs reflect a regional flow pattern, with flow paths up to hundreds of kilometres.

Visible springs represent the other end member. They are overflow springs, so have high discharge variance. They represent the removal of limestone and dolomite with small amounts of anhydrite, via large conduits with rapid, often turbulent flow. Overflow springs represent local flow vectors.

Augmented underflow springs are intermediate in function and characteristics.

The principal problem with the new model is the imprecise role played by the anhydrite. Its presence appears to be ubiquitous in early conduit flow, so it may be that the dissolution of anhydrite is the key to the initiation of conduit flow. As Drake (1974) concluded at the end of his study of the same area, isotopic analysis of the sulphate would help indicate its origin. More sampling of underflow springs in other areas is also needed to establish the concentration and flux of sulphate.

There are perhaps two fields where the results from this thesis will be particularly useful. Mississippi Valley type (MVT) ore deposits are now understood to be emplaced at relatively low temperatures (<200°C) in carbonates, and it has been shown that gravity-driven regional flow is a plausible mechanism (Garven and Freeze, 1984). There has been much computer modelling in recent years, most of which has used the Darcian approach (e.g. Garven and Freeze, 1984), or considered the flow paths as being along tectonic fractures (e.g. Deloule and Turcotte, 1989). It would appear that the ore fluids migrated along dissolutional conduits (Ford and Williams, 1989). It would seem that thermal karst springs provide a direct modern analogue for MVT fluid migration, and modelling using conduit flow should prove fruitful. Also, the investigation of thermal karst springs as modern analogues may better define concepts on the extent of ore bodies.

This thesis may also be useful in providing a theory for understanding karst groundwater flow, which may be applied to give more accurate results in hydrogeological studies.

References

- Alberta Environment, 1980. Surficial geology: Alberta foothills and Rocky Mountains, Sheet 6. Alberta Research Council.
- Albutt, A., 1977. An appraisal of the conductance method for the in situ measurement of total hardness and aggressivity. *Trans. British Cave Research Assoc.*, 4, 431-439.
- Aley, T., and M.W. Fletcher, 1976. Water tracers cookbook. *Missouri Speleology*, 16(3), 1-32.
- Anon., 1988. Cheddar caves, '88. *Descent*, #83, 34-36.
- Anon., 1989a. Major northern link completed. *Descent*, #88, p5.
- Anon., 1989b. Northern news: Lancaster Hole. *Caves and Caving, Bull. of the British Cave Research Assoc.*, #45, p29.
- Arnos, B., 1981. Ice and snow hydrology. In: *Stable isotope hydrology: deuterium and oxygen-18 in the water cycle*, (Eds. J.R. Gat and R. Gonfiantini). Tech. Report Series, #210, Int. Atomic Energy Agency, Vienna, 143-176.
- ARSIP (Association de Recherches Spéléologiques Internationales de la Pierre Saint-Martin), 1985. Le karst de la Pierre Saint-Martin en quelques chiffres (Pyrénées-Atlantiques France et Navarre Espagne). *Karstologia*, #6, 3-6.
- Ashmead, P., 1967. The origin and development of Ease Gill Caverns. *Trans. Cave Res. Group of Great Britain*, 9, 104-112.
- Ashmead, P., 1974. Development of the caves of Casterton Fell. In: *Limestone and caves of north-west England*, (Ed: A.C. Waltham), David & Charles, Newton Abbot, p250-272.
- Ashton, K., 1966. The analyses of flow data from karst drainage systems. *Trans. Cave Res. Group G.B.*, 7(2), 161-203.
- Atkinson, T.C., 1968. The earliest stages of underground drainage in limestone - a speculative discussion. *Proc. British Speleological Assoc.*, 6, 53-70.
- Atkinson, T.C., 1977a. Diffuse flow and conduit flow in limestone terrain in the Mendip Hills, Somerset (Great Britain). *J. Hydrol.*, 35, 93-110.
- Atkinson, T.C., 1977b. Carbon dioxide in the atmosphere of the unsaturated zone: an important control of groundwater hardness in limestones. *J. Hydrol.*, 35, 111-123.
- Atkinson, T.C., 1984. Notes from Karst Hydrology course, Western Kentucky Univ.
- Atkinson, T.C., R.S. Harmon, P.L. Smart and A.C. Waltham, 1978. Palaeoclimatic and geomorphic implications of $^{230}\text{Th}/^{234}\text{U}$ dates on speleothems in Britain. *Nature*, 272, 24-28.

- Atkinson, T.C., and P.L. Smart, 1977. Caves and karst of southern England and South Wales. Guidebook for 7th Internat. Congress of Speleology, Sheffield. Brit. Cave Res. Assoc., Bridgwater, 83p.
- Atkinson, T.C., and P.L. Smart, 1980. Artificial tracers in hydrogeology. In: A survey of British hydrogeology 1980. Royal Society, London, 173-190.
- Atkinson, T.C., P.L. Smart and T.M.L. Wigley, 1983. Climate and natural radon levels in Castleguard Cave, Columbia Icefields, Alberta, Canada. Arctic and Alpine Res., 15, 487-502.
- Atkinson, T.C., and D.I. Smith, 1974. Rapid groundwater flow in fissures in the Chalk - an example from South Hampshire. Q. Jnl. Engng. Geol., 7, 197-205.
- Atmospheric Environment Service, 1985. Monthly records. Meteorological observations in Western Canada, vol. 70, in 12 monthly parts, plus an annual supplement. Environment Canada, Downsview, Ont.
- Atmospheric Environment Service, 1986. Monthly records. Meteorological observations in Western Canada, vol. 71, in 12 monthly parts, plus an annual supplement. Environment Canada, Downsview, Ont.
- Auler, A. 1988. Gruta do Padre (Brésil), la plus longue grotte de l'Amérique du Sud. Spelunca, #32, 18-22.
- Back, W., and B.B. Hanshaw, 1970. Comparison of chemical hydrogeology of the carbonate peninsulas of Florida and Yucatan. J. Hydrol., 10, 330-368.
- Bakalowicz, M., 1973. Les grandes manifestations hydrologiques des karsts dans le monde. Spelunca, 2, 38-40.
- Bakalowicz, M., 1979. Contribution de la géochimie des caux à la connaissance de l'aquifère karstique et de la karstification. Thèse doct. sci. nat., Univ. Curie, Paris, 269p.
- Bakalowicz, M., 1984. Water chemistry of some karst environments in Norway. Norsk geogr. Tidsskr., 38, 209-214.
- Bakalowicz, M., B. Blavoux and A. Mangin, 1974. Apports du traçage isotopique naturel à la connaissance du fonctionnement d'un système karstique - teneurs en oxygène-18 de trois systèmes des Pyrénées, France. J. Hydrol., 23, 141-158.
- Bakalowicz, M., and A. Mangin, 1980. L'aquifère karstique. Sa définition, ses caractéristiques et son identification. Mém. h. sér. Soc. géol. France, #11, 71-79.
- Ball, T.K., and J.C. Jones, 1990. Speleogenesis in the limestone outcrop north of the South Wales Coalfield: the role of micro-organisms in the oxidation of sulphides and hydrocarbons. Cave Science, 17(1), 3-8.
- Bally, A.W., P.L. Gordy, and G.A. Stewart, 1966. Structure, seismic data, and orogenic evolution of southern Canadian Rocky Mountains. Bull. Canadian Petroleum Geology, 14(3), 337-381.
- Barnes, R.G., 1978a. Hydrogeology of the Brazeau - Canoe River area, Alberta. Alberta Research Council, Earth Sciences Report 77-5, 32p.

- Barnes, R.G., 1978b. Hydrogeology of the Mt Robson - Wapiti area, Alberta. Alberta Research Council, Earth Sciences Report 76-5.
- Barsch, D., and N. Caine, 1984. The nature of mountain geomorphology. *Mountain Res. and Development*, 4, 287-298.
- Barton, T., 1981a. The Back Door: Mendips to Yorkshire Pot. *Canadian Caver*, 13(1), 4-10.
- Barton, T., 1981b. Crowsnest Spring dives. *Canadian Caver*, 13(2), 34-36.
- Bass, M., 1990. News North: East Kingsdale water found. *Descent*, #97, 12.
- Bassett, J., 1976. Hydrology and geochemistry of the Upper Lost River drainage basin, Indiana. *NSS Bull.*, 38(4), 79-87.
- Bauer, F., and J. Zötl, 1972. Karst of Austria. In: *Karst. Important karst regions of the Northern Hemisphere*, (Eds. M Herak and V.T. Stringfield), Elsevier, p225-266.
- Beaupré, M., D. Caron and G. Dubuc, 1976. L'exploration spéléologique au Québec. In: *Cave Exploration in Canada*, p19-38.
- Bedinger, M.S., 1966. Electric-analog study of cave formation. *Bull. Nat. Speleol. Soc.*, 28, 127-136.
- Belloni, S., R. Martinis and G. Orombelli, 1972. Karst of Italy. In: *Karst. Important karst regions of the Northern Hemisphere*, (Eds. M Herak and V.T. Stringfield), Elsevier, p85-128.
- Benischke, R., H. Zojer, P. Fritz, P. Maloszewski and W. Stichler, 1988. Environmental and artificial tracer studies in an Alpine karst massif (Austria). In: *Karst hydrogeology and karst environment protection (Proc. IAH 21st congress)*, Eds. Yuan Daoxian and Xie Chaofan. Geological Publ. House, Beijing, p938-947.
- Benoit, P., and B. Collignon, 1988. Rhar Bou'Maza ou la Tafna souterraine, Monts de Tlemcen, Algérie. *Spelunca*, #32, 31-38.
- Blak, R., 1990. Belize expedition '89. *Canadian Caver*, 22(1), 26-29.
- Bögli, A., 1964. Mischungskorrosion - ein Beitrag zum Verstärkungsproblem. *Erdkunde*, 18, 83-92.
- Bögli, A., 1970. Das Höllloch und sein Karst. *De la Baconnière*, Neuchâtel, 109p.
- Bögli, A., 1980. Karst hydrology and physical speleology. Springer-Verlag, Berlin, 284p.
- Bonacci, O., 1987. Karst hydrology, with special reference to the Dinaric karst. Springer-Verlag, Berlin, 184p.
- Boon, J.M., 1974. Escondida - to the sump. *Canadian Caver*, 6(2), 45-54.
- Boon, J.M., 1977a. Down to a sunless sea. Stalactite Press, Edmonton, 105p.
- Boon, J.M., 1977b. A grim journey and a through trip, Sumidero Chicja. *Canadian Caver*, 9(2), 12-14.

- Borneuf, D., 1980. Hydrogeology of the Kananaskis Lake area, Alberta. Alberta Research Council, Earth Sciences Report 79-4.
- Borneuf, D., 1983. Springs of Alberta. Earth Sciences Report 82-3, Alberta Research Council, 95p.
- Bray, L.G., 1976. Recent chemical work in the Ogof Ffynnon Ddu system: A conductimetric study including a novel method for aggressiveness assessment. Trans. British Cave Research Assoc., 3(1), 20-28.
- Bray, L.G., 1977. The role of organic matter in limestone solution in the Ogof Ffynnon Ddu streamway. Proc. 7th Internat. Congress of Speleology, Sheffield. British Cave Res. Assoc., Bridgwater, 65-68.
- Bretz, J.H., 1942. Vadose and phreatic features of limestone caverns. J. Geol., 50, 675-811.
- Brook, D.B., 1974. Cave development in Kingsdale. In: Limestone and caves of north-west England (Ed. A.C. Waltham), p310-334.
- B.R.G.M. (Bureau de Recherches Géologiques et Minières), 1979. Carte géologique de la France à 1:50000, Terrasson, XX-35.
- Brook, D.B., and A.C. Waltham, 1978a. Caves of Mulu. Royal Geog. Soc., London, 44p.
- Brook, D.B., and A.C. Waltham, 1978b. The underworld of Mulu, part 1. Caving International Magazine, #1, 3-10.
- Brook, G.A., 1976. Geomorphology of the North Karst, South Nahanni River region, Northwest Territories, Canada. Unpubl. PhD thesis, McMaster Univ., 627p.
- Brown, M.C., 1970. Karst geomorphology and hydrology of the lower Maligne Basin, Jasper, Alberta. Unpubl. PhD thesis, McMaster Univ., 178p.
- Brucker, T.A., 1989. Cave systems south of the Green River. In: Karst hydrology: concepts from the Mammoth Cave area, (Eds. W.B. White and E.L. White), Van Nostrand Reinhold, New York, p175-188.
- B.S.E.E. (British Speleological Expedition to Ethiopia: S.N. Amatt, D. Catlin, P.R. Ramsden, R.W. Ramsden, T. Raynor, T. Renvoize, S.R.H. Worthington), 1973. The caves of Ethiopia. Trans. Cave Research Group of G.B., 15, 107-168.
- Buchanan, J.P., 1989. Geology and geomorphology of the Bastille karst. Canadian Caver, 21(1), 38-39.
- Buck, M., 1990. Private communication.
- Caine, T.N., 1976. A uniform measure of subaerial erosion. Bull. Geol. Soc. Amer., 87, 137-140.
- Caine, T.N., 1986. Sediment movement and storage on alpine slopes in the Colorado Rocky Mountains. In: Hillslope Processes, Ed. A.D. Abrahams, Allen & Unwin, Boston, 115-137.
- Chabert, C., 1977. Sur trois systèmes karstiques de grande ampleur: Eynif, Kembos et Dumanli (Taurus Occidental). Proc. 7th Internat. Congress Speleology, Sheffield, 1977. Ed: T.D. Ford. Brit. Cave Res. Assoc., Westonbirt, Somerset, p105-108.

- Chabert, C., 1981. *Les grandes cavités Françaises*. Fédération Française de Spéléologie, Paris, 154p.
- Charity, R.A.P. and N.S.J. Christopher, 1977. The stratigraphy and structure of the Ogof Ffynnon Ddu area. *Trans. British Cave Research Assoc.*, 4, 403-416.
- Chen Wenjun, 1988. The study of Disu underground river system, Du'un County, Guanxi. In :Karst hydrogeology and karst environment protection (Proc. IAH 21st congress), Eds. Yuan Daoxian and Xie Chaofan. Geological Publ. House, Beijing, p543-551.
- Chen Yusun and Bian Ji, 1988. The media and movement of karst water. In :Karst hydrogeology and karst environment protection (Proc. IAH 21st congress), Eds. Yuan Daoxian and Xie Chaofan. Geological Publ. House, Beijing, p555-564.
- Chevalier, P., 1951. Subterranean climbers. Faber & Faber. Republished 1975 by Zephyrus Press, Teaneck. Originally published 1948 as Escalades souterraines.
- Christopher, N.S.J. and J.S. Beck, 1977. A survey of Carlswark Cavern, Derbyshire, with geological and hydrological notes. *Trans. British Cave Research Assoc.*, 4(3), 361-365.
- Christopher, N.S.J., J.S. Beck and P.T. Mellors, 1977. Hydrology - water in the limestone. In: Limestone and caves of the Peak District, Ed: T.D. Ford. Geo Books, Norwich, p185-230.
- Christopher, N.S.J., S.T. Trudgill, R.W. Crabtree, A.M. Pickles and S.M. Culshaw, 1981. A hydrological study of the Castleton area, Derbyshire. *Trans. Brit. Cave Res. Assoc.*, 8(4), 189-206.
- Church, M., 1974. Electrochemical and fluorometric tracer techniques for streamflow measurements. *Bull. Geomorph. Res. Group*, #12, 71p.
- Clague, J.J., 1974. The St Eugene Formation and the development of the southern Rocky Mountain Trench. *Can. J. Earth Sci.*, 916-938.
- Clague, J.J., 1975. Late Quaternary sediments and geomorphic history of the southern Rocky Mountain Trench, British Columbia.
- Coase, A., and D. Judson, 1977. Dan yr Ogof and its associated caves. *Trans. British Cave Research Assoc.*, 4, 247-344.
- Cogley, J.G., 1970. Analysis of some hydrological features of the Crowsnest area, western Canada. Unpublished report, 38p.
- Colin, P., and P. Drouin. 1986. La grotte de la Doua. *Spelunca*, #24, 20-24.
- Collignon, B., 1987. La mise en exploitation des aquifères karstiques: quelques exemples algériens. *Karstologia*, #10, 17-24.
- Collignon, B., 1990. Les grandes découvertes de l'expédition franco-chinoise "Gebihe 1989". *Spelunca*, #37, 19.
- Coons, D., 1976. The river caves. *Canadian Caver*, 8(1), 34-41.
- Courbon, P. and C. Chabert, 1986. *Atlas de grandes cavités mondiales*. Union Internationale de Spéléologie / Fédération Française de Spéléologie, Paris, 255p.

- Courbon, P., C. Chabot, P. Bosted and K. Lindsley, 1989. *Atlas of the great caves of the world. Cave books*, St Louis.
- Courbon, P. and J. Dreux, 1976. *Candelaria: étude du réseau hydrospéléologique de Candelaria, Alta Verapaz. Spelunca special #1*, supplement to 1973, #3, p12-17.
- Couturaud, A., and Y. Aucant, 1990. *Un grand réseau du Jura: Le Verneau (Doubs, France)*. *Spelunca*, #38, 30-41.
- Coward, J.M.H., 1975. *Paleohydrology and streamflow of three karst basins in southeastern West Virginia, USA*. Unpubl. PhD thesis, McMaster Univ., 394p.
- Cowell, D.W., 1976. *Karst geomorphology of the Bruce Peninsula, Ontario*. Unpubl. MSc thesis, McMaster Univ., 231p.
- Cox, N.H., 1990. Wisconsin's greatest challenge: Tecumseh (Horseshoe Bay) Cave. *NSS News*, 48(10), 248-254.
- Crowther, J., 1978. Karst regions and caves of the Malay peninsula, west of the Main Range. *Trans. Brit. Cave Research. Assoc.*, 5(4), 199-214.
- Cundill, J.R., 1955. Notes on faulted Mississippian section at Crowsnest Pass. *J. of the Alberta Soc. of Petroleum Geologists*, 3, 138-139.
- Curry, G.E. and A.S. Mann, 1965. Estimating precipitation on a remote headwater area of western Alberta. *Proc. 33rd Western Snowmelt Conf.*, Colorado Springs, 58-66.
- Davis, W.M., 1930. Origin of limestone caverns. *Bull. Geol. Soc. Amer.*, 41, 475-628.
- Davies, W.E., 1960. Origin of caves in folded limestone. *Bull. Nat. Speleol. Soc.*, 22, 5-18.
- Deike, G.H., III, 1989. Fracture controls on conduit development. In: *Karst hydrology: concepts from the Mammoth Cave area*, (Eds. W.B. White and E.L. White), Van Nostrand Reinhold, New York, p259-292.
- Delance, J.H., 1988. *Le karst de Bourgogne*. *Karstologia*, #11-12, 7-16.
- Delannoy, J.J., 1983. *Le complexe souterrain du plateau du Sornin (Vercors, France). Le gouffre Berger et le Scialet de la Fromagère*. *Karstologia*, #2, 3-12.
- Delannoy, J.J., 1984. *Le Vercors: un massif de la moyenne montagne alpine*. *Karstologia*, #3, 34-45.
- Delannoy, J.J. and R. Maire, 1984. *Les grandes cavités alpines: répartition et contexte hydrogéologique*. *Karstologia*, #3, 18-23.
- Denes, G., and F. Szilagyl, 1989. Hydrographische Zusammenhänge im Einzugsgebiet des Baradla-Öhlensystems, Aggtelek, Ungarn. *Proc. 10th Int. Congress of Speleology*, Budapest, 555-558.
- Department of Transport, 1970. Supplementary precipitation data, 1(1). Department of Transport, Meteorological Branch, Ottawa.
- Desloges, J.R., and J.S. Gardner, 1984. Process and discharge estimation in ephemeral channels. Canadian Rocky Mountains. *Can. J. Earth. Sci.*, 21, 1050-1060.

- DeWit, R. and D.J. McLaren, 1950. Devonian sections in the Rocky Mountains between Crowsnest Pass and Jasper, Alberta. Paper 50-23, Geol. Survey of Canada, 66p.
- Dodge, E., 1985. Heterogeneity of permeability in karst aquifers and their vulnerability to pollution. Examples of three springs in the Causse Comtal (Aveyron, France). Ann. Soc. Geol. Belg., 108, 43-47.
- Domenico, P.A. and F.W. Schwartz, 1990. Physical and chemical hydrogeology. John Wiley, New York, 824p.
- Dougedroit, A. and M.-F. Saintignon, 1984. Les gradients de températures et de précipitations en montagne. Rev. Geog. Alpine, 72, 225-240.
- Douglas, R.J.W., 1958. Mount Head map area, Alberta. Memoir 291, Geol. Survey of Canada, 241p.
- Drake, J.J., 1970. The geohydrology of gypsum karst areas. Unpubl. MSc thesis, McMaster Univ., 90p.
- Drake, J.J., 1974. Hydrology and karst solution in the Southern Canadian Rockies. Unpublished PhD thesis, McMaster University, 222p.
- Drake, J.J., 1983. The effects of geomorphology and seasonality on the chemistry of carbonate groundwaters. J. Hydrol. 61, 223-226.
- Drake, J.J., 1984. Theory and model for global carbonate solution by groundwater. In: Groundwater as a geomorphic agent, (Ed: R.G. LaFleur), 210-226. Allen & Unwin, London.
- Drake, J.J. and D.C. Ford, 1974. Hydrochemistry of the Athabasca and North Saskatchewan Rivers in the Rocky Mountains of Canada.
- Drake, J.J., and D.C. Ford, 1976. Solutional erosion in the Southern Canadian Rockies. Canadian Geographer, 20, 158-170.
- Drake, J.J., and R.S. Harmon, 1973. Hydrochemical environments of carbonate terrains. Water Resources Res., 9, 949-957.
- Drew, D.P., 1970a. The significance of percolation water in limestone catchments. Groundwater, 8, 5-11.
- Drew, D.P., 1970b. Limestone solution within the East Mendip area, Somerset. Trans. Cave Research Group of G.B., 12, 259-270.
- Drew, D.P., 1975a. The limestone hydrology of the Mendip Hills. In: Limestone and caves of the Mendip Hills, (Ed. D.I. Smith), David & Charles, Newton Abbot, p171-213.
- Drew, D.P., 1975b. The caves of Mendip. In: Limestone and caves of the Mendip Hills, (Ed. D.I. Smith), David & Charles, Newton Abbot, p214-312.
- Drew, D.P., M.D. Newson and D.I. Smith, 1970. Water tracing of the Severn Tunnel Great Spring. Proc. Univ. Bristol Speleol. Soc., 12(2), 203-212.
- Dreybrodt, W., 1981. Mixing corrosion in $\text{CaCO}_3\text{-CO}_2\text{-H}_2\text{O}$ systems and its role in the karstification of limestones. Chem. Geol., 32, 221-236.

- Dreybrodt, W., 1990. The role of dissolution kinetics in the development of karst aquifers in limestone: a model simulation of karst evolution. *J. Geol.*, 98, 639-655.
- Drogue, C., A.-M. Laty and H. Paloc, 1983. Les eaux souterraines des karsts méditerranéens. Exemple de la région pyrénéo-provençale (France méridionale). *Bull. Bur. Rech. Géol. Minières, Hydrogéologie - géologie de l'ingénieur*, #4, 293-311.
- Droppa, A., 1966. The correlation of some horizontal caves with river terraces. *Studies in Speleology*, 1, 186-192.
- Dublyansky, V., A. Milouchischin, V. Resvan, N. Shulich and L. Shlyaschova, 1989. Some peculiarities of the vauclusian spring Mchishta. *Proc. 10th Int. Congress of Speleology*, Budapest, p590-592.
- Eavis, A.J., 1981. Caves of Mulu '80. The limestone caves of the Gunong Mulu National Park, Sarawak. Royal Geograph. Soc., London, 52p.
- Eavis, A.J., 1985. Caves of Mulu '84. The limestone caves of the Gunong Mulu National Park, Sarawak. Brit. Cave Research Assoc., Bridgwater, 56p.
- Eberenz, P., 1976. Apports des méthodes isotopiques à la connaissance de l'aquifère karstique. PhD thesis (dynamic geology), Univ. Pierre et Marie Curie, Paris, 70p. Data reproduced in Bakalowicz and Mangin, 1980.
- Ecock, K.E., 1984. Karst hydrology of the White Ridges, Vancouver Island. Unpubl. MSc thesis, McMaster Univ., 138p.
- Ede, D.P., 1972. Comment on "Seasonal fluctuations in the chemistry of limestone springs" by E.T Shuster and W.B. White. *J. Hydrol.*, 16, 53-55.
- Ede, D.P., 1975. Limestone drainage systems. *J. Hydrol.*, 27, 297-318.
- Edmunds, W.M., 1971. Hydrogeochemistry of groundwaters in the Derbyshire Dome with special reference to trace constituents. *Inst. Geol. Sci. report 71/7*, HMSO, London, 52p.
- Edmunds, W.M., B.J. Taylor and R.A. Downing, 1969. Mineral and thermal waters of the U.K. In: Mineral and thermal waters of the world; A - Europe. Proc. Symposium II, 23rd Internat. Geol. Congr., 18, 139-158.
- Ek, C., 1961. Conduits souterrains en relation avec les terrasses fluviales. *Ann. Soc. Géol. Belge*, 84, 313-340.
- Elliot, J.V., C.F. Westlake and M.E. Tringham, 1979. Otter Hole, near Chepstow, Wales. *Trans. British Cave Research Assoc.*, 6(4), 143-158.
- Engler, S., 1982. Exploration of Boca del Río Apetlanca. *AMCS Activities Newsletter*, #10. Assoc. Mexican Cave Studies, Austin, 43-48.
- Erdélyi, M., and J. Gálfy, 1988. Surface and subsurface mapping in hydrogeology. Wiley, 384p.
- Eraso, A., 1986. The prediction method of the principal directions of drainage in karst. *Proc. Ninth Internat. Congress of Speleology*, Barcelona, 46-49.

- Even, H., I. Carmi, M. Magaritz and R. Gerson, 1986. Timing the transport of water through the upper vadose zone in a karstic system above a cave in Israel. *Earth Surface Processes and Landforms*, 11, 181-191.
- Ewers, R.O., 1969. A model for the development of subsurface drainage routes along bedding planes. Unpubl. MSc thesis, Univ. of Cincinnati, 84p.
- Ewers, R.O., 1982. Cavern development in the dimensions of length and breadth. Unpubl. PhD thesis, McMaster Univ., 398p.
- Exley, S., 1988. Mante update: Americans set new cave diving records. *NSS News*, 46, 358-359.
- Fabre, G., 1984. Traits généraux de l'hydrologie karstique en basse Cévenne. *Karstologia*, #4, 19-25.
- Farley, A.L., 1979. *Atlas of British Columbia*. Univ. B.C. Press, 136p.
- Farr, M., 1980. The darkness beckons. *Diadem*, London, 207p.
- Farr, M., 1983. A new advance at Wookey Hole. *Caves and Caving* (Bull. British Cave Research Assoc.), #19, 2-3.
- Faulkner, G.L., 1976. Flow analysis of karst systems with well developed underground circulation. In: *Karst hydrology and water resources* (Ed. V. Yevjevich), Water Resource Publications, Fort Collins, p137-164.
- Faulkner, T.J., 1980. Sirjordgrotten and other caves in Eiteradal, Vefsn, Norway. *Trans. Brit. Cave Research Assoc.*, 7, 53-69.
- Field, M.S., 1988. U.S. Environment Protection Agency's strategy for groundwater quality monitoring at hazardous waste land disposal facilities located in karst terrains. In: *Karst hydrogeology and karst environment protection* (Proc. IAH 21st congress), Eds. Yuan Daoxian and Xie Chaofan. Geological Publ. House, Beijing, p1006-1011.
- Fish, J.E., 1977. Karst hydrogeology of Valles - San Luis Potosi region, Mexico. Unpubl. PhD thesis, McMaster University, 469p.
- Forbes, J., 1988. Heave Ho! *Canadian Caver*, 20(1), 6.
- Ford, D.C., 1963. Aspects of the geomorphology of the Mendip Hills. Unpubl. DPhil. thesis, Univ. of Oxford, 499p.
- Ford, D.C., 1965. The origin of limestone caverns: a model from the central Mendip Hills, England. *Bull. of the Nat. Speleol. Soc.*, 27, 109-132.
- Ford, D.C., 1966. Calcium carbonate solution in some Central Mendip caves, Somerset. *Proc. Univ. Bristol Speleol. Soc.*, 11, 46-53.
- Ford, D.C., 1969. Unpublished field notes.
- Ford, D.C. 1971a. Characteristics of limestone solution in the Southern Rocky Mountains and Selkirk Mountains, Alberta and British Columbia. *Can. J. Earth Sci.*, 8, 585-609.
- Ford, D.C., 1971b. Geologic structure and a new explanation of limestone cavern genesis. *Trans. Cave Research Group of G.B.*, 13, 81-94.

- Ford, D.C., 1971c. Unpublished field notes.
- Ford, D.C., 1983a. Alpine karst systems at Crowsnest Pass, Alberta - British Columbia, Canada. *J. Hydrol.*, 61, 187-192.
- Ford, D.C., 1983b. Castleguard Cave and karst, Columbia Icefields area, Rocky Mountains of Canada: a symposium (Editor: D.C. Ford). *Arctic and Alpine Res.*, 15, 425-426.
- Ford, D.C., 1983c. Preface. In: Castleguard Cave and karst, Columbia Icefields area, Rocky Mountains of Canada: a symposium. *Arctic and Alpine Res.*, 15, 425-426.
- Ford, D.C., 1983d. The physiography of the Castleguard karst and the Columbia Icefields area, Alberta, Canada. *Arctic and Alpine Res.*, 15, 427-436.
- Ford, D.C., J.C. Andrews, T.E. Day, S.A. Harris, J.B. MacPherson, S. Occhietti, W.F. Rannie and H.O. Slaymaker, 1984. Canada: how many glaciations? *Can. Geographer*, 28, 205-225.
- Ford, D.C., and J.J. Drake, 1982. Spatial and temporal variations in karst solution rates: the structure of variability. In: *Space and time in geomorphology*, (Ed. C.E. Thorn), Allen and Unwin, London, 147-170.
- Ford, D.C. and R.O. Ewers, 1978. The development of limestone cave systems in the dimensions of length and depth. *Can. J. Earth. Sci.*, 15, 1783-1798.
- Ford, D.C., A.N. Palmer, and W.B. White, 1988. Landform development; Karst. In: Back, W., Rosenschein, J.S., and Seaber, P.R., eds., *Hydrogeology: Boulder, Colorado, Geol. Soc. Amer., The geology of North America*, v. O-2.
- Ford, D.C., H.P. Schwarcz, J.J. Drake, M. Gascoyne, R.S. Harmon and A.G. Latham, 1981. Estimates of the age of the existing relief within the southern Rocky Mountains of Canada. *Arctic and Alpine Research*, 13, 1-10.
- Ford, D.C., P.L. Smart and R.O. Ewers, 1983. Physiography and speleogenesis of Castleguard Cave, Columbia Icefields, Alberta, Canada. *Arctic and Alpine Res.*, 15, 437-450.
- Ford, D.C. and P. Williams, 1989. Karst geomorphology and hydrology. Unwin Hyman, London, 601p.
- Ford, T.D., 1977. Limestone and caves of the Peak District. Geo Books, Norwich, 469p.
- Ford, T.D., 1989. The caves of Nant y Glaes, Vaynor. In: *Limestones and caves of Wales*, Ed. T.D. Ford. Cambridge Univ. Press, 152-154.
- Freeman, J.P., G.I. Smith, T.L. Poulson, P.J. Watson and W.B. White, 1973. Lee Cave, Mammoth Cave National Park, Kentucky. *Bull. of the Nat. Speicol. Soc.*, 35, 109-125.
- Freeze, R.A. and J.A. Cherry, 1979. Groundwater. Prentice-Hall, Englewood Cliffs, NJ, 604p.
- Freeze, R.A. and P.A. Witherspoon, 1967. Theoretical analysis of regional groundwater flow: 2. effect of water-table configuration and subsurface permeability variation. *Water Resources Res.*, 641-656.

- Freixcs i Perich, A., 1986. El carst conglomeràtic experimental de Rellinars: un enfocament sistèmic i hidrogeològic en la recerca del medi càrstic. Doctoral thesis, Univ. of Barcelona, 152p.
- Friederich, H., and P.L. Smart, 1981. Dye trace studies of the unsaturated-zone recharge of the Carboniferous Limestone aquifer of the Mendip Hills, England. Proc. 8th Internat. Congr. Speleology, Bowling Green, Ed: B.F. Beck. National. Speleol. Soc., Huntsville, Alabama, p283-286.
- Friederich, H., and P.L. Smart, 1982. The classification of autogenic percolation waters in karst aquifers: a study in G.B. Cave, Mendip Hills, England. Proc. Univ. Bristol. Speleol. Soc., 16(2), 143-159.
- Gadd, B., 1986. Handbook of the Canadian Rockies. Corax, Jasper, Alberta, 876p.
- Gale, S.J., 1984. The hydraulics of conduit flow in carbonate aquifers. J. Hydrol., 70, 309-327.
- Gamble, B.F., Y. Eckstein and W.M. Edwards, 1990. Evaluation of soil water residence time in a monolith lysimeter from the application of queuing disciplines to water budget data (demonstration - II). J. Hydrol., 113, 27-49.
- Gardner, J.S., 1979. The movement of material on debris slopes in the Canadian Rocky Mountains. Z. Geomorph. N.F., 23, 45-57.
- Gardner, J.S., 1980. Frequency, magnitude and spatial distribution of mountain rockfalls and rockslides in the Highwood Pass area, Alberta, Canada. In: Thresholds in geomorphology, Eds. D.R. Coates and J.D. Vitek, Allen & Unwin, London, 267-295.
- Gardner, J.S., 1982. Alpine mass-wasting in contemporary time: some examples from the Canadian Rocky Mountains. In: Space and time in geomorphology, Ed. C.E. Thorn, Allen & Unwin, London, 171-192.
- Gardner, J.S., 1983a. Observations on erosion by wet snow avalanches, Mt Rae area, Alberta, Canada. Arctic and Alpine Res., 15, 271-274.
- Gardner, J.S., 1983b. Accretion rates on some debris slopes in the Mt Rae area, Canadian Rocky Mountains. Earth Surface Processes and Landforms, 8, 347-355.
- Gardner, J.S., 1983c. Rockfall frequency and distribution in the Highwood Pass area, Canadian Rocky Mountains. Z. Geomorph. N.F., 27, 311-324.
- Gardner, J.S., 1986. Sediment movement in ephemeral streams on mountain slopes, Canadian Rocky Mountains. In: Hillslope processes, Ed. A.D. Abrahams. Allen & Unwin, Boston, 97-113.
- Gardner, J.S., D.J. Smith and J.R. Desloges, 1983. The dynamic geomorphology of the Mt Rae area: a high mountain region in Southwestern Alberta. Dept of Geography Publ. Series #19, Univ. Waterloo, 23'9.
- Garven, G., and A. Freeze, 1984. Theoretical analysis of the role of groundwater flow in the genesis of stratabound ore deposits: 2. Quantitative results. Amer. Jour. Sci., 284, 1125-1174.

- Gascoyne, M., 1977. Hydrogeology and solution chemistry of north Venezuelan karst. In: Karst Hydrology, (Eds. J.S. Tolson and F.L. Doyle), UAH Press, Huntsville, Alabama, 553-566.
- Gascoyne, M., D.C. Ford and H.P. Schwarcz, 1983. Rates of cave and landform development in the Yorkshire Dales from speleothem age data. *Earth Surface Processes and Landforms*, 8, 557-568.
- Gascoyne, M., A.G. Latham, R.S. Harmon and D.C. Ford, 1983. The antiquity of Castleguard Cave, Columbia Icefields, Alberta, Canada. *Arctic and Alpine Res.*, 463-470.
- Gaspar, E., 1987. Flow through hydrokarstic structures. In: Modern trends in tracer hydrology, vol.2, Ed: E. Gaspar, CRC Press, Boca Raton, p32-93.
- Gat, J.R., 1981. Groundwater. In: Stable isotope hydrology: deuterium and oxygen-18 in the water cycle, (Eds. J.R. Gat and R. Gonfiantini). Tech. Report Series, #210, Int. Atomic Energy Agency, Vienna, 223-240.
- Geyh, M.A., G. Michel and W. Wagner, 1988. Environmental isotope identification of catchment areas in karst. In: Karst hydrogeology and karst environment protection (Proc. IAH 21st congress), Eds. Yuan Daoxian and Xie Chaofan. Geological Publ. House, Beijing, p58-63.
- Gèze, B., 1990. Mea culpa d'un sceptique. *Spelunca*, #40, 25-28.
- Gibert, J., R. Laurent and R. Maire, 1983. Carte hydrogéomorphologique au 1/10000 du karst de Dorvan (Jura méridional, Ain, France). Présentation et principales données sur l'hydrogéologie et l'hydrochimie de ce karst. *Karstologia*, #2, 33-40.
- Gill, D., B. Lyon and S. Fowler, 1990. The caves of Bama County, Guangxi, China. *Cave Science*, 17 (2), 55-66.
- Glennie, E.A., 1950. Further notes on Ogof Ffynnon Ddu. *Trans. Cave Res. Group G.B.*, 1 (3), 1-47.
- Glover, R.R., 1974. Cave development in the Gaping Gill System. In: Limestone and caves of north-west England (Ed. A.C. Waltham), p343-384.
- Gospodarič, R., and P. Habič, 1976. Underground water tracing investigations in Slovenia, 1972-1975. Inst. Karst Research, Ljubljana, 312p.
- Grassi, D. and T. Tadolini, 1985. Hydrogeology of the Mesozoic carbonate platform of Apulia (South Italy) and the reasons for its different aspects. *Karst water resources* (Proc. Ankara - Antalya Symposium, July 1985), IAHS Publ., 161, 293-306.
- Gunn, J., 1981a. Hydrological processes in karst depressions. *Z. Geomorph.*, 25, 313-331.
- Gunn, J., 1981b. Limestone solution rates and processes in the Waitomo district, New Zealand. *Earth Surface Processes and Landforms*, 6, 427-445.
- Gunn, J., 1983. Point-recharge of limestone aquifers - a model from New Zealand karst. *J. Hydrol.*, 61, 19-29.
- Gunn, J., 1986a. A conceptual model for conduit flow dominated karst aquifers. *Karst water resources* (Proc. Ankara - Antalya Symposium, July 1985), IAHS Publ., 161, 587-596.

- Gunn, J., 1986b. Solute processes and karst landforms. In: *Solute Processes* (Ed. S. Trudgill), John Wiley and Sons, 363-437.
- Gunn, J., and B. Turnpenny, 1985. Stormflow characteristics of three small limestone drainage basins in North Island, New Zealand. In: *New directions in karst*, Eds: M.M. Sweeting and K. Paterson, Geobooks, Norwich, 233-258.
- Gurnee, R. & J., 1974. *Discovery at the Rio Camuy*. Crown, New York, 183p.
- Gujot, J.-L., 1986. Les monts de Pardailhan. Etude hydrodynamique et hydrochimique des sources karstiques de Poussarou et Malibert (Montagne Noire - Hérault). *Karstologia*, #7, 25-30.
- Halliwell, R.A., J.L. Ternan and A.F. Pitty, 1974. Introduction to the karst hydrology of north-west Yorkshire. In: *Limestone and caves of north-west England*, (Ed: A.C. Waltham), David & Charles, Newton Abbot, p106-114.
- Harris, S.A., 1973. Studies of soil creep, Western Alberta, 1970 to 1972. *Arctic and Alpine Res.*, 5, A171-A180.
- Herak, M., 1972. Karst of Yugoslavia. In: *Karst. Important karst regions of the Northern Hemisphere*, (Eds. M Herak and V.T. Stringfield), Elsevier, p25-84.
- Hess, J.W., and W.B. White, 1989a. Water budget and physical hydrology. In: *Karst hydrology: concepts from the Mammoth Cave area*, (Eds. W.B. White and E.L. White), Van Nostrand Reinhold, New York, p105-126.
- Hess, J.W., and W.B. White, 1989b. Chemical hydrology. In: *Karst hydrology: concepts from the Mammoth Cave area*, (Eds. W.B. White and E.L. White), Van Nostrand Reinhold, New York, p145-174.
- Hewlett, J.D., and A.R. Hibbert, 1967. Factors affecting the response of small watersheds to precipitation in humid areas. In: *Forest Hydrology*, (Eds. W.E. Sopper and H.W. Lull), Pergamon, Oxford, 275-290.
- Hillel, D., 1971. *Soli and water: physical principles and processes*. Academic Press, New York, 288p.
- Hitchon, B., 1969a. Fluid flow in the Western Canada Sedimentary Basin. 1. Effect of topography. *Water Resources Res.*, 5, 186-195.
- Hitchon, B., 1969b. Fluid flow in the Western Canada Sedimentary Basin. 1. Effect of geology. *Water Resources Res.*, 5, 460-469.
- Hitchon, B., 1984. Geothermal gradients, hydrodynamics and hydrocarbon occurrences, Alberta, Canada. *Amer. Assoc. Petroleum Geologists Bull.* 68, 713-743.
- Hobbs, S.L., and P.L. Smart, 1988. Heterogeneity in karst aquifers - a case study from the Mendip Hills, England. In: *Karst hydrogeology and karst environment protection (Proc. IAH 21st congress)*, Eds. Yuan Daoxian and Xie Chaofan. Geological Publ. House, Beijing, p724-730.
- Holter, M.E., 1976. Limestone resources of Alberta. *Economic Geology report 4*, Alberta Res. Council, Edmonton, 91p.

- Houlez, J.-P., 1988. La grotte du Grenouillet, Massif de la Séranne, Hérault. *Spelunca*, #32, 39-41.
- Hribar, F., 1976. Ponors marking and springs observation. In: *Underground water tracing investigations in Slovenia, 1972-1975* (Eds. R. Gospodarič and P. Habic. Inst. Karst Research, Ljubljana, 132-138).
- Hubbert, M.K., 1940. The theory of groundwater motion. *J. Geol.*, 48, 785-944.
- Huntley, D.H., 1990. Hydrogeomorphology of an alpine karst. Unpubl. MSc thesis, Univ. of Western Ontario, 228p.
- Huntley, D. and C. Smart, 1989. Glacier-karst interaction at Small River, B.C. *Canadian Caver*, 21(1), 36-38.
- Inland Waters Directorate, (Water Quality Branch, Ottawa), 1975. Water quality data, Alberta, 1961-1973. Information Canada, Ottawa.
- Inland Waters Directorate, (Western and Northern region, Water Quality Branch, Calgary), 1980. Detailed surface water quality data, Alberta, 1974-1976. Ministry of Supply and Services, Ottawa.
- Inland Waters Directorate, (Western and Northern region, Water Quality Branch, Calgary), 1982. Detailed surface water quality data, Alberta, 1977-1979. Ministry of Supply and Services, Ottawa.
- Inland Waters Directorate, (Western and Northern region, Water Quality Branch, Calgary), 1984. Detailed surface water quality data, Alberta, 1980-1981. Ministry of Supply and Services, Ottawa.
- Inland Waters Directorate, (Water Resources Branch, Water Survey of Canada, Ottawa), 1986a. Surface water data, Alberta, 1985. Ministry of Supply and Services, Ottawa.
- Inland Waters Directorate, (Water Resources Branch, Water Survey of Canada, Ottawa), 1986b. Surface water data, British Columbia, 1985. Ministry of Supply and Services, Ottawa.
- Inland Waters Directorate, (Water Resources Branch, Water Survey of Canada, Ottawa), 1987a. Surface water data, Alberta, 1986. Ministry of Supply and Services, Ottawa.
- Inland Waters Directorate, (Water Resources Branch, Water Survey of Canada, Ottawa), 1987b. Surface water data, British Columbia, 1986. Ministry of Supply and Services, Ottawa.
- Inland Waters Directorate, (Water Resources Branch, Water Survey of Canada, Ottawa), 1989a. Historical streamflow summary, Alberta, to 1988. Ministry of Supply and Services, Ottawa, 1989.
- Inland Waters Directorate, (Water Resources Branch, Water Survey of Canada, Ottawa), 1989b. Historical streamflow summary, British Columbia, to 1988. Ministry of Supply and Services, Ottawa, 1989.
- Isler, O., 1981. La source du Lison, Doubs. *Spelunca*, #4, 38-39.
- Isler, O. and C. Magnin, 1985. La Doux de Coly. *Spelunca*, #18, 19-23.

I.W.D.: see Inland Waters Directorate.

- Izapy, G., and L. Maucha, 1989. Subsurface water chemical matter - transportation values of karstic areas in Hungary. Proc. 10th Internat. Congr. of Speleology, Magyar Karszt- és Barlangkutató Társulat, Budapest, 533-535.
- Jackli, H., 1956. Gegenwartsgeologie des bündnerischen Rheingebiets - ein Beitrag zur exogenen Dynamik alpiner Gebirgslandschaften. Beiträge zur Geologie der Schweiz, Geotech. Ser. #36, 126p.
- Jacobson, R.J., and D. Langmuir, 1974. Controls on the quality of some carbonate spring waters. J. Hydrol., 23, 247-265.
- Jacuš, L., 1959. Neue Methoden der Höhlenforschung in Ungarn und ihre Ergebnisse. Die Höhle, 10, 88-96. Not seen: quoted in Ford and Williams, 1989.
- James, J.M., and H.J. Dyson, 1980. Caves and karst of the Muller Range., Speleol. Res. Council, Broadway, Australia, 150p.
- James, J.M., A.T. Warild, S.R.H. Worthington and A.T. White, 1980. Mamo. In: Caves and karst of the Muller Range, (Eds. J.M. James and H.J. Dyson), Speleol. Res. Council, Broadway, Australia, p50-65.
- Jameson, R.A., 1981. Development of flow paths and cave passages from fault segments in West Virginian caves. Proc. 8th Int. Congress of Speleology, Bowling Green, Kentucky, 717-719.
- Jameson, R.A., 1985. Structural segments and the analysis of flow paths in the North Canyon of Snedegar Cave, Friars Hole Cave System, West Virginia. Unpubl. MSc thesis, 421p.
- Jawad, S.B., and K.A. Hussien, 1986. Contribution to the study of temporal variations in the chemistry of spring water in karstified carbonate rocks. Hydrological Sciences J., 31, 529-542.
- Jeannin, P.-Y., 1990. Néotectonique dans le karst du nord du lac de Thoune (Suisse). Karstologia, #15, 41-54.
- Jennings, J.N., 1985. Karst geomorphology. Basil Blackwell, 293p.
- Karanjac, J., and A. Altug, 1980. Karstic spring recession hydrograph and water temperature analysis: Oymapinar dam project, Turkey. J. Hydrol., 45, 203-217.
- Karmann, I., 1990. Private communication.
- Kiknadze, T., 1982. Some problems of karst hydrogeology of the mountainous countries. Geologia applicata e idrogeologia (Bari), 47-54.
- King, F.H., 1899. Principles and conditions of the movement of groundwater. U.S. Geol. Survey, 19th Ann. Report, part 2, 59-294.
- Kiraly, L., 1975. Rapport sur l'état actuel des connaissances dans le domaine des caractères physiques des roches karstiques. In: hydrogeology of karstic terrains (Eds: A. Burger and L. Dubertret), 53-67. Internat. Union Geol. Sci., Series B, 3. (Not seen: data quoted in Ford and Williams, 1989).
- Kirby, M., 1990. Clearwater - a Mulu success. Desceni, #92, p33.

- Knutson, S., 1979. Cuetzalan - Spring 1979. AMCS Activities Newsletter, #10. Assoc. Mexican Cave Studies, Austin, 64-69.
- Knutson, S., 1984. Sumidero San Bernardo. AMCS Activities Newsletter, #14. Assoc. Mexican Cave Studies, Austin, 80-81.
- Knutson, S., 1988. Sumidero of the Rio San Jose de Atima; the 1987 NSS expedition to Honduras. NSS News, 46(8), 320-326.
- Komatina, M., 1965. Sur le problème de la détermination des bassins versants et des directions de la circulation des eaux souterraines dans le karst dinarique. In: Hydrologie des roches fissurées, Proc. Dubrovnik symposium, October 1965. UNESCO, Paris, Vol. 1, p 190-199.
- Komatina, M., 1984. Hydrogeologic features of the Dinaric karst. In: Hydrogeology of the Dinaric karst, Ed. B.F. Mijatović. Internat. Assoc. of Hydrogeologists, Heise, Hannover, p55-73.
- Koppe, P., 1988. Dry diving at Dezaiko. Canadian Caver, 20(2), 22-23.
- Kovacs, G., 1985. Special aspects of modelling karstic groundwater systems. Karst water resources (Proc. Ankara - Antalya Symposium, July 1985), IAHS Publ., 161, 27-54.
- Kovalevsky, V.S., 1977. Prospects of forecasting the karstic water regime. In: Karst hydrogeology, Eds: J.S. Tolson and F.L. Doyle. UAH Press, Huntsville, p73-80.
- Kox, N., 1990. Wisconsin's greatest challenge: Tecumseh (Horseshoe Bay) Cave. NSS News, 48(10), 248-254.
- Krothe, N.C., and R.D. Libra, 1983. Sulfur isotopes and hydrochemical variations in spring waters of southern Indiana, U.S.A. J. Hydrol., 61, 267-283.
- Kruse, P.B., 1980. Karst investigations of Maligne Basin, Jasper National Park, Alberta. Unpublished MSc thesis, University of Alberta, 120p.
- Lam, H.L., F.W. Jones and C. Lambert, 1982. Geothermal gradients in the Hinton area of west-central Alberta. Can. J. Earth Sci. 19, 755-766.
- Langmuir, D., 1971. The geochemistry of some carbonate waters in central Pennsylvania. Geochim. Cosmochim. Acta., 35, 1023-1045.
- Lauritzen, S.-E. 1981. A study of some karst water, in Norway. Spatial variation in solute concentrations and equilibrium parameters in limestone dissolution. Norsk geogr. Tidsskr. 35, 1-19.
- Lauritzen, S.-E., 1982. The paleocurrents and morphology of Pikhågrottene, Svartisen, North Norway. Norsk Geogr. Tidsskr., 36, 183-209.
- Lauritzen, S.-E., J. Abbott, R. Arnesen, G. Crossley, D. Grepperud, A. Ive and S. Johnson, 1985. Morphology and hydraulics of an active phreatic conduit. Cave Science (Trans. Brit. Cave Res. Assoc.) 12, 139-146.
- Lauritzen, S.-E., 1986. Hydraulics and dissolution kinetics of a phreatic conduit. Proc. Ninth Internat. Congress of Speleology, Barcelona, 20-22.

- Lauritzen, S.-E., 1989. Shear, tension, or both - a critical view of the prediction potential for caves. Proc. Tenth Internat. Congress of Speleology, Budapest, 118-120.
- Lauritzen, S.-E., 1990. Autogenic and allogenic denudation in carbonate karst by the multiple basin method: an example from Svartisen, North Norway. Earth Surface Processes and Landforms, 15, 157-167.
- Lavanchy, Y., I Müller and F. Zwahlen, 1988. Several principal mechanisms of karstic springs in Switzerland related to physical and geological characteristics of their catchment. In :Karst hydrogeology and karst environment protection (Proc. IAH 21st congress), Eds. Yuan Daoxian and Xie Chaofan. Geological Publ. House, Beijing, p386-393.
- Laverty, M., 1980. Water chemistry in the Gunung Mulu National Park including problems of interpretation and use. Geogrl J., 146, 232-245.
- Le Pennec, R., 1989. Les galets d'argiles de la grotte des Moulins "C". Spelmoncel, Jura. Spelunca, #36, 39-40.
- Le Roux, 1989. Réseau de Foussoubie, France. Detailed plan and profile of the cave.
- Li Maogiu, 1981. The deep karsts in Wujiang Valley at Wujiandu dam site. Proc. 8th Int. Congress of Speleology, Bowling Green, Kentucky, 732-734.
- Lismonde, B., 1989. La traversée sima Tonio - cueva Canuela (Arredondo, Monts Cantabriques, Espagne). Spelunca, #34, 25-30.
- Luckman, B.H., 1976. Rockfalls and rockfall inventory data: some observations from Surprise Valley, Jasper National Park, Canada. Earth Surface Processes, 1, 287-298.
- Luckman, B.H., 1977. The geomorphic activity of snow avalanches. Geografiska Annaler, 59A, 31-48.
- Luckman, B.H., 1978a. Geomorphic work of snow avalanches in the Canadian Rocky Mountains. Arctic and Alpine Res., 10, 261-276.
- Luckman, B.H., 1978b. The measurement of debris movement on alpine talus slopes. Z. Geomorph. N.F., Suppl.-Bd., 29, 117-129.
- Luckman, B.H., 1981. The geomorphology of the Alberta Rocky Mountains: A review and commentary. Z. Geomorph. N.F., Suppl.-Bd., 37, 91-119.
- Lu Yaoru, 1988. Hydrological environments and water resource patterns in karst regions of China. In :Karst hydrogeology and karst environment protection (Proc. IAH 21st congress), Eds. Yuan Daoxian and Xie Chaofan. Geological Publ. House, Beijing, p64-75.
- Luckman, B.H., 1973. Scree slope characteristics and processes in Surprise Valley, Jasper National Park, Alberta. Unpubl. PhD thesis, McMaster Univ., 499p.
- MacGregor, K., 1976. Caves of Ontario. In: Cave exploration in Canada, (Ed: P. Thompson), p39-56.
- Majorowicz, J.A., F.W. Jones, H.L. Lam and A.M. Jessop, 1985. Terrestrial heat flow and geothermal gradients in relation to hydrodynamics in the Alberta Basin, Canada. J. of Geodynamics 4, 265-283.

- Maire, R., 1990. *La haute montagne calcaire. Karstologia - Mémoires #3*, 731p.
- Maire, R., and J. Nicod, 1984. Aperçus sur hydrologie karstique des Alpes occidentales. *Karstologia*, #3, 18-24.
- Mandel, S., 1965. A conceptual model of karstic erosion by groundwater. In: Hydrologie des roches fissurées, Proc. Dubrovnik symposium, October 1965. UNESCO, Paris, vol 2, p62-664.
- Mangin, A., 1975. Contribution à l'étude hydrodynamique des aquifères karstiques. Thesis: doct. sci. nat., univ Dijon, publ. in: *Ann. de Spéléologie*, 29(3), 283-332; 29(4), 495-601; 30(1), 21-124.
- Mangin, A., 1984. Pour une meilleure connaissance des systèmes hydrologiques à partir des analyses corrélatoire et spectrale. *J. Hydrol.*, 67, 25-43.
- Mangin, A., 1986. Livret guide de l'excursion à travers l'Ariège karstique. Laboratoire souterrain du CNRS, Moulis, Ariège, France, 52p.
- Margat, J., 1980. Carte hydrogéologique de la France: systèmes aquifères. Bureau de recherches géologiques et minières, Orléans.
- Markova, O.L., 1970. Water balance peculiarities of karst areas. IASH #52, p363-375.
- McKenzie, I., 1984. Fangs for the memories. *Canadian Caver*, 16(1), 12-17.
- McKenzie, I., 1987a. Across Canada: from the Rockies. *Canadian Caver*, 19(2), 6-8.
- McKenzie, I., 1987b. The Backdoor resurvey. *Canadian Caver*, 19(2), 42-44.
- McKenzie, I., 1989a. Explorations near Crowsnest Pass. *Canadian Caver*, 21(1), 14-16.
- McKenzie, I., 1989b. A new survey of Yorkshire Pot. *Canadian Caver*, 21(1), 30-31.
- McKenzie, I., 1990. Further explorations in Snowslope Pot. *Canadian Caver*, 22(1), 6-7.
- McKenzie, I., and J. Pollack, 1986. Dezaiko again. *Canadian Caver*, 18(1), 4-9.
- McPherson, H.J., 1975. Sediment yields from intermediate-sized stream basins in Southern Alberta. *J. Hydrol.*, 25, 243-257.
- Medville, D., 1983. Private communication.
- Medville, D., 1990. Private communication.
- Medville, D.M., G.R. Dasher and E. Werner, 1983. An introduction to the caves of east-central West Virginia. *West Virginia Speleol. Survey*, 146p.
- Medville, D.M., and W.K. Storage, 1986. Structural and stratigraphic influences on the development of solution conduits in the Upper Elk River Valley, West Virginia. *NSS Bull.*, 48, 8-25.
- Meinke, S., 1986. Halfway caves revisited. *Canadian Caver*, 18(2), 58.
- Meus, P., 1990. Private communication.

- Michelot, C. and J. Mudry, 1985. Remarques sur les exutoires de l'aquifère karstique de la Fontaine de Vaucluse. *Karstologia*, #6, 11-14.
- Milanović, P.T., 1976. Water regime in deep karst. Case study of the Ombla Spring drainage area. In: *Karst hydrology and water resources*, Vol. 1, Karst hydrology, Ed: V. Yevjevich. Water Resource Publications, Littleton, Colorado, 165-191.
- Milanović, P.T., 1981. Karst hydrogeology. Water Resource Publications, Littleton, Colorado.
- Miller, T.E., 1979a. A sketch of Columbian karst. *Canadian Caver*, 11(1), 43-53.
- Miller, T.E., 1979b. Darknight, Belize. *Canadian Caver*, 11(2), 14-17.
- Miller, T.E., 1980. Great Expectations Cave. *Canadian Caver*, 12(2), 35-44.
- Miller, T.E., 1982. Hydrochemistry, hydrology and morphology of the Caves Branch karst, Belize. Unpubl. PhD thesis, McMaster Univ., 280p.
- Miller, T., 1986. Chiquibul, 1986. *Canadian Caver*, 16(2), 38-39.
- Miller, T., 1989. Storming the Bastille. *Canadian Caver*, 21(1), 7-11.
- Mills, L.D.J. and A.C. Waltham, 1981. Geomorphology of the Matienzo caves. *Trans. British Cave Research Assoc.*, 8(2), 63-84.
- Minvielle, P., 1977. Grottes et canyons. Denoël, Paris, 231p.
- Miotke, F.-D. and A.N. Palmer, 1972. Genetic relationship between caves and landforms in the Mammoth Cave National Park area. Wurtzburg, Böhler Verlag, 69p.
- Miserez, J.J., 1976. Complements to the water chemistry of the karstic system of the Ljubljanica River. In: *Underground water tracing investigations in Slovenia, 1972-1975*, (Eds: R. Gospodarić and P. Habić. Inst. Karst Research, Ljubljana, 82-92.
- Mixon, W., 1990. Cave geology is not physics. *Geo²*, 17(1), 2-7.
- MKBT, 1989. Baradla Barlang, 1:1000. Magyar Karszt- és Barlangkutató Társulat, Budapest.
- Morris, T., 1984. Speleofest '84. *Canadian Caver*, 16(2), 20-29.
- Moser, H., V. Rajner, D. Rank and W. Stichler, 1976. Results of measurements of deuterium, oxygen-18 and tritium in water samples from test area taken during 1972-1975. In: *Underground water tracing investigations in Slovenia, 1972-1975* (Eds. R. Gospodarić and P. Habić. Inst. Karst Research, Ljubljana, 93-117.
- Mountjoy, E.W. and R.A. Price, 1985. Geology of Jasper, Alberta: Geological Survey of Canada, map 1611A, scale 1:50,000.
- Muir, D., and D.C. Ford, 1985. Castleguard. Canadian Govt. Publ. Centre, Ottawa.
- Mylroic, J.E., and J.L. Carew, 1987. Field evidence of the minimum time for speleogenesis. *NSS Bull.*, 49, 67-72.
- Nash, M., 1983. Fang Cave - and a first caving experience. *Canadian Caver*, 15(1), 9-15.

- Newson, M.D., 1971. A model of subterranean limestone erosion in the British Isles based on hydrology. *Trans. Inst. Brit. Geographers*, 54, 55-70.
- Norris, D.K., 1958. Beehive Mountain, Alberta and B.C. Paper 58-5, Geol. Survey of Canada, 22p.
- NZSB, 1986. Broken River Cave. New Zealand Speleological Bulletin, #140.
- Obarts, F.J., P. Garay and I. Morell, 1988. An attempt to karst classification in Spain based on system analysis. In :Karst hydrogeology and karst environment protection (Proc. IAH 21st congress), Eds. Yuan Daojian and Xie Chaofan. Geological Publ. House, Beijing, p328-336.
- Ogden, A.E., 1976. The hydrogeology of the central Monroe County karst, West Virginia. Unpubl. PhD thesis, West Virginia Univ., 263p.
- Önder, H., 1986. Interaction between conduit - type flow and diffuse flow in karst formation. Karst water resources (Proc. Ankara - Antalya Symposium, July 1985), IAHS Publ., 161, 371-386.
- Ozoray, G., 1977. Groundwater potential of the karst regions of Alberta, Canada. In: Hydrologic problems in karst regions, Eds: R.R. Dilamarter and S.C. Csallany, W. Kentucky, Univ., p235-240.
- Ozoray, G., and R.G. Barnes, 1978. Hydrogeology of the Calgary - Golden area, Alberta. Alberta Research Council, Earth Sciences Report 77-2.
- Palmer, A.N., 1975. The origin of maze caves. *NSS Bull.*, 37, 56-76.
- Palmer, A.N., 1977. Influence of geologic structure on groundwater flow and cave development in Mammoth Cave National Park, U.S.A. In: Karst hydrology (Eds. J.S. Tolson and F.L. Doyle), Univ. of Alabama in Huntsville, 405-414.
- Palmer, A.N., 1984. Geomorphic interpretation of karst features. In: Groundwater as a geomorphic agent (Ed. R.G. LaFleur), Allen & Unwin, 173-209.
- Palmer, A.N., 1987. Cave levels and their interpretation. *NSS Bull.*, 49, 50-66.
- Palmer, A.N., 1989a. Stratigraphic and structural control of cave development and groundwater flow in the Mammoth Cave region. In: Karst hydrology: concepts from the Mammoth Cave area, (Eds. W.B. White and E.L. White), Van Nostrand Reinhold, New York, p293-316.
- Palmer, A.N., 1989b. Geomorphic history of the Mammoth Cave System. In: Karst hydrology: concepts from the Mammoth Cave area, (Eds. W.B. White and E.L. White), Van Nostrand Reinhold, New York, p317-337.
- Palmer, A.N., 1991. Origin and morphology of limestone caves. *Geol. Soc. Amer. Bull.*, 103, 1-21.
- Palmer, A.N., and M.V. Palmer, 1989. Geologic history of the Black Hills, South Dakota. *NSS Bulletin*, 51(2), 72-99.
- Palmer, R., 1986. Cave diving news. *Caves and Caving, Bull. of the British Cave Research Assoc.*, #32, p29.

- Parizek, R.R., 1970. On the nature and significance of fracture traces and lineaments in carbonate and other terranes. In: Karst hydrology and water resources (Ed. V. Yevjevich), Water Resource Publications, Fort Collins, p47-108.
- Pasini, G., 1967. Nota preliminare sul ruolo speleogenetico dell' erosione "antigravitativa". Le grotte d'Italia, 4, 75-87.
- Pernette, J.-F., and R. Maire, 1983. Le BUS6, ou Sima de las Puertas de Illamina, Navarre, Espagne. Spelunca, #9, 25-34.
- Picknett, R.G., 1972. The pH of calcite solutions with and without magnesium carbonate present, and the implications with regard to rejuvenated aggressiveness. Trans. Cave Res. Grp. of G.B., 14, 141-149.
- Picknett, R.G., L.G. Brav and R.D. Stenner, 1976. The chemistry of cave waters. In: The science of speleology, Ed: T.D. Ford, 213-266.
- Pitty, A.F., 1968. Calcium carbonate content of karst water in relation to flow-through time. Nature, 217, 939-940.
- Pitty, A.F., 1974. Karst water studies in and around Ingleborough Cavern. In: Limestones and caves of North-West England, Ed: A.C. Waltham, David & Charles, Newton Abbot, p127-148.
- Pitty, A.F., R.A. Halliwell, J.L. Ternan, P.A. Whittel and R.G. Cooper, 1979. The range of water temperature fluctuations in the limestone waters of the Central and Southern Pennines. J. Hydrol., 41, 157-160.
- Plummer, L.N., and T.M.L. Wigley, 1976. The dissolution of calcite in CO₂-saturated solutions at 25°C and 1 atmosphere total pressure. Geochim. Cosmochim. Acta, 40, 191-202.
- Plummer, L.N., T.M.L. Wigley and D.L. Parkhurst, 1978. The kinetics of calcite dissolution in CO₂-water systems at 5 to 60°C and 0.0 to 1.0 atm CO₂. Am. J. Sci., 278, 179-216.
- Pollack, J., 1984a. Dezaiko Range exploration. Canadian Caver, 16(1), 41-42.
- Pollack, J., 1984b. Dezaiko 1984. Canadian Caver, 16(2), 34-35.
- Pollack, J., 1986. Two dives in Bluebell Cave. Canadian Caver, 18(2), 50-51.
- Pollack, J., 1988. Diving in Twin Falls Resurgence. Canadian Caver, 20(1), 16-17.
- Porter, J.W., R.A. Price and R.G. McCrossan, 1982. The Western Canada Sedimentary Basin. Phil. Trans. R. Soc. Lond. A305, 169-192.
- Powell, R.L., 1976. Joint patterns and solution channel evolution in Indiana. In: Karst hydrology, (Eds. J.S. Tolson and F.L. Doyle), Univ. of Alabama in Huntsville, 255-269.
- Price, R.A., 1962a. Fernie map area, east half, Alberta and British Columbia, 82G E1/2. Paper 61-24, Geol. Survey of Canada, 65p.
- Price, R.A., 1962b. Geologic structure of the central part of the Rocky Mountains in the vicinity of Crowsnest Pass. J. of the Alberta Soc. of Petroleum Geologists, 10, 341-351.

- Price, R.A. 1965. Flathead map area, British Columbia and Alberta. Memoir 336, Geol. Survey of Canada, 221p.
- Price, R.A. and E.W. Mountjoy, 1970. Geologic structure of the Canadian Rocky Mountains between the Bow and Athabasca Rivers - a progress report. In Structure of the southern Canadian Cordillera, Ed. J.O. Wheeler. Geological Survey of Canada, Special Paper 6, 7-25.
- Price, R.A. and P.R. Fermor, 1985. Structure section of the Cordilleran foreland thrust and fold belt west of Calgary, Alberta. Geol. Survey of Canada, Paper 84-14.
- Province of B.C. (Ministry of Energy, Mines and Petroleum Resources), 1982. British Columbia geological highway map. In four folders.
- Puch, C., 1989. La traversée B15 - Fuente de Escuain (Sistema Badalona), Pyrénées centrales, Huesca, Espagne. Spelunca, #33, 22-27.
- Pugsley, C., 1979. Caves of the Mount Arthur region, New Zealand. Caving International, #4, 3-10.
- Pugsley, C., 1986. Private communication.
- Puig, J.M., 1987. Le système karstique de la Fontaine de Vaucluse. Doct. thesis, Fac. Sci., Avignon, 208p. (Summary in: Karstologia, #10, 59)
- Quinif, Y., 1989. La notion d'étages de grottes dans le karst belge. Karstologia, #13, 41-49.
- Quinlan, J.F., 1986. Discussion of "Ground water tracers", by Davis et al. (1985), with emphasis on dye tracing, especially in karst terrains. Groundwater, 24, 253-259; 396-399.
- Quinlan, J.F., 1990. Special problems of ground-water monitoring in karst terranes. In: Ground Water and Vadose Zone Monitoring. ASTM STP 1053, Eds: D.M. Nielsen and A.I. Johnson, Amer. Soc. for Testing and Materials, Philadelphia, 275-304.
- Quinlan, J.F. and R.O. Ewers, 1981. Hydrogeology of the Mammoth Cave Region, Kentucky. In: Geol. Soc. of Amer. Cincinnati 1981 field trip guide books (Ed. T.G. Roberts), Amer. Geol. Inst., Washington, D.C., 3, 457-506.
- Quinlan, J.F., and R.O. Ewers, 1986. Reliable monitoring in karst terranes: it can be done, but not by an EPA-approved method. Ground water monitoring review, 6(1), 4-6.
- Quinlan, J.F. and R.O. Ewers, 1989. Subsurface drainage in the Mammoth Cave area. In: Karst hydrology: concepts from the Mammoth Cave area, (Eds. W.B. White and E.L. White). Van Nostrand Reinhold, New York, p65-103.
- Quinlan, J.F., R.O. Ewers, J.A. Ray, R.L. Powell and N.C. Krothe, 1983. Ground-water hydrology and geomorphology of the Mammoth Cave Region, Kentucky, and of the Mitchell Plain, Indiana. In: Field trips in Midwestern geology: Bloomington, Indiana, (Eds. R.H. Shaver and J.A. Sunderman), Geol. Soc. of Amer. and Indiana Geol. Survey, 2, 1-85.
- Quinlan, J.F. and J.A. Ray, 1981. Groundwater basins in the Mammoth Cave Region, Kentucky. Occ. Publ. #1, Friends of the karst, Mammoth Cave.
- Rapp, A., 1960. Recent development of mountain slopes in Karkevagge and surroundings, northern Scandinavia. Geograf. Annaler, 42, 71-200.

- Rauch, H.W. and W.B. White, 1970. Lithologic controls on the development of solution porosity in carbonate aquifers. *Water Resources Res.*, 6, 1175-1192.
- Ravens, J.M., 1986. Nettlebed Cave, Mount Arthur, New Zealand. Eighth edition, 1:1000 map in two sheets. New Zealand Speleological Society.
- Renault, H.P., 1967. Contribution à l'étude des actions mécaniques et sedimentologiques dans la spéléogénèse: les actions mécaniques à l'échelle du massif. *Ann. Spéléologie*, 22, 209-267.
- Renault, H.P., 1968. Contribution à l'étude des actions mécaniques et sedimentologiques dans la spéléogénèse: les facteurs sédimentologiques. *Ann. Spéléologie*, 24, 529-576.
- Rhoades, R., and N.M. Sinacori, 1941. Patterns of groundwater flow and solution. *J. Geol.*, 49, 785-794.
- Rigal, D., and E. Boyer, 1989. Le Red del Silencio, Monts Cantabriques, Espagne. *Spelunca*, #36, 21-27.
- Rollins, J., 1988. 1987 Speleofest. *Canadian Caver*, 20(1), 3-5.
- Rose, J., 1982. The Melinau River and its terraces. *Cave Science*, 9, 113-127.
- Rose, L., 1983. Alkalinity, its meaning and measurement. *Cave Science*, 10, 21-29.
- Round, S., 1990. Northern news: over a kilometre of passage below Malham Cove. *Caves and Caving*, #48, 13.
- Rouiller, P., and F. Auf der Mauer, 1986. Höhlochnachrichten Nr. 6. *Stalactite*, 1986, #1, p28-29.
- Rutter, N.W., 1987. Glacial processes in the Central Canadian Rocky Mountains. In: *Geomorphic systems of North America*, Ed. W.L. Graf. *Geol. Soc. America*, Boulder, 228-238.
- Sawatsky, K.D., 1987. Diving in Castleguard. *Canadian Caver*, 19(2), 22-28.
- Sawatzky, K.D., 1988. Cave diving camp, Vancouver Island 1988. *Canadian Caver*, 20(2), 10-17.
- Schotterer, U., A. Wildberger, U. Siegenthaler, W. Nabholz and H. Oeschger, 1979. Isotope study in the alpine karst region of Rawil, Switzerland. *Isotope hydrology*, 1978, 1, 351-366. Int. Atomic Energy Agency, Vienna.
- Schmidt, V.A., 1982. Magnetostratigraphy of sediments in Mammoth Cave, Kentucky. *Science*, 217, 827-829.
- Schroeder, J., 1990. Private communication.
- Schroeder, J., and D.C. Ford, 1983. Clastic sediments in Castleguard Cave, Columbia Icefields, Alberta, Canada. *Arctic and Alpine Res.*, 15, 451-461.
- Seiler, K.-P., P. Maloszewski and H. Behrens, 1989. Hydrodynamic dispersion in karstified limestones and dolomites in the Upper Jurassic of the Franconian Alb, F.R.G.. *J. Hydrol.*, 108, 235-247.

- Sesiano, J., 1989. les importantes émergences de Magland, dans la vallée de l'Arve (Haute-Savoie, France): physico-chimie et origine des eaux. *Karstologia*, #14, 47-53.
- Shackleton, N.J. and N.D. Opdyke, 1973. Oxygen isotope and paleomagnetic stratigraphy of equatorial Pacific core V28-238: oxygen isotope temperatures and ice volume on a 10^5 and 10^6 year scale. *Quat. Res.*, 3, 39-55.
- Shaw, J., and R. Kellerhals, 1982. The composition of recent alluvial gravels in Alberta river beds. *Alberta Research Council Bulletin* 41, 151p.
- Shifflett, P., 1987. A return to Great Expectations. *NSS News*, 44(6), 247-252.
- Shuster, E.T., and W.B. White, 1971. Seasonal fluctuations in the chemistry of limestone springs: a possible means for characterising carbonate aquifers. *J. Hydrol.*, 14, 93-128.
- Siddiqui, S.H. and R.R. Parizek, 1971. Hydrogeologic factors influencing well yields in folded and faulted carbonate rocks in Central Pennsylvania. *Water Resources Research*, 7, 1295-1312.
- Simmons, R., 1990. Private communication.
- Slaymaker, O., and H.J. McPherson, 1977. An overview of geomorphic processes in the Canadian Cordillera. *Z. Geomorph. N.F.*, 21, 169-186.
- Sloan, N., 1985. Huautla: exploration of the Peña Colorada. *NSS News*, 43(10), 300-310.
- Smart, C.C., 1983a. The hydrology of a glacierised alpine karst. Unpublished PhD thesis, McMaster Univ., 342p.
- Smart, C.C., 1983b. The hydrology of the Castleguard karst, Columbia Icefields, Alberta, Canada. *Arctic and Alpine Res.*, 15, 471-486.
- Smart, C.C., 1984. Overflow sedimentation in an alpine cave system. *Norsk geogr. Tidsskr.*, 38, 171-175.
- Smart, C.C., 1988a. Quantitative tracing of the Maligne karst system, Alberta, Canada. *J. Hydrol.*, 98, 185-204.
- Smart, C.C., 1988b. Artificial tracer techniques for the determination of the structure of conduit aquifers. *Groundwater*, 26, 445-453.
- Smart, C.C. and D.C. Ford, 1986. Structure and function of a conduit aquifer. *Can. J. Earth Sci.*, 23, 919-929.
- Smart, C. and D. Huntley, 1988. Small River update. *Canadian Caver*, 20(1), 40.
- Smart, P.L., 1976. Catchment delineation in karst areas by the use of quantitative tracer methods. *Proc. 3rd Internat. Symp. of Underground Water Tracing*, Bled, Yugoslavia, 291-298.
- Smart, P.L., 1981a. Underground geomorphology. In: *Caves of Mulu '80*, (compiled by A.J. Eavis), 44-46.
- Smart, P.L., 1981b. Variation of conduit flow velocities with discharge in the Longwood to Cheddar Rising system, Mendip Hills. *Proc. 8th Internat. Congr. Speleology*, Bowling Green, Ed: B.F. Beck. National. Speicol. Soc., Huntsville, Alabama, p333-335.

- Smart, P.L., 1984a. Cave geomorphology. In *Caves of Mulu '84*, (compiled by A.J. Eavis), 46-48.
- Smart, P.L., 1984b. The geology, geomorphology and speleogenesis of the Eastern Massifs, Picos de Europa, North Spain. *Cave Science*, 11(4), 238-245.
- Smart, P.L., and H. Friederich, 1982. An assessment of the methods and results of water-tracing experiments in the Gunung Mulu National Park, Sarawak. *Cave Science* (Trans. Brit. Cave Res. Assoc.), 9(2), 100-112.
- Smart, P.L., and N.S.J. Christopher, 1989. Ogo Ffynnon Ddu. In: *Limestone and caves of Wales*, Ed. T.D. Ford, Cambridge Univ. Press, 177-189.
- Smart, P.L., and C.G. Gardener, 1989. The Mynydd Llangattowg cave systems. In: *Limestone and caves of Wales*, Ed. T.D. Ford, Cambridge Univ. Press, 124-151.
- Smith, D.I., 1971. The concepts of water flow and water tables in limestones. *Trans. Cave Research Group of G.B.*, 13, 95-99.
- Smith, D.I., and T.C. Atkinson, 1976. Process, landform and climate in limestone regions. In: *Geomorphology and climate*, Ed: E. Derbyshire, Wiley, New York, 367-409.
- Smith, D.I., T.C. Atkinson and D.P. Drew, 1976. The hydrology of limestone terrains. In: *The science of speleology*, Eds: T.D. Ford and C.H.D. Cullingford. Academic Press, London, p179-212.
- Smith, D.I., and M.D. Newson, 1974. The dynamics of solutional and mechanical erosion in limestone catchments on the Mendip Hills, Somerset. In: *Fluvial processes in instrumented watersheds*, Inst. Brit. Geographers, Spec. Publ. #6, 155-167.
- Smith, D.I., and T.C. Atkinson, 1977. Underground flow in cavernous limestones, with special reference to the Malham area. *Field Studies*, 4, 597-616. (reported in Jennings, 1985).
- Smith, D.J., 1987. Solifluction in the Southern Canadian Rockies. *Canadian Geographer*, 31, 309-318.
- Smith, D.J., 1988. Rates and controls of soil movement on a solifluction slope in the Mount Rae area, Canadian Rocky Mountains. *Z. Geomorph.*, N.F. Suppl.-Bd, 71, p25-44.
- Smith, D.J., and J.S. Gardner, 1985. Geomorphic effects of ground squirrels in the Mount Rae area, Canadian Rocky Mountains. *Arctic and Alpine Res.*, 17, 205-210.
- Song Lin Hua, 1986. Principal characteristics of karst hydrology in China. *Proc. Ninth Internat. Congress of Speleology*, Barcelona, 55-59.
- Sorriaux, P., 1982. Contribution à l'étude de la sédimentation en milieu karstique. Le système de Niaux - Lombrives - Sabart (Pyrénées Ariégeoises). Thèse 3ème cycle, Univ. Paul-Sabatier de Toulouse, 255p.
- Spahli, R., 1983. Sumidero de Agueyaco. *Canadian Caver*, 15(2), 46-49.
- Sprouse, P., 1987. Camp V - Sistema Purificación 1987. *AMCS Activities Newsletter*, #16, 80-88. Assoc. for Mexican Cave Studies, Austin, Texas.

- Stanton, W.I., 1981. Some Mendip water traces 1976-1980. *J. Wessex Cave Club*, 16 (185), 120-127.
- Stanton, W.I., and P.L. Smart, 1981. Repeated dye traces of underground streams in the Mendip Hills, Somerset. *Proc. Univ. Bristol Speleol. Soc.*, 16, 47-58.
- Stenner, R.D.. 1969. The measurement of the aggressiveness of water towards calcium carbonate. *Trans. Cave Res. Group of Great Britain*, 11(3) 175-200.
- Stone, W., 1984. Peña Colorada. *AMCS Activities Newsletter*, #14, 46-55. Assoc. Mexican Cave Studies, Austin.
- St Pierre, S., and D. St Pierre, 1980. Caves of Velfjord, South Nordland, with particular reference to Sirijordgrotten. *Trans. Cave Res. Group of Great Britain*, 7(2), 70-82.
- Strayle, G., 1970. Karsthydrolische Untersuchungen auf der Ebinger Alb. *Jh. geol. Landesamt Baden-Württemberg* 12, Freiburg i. Br. (reported in Zötl, 1974).
- Stringfield, V.T., 1966. Relation of surface-water hydrology to the principal artesian aquifer in Florida and southeastern Georgia. *U.S. Geol. Survey, Profess. Papers*, 492, 383p.
- Sweeting, M.M., 1950. Erosion cycles and limestone caverns in the Ingleborough district. *Geog. J.*, 115, 63-78.
- Sweeting, M.M., 1973. Karst landforms. *Columbia Univ. Press*, 362p.
- Swinnerton, A.C., 1932. Origin of limestone caverns. *Bull. Geol. Soc. Amer.*, 43, 663-694.
- Tardy, J.-C., 1990a. Siphon de la Mescla, Malaucène. *Spelunca*, #40, 4-5.
- Tardy, J.-C., 1990b. Siphon de Paques; résurgence de la Fou, Saint-Cézaire. *Spelunca*, #40, 5-6.
- Terjesen, S.G., O. Erga, G. Thorsen and A. Væ, 1961. Phase boundary processes as rate determining steps in reactions between solids and liquids. The inhibitory action of metal ions on the formation of calcium bicarbonate by the reaction of calcite with aqueous carbon dioxide. *Chem. Eng. Sci.*, 14, 277-289.
- Ternan, J.L., 1972. Comments on the use of a calcium hardness variability index in the study of carbonate aquifers: with reference to the Central Pennines, England. *J. Hydrol.*, 16, 317-321.
- Thompson, P. and J. Coward, 1973. Report on the winter expedition to Yorkshire Pot. *Canadian Caver*, 5, 4-20.
- Thompson, P., 1972. Caving in Chiapas, Mexico. *Canadian Caver*, 4(1), 8-21.
- Thompson, P., 1976. Cave exploration in Canada. *Canadian Caver Magazine*, Edmonton, 183p.
- Thompson, T.L., 1962. Origin of the Rocky Mountain Trench in southeastern British Columbia by Cenozoic block faulting. *J. Alberta Soc. of Petroleum Geologists*, 10, 408-427.
- Thomson, D., Castleguard 88. *Canadian Caver*, 20(2), 24-27.

- Torbarov, K., 1976. Estimation of permeability and effective porosity in karst on the basis of recession curve analysis. In: Karst hydrology and water resources (Ed. V. Yevjevich), Water Resource Publications, Fort Collins, p121-136.
- Tracey, G., 1975. Caving in the Huixtan area: Cochol. Canadian Caver, 7(1), p14 and 31-33.
- Thraikill, J., 1968. Chemical and hydrologic factors in the excavation of limestone caves. Geol. Soc. of Amer. Bull. 79, 19-46.
- Thraikill, J., 1985. Flow in a limestone aquifer as determined from water tracing and water levels in wells. J. Hydrol., 78, 123-136.
- Tokarsky, O., 1974. Hydrogeology of the Lethbridge - Fernie area. Alberta Research Council, Earth Sciences Report 74-1.
- Tratman, E.K., 1969. The caves of north-west Clare. David & Charles, Newton Abbot.
- Trombe, F., 1952. Traité de Spéléologie. Payot, Paris, 376p.
- UBSS (University of Bristol Speleological Society), 1969. The caves of North-West Clare, Ireland, Ed: E.K. Tratman, 256p.
- van Everdingen, R.O., 1968. Studies of formation water in Western Canada: geochemistry and hydrodynamics. Can. J. Earth Sci 5, 523-543.
- van Everdingen, R.O., 1972. Thermal and mineral springs in the southern Rocky Mountains of Canada. Environment Canada, Water Management Service, 151p.
- Vermette, S.J., 1989. Distribution and sources of atmospheric sulphur, halogen and heavy metal deposition in Hamilton, Ontario. Unpubl. PhD thesis, McMaster Univ., 176p.
- Warwick, G.T., 1960. The effect of knick-point recession on the water-table and associated features in limestone regions, with special reference to England and Wales. Zeit. für Geomorph. Supplementband, 2, 92-99.
- Waltham, A.C., 1970. Cave development in the limestone of the Ingleborough District. Geogr. J., 136, 574-585.
- Waltham, A.C., 1971. Controlling factors in the development of caves. Trans. Cave Research Group of G.B., 13, 73-80.
- Waltham, A.C., 1974. Limestone and caves of north-west England. David and Charles, Newton Abbot, 477p.
- Waltham, A.C., 1976. Tigris Tunnel, Turkey. British Cave Research Assoc. Bull., #14, 31-34.
- Waltham, A.C., 1981. The origin and development of limestone caves. Progress in Physical Geography, 5, 242-256.
- Waltham, A.C., 1977. White Scar Cave. Trans. British Cave Research Assoc., 4(3), 345-353.
- Waltham, A.C., 1983. Valley excavation in the Yorkshire Dales karst. In: New directions in karst (Eds. K. Paterson and M.M. Sweeting), Geo Books, Norwich, 541-550.
- Waltham, A.C., 1986. China Caves '85. Royal Geog. Soc., London, 60p.

- Waltham, A.C. and D.B. Brook, 1980a. The Three Counties System. *Trans. British Cave Research Assoc.*, 7, 121.
- Waltham, A.C. and D.B. Brook, 1980b. Geomorphological observations in the limestone caves of the Gunung Mulu National Park, Sarawak. *Trans. British Cave Research Assoc.*, 7, 123-139.
- Waltham, A.C., D.B. Brook, O.W. Statham and T.G. Yeadon, 1981. Swinsto Hole, Kingsdale: a type example of cave development in the limestone of Northern England. *Geog. J.*, 147, 350-353.
- Waltham, A.C. and P. Hatherley, 1983. The caves of Leck Fell. *Trans. British Cave Research Assoc.*, 10, 245-247.
- Waltham, A.C., R.D. Brown and T.C. Middleton, 1985. Karst and caves of the Jabal Akhdar, Oman. *Cave Science*, 12(3), 69-79.
- Webb, B.C., 1982. The geology of the Melinau Limestone of the Gunung Mulu National Park. *Cave Science*, 9, 94-99.
- Weyl, P.K., 1958. The solution kinetics of calcite. *J. Geol.*, 66, 163-176.
- White, E.L., and B.M. Reich, 1970. Behaviour of annual floods in limestone basins in Pennsylvania. *J. Hydrol.*, 10, 193-198.
- White, W.B., 1969. Conceptual models for carbonate aquifers. *Ground Water*, 7, 15-21.
- White, W.B., 1988. *Geomorphology and hydrology of karst terrains*. Oxford Univ. Press, 464p.
- White, W.B., and J. Longyear, 1962. Some limitations on speleo-genetic speculation imposed by the hydraulics of groundwater flow in limestone. *Nittany Grotto Newsletter* 10, 155-167.
- White, W.B., and V.A. Schmidt, 1966. Hydrology of a karst area in east-central West Virginia. *Water Resources Res.*, 2, 549-560.
- White, W.B. and E.L. White, 1983. Patterns of cave development and speleogenesis in West Virginia. In: *An introduction to the caves of east-central West Virginia*, (Eds. D.M. Medville, G.R. Dasher and E. Werner), NSS Convention guidebook, #23.
- White, W.B. and G.H. Deike III, 1989. Hydraulic geometry of cave passages. In: *Karst hydrology: concepts from the Mammoth Cave area*, (Eds. W.B. White and E.L. White), Van Nostrand Reinhold, New York, p223-258.
- White, W.B., G.L. Jefferson, and J.F. Haman, 1966. Quartzite karst in southeastern Venezuela. *Internat. J. Speleol.*, 2, 309-314.
- White, W.B., and E.L. White, 1974. Base-level control of underground drainage in the Potomac River basin. *Proc. 4th conf. on karst geol. and hydrol.*, W. Va. Geol. and Econ. Survey, 41-53.
- Williams, C.F., and W.K. Jones, 1983. Karst drainage systems of the northern Spring Creek basin, West Virginia. In: NSS annual convention program, Eds: E. Werner and H. Medville. Nat. Speleol. Soc., Huntsville, Alabama, p92-93.

- Williams, D.D., and H.B.N. Hynes, 1974. The occurrence of benthos deep in the substratum of a stream. *Freshwater Biol.*, 4, 233-256.
- Williams, P.W., 1977. Hydrology of the Waikoropupu Springs: a major tidal karst resurgence in northwest Nelson (New Zealand). *J. Hydrol.*, 35, 73-92.
- Williams, P.W., 1983. The role of the subcutaneous zone in karst hydrology. *J. Hydrol.*, 61, 45-67.
- Wolfe, T.E., 1964. Cavern development in the Greenbrier Series, West Virginia. *Bull. Nat. Speleol. Soc.*, 26, 37-60.
- Worthington, S.R.H., 1978. Spain '75 and '77. *Sheffield Univ. Speleol. Soc. J.*, 2 (6), 3-8.
- Worthington, S.R.H., 1980. The Hole in the Wall. *Sheffield Univ. Speleol. Soc. J.*, 3 (1), 38-39.
- Worthington, S.R.H., 1984a. Caving in the Mount Robson area. *Canadian Caver*, 16(1), 25-30.
- Worthington, S.R.H., 1984b. The paleodrainage of an Appalachian fluviokarst: Friars Hole, West Virginia. Unpubl. MSc thesis, McMaster Univ., 218p.
- Worthington, S.R.H., 1984c. Diffuse flow and conduit flow in the Locust Creek catchment. Unpublished term paper, 37p.
- Worthington, S.R.H., S. Mayers, K. Ecock, P. Basco, J. Troester, D. Troester, and S. Allen, 1984d. Unpublished map of Rio Encantado cave.
- Worthington, S.R.H., 1989. Spéléogénèse des cavernes de la Sierra Negra. *Sous Terre*, 6(4), 6-7.
- Worthington, S.R.H., 1990. Unpublished data.
- Yonge, C., 1983a. Gargantua extension. *Canadian Caver*, 15(2), 5-6.
- Yonge, C., 1983b. Castleguard 1983. *Canadian Caver*, 15(2), 7-15.
- Yonge, C., 1984. Castleguard 1984. *Canadian Caver*, 16(2), 36.
- Yonge, C., 1985. The 1984/1985 Castleguard expeditions. *Canadian Caver*, 17, 16-19.
- Yonge, C., 1986. Shorty's Cave is getting longer. *Canadian Caver*, 18(1), 33-35.
- Yonge, C., 1987. Private communication.
- Yonge, C., 1990a. Private communication.
- Yonge, C., 1990b. Rats Nest Cave: Provincial Historic Resource, 1987. Unpubl. report, 51p.
- Yonge, C., and S.R.H. Worthington, 1984. Recent explorations around Mount Robson. *Canadian Caver*, 17, 32-48.
- Yonge, C., D.C. Ford, J. Gray and H.P. Schwarcz, 1985. Stable isotope studies of cave seepage water. *Chem. Geol. (Isotope Geoscience section)*, 58, 97-105.

- Yurtsever, Y., and J.R. Gat, 1981. Atmospheric waters. In: Stable isotope hydrology: deuterium and oxygen-18 in the water cycle, (Eds. J.R. Gat and R. Gonfiantini). Tech. Report Series, #210, Int. Atomic Energy Agency, Vienna, 103-142.
- Yves-Bigot, J., 1989. Trave System: third deepest cave in the world. Caves and Caving, #46, 10-14.
- Zötl, J.G., 1974. Karsthydrogeologie. Springer-Verlag, 291p.
- Zupan, N., 1990. Izvar in mineralna sestava jamskih peskov in ilovic (The origin and mineral composition of cave sands and loams). Unpubl. MSc thesis, Univ. Ljubljana. (Not seen: details from N. Zupan, 1990, private communication).

